FE MODEL UPDATING OF A BASE-ISOLATED NUCLEAR POWER PLANT CONSIDERING AGING EFFECTS OF ISOLATORS

Dookie Kim [1], Thuy Dung Vu [1], Md Iftekharul Alam [1], Sung Gook Cho [2]
[1] Kunsan National University, Kunsan, South KOREA
[2] R&D Center, JACE KOREA Company, Gyeonggi-do, South KOREA
E-mail of corresponding author: kim2kie@chol.com

ABSTRACT

Aging is defined as a continuing time-dependent degradation of material due to service conditions such as normal operation and transient conditions. It is expected that over long periods of time, there is gradual changes in the properties of structural materials. Since nuclear power plants (NPPs) are generally designed for a life cycle of 60 years, their stabilities and working capacity may be lost due to aging effects. The paper presents a new approach to update the finite element (FE) model of NPPs. FE Model updating based on iterative neural networks is proposed as a suitable and reliable tool to estimate the aging effects of NPPs. The method is applied to update the isolator model of a base-isolated NPP in order to validate the studies. Experiments and FE analyses have been also carried out to identify the aging effects of the isolators on the structural behavior. Parameters of which aging can significantly affect the isolator characteristics are identified by performing the sensitivity analysis. The obtained results indicate a great potential of the presented method for practical applications. Static and dynamic structural performances of the NPP are also observed and compared before and after aging. It reveals the considerable effects of aging on the NPP.

INTRODUCTION

Aging effect of NPPs is considered as one of the vital factors for safety and reliability of plant. Requirements and guidance related to degradation of structures and passive components, which include containments, water-control structures, and masonry walls, are available in international code and standards (e.g., ACI 318). Over the years, many researchers and engineers of the nuclear energy area have been developed studies to investigate and comprehend the performance of base-isolated nuclear power plant (base-isolated NPP) caused and affected by aging. They consist of age-related degradation of not only plant structures but also systems and components.

The aging process and aging assessment of containment cooling systems in NPPs were studied in Lofaro *et al.* (1994). The result shows that aging is a concern and should be addressed in the design of NPPs. A methodology was developed in Naus (1996) through a structural aging (SAG) programe, which addressed safety-related concrete structures and longevity considerations in nuclear power plants. Ellingwood (1998) proposed a mathematical formalism of a probabilistic risk assessment (PRA) for identifying aging structural components whose may play a significant role in NPPs due to aging effects. An assessment of age-related degradation of NPP structures and passive components were introduced in Braverman (2000). These studies emphasized that aging and its effects need to be defined and calibrated to account for the performance of NPPs.

Seismic isolation or base isolation systems are commonly used to ensure safety and reliability against earthquake of infrastructures: bridges, buildings and other mission critical structures like nuclear power plants. Since the 1980s, several pressurized water reactor units have been isolated successfully. Research about aging therefore needs to be done to investigate the performance of base-isolated nuclear power plant (base-isolated NPP). Model updating based on iterative neural networks is proposed in this paper in order to study the aging effects of base-isolated NPPs.

The model updating procedure has a natural logical flow: collect data, choose a model set, and then pick the "best" model in this set. It is quite likely, though, that the model first obtained will not pass the model validation tests (Ljung 1999). Neural networks (NNs) as the techniques that seek to build an intelligent program using models to mimic the function of human brain (Lippmann 1987). Adaptive NNs for model updating of structures introduced in Chang *et al.* (2000) open loop in nature and are capable of providing a confidence measure of the accuracy only during the training phase. Finite element (FE) model updating based NNs (Ramuhalli *et al.* 2005) has been developed for estimating the system parameters as well as structural damage detection related application (Kerschen *et al.* 2006, Zapico *et al.* 2008, Rouss *et al.* 2009).

A simplified approach has been adopted for FE model updating based on iterative NNs of a base-isolated NPP using the virtual static deflections of the lead rubber bearing (LRB). Thermal aging test has been performed on the LRB for the verification of the approach. The observed results indicate a great potential of proposed method to update the base-isolated NPP model accounting for aging effects. The static and dynamic analyses obtained estimated and initial parameters are performed and compared. The observed results show the considerable effects of aging on the behavior of the structure.

FE MODEL AND SENSITIVITY ANALYSIS

A FE model (Lee *et al.*, 1999) was developed in Opensees Software (McKenna and Fenves 2001) for an actual base-isolated NPP (Fig. 1). The containment building was modeled with 65.8-meter height using 13 elastic beam column elements. The element lengths were selected in accordance with the key levels of the NPP. The mass was distributed as concentrated loads at two nodes of each element. Diaphragm constrains are applied to connect the elements. The mechanical properties of frame elements were modeled with section properties selected based on sensitivity analysis, which has been done in (Lee *et al.*, 1999). A LRB with specifications described in Table 1 is considered for isolation devices. A bilinear model (Naeim *et al.*, 1999) with a zero length element (Ryan *et al.*, 2005) was built for numerical analysis as shown in Fig. 2 (a). Initially, the load-displacement hysteresis loop illustrated Fig. 2 (b) is observed from the equivalent properties of LRB calculated from the concept presented in Naeim *et al.* (1999).

Table 1 Specifications of laminated rubber bearings

Steel diameter D_s (mm)	Hole diameter D_h (mm)	Steel diameter D (mm)	Rubber thickness t_i (mm)	Number of Layer n	Steel thickness t_s (mm)	1st shape factor S_1	2nd shape factor S_2	Shear modulus G
259	56	279	3	29	3	21.6	2.98	0.4

where

$$S_1 = \left(\frac{D_s - D_h}{4t_i} \right) \quad (1)$$

$$S_2 = \left(\frac{D_s}{nt_i} \right) \quad (2)$$

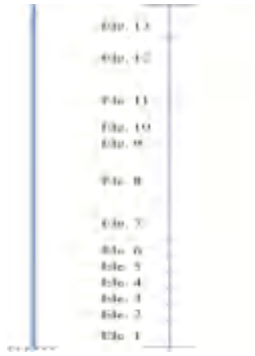

Fig. 1 Stick model of NPP containment building

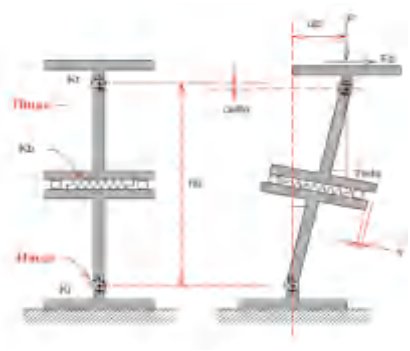

(a) Two-spring mechanical model

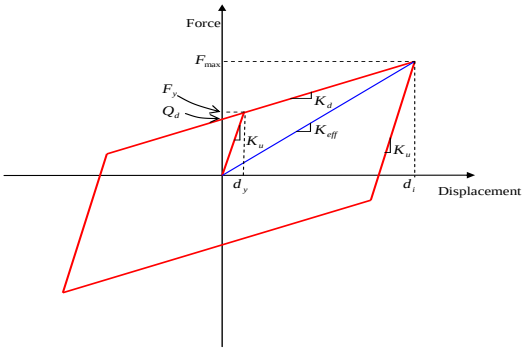

(b) Force-displacement hysteresis loop

Fig. 2 Isolation bearing model (Ryan *et al.*, 2005)

The design of LRB includes the post yield stiffness k_{2o} ; yield displacement d_y ; the ratios $PP_{cr} = P / P_{cr} = 1/SF$ and $PP_o = P / P_o$. Sensitivity analysis was carried out to identify the parameters whose aging can significantly affect the performance of the LRB. Fig. 3 demonstrates variation of input parameters due to an equivalent lateral force cause the approximately the same displacement as design shear load and an axial load of 565 kN .

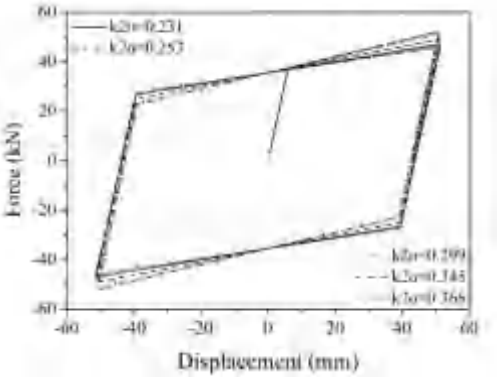

(a) Post-yield stiffness

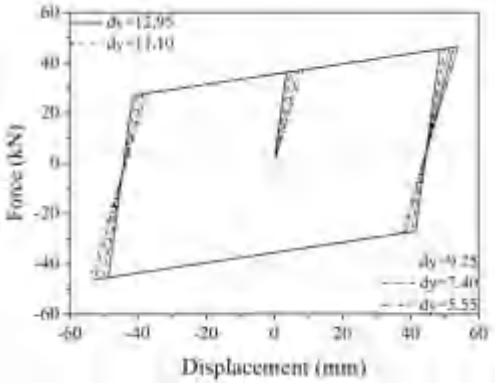

(b) Yield displacement

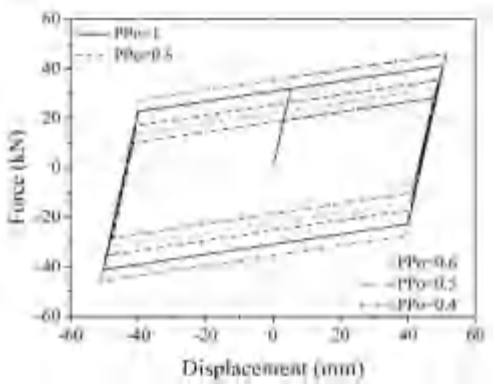

(a) P/Po

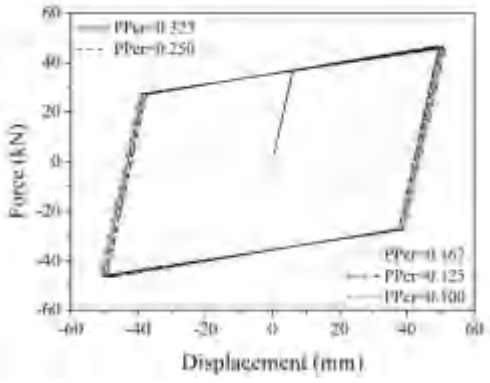

(b) P/Pcr

Fig. 3 Sensitivity Analysis

EXPERIMENT STUDY AND MODEL UPDATING

A LRB with the specimen geometry and specifications given in Table 1 and Fig. 4 was considered for experimental studies (Oh *et al.,* 2010). The bearing was a 275-millimeter diameter including a 10-millimeter thickness of outside surrounding rubber, 171-millimeter depth which consists of 29 layers with thickness of 3-millimeter laminated rubber and 3-millimeter steel plate.

The compressive-shear test was carried out to identify the variation of compressive and shear properties by comparing before and after thermal aging. The thermal aging experiments were performed in the accelerated exposure condition of 70℃ for about 168 hours, which is equivalent to the estimated life of 60 years (ISO 11346). These thermally aged specimens were used for the compression-shear loading test in order to investigate the changes in the LRB parameters due to thermal aging. The vertical load of 565 kN was uniformly applied in order to maintain the designed in-plane pressure. The equivalent lateral load with a 5 Hz sinusoidal wave was employed to cause the approximately the same displacement as design shear load. The load was incurred and repeated 11 times. The obtained compression-shear loading curves for LRB before and after aging are shown in Fig. 5.

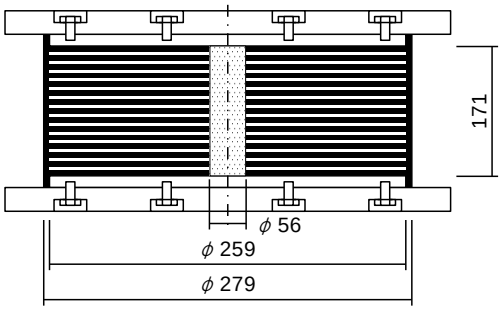

Fig. 4 Specimen geometry and specification

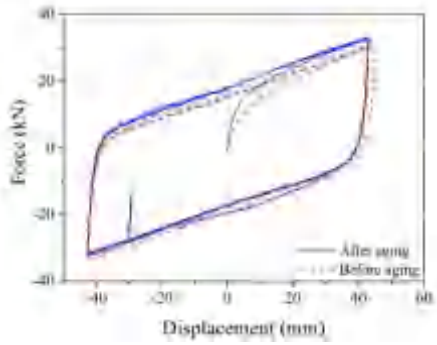

Fig. 5 Compression-shear loading curves

According to the sensitivity analysis represented by the objective function value (OFV), the ratio PP_o, k_{2o} and d_y are found to be largely affecting the LRB behavior while PP_{cr}, which is calculated according to the buckling load, is found to have small effect. It can therefore be concluded that the post yield stiffness (k_{2o}), yield displacement

(d_y), the ratio PP_o (between compressive and axial loads) are the key parameters in performance of LRB. Updating the model is therefore to estimate the representative stiffness, yield displacement and the ratio PP_o.

The optimization toolbox in MATLAB, which uses the objective function (Eq. 3) as the objective function, was employed to perform the model updating (an optimization process actually). The process of model updating method was a process of optimization as shown in Fig. 6.

$$OFV = \sum_{j=1}^{6} \left(\left(\frac{d_j^{\exp} - d_j^{num}}{d_j^{\exp}} \right)^2 \right) \tag{3}$$

where OFV is the cost function, $d_j^{\exp}$ is the experimental displacement and d_j^{num} is the corresponding numerical displacement.

The optimization was converged at the end of about seven iterations. The value of the cost function is 1.636656 after the optimization process, which can conclude that the optimization process worked effectively. Fig. 7 shows the comparisons of the numerical compression-shear curve, after model updating, and the experimental curve. An agreement between the numerical and experimental results demonstrates that the presented method is effective and efficient to estimate the structural parameters considering aging effect.

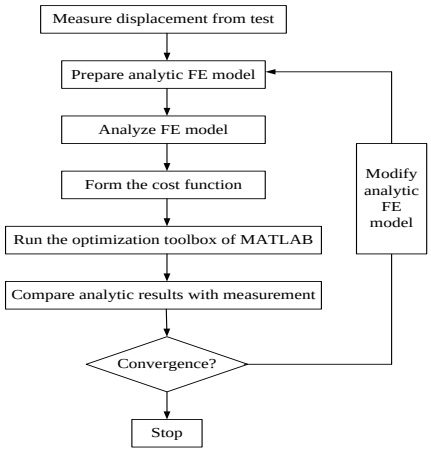

Fig. 6 Flowchart of the identification method

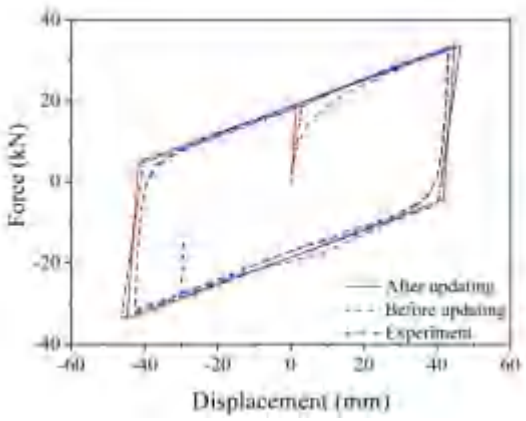

Fig. 7 Model updating

SEISMIC PERFORMANCE OF THE BASE-ISOLATED NPP

After model updating, dynamic and static behavior of the base-isolated NPP were performed in order to evaluate the aging effects on the structure. The observed results were compared before and after thermal aging of LRB. Table 2 shows the comparison of natural frequencies before and after aging. While Fig. 8 shows the comparison of seismic response under EI Centro earthquake.

Table 2 Effects of aging

Parameters	Input parameters			Natural frequencies		
	k_{2o} kN/mm	d mm	PP_o	1st mode Hz	2nd mode Hz	3rd mode Hz

Before updating	0.3291	9.25	0.45	0.5965	9.9436	25.0978
After updating	0.3465	4.63	0.40	0.6030	9.9436	25.0978

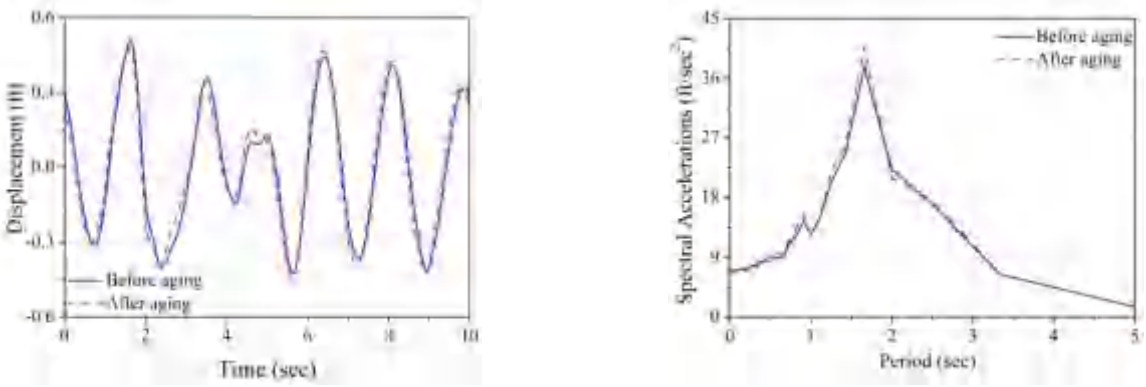

Fig. 8 Earthquake response

CONCLUSION

FE model updating based on neural networks is proposed in this paper in order to estimate the aging effects of the lead rubber bearings of the base-isolated nuclear power plants (base-isolated NPPs). The sensitivity analysis was performed in order to identify the parameters which may have critical effects on the LRB behavior in terms of aging. Numerical and experimental studies have been carried out in order to verify the effectiveness and accuracy of the presented method. The observed behaviors of the base-isolated NPP, both before and after model updating, were compared in order to indicate the aging effects on the structure. The main conclusions can be drawn from this study as follows:

1. Based on the sensitivity analysis presented by the objective function value (OFV), the ratio PP_o, k_{2o} and d_y are found to be largely affecting the LRB behavior while PP_{cr}, which is calculated according to the buckling load, is found to have a small effect. It can therefore be concluded that the post yield stiffness (k_{2o}), yield displacement (d_y), and the ratio PP_o (between compressive and axial loads) are the key parameters in the performance of the LRB.
2. It is observed that the post yield stiffness of the LRB is increased about 5% after optimization process, while observed value is about 3% from experiment. It indicates that FE model updating was successfully applied to estimate the effects of aging on the base-isolated NPP. It strengthens the suitability and efficiency of the proposed method in practice.
3. The static and dynamic behaviors of the base-isolated NPP were performed and compared before and after considering aging effects. The peak spectral acceleration at the top of the containment building was increased about 7.2 % due to aging. The displacement was also decreased remarkably. They show considerable effects of aging-related degradation on performances of the NPP. Aging effects are therefore required to be assessed and managed.

ACKNOWLEDGEMENTS

This work was supported by the Nuclear Research & Development of the Korea Institute of Energy Technology Evaluation and Planning (KETEP), through a grant funded by the Ministry of Knowledge Economy (2011T100200079). The authors would like to express their appreciation for the financial support.

REFERENCES

[1] ACI 318 (2005), Building Code Requirements for Structural Concrete and Commentary, American Concrete Institute, Detroit, Michigan.

[2] Lofaro, R. and Subudhi. M. (1994), Effects of Age on Nuclear Power Plant Containment Cooling Systems, NUREG/CR – 5939, BNL-NUREG-2345, Washington, DC: US Nuclear Regulatory Commission

[3] Naus D.J., Oland C.B. and Ellingwood B. (1996), Report on aging of nuclear power plant reinforced concrete structures. NUREG/CR-6424, Washington, DC: US Nuclear Regulatory Commission

[4] Ellingwood, B. (1998), "Issues related to structural aging in probabilistic risk assessment of nuclear power plants", Reliability Engineering and System Safety, 62, pp. 171-183

[5] Braveman, J.J., Hofmayer, R.J. and Morante, R.J. (2000), Assessment of age-related degradation of structures and passive components for U.S. Nuclear Power Plant, NUREG/CR-6679, Washington, DC: US Nuclear Regulatory Commission

[6] Ljung, Lennart (1999), System Identification: Theory for the Use, 2nd Ed., PTR, Prentice-Hall, Upper Saddle River, N.J.

[7] Lippmann, R.P. (1987), "An introduction to computing with neural networks", IEEE ASSP Magazine, 4(**2**), pp. 4-22

[8] Chang, C.C, Chang, T.Y.P and Xu. Y.G (2000), "Adaptive neural networks for model updating of structures", *Smart materials & structures*, 9, pp. 59-68

[9] Ramuhalli, P., Udpa, L. and Udpa, S.S. (2005), "Finite-element neural networks for solving differential equations", *IEEE Trans. Neural Networks*, 16(**6**), pp. 1388-1391

[10] Kerschen, G., Worden, K., Valakis, A.F. and Golinval, J.C. (2006), "Past, present and future of non-linear system identification in structural dynamics", *Mechanical System and Signal Processing*, **20**(3), pp. 505-592

[11] Zapico, J.L., González-Buelga, A., González, M.P., Alonso, R. (2008), "Finite element model updating of a small steel frame using neural networks", *Smart Materials and Structures*, **17**(4), pp. 1-11

[12] Rouss, V., Charon, W., Cirrincione, G. (2009), "Neural model of the dynamic behaviour of a non-linear mechanical system", *Mechanical System and Signal Processing*, **23**(4), pp. 1145-1159

[13] Lee, N.H. and Song, K.B. (1999), "Seismic Capacity Evaluation of the Prestressed/Reinforced Concrete Containment, Young-Gwang Nuclear Power Plant Units 5 & 6", *Nuclear Engineering and Design*, 192, pp. 189-203.

[14] McKenna, F. and Fenves, G. L. (2001), *OpenSees, the Open System for Earthquake Engineering Simulation*, http://opensees.berkeley.edu

[15] Ryan, K. L., Kelly, J. M. and Chopra, A. K. (2005), "Nonlinear model for lead-rubber bearings including axial-load effects", *J. Engineering Mechanics (ASCE)*, 131(**12**), pp. 1270-1278.

[16] Naeim, F. and Kelly, J.M. (1999), *Design of seismic isolated structures*, John Wiley & Sons Inc

[17] Oh, J. and Jung, H.Y. (2010), "Effects of Accelerated Thermal Aging on Dynamic Properties of Laminated Rubber Bearings", Journal of Korean Society of Civil Engineers, KSCE, 30(**5**), pp. 417-424 (in Korean).

APPENDIX

Q_d : Characteristic strength

F_y : Yield force

F_{max} : Maximum force

k_d : Post yield stiffness

k_u : Elastic (unloading) stiffness

k_{eff} : Effective stiffness

d_y : Yield displacement

d_i : Maximum bearing displacement

P : Compressive load

P_o : Axial load

P_{cr} : Critical load

PP_{cr} : Ratio between compressive load and critical load

SF : Safety factor against buckling of LRB

SEISMIC PERFORMANCE OF THREE-DIMENSIONALLY BASE-ISOLATED NUCLEAR POWER PLANT

T. Wang[1], F. Wang[1]
[1]Institute of Engineering Mechanics, China Earthquake Administration, Yanjiao, Sanhe, Hebei, 065201, China
E-mail of corresponding author: wangtao2004@gmail.com

ABSTRACT

In order to render nuclear power plants a larger seismic margin from design earthquakes and standardize the seismic design procedure for different locations with various seismic fortification intensities, the base isolation technique that has been successfully applied in traditional civil engineering, is proposed for nuclear power plants. Considering the seismic demand from installed facilities and pipes within the plants, a three-dimensional base isolation technique is developed in this study. It was first examined by simplified single-degree-of-freedom models to search for the suitable parameters for the base isolation layer. It is found that the vertical frequency of the base-isolated plant shall be larger than 1.0Hz to avoid the dominated rocking mode. A set of time history analyses were then conducted to further explore the damping effect of the base isolation layer on the structural response indices. It is observed that the damping within the reasonable range, commonly less than 30%, is helpful to suppress structural displacement, velocity and acceleration.

INTRODUCTION

Nuclear power plant is one of the sustainable and green power sources, playing significant role in human society. However, recent earthquakes, particularly the 2011 Sendai earthquake and tsunami of Japan lead to the deadly failure of Fukushima Nuclear Power Plant. Massive radioactive material was burst out, resulting in serious environment problem. It was reported that all reactors of Fukushima plant automatically shut down when being hit by the huge earthquake. However, the emergency power failed during earthquake which was supposed to provide coolant water to reactors. Also in Japan, the Kashiwazaki-Kariwa Nuclear Power Plant, one of the largest nuclear generating stations in the world, locates approximately 24 kilometers from the epicenter of the Mw 6.6 July 2007 Chuetsu offshore earthquake. The seismic intensity was larger than the design basis earthquake and initiated an extended shutdown for inspection, which indicated that greater earthquake-proofing was needed before operation could be resumed. The plant was completely shut down for 21 months following the earthquake. To mitigate the disaster resulted by potential earthquakes, the seismic reliability shall be enhanced in the design stage.

To support China's quick development, nuclear power plants are being constructed in many places of mainland, China. The dominated reactors are AP1000 and EPR600 introduced from American and Europe, respectively. The design earthquakes for these two types of reactor are 0.3 and 0.2g, correspondingly. Some plants, however, are to be constructed at the region with higher seismic intensity, and the investigated seismic intensity with the expected probability of exceedance is higher than the design earthquake. To avoid redesigning the station, the seismic effect shall be reduced effectively.

To this end, the base isolation technique, which has been successfully applied in traditional civil engineering, is proposed. It is a reasonable option for nuclear power plants and is able to render nuclear power plants a larger seismic margin from design earthquakes and standardize the seismic design procedure for different locations with various seismic fortification intensities. France is the first country to have constructed two isolated nuclear power plants. Consequently, the standard design of nuclear facilities has been propelled [1]. Since the 1980's, Japan has developed a series of research on the isolation technology for nuclear power plants, and published a guideline of the base isolation design for nuclear power plants [2], systematically discussing structural dynamics and extreme load analysis, seismic response analysis and design, structural reliability and probabilistic safety assessment and qualification management and maintenance of isolators. In 1995, European Atomic Energy Community (EAEC) raised a proposal for design guidelines of base isolated nuclear facilities, mainly using high damping steel-laminated rubber bearings (HDRB) [3]. Numerous experiments and analyses of three dimensional models by both simple bearing models and detailed finite-element were completed, which verified that isolation technology is feasible and economic.

Traditional horizontal isolation technique, however, still allows the seismic energy to pass through vertically into the superstructure. The vertical response commonly vibrates within a frequency range of 10-20Hz, which covers most facility frequencies, indicating an adverse effect of the horizontal base isolation. Therefore, the

concept of three-dimensional base isolation was introduced into the seismic design of nuclear power plant. The practice so far is still limited within laboratories, and can be classified into two categories, i.e., overall three-dimensional base isolation, and separated base isolation combining both overall horizontal isolation of nuclear building and local vertical isolation of specific facilities.

Proposed in this paper is an overall three-dimensional base isolation system consisting of polymeric bearings and a hydraulic rocking suppression system. The polymeric bearing is featured with thick rubber layers. The hydraulic rocking suppression system is used not only to limit the rocking response of the superstructure, but also to provide extra damping in the vertical direction. In this preliminary study, the design parameters of the three-dimensional base isolation system, such as the horizontal and vertical frequencies and damping ratios, were identified through numerical analysis using a simplified mass-spring model. The modal analysis was first conducted to find suitable values for the vertical stiffness of the base isolation layer. Then time history analyses were conducted to examine the damping effect.

PARAMETRIC STUDY USING RIGID BLOCK MODEL

Two models were adopted to examine the parameters of the base isolation layer. The first model is shown in Fig.1 where, the superstructure is treated as a rigid block with the gravity center half height above the base isolation layer. The base isolation layer is modeled with distributed vertical springs representing the isolators, while the horizontal behavior is represented by a horizontal spring. The damping is implemented by the similar way as the dashpots. Under the small displacement condition, the vertical response is decoupled with the horizontal and the rocking responses. To examine the coupling between the horizontal and the rocking response, the natural frequencies are calculated and compared, taking the aspect ratio of h/b and the vertical frequency f_v as the parameters. The equation of motion of rigid-block model is then formulated as Eq.1, and the symbols are listed in Table.1. The nominal frequencies are calculated for reference by Eqs.2-4 without considering the coupling between the rocking and horizontal components.

$$\begin{bmatrix} m & 0 & mh_0 \\ 0 & m & 0 \\ mh_0 & 0 & m_\theta + mh_0^2 \end{bmatrix} \begin{Bmatrix} a_h \\ a_v \\ a_\theta \end{Bmatrix} + \begin{bmatrix} c_h & 0 & 0 \\ 0 & c_v & 0 \\ 0 & 0 & c_\theta \end{bmatrix} \begin{Bmatrix} v_h \\ v_v \\ v_\theta \end{Bmatrix} + \begin{bmatrix} k_h & 0 & 0 \\ 0 & k_v & 0 \\ 0 & 0 & k_\theta \end{bmatrix} \begin{Bmatrix} d_h \\ d_v \\ d_\theta \end{Bmatrix} = \begin{bmatrix} -m & 0 \\ 0 & -m \\ -mh_0 & 0 \end{bmatrix} \begin{Bmatrix} a_{gh} \\ a_{gv} \end{Bmatrix} \quad (1)$$

$$f_{v0} = \frac{1}{2\pi}\sqrt{\frac{k_v}{m}} \quad (2)$$

$$f_{h0} = \frac{1}{2\pi}\sqrt{\frac{k_h}{m}} \quad (3)$$

$$f_{\theta 0} = \frac{1}{2\pi}\sqrt{\frac{k_\theta}{m_\theta + mh_0^2}} = \sqrt{\frac{1}{1+(2h/b)^2}}\, f_{v0} \quad (4)$$

Table1: Symbols used in rigid-block model

Symbol	Physical meaning
b, h, h_0	Width, total height, and height of gravity center of rigid block
C, X	Gravity center, and center of base-isolation layer
m, m_θ	Mass and inertial of rotation around gravity center
k_0, c_0	Distributed vertical stiffness and damping at base isolation layer
k_h, c_h	Horizontal stiffness and damping at base isolation layer
k_v, c_v	Vertical stiffness and damping at base isolation layer
k_θ, c_θ	Rocking stiffness and damping at base isolation layer
d_h, d_v, d_θ	Relative displacements at center of base isolation layer
$d_{hc}, d_{vc}, d_{\theta c}$	Relative displacements at gravity center

a_{gh}, a_{gv}	Horizontal and vertical ground accelerations
$a_{hc}^{total}, a_{vc}^{total}, a_{\theta c}^{total}$	Absolute accelerations at gravity center
f_h, f_v, f_θ	Frequencies of the horizontal, vertical and rocking components
$f_{h0}, f_{v0}, f_{\theta 0}$	Nominal frequencies without considering coupling effect

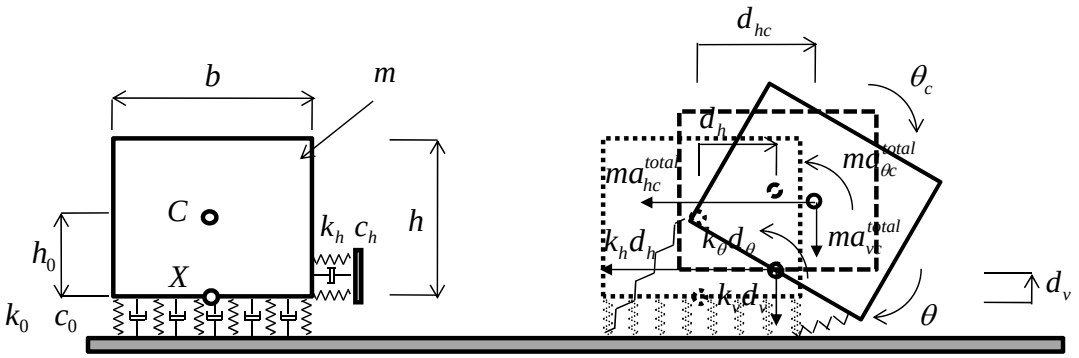

Fig.1 Rigid-block model and its motion along with base isolation layer

The first study took the aspect ratio h/b as the variable, while set the nominal horizontal frequency f_{h0} as a constant, 0.5Hz. Five cases were considered, each adopts different nominal vertical frequency f_{v0} as 0.5, 1.5, 2.5, 3.5, and 4.5Hz. Note that the vertical motion is uncoupled from the rocking motion because small displacement was considered here, so that the actual vertical frequency f_v is identical as the nominal vertical frequency f_{v0}. The eigen values of rigid-block model are calculated and plotted in Fig.2 with respect to the aspect ratio. Several findings are listed as follows:

(1) The rocking frequency is always smaller than the vertical frequency;

(2) If the vertical frequency is as low as the case with $f_v = 0.5$ Hz, the rocking mode is always dominated regardless of the aspect ratio;

(3) For other cases, with the increase of the aspect ratio, the horizontal frequency decreases at first then increases, while the rocking frequency keeps decreasing. It is noteworthy that the horizontal mode and the rocking mode interchange at some special aspect ratio. Taking the case with $f_v = 1.5$ as an example, the horizontal mode jumps to be the third mode at the aspect ratio of about 1.4, while the rocking mode becomes to be the first vibration mode, meaning that for cases with the aspect ratios larger than 1.4, the rocking mode dominates. The frequency jumping points are denoted in Fig.2 as the switching points, which can also be determined by the intersection between the nominal rocking frequency and the nominal horizontal frequency.

Further study examines the influence from the vertical stiffness of base isolation layer. The aspect ratios are selected as 0.5, 1.0, 1.5, 2.0, 2.5, and 3.0. Similar conclusions are obtained as the previous study. The other information obtained from Fig.3 is that the vertical frequency shall not be too small for a given aspect ratio, otherwise the rocking mode dominates. For the case with the aspect ratio of 1.0, the vertical frequency is suggested larger than 1.1Hz approximately.

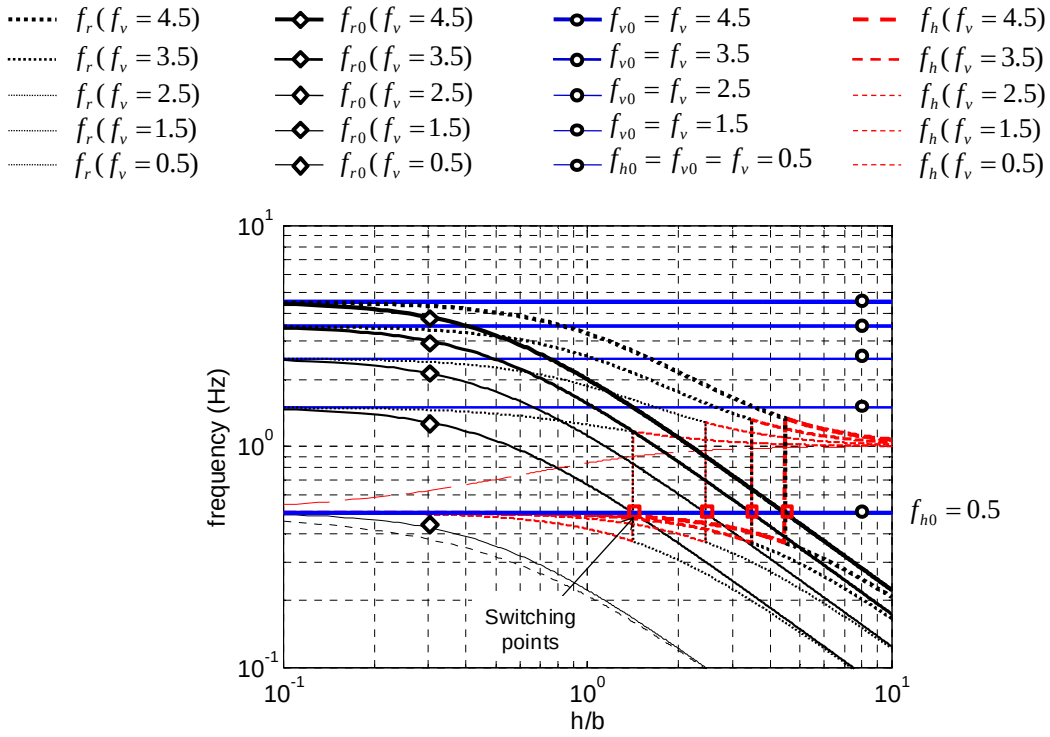

Fig.2 Mode switching curves of rigid-block model with respect to aspect ratio

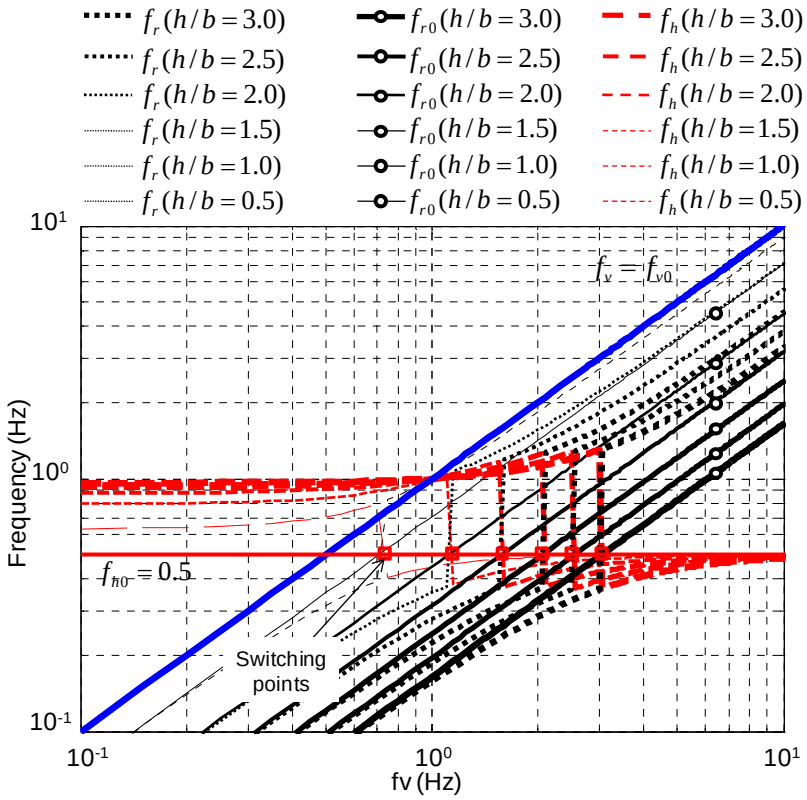

Fig.3 Mode switching curves of rigid-block model with respect to vertical frequency

PARAMETRIC STUDY USING FLEXIBLE MODEL

In this section, a flexible model is developed. Time history analyses using a set of 20 near fault ground motions [4] were conducted to find the influence of damping ratios. The model represents a virtual nuclear power plant. It is simplified as a single-degree-of-freedom model with a mass at the top of a flexible column, as shown in Fig.4. The section of the column is selected to reproduce the horizontal and vertical flexibility of the nuclear power plant. The periods in both horizontal and vertical direction are 0.2s and 0.07s, respectively. The mass of the superstructure is taken as 8.95e7kg, while the bottom slab above the base isolation layer is 3.61e7kg. The effective height was calculated to reproduce the same overturning moment at the bottom slab, which is 27.5m. Three springs were inserted in the base isolation layer to represent the isolators, two in vertical and one in horizontal. The distance between the two vertical springs is decided by the expected rocking stiffness. Similar implementation is also given to the dash pots which represent the damping coefficients in three directions.

Analysis parameters are shown in Table.2 where, the horizontal frequency varies from 0.5 to 0.25 Hz, which are typical frequencies that can be easily achieved by using of steel-laminated rubber bearings. Based on the previous parametric study, the vertical frequency is adopted from 1.0 to 20Hz, where the vertical frequency of 20Hz represents the traditional horizontal base isolation buildings. Previous study [5] indicated that larger damping ratio may result in larger acceleration in the superstructure, so that the damping ratio is selected ranging from 2 to 30% for both directions. The damping ratio of 2% implies no damper is installed while a bigger ratio is necessary to mitigate response of nuclear structures and reactor components.

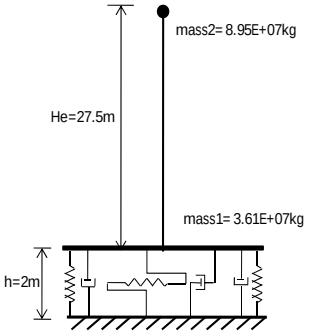

Fig.4 Flexible model with base isolation layer

Table.2 Analysis parameters

Th(s)	1.0	1.5	2.0	2.5	3.0	3.5	4.0
Hh(%)	2.0	5.0	10.0	15.0	20.0	25.0	30.0
Tv(s)	0.05	0.1	0.2	0.25	0.5	1.0	
Hv(%)	2.0	5.0	10.0	15.0	20.0	25.0	30.0

Note:
(1)Th(Hh):Period(damping ratio) in horizontal direction;
(2) Tv(Hv): Period(damping ratio) in vertical direction.

The averaged maximum responses of each model are given in Fig.5 in terms of displacements, velocities and absolute accelerations. It is observed from these figures that:

(1) A system that has a longer period exhibits smaller acceleration and bigger displacement, no matter in horizontal or vertical direction. And damping is able to effectively suppress maximum responses, includes displacement, velocity and acceleration. Without additional damping (damping ratio equals to 2%), the maximum horizontal displacement and vertical displacement are 0.8m and 0.3m, respectively. However, if the damping ratio of 30% is adopted, the values decrease to 0.4 and 0.15m, correspondingly;

(2) Comparatively, the damping is more effective in horizontal than in vertical direction regarding of the displacement. However, it is more effective to reduce the acceleration response in the vertical direction than in horizontal;

(3) The velocity is not sensitive to horizontal period, while vertical velocity becomes bigger when vertical period increases.

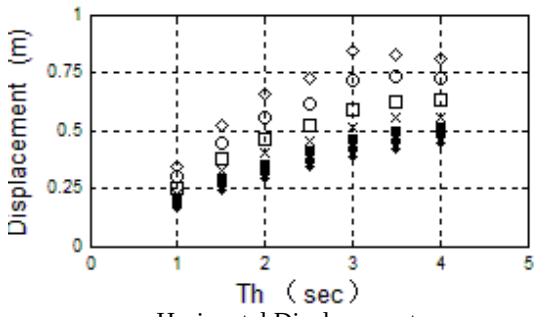

Horizontal Displacement

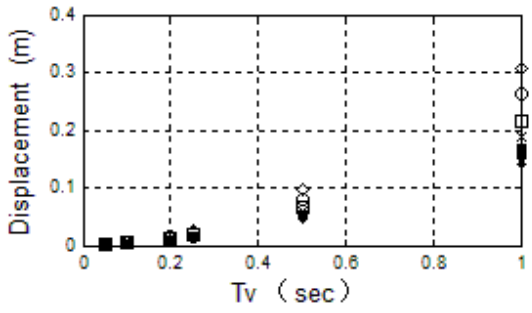

Vertical Displacement

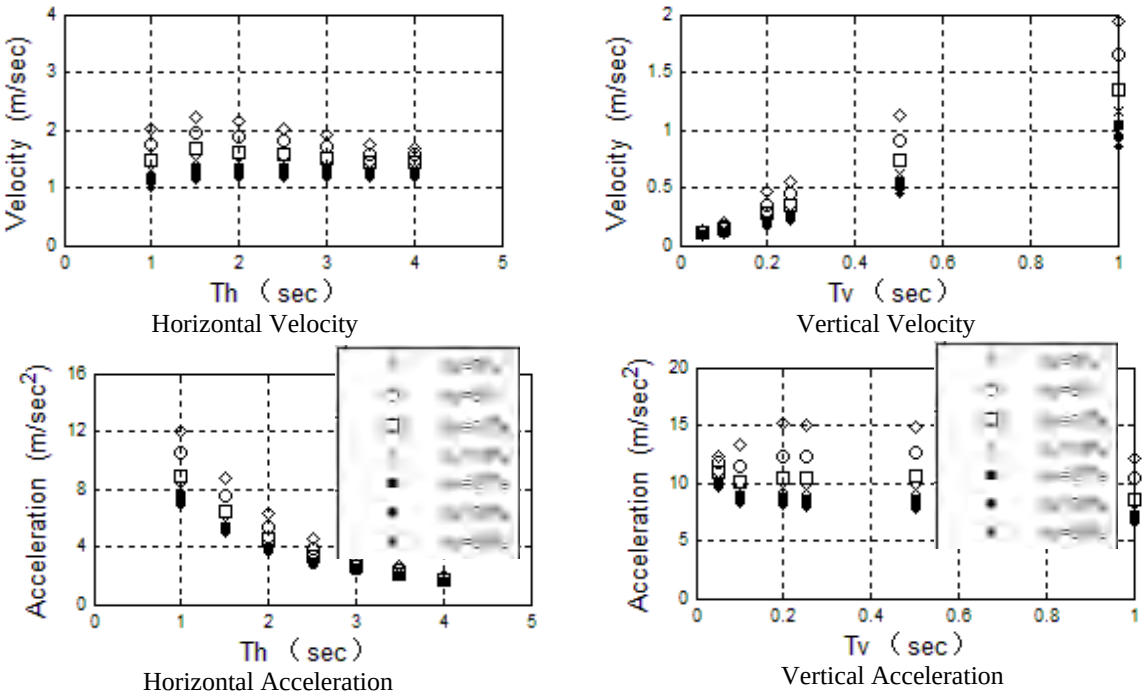

Fig.5 Seismic responses of flexible model

CONCLUSIONS

This preliminary study searches for suitable parameters for the base-isolation design of nuclear power plants. A rigid-block model was used to find the suitable vertical stiffness of the base isolation layer, while a flexible model was employed to examine the damping effect. Major findings are as follows:

(1) To effectively suppress the adverse rocking motion and to reduce the initial deformation under the gravity of the superstructure, the vertical stiffness shall not be too small. Also considering the acceleration reduction effect, the vertical stiffness shall not be too large as well. The suggested value ranges from 1Hz to 5Hz;

(2) To suppress the deformation of the base isolation layer, a large damping ratio is needed. The suitable damping ratio can be selected from Fig.5 for any expected responses. However, the damping ratio shall not be too large. It is better limited within 30%.

ACKNOWLEGEMENT

This project was supported by Central Public-Interest Scientific Institution Basal Research Fund of China (021800210), and National Natural Science Foundation of China (51008287). Any opinions, findings, and conclusion expressed in this paper are those of the authors and do not necessarily reflect the views of the sponsors.

REFERENCES

[1] Malushte, S., and Whittaker, A., “Survey of past base isolation applications in nuclear power plants and challenges to industry/regulatory acceptance”, 18th SMiRT, Beijing, China, K10-7, 2005.

[2] JEAG, Specifications for base isolation design of nuclear power plants, JEAG-4614, 2000.

[3] Martelli, A., Forni, M., Bergamo, G., Bonacina, G., and Cesari, “Proposal for design guidelines for isolated nuclear facilities”, 13th SMiRT, Italy, 1995.

[4] Somerville, P., “Development of ground motion time histories for phase 2 of the FEMA/SAC steel project”, SAC Background Document, Report No. SAC/BD-99-03, 1999.

[5] Politopoulos, I., “A review of adverse effects of damping in seismic isolation”, Earthquake Engineering & Structural Dynamics, 2008, Vol. 37, pp. 447–465.

FRAMEWORK FOR PERFORMANCE-BASED EVALUATION AND DESIGN OF SEISMIC ISOLATION FOR NUCLEAR ENERGY FACILITY STRUCTURES

E. Keldrauk[1], P.F. Peterson[2], B. Stojadinovic[3]
[1]Doctoral Candidate, Dept. of Civil and Env. Eng. Univ. of California, Berkeley, USA
[2]Professor, Dept. of Nuclear Eng. Univ. of California, Berkeley, USA
[3]Professor, Dept. of Civil and Env. Eng. Univ. of California, Berkeley, USA

ABSTRACT

Seismic isolation response modification technology has been used for buildings and non-building structures for more than forty years. Advances in this technology have spurred the use of seismic isolation systems for safety-related nuclear facility structures because of the ability to standardize the design above the isolation plane (i.e. superstructure) and, thus, significantly improve the economy of new facilities while maintaining the required levels of seismic safety and performance. The successful design and licensing of new plants requires a well-defined, risk-informed, performance-based framework for seismic isolation of safety-related nuclear facility structures. The elements of such framework addressing the beyond-design basis earthquake and aircraft impact loads are presented. Basic analyses of the structural response of idealized nuclear power structures to beyond-design basis events enable design recommendations for location, layout, and protective systems.

INTRODUCTION

Seismic isolation is a means of reducing structural accelerations and forces by introducing a laterally flexible layer which decouples the responses of the superstructure and foundation [1]. The subsequent reduction of lateral stiffness results in a lengthening of the fundamental structural period well past the predominant period range of typical seismic activity. **Error! Reference source not found.** illustrates the reduction in spectral accelerations as a result of this so-called “period shift”.

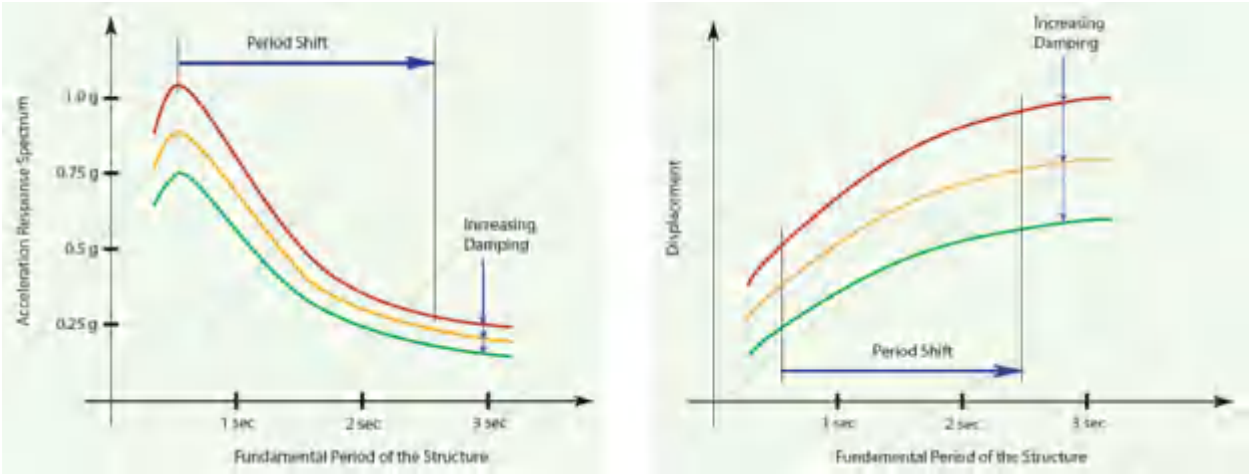

(a) (b)

Fig. 1 The effect of period shift on (a) spectral acceleration response, and (b) displacement response [2]

A seemingly unfortunate corollary of the shift is the increase of induced spectral displacements, however, within the primary mode of the isolated structure, interstory drifts are almost exclusively concentrated in the isolation layer. The isolation system is designed to accept this displacement, thereby minimizing deformation in the superstructure from the fundamental mode. Additionally for elastomeric bearings, the first mode shape closely resembles the force-influence vector due to earthquake excitation, meaning higher modes are "filtered-out" of the response as a result of the principle of modal orthogonality. Thus, seismic isolation works dually by reducing negative spectral effects in the superstructure from the fundamental mode, and additionally reducing the influence of higher-frequency modes on the total response.

Seismic Isolation Types

The practice of seismic isolation in the US is focused on two main types of passive seismic isolators. The first type is an elastomeric bearing, typically comprised of alternating steel and natural rubber laminates which assure the rubber deforms in shear and remains stable under compressive loading. The rubber supplies the large deformation capacity and low shear stiffness which is a function of bonded rubber area, height, and shear modulus. Various types of elastomeric bearings are differentiated by their methods of energy dissipation. Low-damping rubber (LDR) bearings use natural rubber with very little inherent damping and, therefore, systems utilizing these bearings often employ supplemental dampers. High-damping rubber (HDR) bearings use rubber infused with fillers (i.e. carbon black, oils, and resins) which absorb energy during extension of molecular chains. Because the response of HDR bearings is highly non-linear and degrades under repeated loading, it is not preferred for nuclear application. Lead rubber (LR) bearings use one or more embedded vertical lead plugs which absorb energy by yielding and may considerably soften under repeated cyclic loading.

The second type of seismic isolators are sliding bearings, which limit the force transmitted to the superstructure by introducing one or more low-friction interfaces for sliding. The first widely-used sliding isolation bearings were friction pendulum (FP) bearings. These bearings have Teflon-coated sliding surfaces which are concave to provide restoring action after deformation. It can be shown that the isolated period of these bearings depends only on these radii of curvature. Energy dissipation is determined by the friction coefficient of the surfaces, which defines the width of the hysteretic loop upon load reversal. By placing smaller sliding "disks" between the outer concaves, multiple pendulum mechanisms can form which enable the engineer to design a bearing with optimal stiffness and damping properties at various levels of displacement. Thus the resulting triple pendulum (TP) bearing is considered a more robust design, capable of a stiff response to low amplitude wind and seismic excitation, flexible response to moderate seismicity, and stiffening under high-amplitude excitation to dissipate energy and limit maximum displacements.

Existing Seismically-Isolated Nuclear Energy Facilities and Codes

Given the high level of safety and reliability required of nuclear power plant structures, seismic isolation has been considered since the late 1970's [3]. As a result of intense research and engineering work in France, there are now six seismically isolated PWR units: Four at the Cruas-Meysse site in France and two at the Koeberg site in South Africa [4]. All of these plants use large neoprene pads which have since been deemed improper for nuclear application in the US [5]. In Japan, a number of industry and regulatory research and development programs [6] resulted not only in development and proof-testing of new seismic isolator units, but also in regulatory documents [7][8].

DYNAMIC ANALYSIS

To ascertain the approximate dynamic response of nuclear power plants to beyond-design basis lateral excitation, computer simulations were undertaken. Focusing on the displacement and acceleration response of the structure will assist in developing design recommendations and illuminating potential design issues which require further research.

Structural Model

Separate structural models are used for the seismic and impact analyses. In each case, all analyses are unidirectional, with no coupled lateral bidirectionality or vertical component considered. The seismic model has a single-degree-of-freedom elastic superstructure ("lollipop") with a fixed-based period of 0.3 seconds. This superstructure is mounted atop 3 separate systems: a rigid system representing the non-isolated case, an LDR-like, linear-elastic isolation system with an isolated period of 3 seconds, and an LRB-like, bilinear system with the same isolated period and a pre-yield to post-yield stiffness ratio of 10. For each ground motion, the latter two isolated responses are compared to the fixed-base case.

The impacted superstructure model is a three-story structure with shear columns (floors idealized as rigid) used as part of a parametric analysis comparing nine different structures with varying isolated periods (1.35, 2.00, and 2.99 seconds) and masses (20,000 metric tons [44,000 kips], 50,000 metric tons [110,000 kips], and 100,000 metric tons [220,000 kips]). Although impact is expected to impart inelastic deformations, the superstructure is modeled as linear-elastic and acceleration levels are used to determine if inelasticity is expected. The isolators are assumed to be linear-elastic, with 10% supplemental damping.

Seismic Excitation Records and Impact Forces Used

The groundmotion records chosen were created for the SAC project at a hazard level of 2% in 50 years ($4x10^{-4}$ annual) probability of exceedence [9]. Although this hazard level is below the design level for nuclear structures, they are adequate for displaying the beneficial effects of seismic isolation. The 60 ground motions are comprised of three groups of 10 two-component records representing three separate US sites: Boston, Seattle, and Los Angeles. These three sites represent a variety of tectonic regions with associated issues. The East Coast site has high-frequency motions, whereas the West Coast motions represent higher amplitude seismicity and poorer soil conditions.

The aircraft loading time history was formulated through scaling of the original Riera [10] time history in both time and magnitude for the Boeing 747-400 and 737-900. The large increase in peak forces are a result of the longer, heavier aircrafts that exist today, as well as the increased speed that results from not only the newer planes, but also from considering malicious impacts above cruising velocity. These time histories are applied at the center of the top floor of the isolated model structure, orthogonal to the building face.

Results

The results demonstrate the reduction in acceleration response compared to the fixed-based structure. The linear isolator model showed median peak acceleration reductions of 97%, 92%, and 80% in comparison to the non-isolated structure in response to the Boston, Seattle, and Los Angeles ground motions, respectively, and reductions of 90%, 80%, and 56% from the PGA [11]. The bilinear isolator model had similar median peak acceleration reductions of 93%, 90%, and 75% compared to the fixed base structure as well as 84%, 73% and 41% compared to the PGA for the respective ground motion groups. The peak deformations were also shown to have much less scatter than the peak accelerations suggesting the design of the isolation gap may depend almost solely on the period.

The impact analysis showed that peak structural accelerations were large for most cases [11]. Median peak elastic accelerations for 747 (737) collisions were found to be 7.6g (2.1g) for the smallest reactor, 3.0g (0.85g) for the middle-weight reactor, and 1.5g (0.43g) for the heaviest reactor. The analysis proved that period has a very small effect of less than 10% on the acceleration response of impacted structures, and that aircraft impacts for smaller plants are almost impossible to accommodate by the reactor superstructure. Thus, extensive inelasticity is expected in the superstructure as a result of aircraft impact.

The deformation of the base isolation system when an aircraft impacts a seismically isolated nuclear facility structures depends on the ratio of the masses of the aircraft and the balance of the facility above the isolation layer. This is because the duration of the impact (about 0.3 sec) and the time when the structure attains peak acceleration is significantly shorter than the isolated period of the structure (about 2.0 sec), making the impulse momentum balance the primary determinant of peak post-impact isolation system displacement. Therefore, given that the mass of the model aircraft is constant, the displacement of the isolation system will be inversely proportional to the weight of the

plant above isolation layer. In contrast, deformation of the isolation system under seismic loading depends on the fundamental period of the isolated system, making it, in general, directly proportional to the weight of the balance of the plant above the isolation layer. Therefore, deformation of the seismic isolation layer of a relatively light plant may be controlled by aircraft impact, while that of a relatively heavy plant is likely to be controlled by seismic demands. This situation is further complicated by the different seismicity in the West and the Central and Eastern US, and different estimates of the magnitude of beyond-design basis seismic demand.

ISOLATION OF NEW NUCLEAR ENERGY FACILITIES

Initial preparations for the new Generation III nuclear power plants in the US have already started. Consequently, commercial development of the next generation of nuclear power structures and reactors, based on Small Modular Reactor technologies, in North America is imminent. There are strong indications that nuclear power plant vendors are considering seismic isolation in their designs to maintain and improve safety. Isolation technology is capable of offering many design and safety benefits enumerated below, as well as some design challenges which must be considered and solved prior to full implementation into a functioning nuclear energy facility.

Benefits

The motivation for implementing seismic isolation is, first and foremost, to improve the safety and reliability of nuclear power plants. A properly engineered seismically-isolated superstructure will, with high confidence, be decoupled from the earthquake-induced motion of its foundation and experience significantly smaller inertial forces than its non-isolated counterpart. The reduced forces make it easier to design the superstructure to remain essentially elastic: this, in turn, ensures that the deformations of the structure will remain small and in the acceptable range, improving its seismic performance and protecting the internal systems and components. Taken together, reduction in inertial forces and deformations experienced by the superstructure achieved by the seismic isolation system, and the repeatable performance of seismic isolator units, can substantially reduce the contribution of seismic hazard to the total probability of large radiation release. This directly increases the safety margins of seismically isolated nuclear facilities. Seismic isolation can be custom-engineered to specific nuclear facility site characteristics, both with respect to site seismic hazard exposure and to local soil conditions and configurations. Engineering the substructure and the seismic isolation system provides an opportunity to engineer the isolated superstructure for essentially the same level of seismic demand regardless of the site characteristics. This, in turn, facilitates standardization of nuclear facility design and makes the seismic behavior of the isolated superstructure more predictable, leading to increased reliability of isolated nuclear facilities. Equally important, standardization facilitates regulatory review and design certification of seismically isolated nuclear facilities.

While seismic isolation adds a structural system between the substructure and superstructure, the added cost and complexity is very likely to be compensated for by the savings realized through the increase of safety margins despite the smaller strength, size and complexity of the superstructure. However, a significantly larger economy can be derived from simplified, standardized designs made to suite modular construction methodology. Today, modular construction is being implemented at the level of components and systems: the use of seismic isolation enables expansion of the modular concept to the entire isolated superstructure and provides the all-important cost driver for use of seismic isolation in new nuclear power plants.

Challenges

The use of seismic isolation systems brings about a number of challenges. Seismic hazard analysis for seismically isolated structures must consider the long fundamental vibration period of such structures, typically 2 seconds or longer. Thus, ground motion records must be filtered differently to provide reliable data in this long-period (low-frequency) range, ground motion attenuation relations must be developed accordingly, and design spectra and ground motion selection procedures must be modified. Maximum horizontal deformation of the isolator units occurs under combined effects of the horizontal components of ground motion and the relative eccentricity of the isolated superstructure with respect to the isolation system. The effect of the vertical motion of the isolated

superstructure on the isolator units must be accounted for, regardless of the cause: overturning moment in the superstructure, ground motion in the vertical direction, or the rotational (rolling) components of the ground motions. Therefore, ground motion selection and scaling must account for all components of ground motion. Modeling of the response of seismically isolated structures must directly account for the three-dimensional, non-linear behavior of seismic isolators under both design-basis and beyond-design-basis earthquake ground motions. This is particularly challenging for the traditional frequency-domain methods used to evaluate the effects of soil-structure interaction on the structural demands and floor spectra. To overcome this challenge, it is imperative to develop effective time-domain non-linear modeling and analysis methods to account for soil-structure interaction between the foundation, the seismic isolation system, and the isolated superstructure, as well as to develop validated and verified models of the isolator units.

Non-redundancy of the seismic isolation system is a profound challenge. The seismic isolation system comprises a large number of essentially identical seismic isolation units that act in parallel. The performance of the seismic isolation system will not be significantly affected by failure of a one or even a few seismic isolation units or components. However, the seismic isolation layer connects the isolated superstructure to the substructure forming a series system. As such, the seismic isolation layer, as a whole, is not redundant. Therefore, engineering measures must be taken to prevent simultaneous or cascading failure of many seismic isolation units due to exceeding their deformation or force capacities. Such engineering measures include fail-safe system such as deformation limiters achieved by physical (bumpers, stoppers, walls) or mechanical (increasing isolator unit stiffness, slider breaks) means, and additional passive or semi-active dampers. These measures, when engaged, may result in impact and/or gradual increase in forces transmitted to the isolated superstructure. The engineering objective is to provide sufficient space for the isolation system to move without obstacles and for graceful degradation of the seismic isolation layer in extreme situations: a cliff-edge sudden seizure of its isolation function must be avoided.

This engineering objective is particularly challenging when another important beyond-design basis load is considered: aircraft impact. The U.S. Nuclear Regulatory Commission issued a final rule that requires new reactor applicants to assess the ability of their reactor designs to avoid or mitigate the effects of a large commercial aircraft impact. The specific aircraft attributes the USNRC requires applicants to consider are considered to be “safeguarded” information and are restricted from public disclosure. This was the motivation behind the dynamic impact analyses previously described. The results of these simulations showed high accelerations for all 747 impacts as well as 737 impacts with lighter reactors. As such, the recommendation is to shield the isolated reactor structure from the possibility of aircraft collision through the use of protective “barrier” walls, undergrounding, or some combination of the two. Each of these has inherent cost and design considerations which must be handled.

PERFORMANCED-BASED EVALUATION AND DESIGN FRAMEWORK

A framework, defined as a consistent set of requirements and guidelines for design and regulatory approval, is needed to successfully design seismically isolated nuclear power plant structures. The framework proposed in this paper builds on the design framework for conventional seismically isolated structures defined in Chapter 17 of ASCE 7-10, on the design objectives for nuclear facility structures contained in ASCE 43-05 [12] and on design provisions proposed for the upcoming ASCE 4-11 standard.

The proposed framework is performance-based. It comprises the following phases: 1) setting the performance objectives for the seismic isolation system; 2) preliminary design of the seismic isolation system for seismic and aircraft impact loads; 3) design, manufacturing and prototype testing of the seismic isolation units; 4) detailed modeling of the seismically isolated structure; 5) evaluation of the design-basis and beyond-design-basis performance under seismic and aircraft impact loads; 6) specification of quality acceptance and quality control for manufacturing and installation of seismic isolator units; and 7) specification of in-service monitoring of the seismic isolation system.

Performance Objectives for a Seismically Isolated Nuclear Power Plant Structure

ASCE 43-05 [12] sets the performance objective for seismically isolated nuclear power plants as Seismic Design Category 5 with Limit State 4 (SDC5-4). These designate the structure as nuclear facility with the requirement that it remain operational (i.e. no significant damage) under the design loading, the strictest case. It also defines the Design Basis Earthquake (DBE) using a Probabilistic Seismic Hazard Assessment (PSHA) to derive a Uniform (or Equal) Hazard Response Spectrum (UHRS) for the site and modifies it further using a Design Factor. The Design Factor is calibrated to achieve a mean annual seismic core damage frequency of 10^{-6} considering the failure probabilities inherent to current design codes and the design goal proposed in ASCE 43-05 [13]. The design goal for structural components not explicitly covered in ASCE 43- 05 is to reasonably achieve both of the following design objectives (Section 2.0 of ASCE 43-05):

1. Less than 1% probability of unacceptable performance for the DBE ground motion.
2. Less than 10% probability of unacceptable performance for 150% of the DBE ground motion.

Acceptable performance of the seismically isolated structure is defined through acceptable behavior of its components. The foundation and the seismically isolated superstructure are expected to remain in Limit State D, i.e. "essentially elastic", even if some of the isolator units fail. Additionally, the structures, systems and components are expected to remain operational in case of impact generated by failure of the seismic isolation system. The seismic isolation system is expected to also develop no significant damage and remain in operational condition. Unacceptable performance of the seismic isolator units under seismic and aircraft impact loads is defined as:

1. Permanent damage to the seismic isolator unit, such as tearing, buckling or disassembly, that prevents it from functioning as intended;
2. Exceedance of the design displacement limit of the seismic isolator unit.

It is important to note that ASCE 43-05 is calibrated to the mean annual frequency. US NRC requires a design to achieve high confidence of low probability of failure (HCLPF).

Preliminary Design of the Isolation System

A preliminary assessment of seismically isolated nuclear structures for design and beyond-design basis ground motions at three different sites has recently been conducted by Huang, Whittaker, Kennedy and Mayes [14] The main outcome of this study is a triplet of performance statements aimed at achieving the two ASCE 43-05 probability-based design goals. Namely:

1. Individual isolators shall suffer no damage in DBE shaking.
2. The probability of the isolated nuclear structure impacting the surrounding structure (moat) for 100% (150%) DBE shaking is 1% (10%) or less.
3. Individual isolators shall sustain gravity and earthquake-induced axial loads at 90th percentile lateral displacements consistent with 150% DBE shaking.

These performance statements, derived for seismic loading, are extended to aircraft impact loading by considering it as beyond-design basis event in the same category as the 150% DBE event. Preliminary design of the seismic isolator units can be conducted using the following procedure. A target isolation system horizontal fundamental vibration period can be at least 4 times longer than the fundamental vibration period of the isolated superstructure, and outside any regions where UHRS has an unusual amplification. Typical values are between 2 and 4 seconds. A target characteristic horizontal strength of the isolation system may be between 3% and 9% of the weight of the isolated superstructure. These values are based on the ranges of parameters considered in Huang, et. al [14]. A target effective damping may be between 15% and 20% of critical damping [1].

Performance statements 1 and 2 can be utilized for preliminary assessment of the design displacement of the seismic isolator unit. To do this, a stick model representing the principal mass and stiffness characteristics of the isolated superstructure should be combined with a model of the seismic isolator unit capable of representing the force-deformation response of the unit in two horizontal directions. Best-estimate values for mechanical properties of the units should be used at this stage. Huang, et. al [14] found that the seismic displacement with a 10% exceedance probability in 150% DBE shaking governs the design. Using their Approach I, select or generate 11 seed three-component ground motions to appropriately represent the site conditions and the controlling hazard, spectrally

match these motions to the DBE spectra, perform 11 non-linear response history analyses, compute the vector-sum maximum displacement of the seismic isolator units in each analysis and then find the median value of these maxima. Multiply this median value by 3 to determine the seismic design displacement of the isolator unit. The aircraft impact displacement can be computed using the same computer model of the facility used for preliminary seismic analysis as well as the scaled aircraft impact models [10][11] and the USNRC aircraft impact model. The resultant aircraft impact displacements are expected to represent the mean and HCLPF displacements, respectively. The mean aircraft impact and the mean seismic displacements of the isolation system should be compared to determine the governing displacement for the next design phase. A procedure suggested in [1] or in [15] can be used to compute the remaining properties of the seismic isolator unit and to design the unit. Using a procedure suggested in [1], a manufacturer should be selected and a proof-test isolator unit should be manufactured. The proof-test should be conducted using a test procedure suggested in [15].

Modeling and Evaluation

Design of the seismic isolation system may also include design of supplemental dampers intended to further reduce design displacements, vertical restraint or isolation devices, and fail-safe devices intended to reduce or eliminate adverse consequence of superstructure impact on the surrounding soil or structure. A detailed model of the seismically isolated nuclear power plant can then be made. This model should be used to evaluate the response of the nuclear power plant structure under design and beyond-design basis earthquake shaking. The limit states associated with the seismic isolation system include (but are not limited to): 1) failure of isolator units due to exceedance of design displacement; 2) failure due to tearing or instability such as buckling, rollout or disassembly; 3) impact of the isolated superstructure against the isolation mote; and 4) vertical motion and uplift due to ground motion, and overturning or rocking due to aircraft impact.

The challenge posed by seismic isolation response modification technology is that the seismic isolator units are expected, and relied upon in design, to behave in a non-linear manner during design-basis and beyond-design-basis earthquake shaking. Even though the isolated superstructure is expected to remain essentially elastic (and can be modeled assuming it remains within its elastic response range), and the soil and the foundation may behave in a manner such that they can be modeled using equivalent elastic properties, the seismic isolator units must be modeled as non-linear using at least a bi-linear model capable of accurately computing the isolator force-deformation response under bi-directional horizontal excitation. Even such relatively simple non-linear models cannot be linearized with sufficient accuracy to represent the response of the seismically isolated structure over the range of excitations of interest. Yet, it is likely that more sophisticated models of seismic isolators and other devices, such as dampers and displacement restrainers if used in design, will be needed to demonstrate satisfactory performance of the seismically isolated structure with the high confidence required by licensing regulators.

Development of verified and validated tools for time-domain non-linear analysis of seismically isolated structures and soil is on the critical path for successful design and licensing of new seismically isolated nuclear power plants. Such tools should include sophisticated 3-directional interaction models of seismic isolators, models of contact, uplift and impact, and non-linear models of soil. Ideally, such models should enable propagation of seismic wave excitation from the source (or rock layer), eliminating the need for additional software. Finally, these tools should enable non-linear modeling of the response of the isolated superstructure capable of capturing its response in higher vibration modes, propagation of horizontal and vertical excitation through the isolation system and into the structure, and the corresponding floor response spectra to enable coupling to equipment fragility evaluation. The time scales of the response quantities of interest span approximately three orders of magnitude (0.1Hz to 10 Hz). The dimensions of the model elements also span roughly four orders of magnitude (0.1m to 100m). Even without non-linear behavior, the time and length scales present a significant challenge for development and implementation of efficient and accurate solution algorithms. Nevertheless, some of solid finite element software package used by industry today can handle such complex problems. But, they need to be verified and validated for seismically isolated structures, and sped-up, simplified and hardened for use in design practice.

CONCLUSIONS

Seismic isolation response modification technology is mature and ready for application in safety critical nuclear power plants. The benefits of using seismic isolation (improved safety, reliability and economy) clearly outweigh the challenges of this technology. Three major issues are on the critical path for adoption of seismic isolation in nuclear engineering practice and regulation. The first is the development of the regulatory guidelines to define the way seismically isolated nuclear power plant license applications are going to be evaluated. Work in this direction is ongoing. The second is the development of practical non-linear seismic and aircraft impact soil-structure interaction response analysis of the seismically isolated nuclear power plants. Research in this direction is starting. Third is the work by vendors to develop seismically isolated nuclear power plant designs and the willingness of the utilities to support the licensing process of the first such license application. The risk for such first movers is significant, but taking this risk on is essential.

REFERENCES

[1] Naeim, F., and Kelly, J. M. (1999). ***Design of seismic isolated structures: from theory to practice***, John Wiley, NY.

[2] Seismic Isolation for Buildings and Bridges. Sparks, NE: Dynamic Isolation Systems (DIS) Inc., 2007.

[3] Renault, J., Jolivet, F., Plichon, C., & Bordet, R. (1976) Patent 05/697632, "***Device for protecting a structure against the effects of high horizontal dynamic stresses"***

[4] Plichon, C. (1980). Protection of nuclear power plants against seism. ***Nuclear Technology, 49***, 295-306.

[5] Malushte, S. and Whittaker A. (2005). "Survey of Past Base Isolation Applications in Nuclear Power Plants and Challenges to Industry/Regulatory Acceptance." Transitions of 18th International Conference on Structural Mechanics in Reactor Technology (SMiRT 18), K-10-7.

[6] Kato, A., Moro, S., Morishita, M., Fujita, T., and Midorikawa S. (2003) "A Development program of 3-Dimensional Seismic Isolation for Advanced Reactor Systems in Japan", Transitions of 17th International Conference on Structural Mechanics in Reactor Technology (SMiRT 17), K09-1.

[7] Japan Electric Association (2000). "Technical Guidelines on Seismic Base Isolation Systems for Structural Safety and Design of Nuclear Power Plants", JEAG-4614, Special Subcommittee on Nuclear Power.

[8] Japan Nuclear Energy Safety Organization (JNES). (2010). "Regulatory Guidelines for Reviewing Seismic Isolation Structures", JNES-SS-1001, Seismic Safety Division.

[9] Woodward-Clyde Federal Services (SAC project). "Suites of Earthquake Ground Motions for Analysis of Steel Moment Frame Structures." National Information Service for Earthquake Engineering. 1997. University of California, Berkeley. 8 March, 2009.

[10] Riera, Jorge D. "On the Stress Analysis of Structures Subjected to Aircraft Impact Forces." Nuclear Engineering and Design (1968): 415 – 426.

[11] Blandford, E., Keldrauk, E., Laufer, M., Mieler, M., Wei, J., Stojadinovic, B. and Peterson, P. F, "Advanced Seismic Base Isolation Methods For Modular Reactors", Technical report UCBTH-09-004, Dept. of Civil and Env. Engineering and Dept. of Nuclear Engineering, UC Berkeley, Berkeley, CA, USA.

[12] American Society of Civil Engineers (ASCE). (2005). "Seismic design criteria for structures, systems, and components in nuclear facilities." ***ASCE/SEI 43-05***, ASCE, Reston, VA.

[13] Kennedy, R., (2007). "Performance-Goal Based (Risk Informed) Approach for Establishing the SSE Site Specific Response Spectrum for Future Nuclear Power Plants', Transitions of 19th International Conference on Structural Mechanics in Reactor Technology (SMiRT 19), Jaeger lecture.

[14] Huang, Y.-N., Whittaker, A. S., Kennedy, R. P. and Mayes, R. L. (2009). "Assessment of base-isolated nuclear structures for design- and beyond-design basis earthquake shaking." ***MCEER-09-0008***, Multidisciplinary Center for Earthquake Engineering Research, SUNY Buffalo, Buffalo, NY.

[15] Buckle, I., Constantinou, M., Dicleli, M. and Ghasemi, H. (2006), "Seismic Isolation of Highway Bridges", Technical Report MCEER-06-SP07, University at Buffalo, The State University of New York.

SEISMIC ISOLATION OF GEN IV LEAD-COOLED REACTORS

S. De Grandis[1], M. Forni[2], D. De Bruyn[3], S. Cardini[4]
[1]SINTEC S.r.l., Bologna, Italy
[2] ENEA Seismic Engineering Technical Unit, Bologna, Italy
[3] SCK•CEN, Mol, Belgium
[4] Ansaldo Nucleare S.p.A, Genoa, Italy
E-mail of corresponding author: silvia.degrandis@sintec-nt.it

ABSTRACT

Nowadays, seismic isolation is widely used to protect not only civil buildings (over 10,000 all over the world [1]) but also bridges, viaducts and industrial plants, and is considered the most promising technology to protect nuclear reactors from violent earthquakes. In spite of this, only two nuclear plants are currently provided with base isolation: 4 PWRs at Cruas (France), and 2 PWRs at Koeberg (South Africa). In addition, the Jules Horowitz Reactor, now under construction at Cadarache (France), must be cited.

The extremely limited number of existing isolated nuclear reactors is probably due to the relatively low seismic input assumed as design for the Generation II reactors, and also because most of them were water reactors, which are characterized by quite stiff structures and rigid components. As a matter of fact, among the new designs of water reactors, only IRIS (International Reactor Innovative and Secure) and 4S (Super Safe, Small and Simple) are provided with base isolation. On the contrary, among the fast reactors, most of the recent designs already include seismic isolation: ALMR (Advanced Liquid Metal Reactor), S-PRISM (Power Reactor Innovative Small Module), DFBR (Demonstration Fast Breeder Reactor), DFBR (Demonstration Fast Breeder Reactor), STAR-LM (Secure Transportable Autonomous Reactor-Liquid Metal) and EFR (European Fast Breeder Reactor). Unfortunately, no application of these reactors has been done, yet, and there is a dramatic lack of information and experimental results about the behavior of large isolators under severe dynamic conditions.

As far as lead cooled reactors is concerned, the most recent designs do not include seismic isolation (with the exception of the “small” STAR-LM). However, such reactors, in addition to structural problems similar to those of the abovementioned sodium reactors, have to deal with the high density of the coolant, which induces sloshing effects and transmits higher inertial forces to the tank and pipelines.

The paper, after a short presentation of the world state-of-the-art of seismically isolated nuclear reactors (included new designs), focuses on the main problems encountered in the application of this technology to lead reactors, such as the need of manufacturing and testing very large isolators and to design interface components, and the lack of standards specifically addressed to isolated nuclear reactors.

INTRODUCTION

On September 21, 2007 the Sustainable Nuclear Energy Technology Platform (SNE-TP) was launched in Brussels, through which the European research nuclear fission community joined its efforts to issue a Strategic Research Agenda (SRA) for achieving sustainable nuclear fission energy. The main objective of the SRA is to provide decision makers as well as the scientific community with clearly identified technological road-maps for the development of fission technologies, being the nuclear energy considered as one of Europe’s main low carbon energy technologies.

The SRA of SNETP has been based, substantially, on the following ideas:

- Generation II and III Light Water Reactors (LWR) nuclear reactors contribute already very positively to the objectives in the EU's energy policy. Existing reactors have an outstanding safety track record and they offer inexpensive base-load electricity; uranium supply is secure. In addition, nuclear power plants emit very low lifecycle greenhouse gases.
- Innovative Generation IV fast reactor systems with a closed fuel cycle will offer greatly improved sustainability. They will produce 50 to 100 times more electricity than current reactors from the same amount of uranium enabling natural resources to last thousands of years. In addition, with advanced fuel cycles and the partitioning and transmutation (i.e. recycling) of minor actinides and long-lived fission products, they will produce significantly less waste for disposal (in terms of volume, thermal load and radio-active inventory) thereby further reducing environmental impacts.

- Other Generation IV reactors operating at very high temperature will provide low carbon process heat for the mass production of hydrogen and other industrial processes, including desalination, thereby addressing major challenges for the future, i.e. replacing oil or extending its exploitation and supplying arid regions with drinking water.

Looking at the area of the development of fast neutron systems, European stakeholders have chosen to concentrate their efforts along two directions:

- Sodium-cooled fast neutron reactor (SFR) is considered as a known and proven technology but for which innovations are necessary to fulfill the criteria of Generation IV reactors.
- In parallel, a coolant technology alternative to sodium, either lead or gas, will be selected between 2010 and 2012 to offer decision makers a choice of reactor systems and to limit technological risks. In this time-frame, the two systems will be compared in terms of potential, R&D needs and developmental timeline.

It is clear, therefore, that great efforts have to be put in identifying and addressing all the topics of major relevance for the demonstration of the abovementioned fast spectrum technologies in a short timeframe. In this context, a topic of particular relevance is certainly the one of safety and mitigation of risks. In general, in fact, it has to be noticed that to be sustainable energy production must avoid endangering the well-being of future generations, not only by reducing the use of natural resources but also by minimizing detrimental effects on public health and environment. This means that electricity production must achieve high levels of safety, both against internal and external damage events, and limit harmful emissions over the full lifecycle of the plant (cradle to grave).

In particular, for Generation IV reactors maintaining and enhancing the safe and reliable operation is an essential priority in the development. Generation IV reactors have to be highly secure and designed to withstand failure-driving events: their many protective features considerably reduce the impact of external or internal threats through the redundancy, diversity, and independence of the safety systems. This goal, strongly outlined in the Generation IV International Forum (GIF) roadmap, points out the need to increase public confidence in the security of nuclear energy facilities.

In this light, a huge effort have been dedicated, ever, to continuously increase the level of safety of Nuclear Power Plants against internally initiated events, reducing the associated core damage frequencies. This has, therefore, forced the nuclear engineering community to concentrate a significant research effort also on the evaluation and mitigation of risks associated to external events such as natural hazards (earthquakes, hurricanes, tornadoes, flooding, tsunamis and so forth) as well as other external risks, such as terroristic attack (i.e. aircraft or missile impacts). Note that there have been recently a large number of external events that have severely challenged structures and operations of nuclear plants: flooding in France and Finland, several big earthquakes (one of them struck Kashiwazaki-Kariwa, the largest nuclear power plant of the world), the 2004 Indian Ocean tsunami (which affected the Tamil Nadu reactor in India) and the more recent catastrophe in Japan, which severely damaged the Fukushima plant.

For the Lead Fast Reactor (LFR) and Accelerator Driven Systems (ADS) design, important R&D technology gaps are identified in the SNE-TP SRA as well as in the Generation IV Roadmap, in system design at level of seismic protection, in particular with respect to selected components as, e.g. core internals support and refueling machine design. The structural support of the reactor vessel, for example, containing dense Lead or Lead-Bismuth Eutectic (LBE) coolant, in fact, will require design development in seismic isolation approaches and sloshing suppression.

SEISMIC RISK IN LEAD-COOLED SYSTEMS

Safety concerns related to seismic events in lead-cooled systems

Main safety concerns related to immediate consequence of a seismic event in a heavy liquid metal reactor, therefore, are related to:

1. structural failures due to the dynamic loading,
2. core voiding by gas entrapped into primary coolant system,
3. functional failures of equipment due to coolant spill-out.

1) Dynamic loading on the elements of primary system in case of intensive seismic event can cause early core damage due to the following phenomena:

- *Loss of coolant from the primary system*. In most of contemporary pool-type designs loss of primary coolant is considered as very low probability because there is no piping below the coolant level and integrity of the vessel is considered as highly reliable. However, seismic events which can cause loss or leaks of primary coolant have to be considered seriously due to their consequences, even though the associated probability is very low.

- *Flow blockage in a fuel assembly*. Most likely outcome of the coolant flow blockage in a fuel assembly is overheating and eventual disintegration of the fuel. In a worst case scenario degradation of one fuel assembly may lead to propagation of core damage to the neighboring assemblies. Thus quantification of dynamic loading which may lead to a damage of an assembly in a seismic event is important element of safety assessment.
- *Steam generator tube rupture (in LFR pool design)*. Steam generator tube is highly loaded thin element of the system. There is a number of threats which originates from steam generator tube rupture (SGTR) or leakage (SGTL). In a nutshell, a SGTR event generates a pressure shock wave and discharges steam/water into a molten lead environment, bringing the fluid (lead) into motion and creating a potentially energetic situation that imposes a dynamic loading on the surrounding structure. There is also gradual pressurization of the vessel after SGTR due to inflow of the steam which also requires design of appropriate protection measures for isolation of ruptured tube and safe depressurization of the vessel.

2) Core voiding is one of the major threats which can lead to rapid reactivity insertion and consequent core disruptive accident in Lead cooled Fast Reactors. In compact pool designs the flow path to the core inlet is, in fact, rather short. Gas bubbles can be dragged down by the coolant flow to the inlet of the core and cause core voiding and transient overpower (TOP) accident. Gas bubbles can originate from:

- *sloshing* and violent breakup of coolant free surface,
- s*team leaking* from a ruptured steam generator tube (in a LFR pool design).

3) There are also risks related to malfunction of different elements of the primary system due to spill-out of the coolant during the seismic excitation. These threats are design specific and can affect such systems as gas-dam thermal insulators.

Considering the abovementioned critical risks related to earthquake events, then, seismic isolation represents a highly attractive strategy. For example, for the Lead-cooled fast reactor concepts, seismic isolation is explicitly regarded as a viability issue, as from the SNE-TP SRA.

Seismic isolation consists in the insertion, between the ground and the base of the structure, of suitable devices, called seismic isolators, which are very stiff in the vertical direction, to carry the dead load, and flexible in the horizontal ones, to allow lateral movements. In addition, seismic isolators usually dissipate a considerable amount of energy and provide a restoring force to limit the displacement during earthquake and the final off-set. Thus, the isolated structure assumes a quite low natural frequency (in a range where, generally, earthquakes have low input energy) and behaves like a rigid body above the isolation systems: accelerations and inertial forces, and then strains and stresses, are dramatically reduced and are almost the same at each level of the plant. This simplifies a lot the anti-seismic design of the structure and internal components and allows the standardization of the design, which become practically site-independent (for the horizontal component of the acceleration, at least). This is particularly important in the phase of development of new reactors, like those of Generation IV, when the construction site of the plant is still unknown and the economics is one of the GIF criteria. More generally, seismic isolation is an effective tool for reducing or almost eliminating the devastating effects of earthquakes on people, equipments and structures. In particular, the use of seismic isolation can provide higher safety margins against failure of equipment and structural components in case of beyond design earthquakes, because the acceleration level at which the safe shutdown occurs can be significantly increased. This is extremely important not only from the safety point of view, but also from the economics, in terms of operability of the plant. It is worth noting that seismic isolation, being quite diffused in civil applications and already known especially in seismic countries like Japan and Italy, is positively perceived by the population and its application to nuclear plants certainly should have a good effect on the public opinion. In the last years, several extremely violent earthquakes occurred all over the world as, for example, the Niigata-Chuetsu-Oki earthquake (Japan, 2007), the Wenchuan earthquake (China, 2008), those which strongly struck Haiti and Chile in 2010 and that near the east coast of Honshu, Japan (March 11, 2011), which caused a devastating tsunami. These earthquakes were well higher than the expected design event (beyond design) and some of them struck large nuclear plants. Thus, the lesson learned from these events is that the demand for seismic capacity often exceeds our current regulations by a factor of 2 or even more. This implies that enhanced design solutions and methodologies, like base isolation, will gain considerable importance. This requires a new attention to the general layout of the plant in order to give adequate protection not only to the reactor core and vessels, but also to all the systems directly or indirectly related to safety to avoid situations like that recently occurred for the Fukushima plants.

State of the art on seismic isolation in NPPs

Application to Light Water Reactors

The first application of seismic isolation to a nuclear power plant was completed at Cruas, France (see Figure 1) where 4 PWRs (with a total electric power of 3600 MWe) were isolated at the end of the '70s (the construction began in 1978 and the reactors became operative between 1983 and 1984). The choice of seismic isolation was done to keep the design unchanged with respect to other reactors already designed or built by EdF in France, in places with lower seismicity (typically 0.2 g peak ground acceleration, being 0.3 g that of Cruas). For the same reason, two 900 MWe PWR units (same model of Cruas), were provided with seismic isolation in Koeberg, South Africa (30 km north of Cape Town, Figure 2). The construction began in 1976 (even before than Cruas) but the reactors were completed in 1984-1985. It is worth noting that the first new application after Cruas and Koeberg, is represented by the Jules Horowitz Reactor, now under construction at the Cadarache Nuclear Centre site (France) with an isolation system composed by 195 neoprene bearings (900x900x181 mm size, manufactured by NUVIA, Freyssinet Group) already installed, see Figure 3).

Fig 1: the four PWR units of Cruas, France, provided with seismic isolation.

Fig 2: the two PWR units of Koeberg, South Africa, provided with a seismic isolation system composed by rubber bearings coupled with friction plates.

Fig 3: sketch of the Jules Horowitz reactor and view of the isolation system during installation.

In addition, the ITER (International Thermonuclear Experimental Reactor) will be erected soon with base isolation, again at the Cadarache site. Among new water reactor designs, the IRIS (International Reactor Innovative and Secure) and the 4S (Super Safe, Small and Simple) reactor, developed by Toshiba-Westinghouse, must be cited. It is worth noting that for the IRIS, lot of activities on seismic isolation, even experimental, have been carried out, especially by the Italian partners of the consortium (see [2, 3]).

The case of Liquid Metal Reactors

The studies carried out up to now have shown as the issue of seismic protection of the plant is particularly felt in Liquid Metal systems. Compact pool-type designs of liquid metal cooled systems, in fact, alleviate plant construction costs, at the same time compactness can introduce new safety issues. For the lead-cooled concepts, seismic design challenges are specifically related to the large mass of lead. Moreover, peculiar to a LFR design, besides the high density of the coolant, is the integration of the steam generators or heat exchanger equipment inside the reactor vessel: this implies the risk of a large potential load in the case of an earthquake and of a new load brought about by the Steam Generator Tube Rupture (SGTR) or Heat Exchange tube rupture accidents.

At now, several studies have been carried out. The ALMR (Advanced Liquid Metal Reactor) is a sodium reactor developed by General Electric-Hitachi Nuclear Energy in the 80's; the project was sponsored by U.S. Department of Energy (DOE). The ALMR isolated structural configuration consists of a stiff steel-concrete box structure, which supports the reactor vessel, the containment dome, and the reactor vessel auxiliary cooling system stacks. The total isolated mass is about 23,000 t, supported by 66 high damping rubber bearings made of hard compound (shear modulus G = 1.1 MPa). The Safe Shutdown Earthquake (SSE) is characterized by an horizontal and vertical peak ground acceleration (PGA) of 0.5g. The horizontal isolation frequency is 0.7 Hz, and the vertical frequency is greater than 20 Hz. ENEA participated in the verification of the design of the isolators. More information on the ALMR is given in reference [4]. The S-PRISM (Power Reactor Innovative Small Module) is a modular reactor (415 MW for each module), again developed by GE in the 80's. Of course, for this kind of reactor the standardization of the design is a very critical issue. Seismic isolation was considered the most promising solution to keep the design unchanged independently of the construction site. The reactor module was supported by 20 HDRBs which give to the system an horizontal frequency of 0.7 Hz and provide a reduction of the horizontal shear forces by a factor 3. The PGA was 0.5 g at the SSE. More information on the S-PRISM is given in references [5, 6]. It is worth noting that this project was abandoned in 1994 before obtaining the licensing and now a new design, including seismic isolation, is in progress and aims to satisfy the severe requirements of GEN IV reactors. For the STAR-LM (Secure Transportable Autonomous Reactor-Liquid Metal) reactor, now under development at the Argonne National Laboratory (ANL), the standardization of the design is a key issue even more important than for S-PRISM, also due to the severe requirements of GEN IV for lead reactors. The SSE and OBE are characterized by a PGA of 0.3g and 0.2 g, respectively. The isolation system is made of cylindrical isolators with a diameter of 1.2 m and a rubber height of 0.5 m; the isolation frequency is 0.5 Hz in the horizontal direction and 21 Hz in the vertical one. For this reactor, a study for the seismic isolation in the vertical direction (with a frequency of 1.1 Hz) is being carried out. More information on the STAR-LM is given in [7]. The KALIMER (Korea Advanced LIquid MEtal Reactor) is an economically competitive, inherently safe, environmentally friendly, and proliferation-resistant sodium cooled reactor which is now being developed by the Korea Atomic Energy Research Institute. A total of 164 HDRBs (1.2m diameter) are installed between the ground and the lower base mat in the KALIMER-600 reactor and fuel handling buildings. The seismic gap between the isolated reactor building and the non-isolated wall is about 1.2 m, sufficient to avoid contacts ("hammering") even when the plant is subjected to a beyond design earthquake with a peak ground acceleration of 1.0 g. Further information about the KALIMER is provided in [8]. The ESFR (European Sodium Fast Reactor) is under development in the framework of the European Collaborative Project CP-ESFR, with the aim of evaluating pros and cons of the loop and pool solutions. In this project, ENEA is responsible of the task *Design measures for consequence mitigation of seismic loads*, in the framework of which the seismic isolation of the whole reactor building has been proposed. Aim of the task is also the development of guidelines and recommendations to provide techniques and methods for the reduction of seismic vulnerability.

Specifically on lead-cooled systems, some preliminary studies have been carried out in ELSY FP6 and LEADER FP7 projects [12], evaluating the general plant behavior up to the vessel in pool-type LFR systems, showing that the issues of coolant sloshing, gas entrapment and core voiding are important phenomena which need a further, detailed, study. The necessity to mitigate the earthquake damaging effects has been outlined in these projects and the seismic isolation is explicitly regarded as a viability issue, as from the SNE-TP SRA.

SEISMIC ISOLATION IN LEAD-COOLED SYSTEMS: THE SILER PROJECT

SILER (*Seismic-Initiated events risk mitigation in LEad-cooled Reactors*) is research project now (June 2011) under negotiation with EURATOM in the frame of the Seventh Framework Programme. The consortium is composed by ENEA (Coordinator, Italy), AREVA (France), SCK-CEN (Belgium), FIP Industriale (Italy), MAURER-SOEHNE (Germany), JRC (Ispra, Italy), SINTEC (Italy), KTH (Sweden), BOA (Germany), IDOM (Spain), ANSALDO (Italy), IPUL (Latvia), NUMERIA (Italy), VCE (Austria), SRS (Italy), CEA (France), EA (Spain), NUVIA (France). SILER addresses all the above-mentioned seismic topics making reference to two reactor concepts: ELSY [13]and MYRRHA.

The main goal of SILER is the development and application of seismic isolators for lead-cooled reactors. Two device typologies are considered in the Project: High Damping Rubber Bearings (HDRB, Figure 4) and Lead Rubber Bearings (LRBs, Figure 5). HDRBs are composed by alternate rubber layers and steel plates, bonded together during the vulcanization phase of the isolator. The capacity of supporting the axial (vertical) forces is given by the reinforcing steel plates which hinder the radial deformation of the rubber. Horizontal (shear) deformations are allowed by the elasticity (or, better, hyper-elasticity) of the rubber, that also provides the restoring force. The shear modulus (G) of the rubber ranges between 0.4 MPa (soft compound) to 1.4 MPa (very hard compound). For civil building applications, a medium compound (G=0.8 MPa) is often used. For nuclear applications, due to the large masses to be isolated (and, consequently, the high stiffness needed), the hardest compound is often necessary. In this case, particular attention must be paid to the bonding between rubber and steel. Finally, the energy dissipation is obtained by using suitable chemical components in the rubber compounds; the equivalent viscous damping can range from 5% (natural rubber) to 15% (high damping rubber). It is worth noting that higher is the damping factor, lower is the failure limit of the isolator. Typically, natural rubber and high damping rubber fail beyond 500% and 300% shear strain, respectively. If higher damping values are needed, the use of lead rubber bearings is recommended instead of additional energy dissipaters. The isolators used for nuclear application are usually quite large, due to the high mass of the superstructure. This introduce difficulties in the manufacturing process. In fact, the abovementioned vulcanization phase requires a quite uniform temperature distribution in the whole isolator, which is more difficult to be obtained for large volumes. Thus, particular attention must be paid to the production process controls and in the qualification of the device. The insertion of one or more lead cores within a rubber bearings can increase the equivalent viscous damping of the isolator up to 25-30% (LRBs). The advantage to dissipate energy trough the lead core is that the isolator can be made in low damping natural rubber, which is more resistant to failure, as stressed above. The disadvantages are a more difficult manufacturing process and a lower re-centering capability. The isolators developed in the SILER Project will be tested in full-scale and real dynamic conditions up to failure, with the aim of carefully evaluating the safety margins in case of beyond design earthquakes.

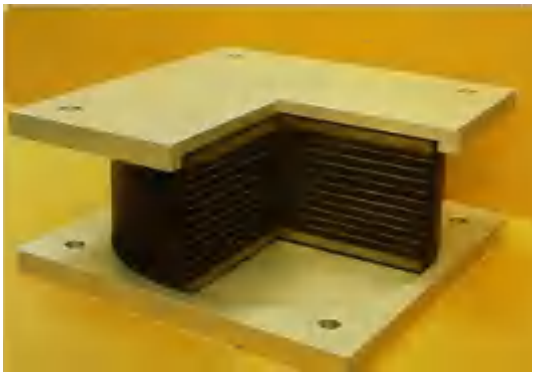

Fig 4: High Damping Rubber Bearing

Fig 5: Lead Rubber Bearing

Interface components

The adoption of base isolation introduces significant relative displacements between the isolated and non isolated parts of the plant. Thus, a seismic gap must be present all around the isolated part and shall be adequately protected and kept free during the whole life of the structure, in order to allow the relative movements in case of earthquake. All the service networks and pipelines crossing the seismic gap shall be provided with suitable expansion joints.

Seismic gap

The seismic gap shall be covered with a weatherproof joint capable not only to absorb bi-directional horizontal displacements in case of earthquake, but also to avoid infiltrations of water in the room where the isolators are installed (not only in case of rain and snow, but also for floods and tsunamis). The seismic joint protection must also be fireproof. In fact, in case of airplane crash, some burning fuel can reach the gap; in this case it's necessary to avoid that it reaches the isolators. Moreover, some wreck of the plane can fall over the cover gap; thus, it shall be adequately protected or designed to resist to the impact.

Expansion joints

For the regular service networks (pipes, wires and cables) several kind of expansion joints are already available on the market, used in the isolation of civil buildings, and no particular design solutions are necessary for applications in nuclear plants. When the whole nuclear island is isolated, one of the most critical systems crossing the seismic gap is the pipeline which goes to the turbines (containing hot and pressurized steam). Expansion joints similar to those needed in this case were tested in the framework of the INDEPTH project [9] for an isolated tank of a petrochemical plant. The technology for this kind of devices already exists also for high temperatures and pressure. It is worth noting that a smart disposition of two gimbals and one angular joints along the pipeline provide 6 degree of freedom to the system and can accommodate even huge displacements with very limited rotations (and then stresses) of the joints.

Horizontal fail safe system

Even in case of beyond design earthquakes, the isolators shall never loose the capability of supporting the vertical load. Thus, the adoption of an horizontal fail safe system to limit the isolator deformation must be foreseen. It is also strongly recommended that the fail safe system includes some shock absorber (for example a rubber bumper) to soft the hammering between the isolated building and the foundation. These devices are not present in the Cruas, Koeberg and Jules Horowitz Reactors, and are seldom used in civil buildings.

Guidelines and standardization procedures

Aim of SILER is also the development of guidelines proposal for the design, qualification, in-service inspection, maintenance and replacement of isolators.

The design and construction of nuclear plants are regulated, all over the world, by well known standards (issued by the NRC, IAEA, JAEA, etc.) that also include the seismic conventional design, but without seismic isolation. Moreover, there are several standards for the design and construction of isolated civil buildings like EURODE 8 and others. Finally, there are some standards addressed to the design, manufacturing and testing of seismic isolators for civil applications, like EN 15129, which came into force in 2010 in all European countries [10]. But no standard, at present, is specifically addressed to seismically isolated nuclear reactors or to isolators to be used in such plants (apart the Japanese standard cited in [11], that, unfortunately, is available in Japanese, only).

The lack of existing specific standards is one of the most important problems in the application of seismic isolation to nuclear plants, especially for what concerns the qualification of the isolators. New guidelines and/or recommendations are necessary to regulate the qualification of these very critical components, maybe developed starting from the existing ones.

EN15129 is going to be mandatory (August 2011) in all European countries for any kind of application where seismic isolators are used. However, it is not specifically addressed to nuclear plant. Thus, EN15129 can be used as a sort of *minimum requirement* in nuclear applications and improvements shall be done. To this aim, some activities are already foreseen in SILER, for showing that EN15129 is basically suitable for applications in nuclear plants but with some, not always minor, improvements. In particular it is recommended:

a) To design the isolator in order to have a rubber shear strain at the SSE lower than 100%. In this way the isolators will have the minimum stiffness at SSE and will have large safety margins in case of beyond design earthquakes.

b) To perform the type tests on full scale isolators and to test them with real three-directional dynamic excitations.

c) To perform the factory tests on the whole isolator production (concerning the vertical load capacity, at least).

CONCLUSIONS

The paper presented the world state-of-the-art of seismically isolated nuclear reactors (included new designs), focusing on the main problems encountered in the application of this technology to lead reactors, such as

the need of manufacturing and testing very large isolators and to design interface components, and the lack of standards specifically addressed to isolated nuclear reactors.

It is recognized that for HLM-cooled reactors the seismic risk mitigation is a key issue to be addressed for the development of such systems, to guarantee the safe operation of such systems.

In general, it can be stressed that:

- All the present applications or recent new designs of isolated NPPs use rubber isolators (with or without lead plugs) acting in the horizontal directions only. These devices are the best candidate to isolate nuclear plants.
- The isolation in the vertical direction of the whole nuclear island is not possible, yet; at present, if necessary, this kind of protection shall be limited to some critical components and equipments through suitable energy dissipaters (spring-dashpot devices).
- The technology for pipe expansion joints connecting the isolated part of the plant with the conventionally founded one, is almost already available, but requires some improvements.
- The adoption of an horizontal fail-safe system is strongly recommended, to avoid the isolator failure or instability in case of extremely violent earthquakes (beyond design).
- EN15129 can be used as reference standard for the design, qualification, in-service inspection, maintenance and replacement of isolators. However, since this standard is not specifically addressed to NPPs, EN15129 shall be used as a sort of "minimum requirement" and some improvements shall be done.

The SILER Project, that hopefully will start on November 2011, will deal with the most critical issues related to the seismic isolation of lead-cooled reactors and will certainly provide significant improvements with respect to the present state-of-the-art also by means of experimental campaigns on full-scale isolator (tested with dynamic three-directional excitations up to failure) and expansion joints.

REFERENCES

[1] A. Martelli, M. Forni, "State of the Art on Application, R&D and Design Rules for Seismic Isolation, Energy Dissipation and Vibration Control for Civil Structures, Industrial Plants and Cultural Heritage in Italy and other Countries", Proc of the 11th World Conference on Seismic Isolation, Energy Dissipation and Active Vibration Control of Structures, Guangzhou, China, Nov. 17-21, 2009.

[2] M. Forni, A. Poggianti, F. Bianchi, G. Forasassi, R. Lo Frano, G. Pugliese, F. Perotti, L. Corradi dell'Acqua, M. Domaneschi, M. D. Carelli, M. A. Ahmed, A. Maioli, "Seismic Isolation of the Iris Nuclear Plant", Proceedings of the 2009 ASME pressure Vessel and Piping Conference, PVP 2009, July 26-30, 2009, Prague, Czech Republic.

[3] G. Bergamo, F. Bianchi, M. G. Castellano, M. Forni, A. Poggianti, "Testing of Elastomeric Isolators for Nuclear Power Plants", Structural Engineering World Congress, April 4 to 6, 2011,Villa Erba (CO), Italy.

[4] E.L. Gluekler, C.C. Bigelow, V. DeVita2, J.M. Kelly, R.W. Seidensticker and F.F. Tajirian, "Seismic isolation development for the US advanced liquid-metal reactor program", Nuclear Engineering and Design 127 (1991) 295-301 295, North-Holland.

[5] M.R. Schrag and F.F. Tajirian, "Qualification of Seismic Isolation for the PRISM Liquid Metal Reactor", 9th SMiRT Conference, Vol K2, Lausanne, Switzerland, 1987.

[6] F.F. Tajirian, J.M. Kelly and E.L. Gluekler, "Testing of Seismic Isolation for the PRISM Advanced Liquid Metal Reactor Under Extreme Loads", SMIRT 10 Conference, Vol. K, San Francisco, California, 1989.

[7] B. Yoo, R.F. Kulak, "Application of Seismic Isolation to the STAR-LM Reactor", Proceedings of ICONE10: 10th International Conference on Nuclear Engineering, Arlington, Virginia, USA April 14-18, 2002.

[8] J.H. Lee, C.G. Park, J.B Kim, and G:H Koo, "Mechanical Structure Design Features of the KALIMER-600 Sodium-cooled Fast Reactor", Transactions, SMiRT 19, Toronto, August 2007, Paper S02/1.

[9] Enel.Hydro, IKI, ENEA, FIP, Principia, MMI, University of Patras, HELPE and IWKA (2002), "INDEPTH, Development of INnovative DEvices for seismic protection of PeTrocHemical facilities", Contract EVG1-CT-2002-00065, Bruxelles, Belgium.

[10] Eurpean Norme EN 15129, Anti-seismic devices.

[11] Japan Electric Association (JEA), Nuclear Standard Committee of JEA, Design and Technical Guideline of Seismic Isolation Structure for Nuclear Power Plant, JEAG 4614-2000, (in Japanese, only).

[12] http://myrrha.sckcen.be/en

[13] http://www.elsy-lead.com/PublicPages/TheReactor/reactor.htm

TUNED MASS DAMPER ON BASE-ISOLATED BUILDING UNDER NEAR-FAULT EARTHQUAKES

Naveet Kaur[1], V.A. Matsagar[2]
[1]Graduate Student, Department of Civil Engineering, Indian Institute of Technology (IIT) Delhi, Hauz Khas, New Delhi - 110 016, INDIA.
[2]Assistant Professor, Department of Civil Engineering, Indian Institute of Technology (IIT) Delhi, Hauz Khas, New Delhi - 110 016, INDIA.
E-mail of corresponding author: naveet.kaur1985@gmail.com

ABSTRACT

The effectiveness of a tuned mass damper provided at the top floor level of a base-isolated building subjected to near-fault earthquake ground motions is investigated. Since the near-fault earthquake ground motion consists of limited number of large acceleration pulses, it can be represented as sine-pulse. The buildings are modelled as shear-type structures considering four cases such as: conventional fixed-base building (FB), base-isolated building (BIS), building installed only with a tuned mass damper (STMD), and base-isolated building installed with a tuned mass damper (BI+TMD) referred to as the hybrid-passive structure. The investigation involved modelling of the buildings of varying heights ranging from five storeys to twenty storeys subjected to real near-fault earthquake ground motions. Time history analyses are carried out to study the variation of the top floor acceleration, top floor displacement and base-shear. A parametric study is also conducted to investigate the effects of isolation time period and isolation damping. It is concluded that, base isolation technique is quite effective in reducing the seismic response in terms of top floor acceleration up to eight storey buildings. However, response reduction reduces as the number of storeys increases, especially when time periods of the non-isolated building and that of the base-isolated building are nearly the same. On the other hand, considerable seismic response reduction is achieved for the buildings greater than sixteen storeys when a tuned mass damper is installed. The hybrid-passive system results in higher response reduction than the other two passive control systems for the eight to sixteen storey buildings. With increase in isolation time period, the structural response in terms of peak top floor acceleration and peak normalised base shear does not show as much variation as it does in case of the peak top floor displacement, which increases substantially. With increase in damping of the isolator, the response quantities namely, peak bearing displacement, peak top floor acceleration, and peak normalized base shear reduce. It is observed that, the dynamic response obtained for the near-fault ground motions and short duration pulses are quite similar.

INTRODUCTION

Base isolation works on the principle of decoupling of superstructure from earthquake ground motion. Further, the flexibility in lateral direction introduced by the base isolation shifts the fundamental time period of the structure to a larger value than the time period of fixed-base (FB, i.e. non-isolated) structure. Fundamental frequency of a base-isolated structure (BIS) is much lower than that of the FB [1]. Owing to the reduced stiffness, floor accelerations are controlled while top floor displacements and base displacements increase.

Tuned mass damper (TMD) is a device consisting of a mass attached to the structure via a spring-dashpot system, such that it oscillates at the same frequency as the main structure (resonance), however with 180° phase shift. The system dissipates energy due to the relative motion developed between the mass of the TMD and the structure.

The aim of using base isolation and TMD together in a structure, called hybrid-passive system (BI+TMD) is to effectively control both, the acceleration response and excessive displacement. Basic dynamic properties of the BI+TMD are mass ratio (μ_t) and tuning of the TMD; sensitivity of and interaction between isolator and TMD needs to be accounted for. The TMD parameters such as μ_t and tuning ratio are adjusted to ensure effectiveness. Resulting from the three sub-systems i.e. the structure, the TMD and the isolators, the hybrid-passive structure is non-classically damped.

The common feature of earthquake ground motions in the near-fault region is the presence of a limited number of large acceleration pulses occurring in the form of a shock, rather than a gradual build-up and a velocity pulse with a long period component as well as a large displacement [2]. The BIS is considered vulnerable to near-fault ground motions owing to possible matching of major frequency contents [3, 4]. Dynamic behaviour of both the

BIS and the FB under the near-fault motion has already been extensively studied [5, 6]. However, very few studies are reported for dynamic response of the hybrid-passive structure such as the BI+TMD [7, 8]. Therefore, it is important to study the effects of such pulse-type ground motions on long time period structures such as the BI+TMD.

In view of the above, the primary objective of the study is to investigate effectiveness of a tuned mass damper on the BIS in controlling the accelerations and large displacements under near-fault earthquakes. The specific objectives of the study include: (1) to investigate the number of storeys for which the BI+TMD is the most effective under near-fault earthquakes; (2) to further carryout parametric study for investigating effects of (a) variation in number of storeys, (b) variation in time period of base isolation, and (c) variation in damping of base isolation; and (3) to compare the response of base-isolated structures under near-fault earthquake with sine-pulse motion.

MATHEMATICAL MODELLING

Mathematical models of (a) FB; (b) BIS; (c) STMD; (d) BI+TMD considered in the study are shown in Fig. 1. Numerical study is carried out to find the range of number of stories for which the hybrid-passive system is comparatively the most efficient, by modelling the four types of structures from five storeys to twenty storeys. Key parameters are identified for further investigation, such as the time period of isolation and damping of base isolation. Assumptions made in the study are: (1) mass is lumped at each floor level; (2) one lateral degree of freedom at each floor level is considered; and (3) soil-structure interaction is neglected. In this study, laminated rubber bearing (LRB) is considered for base isolation, and single TMD at top floor level is considered to be attached.

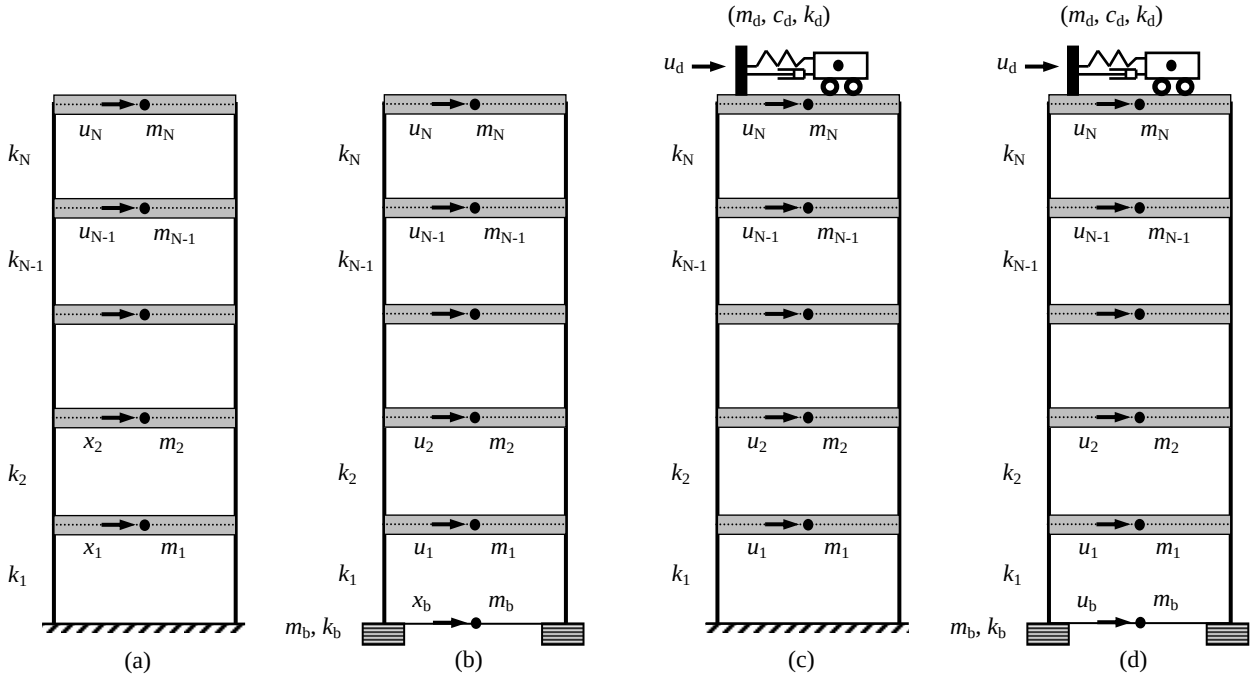

Fig. 1: Mathematical models of *N*-storey (a) fixed-base structure (FB), (b) base-isolated structure (BIS), (c) structure with a TMD (STMD), and (d) hybrid-passive structure (BI+TMD)

Conventional fixed-base structure (FB)

The general equation of motion for a FB (non-isolated) subjected to a horizontal ground motion is described here. The displacement of the ground is denoted by u_g, the total (or absolute) displacement of the mass m_j by u_j^t, and the relative displacement between this mass and the ground by u_j. Hence, the acceleration, velocity, and displacement are the resultant of motion of ground and superstructure, due to the earthquake. At each instant of time these displacements are related by,

$$u_j^t(t) = u_j(t) + u_g(t) \tag{1}$$

The governing differential equation of motion, Eq. 2 for a FB (non-isolated) subjected to a horizontal ground motion hence can be written as,

$$[M_s]\{\ddot{u}(t)\} + [C_s]\{\dot{u}(t)\} + [K_s]\{u(t)\} = -[M]\{r\}\ddot{u}_g(t) \tag{2}$$

where, $[M_s]$, $[C_s]$, and $[K_s]$ are the mass, damping, and stiffness matrices of the superstructure, respectively; $\{\ddot{u}\}$, $\{\dot{u}\}$, and $\{u\}$ are the acceleration, velocity, and displacement vectors, respectively; $\{r\}$ is the influence coefficient vector. Total mass of the structure is, $M = \sum m_j$.

Base-isolated structure (BIS)

The displacements in the BIS are related as in Eq. 3, where, u_j is the relative floor displacement at j^{th} floor with respect to the isolator, u_b is the displacement of the isolator and m_b is the mass of the isolator.

$$u_j^t(t) = u_j(t) + u_b(t) + u_g(t) \tag{3}$$

The general governing equation of motion, Eq. 4 for the BIS is given by,

$$[M_b]\{\ddot{u}^t(t)\} + [C_b]\{\dot{u}^t(t)\} + [K_b]\{u^t(t)\} = -\{\overline{M}_b\}\ddot{u}_g(t) \tag{4}$$

where,

$$[M_b] = \begin{bmatrix} m_N & \cdots & 0 & 0 & m_N \\ \vdots & \ddots & \vdots & \vdots & \vdots \\ 0 & \cdots & m_2 & 0 & m_2 \\ 0 & \cdots & 0 & m_1 & m_1 \\ 0 & \cdots & 0 & 0 & m_b \end{bmatrix} \tag{5}$$

$$[K_b] = \begin{bmatrix} k_N & -k_N & \cdots & 0 & 0 \\ -k_N & k_N + k_{N-1} & \cdots & 0 & 0 \\ \vdots & \vdots & \ddots & \vdots & \vdots \\ 0 & 0 & \cdots & k_2 + k_1 & 0 \\ 0 & 0 & \cdots & -k_1 & k_1 + k_b \end{bmatrix} \tag{6}$$

$$\{\overline{M_b}\} = [M_b]\{r\} = \{2m_N \quad 2m_{N-1} \quad \cdots \quad 2m_2 \quad 2m_1 \quad m_b\}^T \tag{7}$$

Structure with tuned mass damper (STMD)

Consider a FB having a TMD of mass m_d , damping c_d and stiffness k_d attached at the top floor. The mass, damping, and stiffness of the superstructure are same as described earlier. The equation of motion, Eq. 8 for the STMD is,

$$[M_t]\{\ddot{u}(t)\} + [C_t]\{\dot{u}(t)\} + [K_t]\{u(t)\} = -\{\overline{M}_t\}\ddot{u}_g(t) \tag{8}$$

where, $\{\ddot{u}\}$, $\{\dot{u}\}$, and $\{u\}$ are vectors of horizontal acceleration, velocity, and displacement, respectively, relative to the ground, with components for the TMD and the superstructure. The mass and stiffness matrices for the system can thus be written as,

$$[M_t] = \begin{bmatrix} m_d & 0 & \cdots & 0 & 0 \\ 0 & m_5 & \cdots & 0 & 0 \\ \vdots & \vdots & \ddots & \vdots & \vdots \\ 0 & 0 & \cdots & m_2 & 0 \\ 0 & 0 & \cdots & 0 & m_1 \end{bmatrix} \tag{9}$$

$$[K_t] = \begin{bmatrix} k_d & -k_d & \cdots & 0 & 0 \\ -k_d & k_d + k_5 & \cdots & 0 & 0 \\ \vdots & \vdots & \ddots & \vdots & \vdots \\ 0 & 0 & \cdots & k_3 + k_2 & -k_2 \\ 0 & 0 & \cdots & -k_2 & k_2 + k_1 \end{bmatrix} \tag{10}$$

The damping matrix of the superstructure is not known explicitly. It is constructed by assuming the modal damping ratio in each mode of vibration for superstructure, which is kept constant. Ratio of mass of TMD to that of the superstructure is called mass ratio (μ_t).

Hybrid-passive structure (BI+TMD)

With all mathematical notations same as mentioned in the preceding paragraphs, the governing differential equation of motion, Eq. 11 for the BI+TMD can be written as,

$$[M_h]\{\ddot{u}^t(t)\} + [C_h]\{\dot{u}^t(t)\} + [K_h]\{u^t(t)\} = -\left\{\overline{M}_h\right\}\ddot{u}_g \tag{11}$$

where,

$$[M_h] = \begin{bmatrix} m_d & 0 & \cdots & 0 & m_d \\ 0 & m_N & \cdots & 0 & m_N \\ \vdots & \vdots & \ddots & \vdots & \vdots \\ 0 & 0 & \cdots & m_1 & m_1 \\ 0 & 0 & \cdots & 0 & m_b \end{bmatrix} \tag{12}$$

$$[K_h] = \begin{bmatrix} k_d & -k_d & \cdots & 0 & 0 \\ -k_d & k_d + k_5 & \cdots & 0 & 0 \\ \vdots & \vdots & \ddots & \vdots & \vdots \\ 0 & 0 & \cdots & k_2 + k_1 & 0 \\ 0 & 0 & \cdots & -k_1 & k_1 + k_b \end{bmatrix} \tag{13}$$

$$\left\{\overline{M}_h\right\} = \left\{2m_d \quad 2m_N \quad 2m_{N-1} \quad \cdots \quad 2m_2 \quad 2m_1 \quad m_b\right\}^T \tag{14}$$

where, $[M_h]$ is a diagonal matrix with diagonal element $m_{jj} = m_j$, mass lumped at the j^{th} floor.

NUMERICAL STUDY

Seismic response of (a) FB; (b) BIS; (c) STMD; and (d) BI+TMD for 5, 8, 12, and 20 storeys is investigated under real near-fault earthquake ground motions. Earthquake motions selected for the study are Imperial Valley, 1979 recorded at Array#5; normal component of 1992 Landers earthquake recorded at Lucerne Valley; normal component of 1992 Northridge earthquake recorded at Rinaldi station; and normal component of 1992 Northridge earthquake recorded at Sylmar station. The peak ground accelerations (PGA) of Imperial Valley, Landers, Northridge (Rinaldi), and Northridge (Sylmar) earthquake motions are 0.36, 0.71, 0.87, and 0.71 *g*, respectively; where, *g* is the acceleration due to gravity. Structural damping is 5% (kept constant in all modes) for all structures except for the BIS and the BI+TMD, where 10% damping is assumed in the first mode owing to isolation

damping governing the first mode of vibration. Time period (T_b) and damping ratio (ξ_b) characterise the isolation system. The mass and stiffness properties are assumed uniform over the height of the structure. Time periods for the first and second mode are shown in Table 1.

Table 1: Modal time periods of different structures considered.

Description of Structure	Mode	Time Period (sec)			
		5 Storey	8 Storey	12 Storey	20 Storey
Conventional fixed-base building (FB)	1	0.50	0.77	1.13	1.85
	2	0.11	0.26	0.38	0.62
Base-isolated building (BIS)	1	2.01	2.30	2.51	2.50
	2	0.27	0.40	0.55	0.78
Building installed only with a tuned mass damper (STMD)	1	0.64	0.81	1.14	1.86
	2	0.40	0.43	0.44	0.65
Base-isolated building installed with a tuned mass damper (BI+TMD)	1	2.02	2.31	2.51	2.51
	2	0.50	0.46	0.62	0.80

Effect of number of storeys

The isolation system considered for the study is laminated rubber bearing (LRB). Peak bearing displacement, peak top floor acceleration, and peak normalised base shear for the four structures with varying number of storeys under different earthquakes are shown in Table 2. The base shear is normalised with weight of structure $\left(W = \sum m_j \times g\right)$. The considered response parameters are compared with response under sine-pulse motion and it is concluded that, the dynamic response obtained for the near-fault ground motions and the short duration pulses are quite similar.

Table 2: Peak response of different structures with varying storeys under different earthquakes.

Earthquake	Storey	Peak Bearing Displacement (cm)		Peak Top Floor Acceleration (g)				Peak Normalized Base Shear (W)			
		BIS	BI+TMD	FB	BIS	STMD	BI+TMD	FB	BIS	STMD	BI+TMD
1979 Imperial Valley (Array#5)	5	30.19	30.10	1.32	0.34	0.91	0.33	0.91	0.31	0.65	0.31
	8	45.61	45.51	0.70	0.42	0.63	0.34	0.45	0.38	0.43	0.38
	12	50.89	50.51	0.68	0.42	0.65	0.46	0.48	0.39	0.47	0.39
	20	27.93	27.60	0.50	0.58	0.56	0.55	0.28	0.36	0.27	0.36
1992 Landers (Lucerne Valley)	5	33.07	32.58	2.70	0.38	1.62	0.36	1.72	0.35	1.40	0.34
	8	29.11	28.79	2.27	0.33	1.97	0.25	1.59	0.25	1.25	0.25
	12	26.32	26.06	2.00	0.32	1.89	0.28	1.08	0.20	1.01	0.20
	20	14.03	13.97	1.11	0.60	1.05	0.59	0.38	0.18	0.40	0.18
1992 Northridge (Rinaldi)	5	51.26	50.66	2.03	0.59	1.66	0.56	1.71	0.54	1.34	0.52
	8	45.73	45.51	2.51	0.45	2.34	0.43	1.89	0.38	1.66	0.38
	12	39.99	39.99	2.19	0.46	2.26	0.45	1.40	0.32	1.34	0.32
	20	24.32	24.80	1.52	1.98	1.59	0.97	0.59	1.80	0.53	0.31
1992 Northridge (Sylmar)	5	48.93	48.42	1.35	0.56	1.28	0.54	0.93	0.51	0.81	0.50
	8	55.76	55.51	1.32	0.53	0.95	0.53	0.70	0.46	0.59	0.46
	12	58.11	58.13	1.66	0.53	1.23	0.50	0.89	0.44	0.82	0.44
	20	33.90	34.07	1.25	0.61	1.04	0.58	0.54	0.43	0.54	0.43
Sine-Pulse Motion	5	29.94	29.29	2.97	0.32	2.38	0.32	0.24	0.31	0.20	0.31
	8	43.02	43.02	0.29	0.38	0.23	0.38	0.22	0.36	0.21	0.36
	12	46.71	46.63	0.28	0.41	0.26	0.41	0.20	0.36	0.20	0.35
	20	26.58	26.45	0.39	0.44	0.42	0.44	0.31	0.34	0.31	0.34

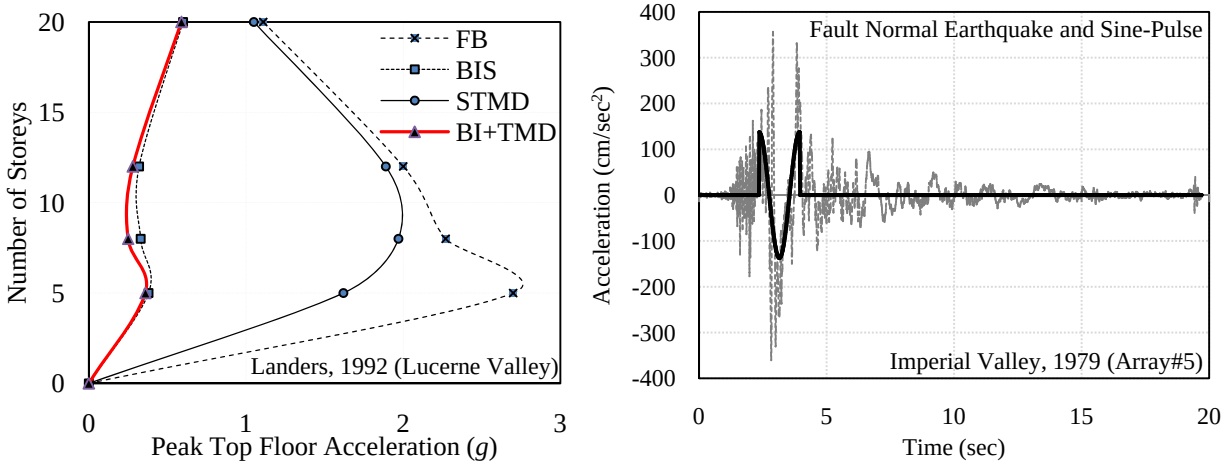

Fig. 2: (a) Peak top floor acceleration for four types of structures with 5, 8, 12, and 20 storeys (b) Time plot of near-fault ground acceleration and the modelled sine-pulse

Peak top floor acceleration for four types of structures with 5, 8, 12, and 20 storeys under Landers, 1992 (Lucerne Valley) is shown in Fig. 2(a) and a sine-pulse motion modelled for Imperial Valley, 1979 (Array#5) is shown in Fig. 2(b). It is observed that, in comparison, the BI+TMD shows the least top floor acceleration. Effectiveness of the BI+TMD is observed to be the maximum for 8 to 16 storeys. The resulting hybrid-passive system reduces the bearing displacement (resulting due to increase in flexibility) along with acceleration and base shear. Time history for bearing displacement and top floor acceleration of 8 storey structures under Northridge, 1992 (Rinaldi) is shown in Fig. 3. Mass ratio (μ_t) is taken as 1.98%. It is observed that, the BI+TMD results in the maximum seismic response reduction.

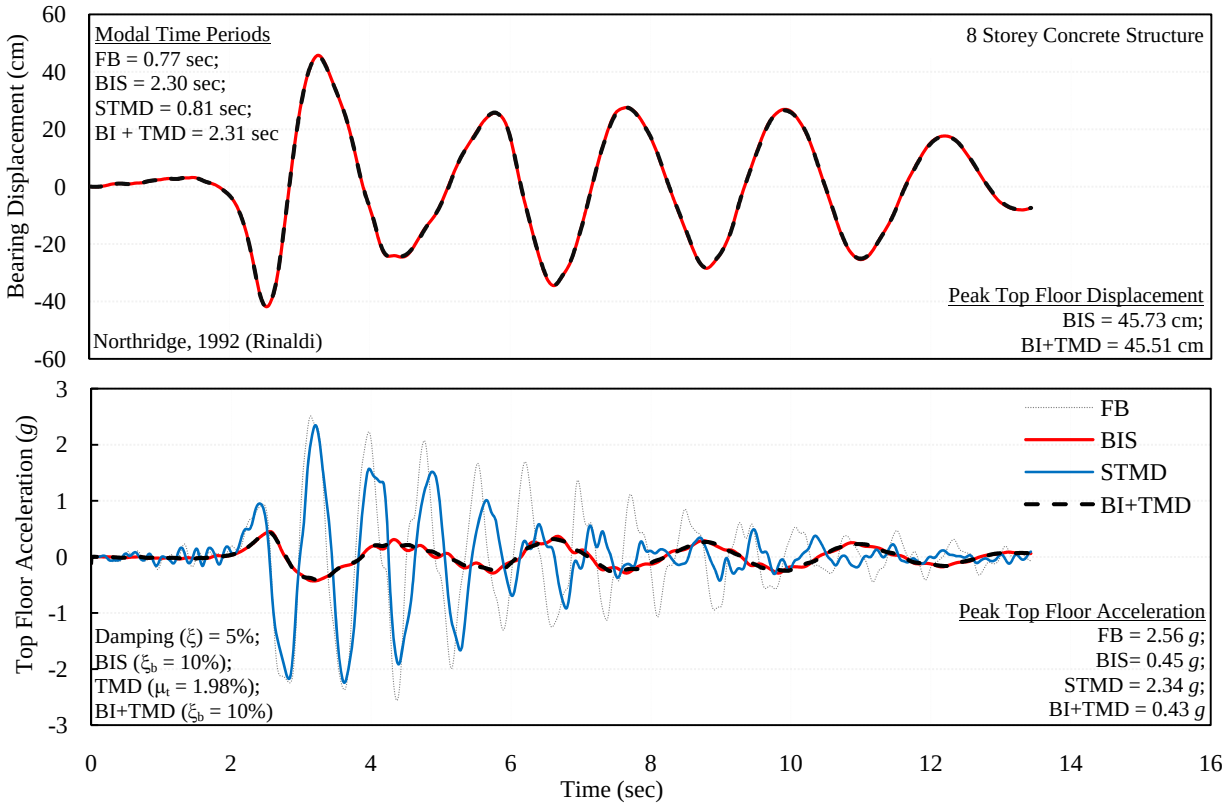

Fig. 3: Time history of bearing displacement and top floor acceleration of 8 storey structure under Northridge, 1992 (Rinaldi)

Effect of isolation time period

The isolation time periods considered for the study are: (a) 1.25 sec; (b) 1.5 sec; (c) 2.0 sec; (d) 2.2 sec; (e) 2.4 sec; and (f) 2.5 sec. For all investigations, TMD of the STMD is tuned to the fundamental frequency of the FB, and the TMD of the BI+TMD with the fundamental frequency of the BIS. Time periods of the BIS and the BI+TMD (T_t) is 2.51 sec. It is observed both for the BIS and the BI+TMD that, with increase in isolation time period, the structural response in terms of peak top floor acceleration and peak normalised base shear does not show as much variation as it does in case of the peak top floor displacement, which increases substantially. It is also observed that, effectiveness of the BI+TMD in reduction of top floor acceleration and peak normalized base shear reduces with increase in time period of isolation (Fig. 4). The BI+TMD is the most effective, in terms of peak top floor acceleration response reduction for the fundamental time period of the FB ranging from 0.8 sec to 1.8 sec. For a stiffer structure, fundamental time period is low; addition of flexible base isolation considerably reduces its seismic response. However, the BI+TMD does not help in significantly reducing peak bearing displacement with increase in isolation time period as compared to the BIS.

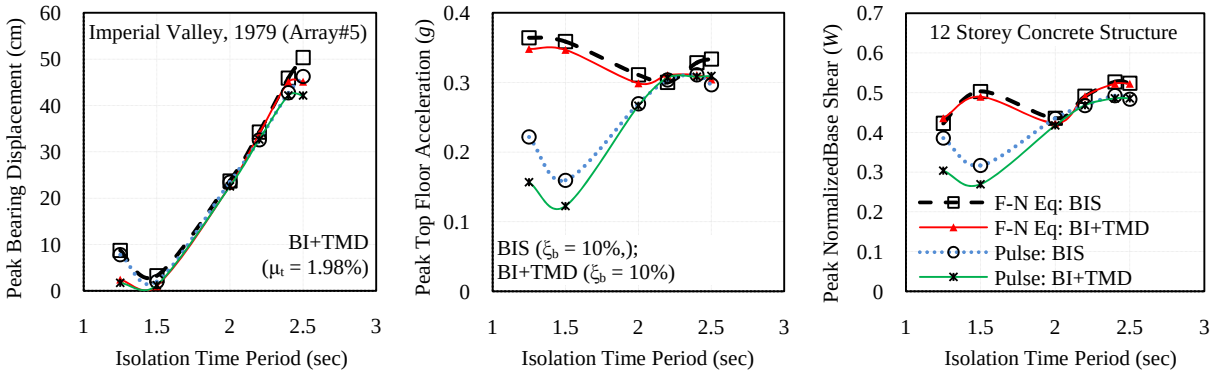

Fig. 4: Variation of peak bearing displacement, peak top floor acceleration and peak normalised base shear against varying isolation time period [F-N Eq: Fault-Normal Earthquake and Pulse: Sine-Pulse Motion]

Effect of isolation damping

For the eight storey BIS and BI+TMD subjected to Imperial Valley, 1979 (Array#5) isolation damping considered for this study are: (a) 5%; (b) 10%; (c) 15%; and (d) 20% in the first mode and 5% damping in all other modes with other structural parameters kept constant. As the damping of the isolator increases, it is observed that, peak bearing displacement, peak top floor displacement, and peak normalised base shear are reduced both for the BI+TMD and the BIS. For an eight storey structure, increase in damping of the isolator reduces the peak top floor acceleration response of the BI+TMD more than the BIS showing its effectiveness (Fig. 5). These observations related to the improved seismic performance of the BI+TMD as compared to the BIS and the STMD are similar to those reported for high-rise structures as well [9].

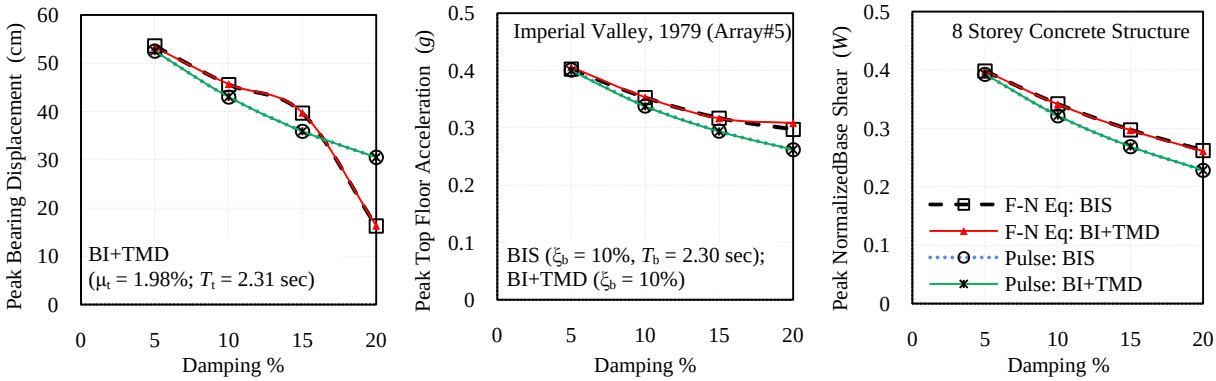

Fig. 5: Variation of peak bearing displacement, peak top floor acceleration and peak normalised base shear against isolation damping [F-N Eq: Fault-Normal Earthquake and Pulse: Sine-Pulse Motion]

CONCLUSIONS

From the study conducted herein the following conclusions are arrived at: (1) Base isolation is quite effective for seismic response reduction for structures up to eight storeys; (2) A tuned mass damper is effective for seismic response reduction for structures with more than sixteen storeys; (3) The hybrid-passive structure constituting of base isolation and a tuned mass damper is comparatively more effective in seismic response reduction for structures with number of storeys ranging from eight to sixteen; (4) For lower isolation time periods, the seismic responses for the base-isolated structure and hybrid-passive are quite different; i.e., for flexible isolated systems, effectiveness in seismic response reduction of base-isolated structure and hybrid-passive structure are almost similar; (5) With increase in damping of the isolator, the response quantities namely, peak bearing displacement, peak top floor acceleration, and peak normalized base shear reduces; and (6) The dynamic response obtained for the near-fault ground motions and short duration pulses are quite similar.

ACKNOWLEDGEMENTS

In accomplishing the reported work, discussions with Lt. Col. Rohit Gogna and the help extended by him by sharing his experiences with the hybrid-passive system are gratefully acknowledged.

REFERENCES

[1] Matsagar, V.A. and Jangid, R.S., "Influence of isolator characteristics on the response of base-isolated structures", *Engineering Structures*, 2004.
[2] Matsagar, V.A. and Jangid, R.S., "Response of base-isolated structures during impact to near-fault motions", *Fourth International Conference of Earthquake Engineering and Seismology*, Tehran, Islamic Republic of Iran, May 2003.
[3] Hall, J.F., Heaton, T.H., Halling, M.W. and Wald, D.J., "Near-source ground motion and its effects on flexible buildings", *Earthquake Spectra*, Vol. 11, 1995.
[4] Heaton, T.H., Hall, J.F., Wald, D.J., Halling, M.W., "Response of high-rise and base-isolated buildings to a hypothetical MW 7.0 blind thrust earthquake", *Science*, Vol. 267, 1995.
[5] Markis, N., "Rigidity-plasticity-viscosity: can electro rheological dampers protect base-isolated structures from near source ground motions?", *Earthquake Engineering and Structural Dynamics*, Vol. 26, 1997.
[6] Jangid, R.S. and Kelly, J.M., "Base isolation for near-fault motions", *Earthquake Engineering and Structural Dynamics*, Vol. 30, 2000.
[7] Tsai, H.C., "The effect of tuned mass dampers on the seismic response of base-isolated structures", *International Journal Solids Structures*, Vol. 32, 1995.
[8] Taniguchi, T., "Effect of tuned mass damper on displacement demand of base-isolated structures", *Engineering Structures*, Vol. 30, 2008.
[9] Gogna, R., "Base-isolated structure with tuned mass damper", Masters Thesis, Indian Institute of Technology (IIT) Delhi, 2011.

ASSESSMENT OF PASSIVE CONTAINMENT ISOLATION FEATURE OF ADVANCED NATURAL CIRCULATION REACTOR

A. Srivastava, H. G. Lele, K. K. Vaze
Reactor Safety Division, Bhabha Atomic Research Centre, Mumbai, INDIA-400085
E-mail of corresponding author: abhisri@barc.gov.in

ABSTRACT

Recent inclination in nuclear industry is towards providing as many passive features as possible. These passive features enhance safety substantially. The Passive Containment Isolation System (PCIS) system is one of the important passive features in the conceptual design of advanced natural circulation reactor. This system isolates the primary containment from the atmosphere in the event of Loss of Coolant Accident (LOCA), thus reducing the possible escape of radioactivity outside containment. The pressure transient in the V1 and V2 zones of the primary containment following the postulated accident provides the driving force to the passive system and ensures the isolation of containment from atmosphere by establishing a liquid seal in the U-shaped ventilation duct. The time required to form the effective liquid seal as well as leakage to atmosphere are some important aspect during the postulated accident.

The PCIS performance can be challenged by its various system parameters i.e. water inventory in the passive containment isolation tank, filter resistance at end of ventilation duct and pressure transient in the containment following various sizes of inlet header break. The present work aim to look in these aspects and evaluate the performance of the system under various important parameters combination.

The paper elaborate modelling of PCIS in two different system code i.e. RELAP5 and CATHARE and results of intercode comparison for time required to form the effective liquid seal as well as leakage to atmosphere along with levels in the u-shape ventilation duct during large break LOCA. Then paper further addresses the PCIS behaviour under different system parameter combination during LOCA transient for sustained liquid seal formation.

INTRODUCTION

The existing reactors mostly use active safety systems. The reliability of the active systems cannot be increased above a threshold and further promptness of operator action, to prevent probable fuel failure and fission product release, is debatable. In view of this, advanced reactors are designed with adequate passive and inherent safety features to provide protection for any event that may lead to a serious accident [1]. The function of confinement of any radioactivity released in the containment is also made more reliable by adopting robust, redundant, and passive design features. The Passive Containment Isolation System (PCIS) is one of the important passive features to limit the escape of radioactivity release to atmosphere in advanced natural circulation reactor. This advance reactor employs a double containment system i.e. primary containment & secondary containment. The primary containment is further zoned as V1 (high enthalpy) and V2 (low enthalpy) regions. Under normal operating conditions, the V1 and V2 regions are connected only through vent shafts, with downstream ends of vent shafts submerged in GDWP that also acts as a suppression pool. Blow Out Panels (BOP) are also provided in the reactor building to limit the pressure on the containment building structure under accidental conditions by directly connecting V1 and V2 volumes. The PCIS consists of a water tank i.e. Passive Containment Isolation Tank (PCIT) with water level maintained at a preset value as shown in Fig.1. The space above the water level is kept in communication with volume V1 through a vent shaft. From the bottom of the tank, where an outlet is provided in the form a vertical pipe, the system is in communication with volume V2 via the connection with the ventilation duct at an appropriate elevation. It may be noted that the volume V2 is ventilated to atmosphere through a 'U' duct, from which a branched connection to PCIT is taken. So, under any operating conditions, the top space of the PCIT would experience the pressure of V1 volume while the pipe connected to the outlet of the tank would experience the pressure of V2 volume. Hence, at any instant, hydrostatic differential pressure head between the two volumes would govern the water level in the outlet pipe. In the event of volume V1 pressurizing to certain pressure beyond the V2 pressure, the water in pipe at the outlet of PCIT rises to spill into the ventilation duct.

Under postulated LOCA conditions, V1 and V2 regions undergo a pressure transient. The V1 pressure rises more rapidly than V2 pressure. This leads to spilling of water from the tank into ventilation duct. However after opening of BOPs, the pressures tend to equalize as V1 and V2 are brought in direct communication. The high-

pressure condition in the V2 demands for the quick isolation of containment system from atmosphere to prevent any eventual release to the atmosphere. The isolation of containment is achieved by establishing a liquid U- seal in the ventilation duct [2].

In this paper, PCIS model is developed for system code RELAP5 [3] and further with CATHARE [4]. The transient analysis post 200% LOCA in the containment is analysed using both the model. The results obtained from these two codes are compared for time required to form the effective liquid seal as well as leakage to atmosphere along with levels in the u-shape ventilation duct during large break LOCA. Further as passive safety systems rely on natural forces, such as gravity or natural convection to perform their accident prevention and mitigation functions once actuated and started. Because the magnitude of the natural forces, which drive the operation of passive systems, is relatively small, counter-forces (e.g., friction) can be of comparable magnitude and cannot be ignored [5]. To address this issue, a parametric study with different system parameter combination during LOCA transient has been done to assess the PCIS behaviour for sustained liquid seal formation.

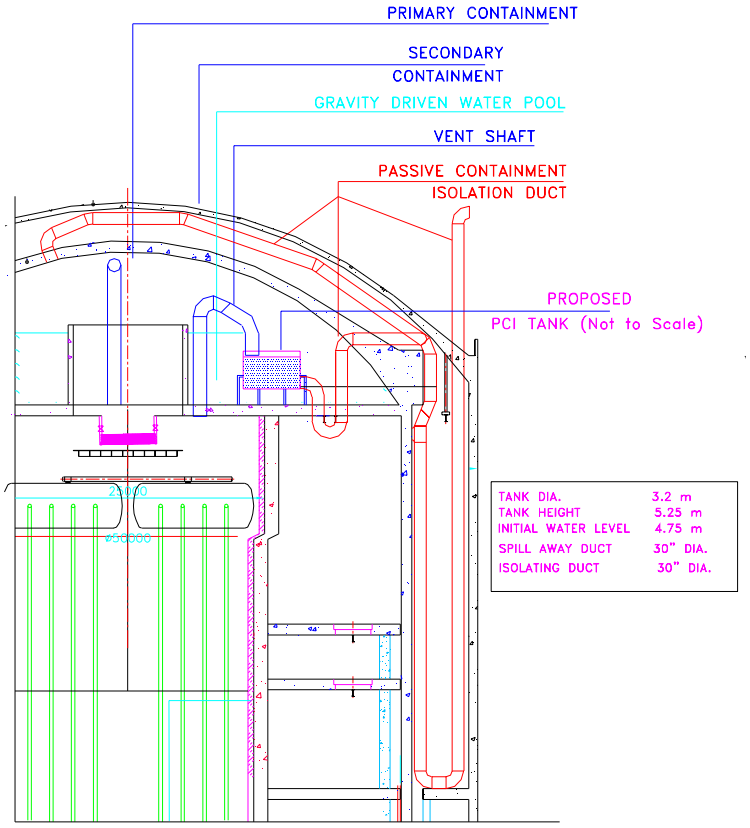

Fig.1: Layout of Passive Containment Isolation System

PASSIVE CONTAINMENT ISOLATION SYSTEM MODELLING

The PCIS system is modelled in best estimate code RELAP5 as well as CATHARE as shown in Fig 2 and Fig 3. The RELAP5 modelling is being described in detail in following paragraph. The CATHARE modelling is kept similar for comparative studies.

The PCIT is modelled with component 203 having 3 control volumes. The first volume i.e. 203-01 is initialized with air and bottom two volumes are initialized with water. The exit pipe is modelled with the help of component 204 having 3 control volumes in it. The ventilation duct is modelled with the component 206. There are first 40 control volumes simulating the vertical downward part of the duct, 206-41 control volume simulates the horizontal portion of the duct and 206-42 to 206-81 i.e. remaining 40 volumes simulates the upward portion of the ventilation duct. RELAP5 specific Time Dependant Volume (TDV) is used to represent the conditions in V1, V2

and atmosphere. The TDV 207, TDV 201 and TDV 205 simulate the atmosphere, V1 condition and V2 conditions respectively. The single volume 202 simulates the vent shaft connecting the V1 volume with the PCIT. The component 208 models the part of ventilation duct connecting the V2 volume. Appropriate junction connection are used to link the above described control volume at various places. The details of the various control volume and junctions are presented in the table 1.

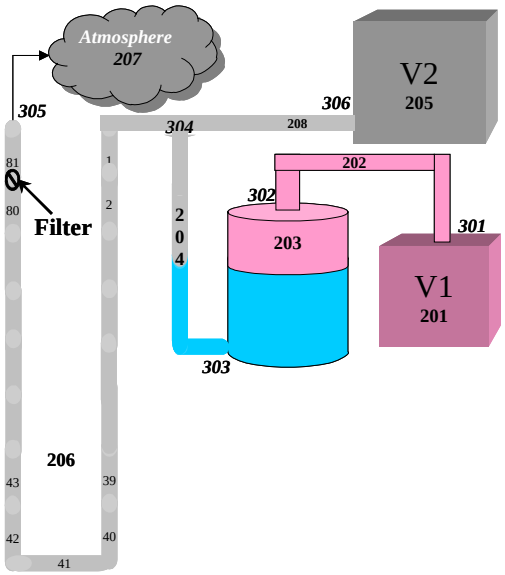

Fig. 2: PCIS model in RELAP5

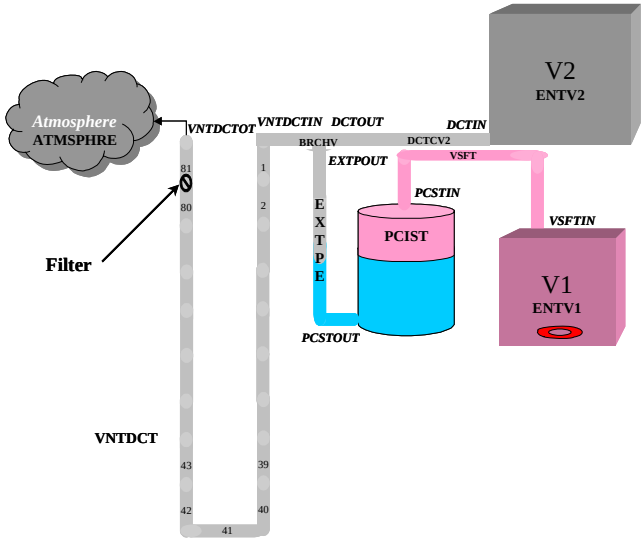

Fig. 3: PCIS model in CATHARE

Table 1: Description of the Hydrodynamic Components and Junctions

RELAP5	CATHARE	Description of the volume
Vol. No./Junction no.	Name of axial/Volume /junction	
201	ENTV1	Volume V1
202	VSFT	Vent shaft connection between V1 and PCIT
203-01, 203-02 and 203-03	PCIST	PCIT volumes
204-01, 204-02 and 204-03	EXTPE	Exit pipes
205	ENTV2	Volume V2
206-01 to 206-81	VNTDCT	Ventilation duct
207	ATMSPHRE	Atmosphere
208-01 and 208-02	DCTCV2	Duct connection from V2
301	VSFTIN	Connection between V1 and vent shaft
302	PCSTIN	Connection between vent shaft and PCIT
303	PCSTOUT	Connection between PCIT and exit pipe
304	BRCHV	Branch to connect exit pipe, V2 duct

		and ventilation duct
305	VNTDCTOT	Connection between duct and atmosphere
306	DCTIN	Connection between V2 duct and V2

The model is initialized with atmospheric conditions i.e. normal operating condition and run for the 100 s to get the stabilized conditions in the circuit.

Further from separate analysis [6], containment V1 and V2 pressure transients are obtained following 200% inlet header break. These pressure transients are applied to present PCIS model in V1 and V2 volumes as boundary condition to run the transient calculations for the PCIS in case of inlet header break. The objective is to observe the sustained liquid seal formation. This seal formation in the ventilation duct is challenged by several parameters i.e. water inventory in the PCIT, filter resistance at end of ventilation duct and pressure transient in the containment following various sizes of inlet header break. The first analysis has been performed with all the system at design conditions. In this case, the filter resistance has been simulated using restricted exit area.

TEST MATRIX

A intercode comparison is done for post 200% IH break LOCA with model developed in RELAP5 and CATHARE for water seal formation in the ventilation duct. Further, a sensitivity study is performed to cover the various initial tank inventories at the time of accident and various filter loss coefficient effect on effective seal formation. In the present analysis, 200% inlet header break pressure transient for V1 and V2 has been utilized to evaluate the performance of PCIS. The test matrix is given in table 2.

Table 2: Test matrix for parametric study

Case ID	IH Break size	Tank inventory	Filter resistance	
			Restricted area	Filter loss coefficient
1	200%	100%	Yes	-
2	200%	80%	Yes	-
3	200%	60%	Yes	-
4	200%	40%	Yes	-
5	200%	20%	Yes	-
6	200%	100%	-	K = 130
7	200%	100%	-	K = 65
8	200%	100%	-	K = 260
9	200%	20%	-	K = 130
10	200%	20%	-	K = 65
11	200%	20%	-	K = 260

RESULTS AND DISCUSSION

Intercode Comparison Results

The comparison results of PCIS performance for seal formation and other important parameters during 200% IH break have been presented using RELAP5 and CATHARE code. These results bring out the comparison of the integrated discharge from the tank (fig 4), leak to the atmosphere (fig 5) for both the codes.

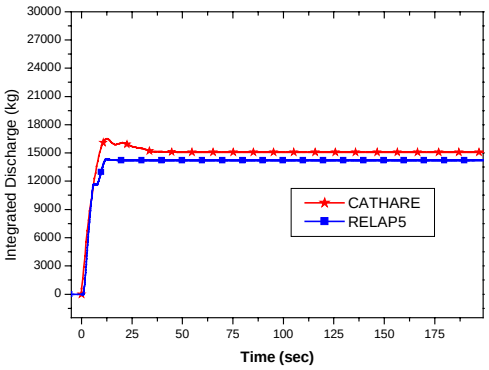

Fig. 4: Water Inventory Discharge from PCIT in to ventilation duct

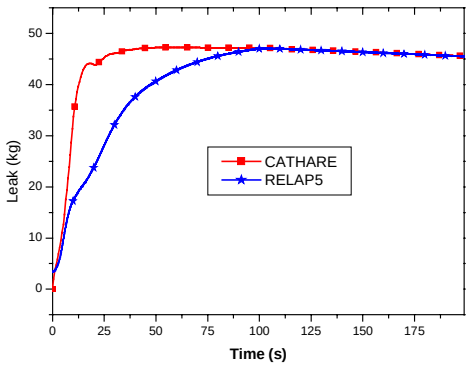

Fig. 5: Integrated leak from Ventilation duct to atmosphere

Fig 6 presents the water level variation in the both side of the U-duct with time against the containment V2 pressure transient for CATHARE and RELAP5. After spilling the water in containment side of u-duct, the water level rise in atmosphere side of U-duct is faster in CATHARE compare to RELAP5.

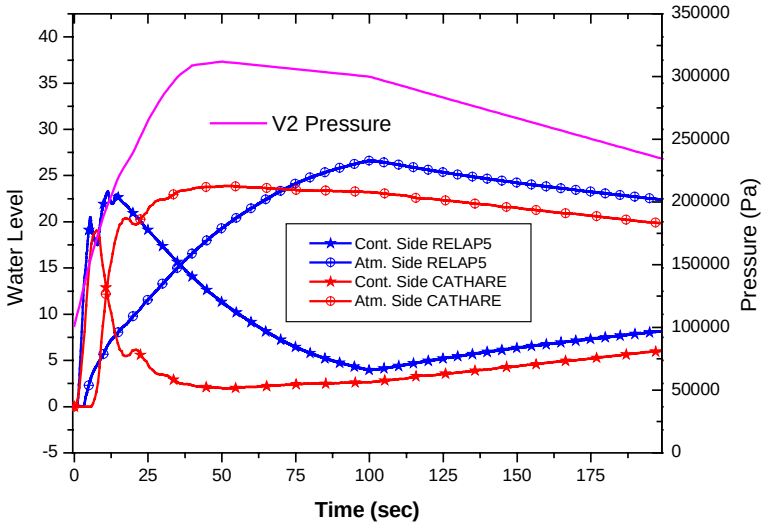

Fig. 6: Water level in ventilation duct & V2 volume pressure

Results of Sensitivity/parametric Studies

The tank water inventory has important role in the liquid seal formation in U tube ventilation duct. With higher pressure in the V1 area than V2 area during LOCA transient in the containment, this pressure difference cause the water in the tank to spill into ventilation duct leading to seal formation. It is clear from the Fig. 7 that till 40% tank inventory, the spilled water is sufficient to form the effective seal in the ventilation duct. The seal formation can be observed for the 100% water inventory case in Fig. 8. The sustained liquid level found in the both leg of U-tube is indicator of water seal formation. The variation in the level in both the legs of ventilation duct during course of the transient can be attributed to change in the V2 pressure over transient duration. The level behaviour during 80% to 40% cases is similar in nature.

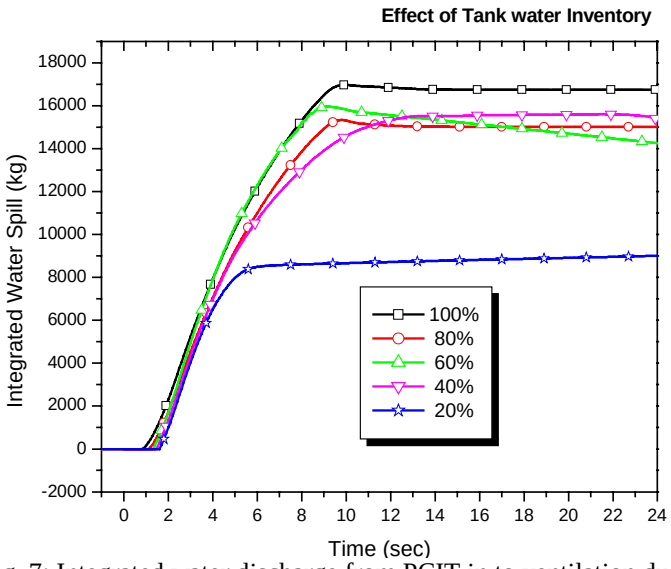

Fig. 7: Integrated water discharge from PCIT in to ventilation duct

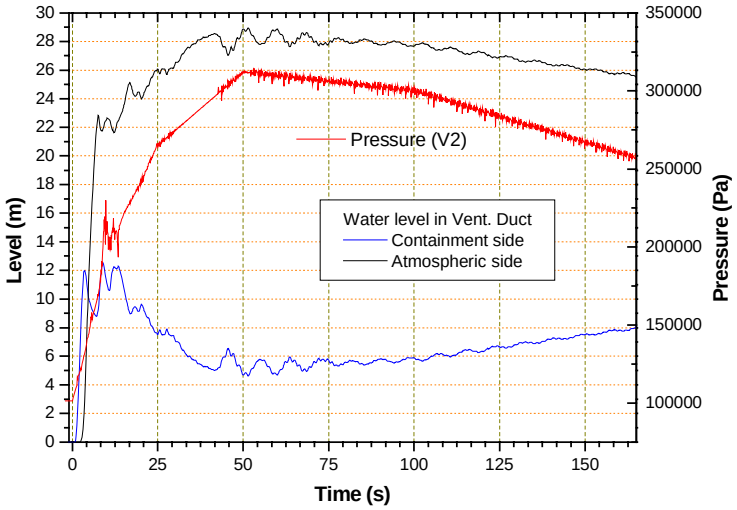

Fig. 8: Water level in ventilation duct & V2 volume pressure (100% inventory)

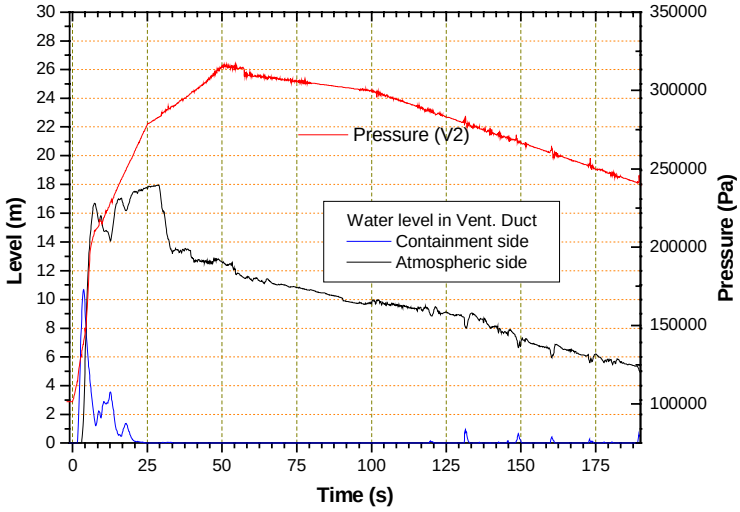

Fig. 9: Water level in ventilation duct & V2 volume pressure (20% inventory)

For the case of 20% tank inventory, the amount of water is not sufficient to hold the water in the duct for seal formation as shown in Fig. 9. The falling level in the atmospheric side leg of the ventilation duct is clearly indicating that water is getting flushed out of the duct over transient and no seal formation is observed.

The leak behaviour during the transient also shows that water seal formation for cases i.e. 105, 80%, 60% and 40% as shown in Fig. 10. It can be seen that leak took place during initial 20 s. The water spilled in the duct pushes the initial air column present in the duct. After the water column is established in both side of ventilation duct, there is no further leak once effective seal formation is observed. This behaviour is not present in the 20% tank inventory case. The case of 20% water inventory, the large amount of water is lost throughout the transient is clear indicator of no seal formation.

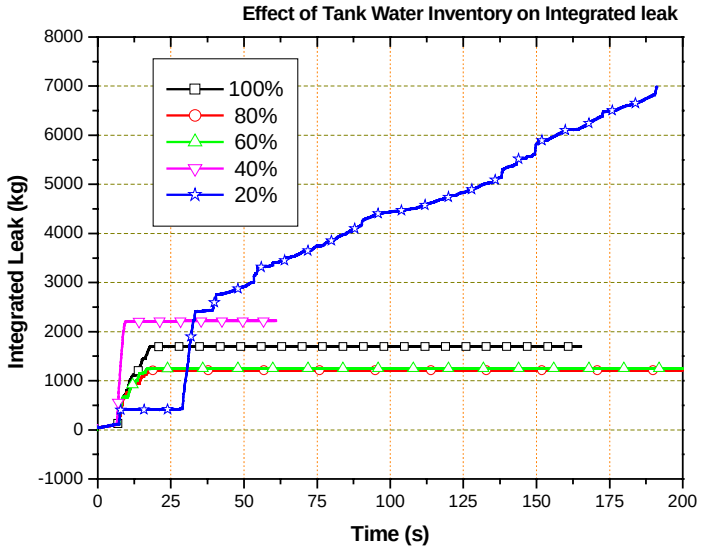

Fig. 10: Integrated leak from ventilation duct in to atmosphere

So, it can be established that except for water inventory less than 20%, the effective seal formation in ventilation duct in a passive manner is observed. The integrated leak is found to be large before seal formation in all the cases. Few more case studies have been performed for 100% tank inventory with varying filter loss coefficient. The results for integrated leak are shown in the Fig. 11. It can be seen that with appropriate loss coefficient, the leak to atmosphere has been reduced quite satisfactorily during the transient duration. This leak is very less compare to earlier cases as shown in Fig. 10.

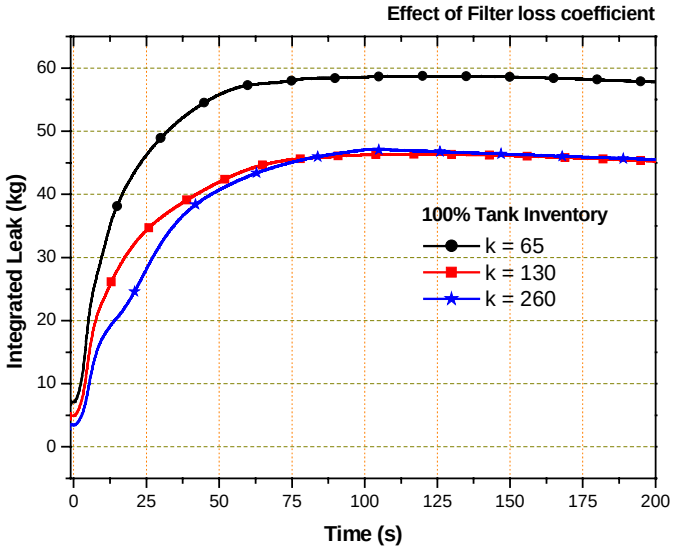

Fig. 11: Integrated leak from ventilation duct (with variation of Filter loss coefficient)

CONCLUSION

The performance of the PCIS is found to be satisfactory for different tank inventory except for 20% tank inventory case. The pressure drop in filter modelled by restricted area is giving higher integrated leak before seal formation. However, modelling with suitable loss coefficient, leak to atmosphere is reduced significantly. The sensitivity studies with different loss coefficient shows that loss coefficient above normal value has no advantage in reducing the leak further. Further, the PCIS has to be tested for the different lower break sizes with varying tank inventory to check the adequacy of design for water seal formation. A coupled calculation of MHT, containment and PCIS system and further reliability study is desired.

REFERENCES

[1] Nayak A. K. and Sinha R. K., "Role of passive systems in advanced reactors" Progress in Nuclear Energy, Vol.49, 2007, pp. 486-498.
[2] Ghosh A.K., Raj V.V., Kakodkar A., "A scheme for passive isolation of the containment of a reactor", Nuclear Safety, Vol.34, No.1, 1993.
[3] Fletcher, G.D., Schultz, R.R., "RELAP5/MOD3.2 Code Manual", Idaho National Engineering Laboratory Idaho, 1995.
[4] Barre F. and Bernard M., "The CATHARE Code strategy and Assessment", Nuclear Engineering and Design, 1990, Vol. 124, pp. 257-284.
[5] Burgazzi L., "State of the art in reliability of thermal-hydraulic passive systems", Reliability Engineering and System Safety, Vol.92, 2007, pp. 671-675.
[6] Haware S.K. et al, "Analysis of Containment of AHWR (920 MWth) following 200% break LOCA", RSD, BARC (2004).

THE SEISMIC FRAGILITY OF BASE-ISOLATED NPP BUILDINGS

F.Perotti[1], M.Domaneschi[1], L.Corradi[2], D.C.Mantegazza[1], G.Bianchi[1]
[1]Department of Structural Engineering, Politecnico di Milano, Piazza Leonardo da Vinci 32, 20133 Milan, Italy
[2]Department of Energy, Politecnico di Milano, Via Lambruschini 4, 20156 Milan, Italy
E-mail of corresponding author: perotti@stru.polimi.it

ABSTRACT

The research work here described is devoted to the development and testing of a numerical procedure for the computation of seismic fragilities for equipment and structural components in Nuclear Power Plants (NPP). The proposed procedure for fragility computation makes use of the Response Surface (RS) Methodology to model the influence of the random variables on the dynamic response. To account for stochastic loading the latter is computed by means of a simulation procedure. Given the RS, the Monte Carlo method is used to compute the failure probability. The procedure is here applied to the preliminary design of the NPP reactor building within the IRIS international project; a base isolation system based on the introduction of HDRB (High Damping Rubber Bearing) elements is considered, leading, on one hand, to a markedly non linear behavior. On the other hand, when supported by an isolation system, the building tends to behave as a rigid body, this allowing for a low-dimensional model for capturing the dynamic response under seismic excitation. The fragility analysis is performed on the basis of a tentative limit-state function relating horizontal and vertical loads applied to isolation devices.

INTRODUCTION

The introduction of isolation systems in the design of strategic buildings is likely to become, in the next future, a widespread seismic protection measure. In fact, the anticipated better performance, when compared to the one of traditional buildings, in terms of acceleration response to design seismic actions, makes isolation techniques a very attractive choice for buildings whose functionality after the event is of utmost importance.

This is the typical case of reactor buildings in future Nuclear Power Plants, where the adoption of isolation systems seems to be almost mandatory if the frequency of earthquake-induced accident scenarios must drop to values of the order of E-08/ry to make the seismic risk of the same order of magnitude if compared to risk related to internal events. In this respect, isolation systems based on High Damping Rubber Bearings (HDRB) represent a highly reliable design solution, given their diffusion and proven reliability; in [9] the application of this solution to the Nuclear Steam Supply System (NSSS) building designed within the IRIS international project [3] is described and some preliminary results are given. These results show how the isolation system is extremely effective in reducing the seismic acceleration transmitted to all structural and equipment components inside the building, this resulting in significant advantages for the design and standardization of the equipment. It must be observed, however, that in such conditions the isolation devices themselves are prone to become the critical components in terms of seismic fragility, since the response attenuation is obtained as the result of large relative displacements between the building and the foundation. Therefore, the need arises to assess the risk associated to the failure of the isolators, this being obviously related to “beyond design” loading conditions.

When the problem of risk evaluation is addressed, the fundamental role played by the hazard definition in the estimation of the seismic-induced CDF is immediately evident; both randomness and uncertainty, however, significantly affect also the evaluation of structural behaviour under extreme loads and thus of seismic reliability. Though randomness cannot be avoided, since is inherent to most of the input data of the analysis, uncertainties, being related to the lack of complete and accurate knowledge about models and methods, must be reduced as much as possible by refining analysis procedures.

In light of the above considerations, the research activity described in the present paper is devoted to the probabilistic evaluation of the seismic performance of a NPP reactor building, focusing on the case in which an isolation system is introduced. An innovative procedure for fragility estimation [6] will be summarized in the next section; an example of application will be subsequently shown with reference to the IRIS (International Reactor Innovative and Secure) system. This is a medium power (335 MWe) pressurized light water reactor under development by an international consortium which includes more than 20 partners from 10 countries (see [3,10])

FRAGILITY ANALYSIS OF NPP BUILDING COMPONENTS

Formulation

Single Following the PEER (Pacific Earthquake Engineering Research) approach (see [7] and references herein), the annual failure rate for a mechanical component under seismic loading can be obtained from the integral:

$$P_f = \iint P\left\{DM > dm_f \,\middle|\, EDP = edp\right\} p_{EDP}(edp \,|\, IM = im)\, p_{IM}(im)\, d(edp)\, d(im) \tag{1}$$

where ***DM*** is a Damage Measure, associated to the assumed limit state (***dm_f*** denotes the damage level at failure), ***EDP*** is an Engineering Demand Parameter (support acceleration, relative displacement,…) expressing the level of the dynamic excitation imposed to the component due to the global seismic response of the structure (reactor building) and ***IM*** is an Intensity Measure (peak ground acceleration, spectral acceleration,…) characterizing the severity of the earthquake motion at the reactor site. As pointed out in [7] all statistics in (1) must be intended in term of annual extreme values, so that the equation delivers a risk estimate in terms of annual probability of failure of the component. For a "simple" equipment component, or for a preliminary evaluation, the limit state can be directly defined in terms of the ***EDP*** value at failure ***edp_f***, thus avoiding the damage analysis step, i.e:

Errore. Non si possono creare oggetti dalla modifica di codici di campo. (2)

where the integrand function can be written in terms of the fragility function ***F(edp,im),*** defined as:

$$F(edp, im) = P\left\{EDP > edp \,\middle|\, IM = im\right\} = 1 - P_{EDP}(edp \,/\, IM = im) \tag{3}$$

When a traditional non-isolated building is considered a typical choice for ***edp*** within the above context is represented by the peak acceleration at the support point of critical pieces of equipment. If a base-isolation system based on HDRB (High Damping Rubber Bearings) is introduced (see for example [11]) the acceleration values inside the building undergo a dramatic decrease. This is obtained at the price of significant relative displacements imposed to isolation devices, which are likely to become the "weakest link" in terms of seismic safety of the building; therefore the extreme value ***u*** of the relative displacement across the most strained isolator is a quite obvious first choice for the ***edp***. The fragility function is therefore expressed as:

$$F(edp, im) = P\left\{U > u \,\middle|\, A_g = a_g\right\} = P_{exc}(u, a_g) \tag{4}$$

For a system under stochastic dynamic excitation, the associated limit state function can be expressed in the following "capacity minus demand" format:

$$g(\mathbf{X}, u, a_g) = C - D(\mathbf{X}, a_g) = u - U(\mathbf{X}, a_g) = 0 \tag{5}$$

where ***U*** is the random variable whose distribution delivers, for fixed **X**, the result of the random vibration analysis.

In [6] linearity of the building response was exploited, in the non-isolated case, for the probabilistic evaluation of the peak motion at the supports of an equipment component; differently, no linearization is here exploited, since the behaviour of HDRB is markedly non-linear, especially at the high level of deformations here anticipated. Once selected the probability distributions of X and U the probability of exceeding the limit state (6), i.e. the integral

$$P_{exc}(u, a_g) = \iiint_{g<0} p_U(u, \mathbf{x})\, du\, d\mathbf{x} \tag{6}$$

could be computed, in principle, by direct application of the Monte Carlo Simulation (MCS) method; in fact the statistics of response U(X) is algorithmically known, i.e. can be deterministically computed by structural dynamic analysis for every realization of the random variables **X**. It must be considered, however, that a huge computing time and cost would be required for running a non-linear dynamic analysis, as it is the case for isolated systems of the

type here considered, for the number of evaluations which are necessary for MCS, especially for the estimation of small probabilities.

Limit-state approximation via Response Surface Methodology

For the above consideration, according to the well-established Response Surface Methodology (RSM - [8], the "true" response function is replaced by a simple analytical representation. Here, assuming that the distribution of $\boldsymbol{U}$ can be described by its mean value μ_U and its standard deviation σ_U, the so called "dual response surface" approach [12] has been adopted for modelling their dependency on X. Assuming that the same model can be used for the mean and the standard deviation the following response functions have been introduced:

$$\mu_U(\mathbf{X}) = \sum_{i=1}^{m} \boldsymbol{a_i} \boldsymbol{z_i}(\mathbf{X}) + \varepsilon_\mu \qquad \sigma_U(\mathbf{X}) = \sum_{i=1}^{m} \boldsymbol{b_i} \boldsymbol{z_i}(\mathbf{X}) + \varepsilon_\sigma \tag{7}$$

where the $\boldsymbol{a_i}$'s and $\boldsymbol{b_i}$'s are coefficients to be estimated, the $\boldsymbol{z_i}$'s are usually polynomial functions and two "error" terms (ε_μ, ε_σ) are introduced as a zero mean random deviations. The latter account for the variability of estimated quantities and for the lack of fit of the adopted model, i.e. for the inadequate analytical form of the RS's and for missing variables (i.e. not comprised in (8) though influencing the response). To compute the coefficients in (8) a number of experiments must be run according to the chosen experimental design; at each of them the random vibration problem can be addressed via either an analytical or a simulation approach. In the second solution, here adopted, a sample of ground motion realizations must be generated, according to the spectral parameters appearing in X. For each realization, the extreme value of $\boldsymbol{U}$ is computed (e.g. via FE modelling and step-by-step analysis); the mean and variance of $\boldsymbol{U}$ are then estimated. The procedure is repeated for all experimental points, leading to n observed values for the statistical parameters of $\boldsymbol{U(X)}$.

We shall assume in the following that the experiments are performed in homogeneous conditions (i.e. differing for the $\boldsymbol{x_i}$ values only), that their results are independent and that the error terms are normal with constant variance; under these hypotheses an unbiased estimate of the coefficients $\boldsymbol{a_i}$,$\boldsymbol{b_i}$ can be obtained by the Least Square (OLS) method, independently of the variance of the error terms (ε_μ, ε_σ). An unbiased estimate of the latter terms can be subsequently obtained is defined, in terms of the residual values. Once models (8) are established, MCS can be carried on. In all applications here shown a Central Composite Design has been adopted for defining the experimental points.

Note that, differently from the linear case, analyzed in [6], the Response Surface evaluation must be repeated for every value of peak ground acceleration, this representing, potentially, a huge computational task. It can be considered, however, that in the isolated case the seismic behavior of the building can be captured, to the aim of evaluating the isolators' performance, by means of very simple mechanical models; the latter, in fact, can be based on the hypothesis of rigid-body motion of the building above the isolators.

As a second option the "capacity minus demand" function (10) can be associated to a limit state function [5] expressed in terms of horizontal and vertical loads acting on the most severely strained isolator; for typical HDRBs, made by alternate rubber and steel layers, the limit state here considered is the "first damage" condition related to the attainment of an admissible peak tensile stress at the steel-rubber interface. In this light and with reference to Fig. 1, demand is here defined, at each instant, as the distance between the points describing the static vertical loading on the isolator (point S) and the current loading (point C), while capacity is computed as the total distance, measured along SC, between the static loading condition and the limit state surface (point L). Both are made non-dimensional with respect to the capacity so that the EDP is represented by the ratio SC/SL, this being the inverse of the "instantaneous" safety factor, while the limit value $\boldsymbol{edp_f}$ takes a constant unit value. Under these assumption and criteria the limit-state function takes the form:

$$\boldsymbol{g}(\mathbf{X}, \boldsymbol{a_g}) = \boldsymbol{C} - \boldsymbol{D}(\mathbf{X}, \boldsymbol{a_g}) = 1 - \frac{\boldsymbol{SC}(\mathbf{X}, \boldsymbol{a_g})}{\boldsymbol{SL}(\mathbf{X}, \boldsymbol{a_g})} = 0 \tag{8}$$

As an alternative, the actual distance CT can replace CL in the formulation of the safety factor. Note that considering first damage instead of actual failure in the formulation of the limit state surface appears to be reasonable choice until a complete experimental characterization of the behaviour of large HDRBs at collapse will be available.

Finally, in [6], a risk-based procedure for refining the Response Surfaces and the evaluation of the failure probability is proposed for the linear case; application to non-linear systems is at study.

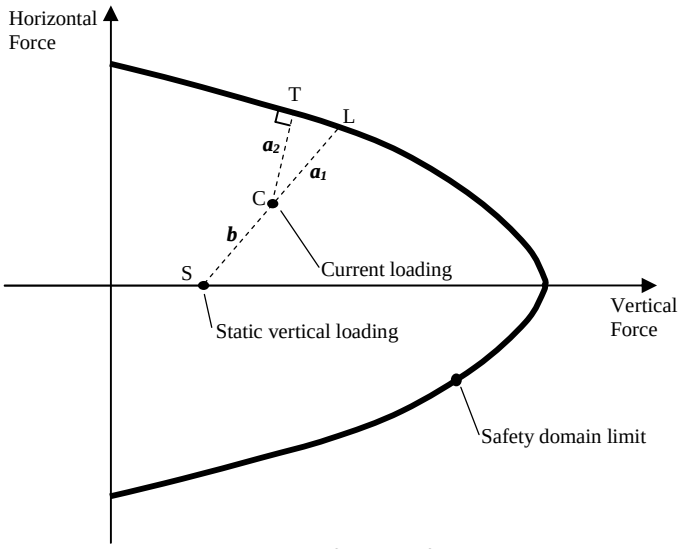

Fig.1: Limit state function for the isolator

EXAMPLE OF APPLICATION

The isolated IRIS NSSS building

The above described procedure has been applied to the analysis of a preliminary design of the reactor building of IRIS (International Reactor Innovative and Secure). This is a medium power (335 MWe) pressurized light water reactor under development by an international consortium which includes more than 20 partners from 10 countries (see [3,10]). Installation in a site characterized by a low-to-average seismicity level has been here assumed.

In a tentative design of the NSSS building (see Fig. 2a), the introduction of an isolation system was considered; the system is made by High Damping Rubber Bearings (HDRB) installed between the foundation slab and the base (Fig. 2b). The main scheme of the isolators layout, as considered in the preliminary design approach, is depicted in Figs 2c-d. The HDRB devices are made of alternated rubber layers and steel plates, bonded through vulcanization. Damping factor ranges from 10% to 20%, while shear modulus (G) lies in the 0.8-1.4 MPa range.

Steel plates give a high vertical stiffness to the isolator, though allowing large horizontal deformations. Therefore, the isolated building has low natural frequencies for motions lying in the horizontal plane, typically in the range 0.5 - 0.7 Hz, where the spectrum of ground motion has generally quite low energy. In such vibration modes the isolated building moves like a rigid body over the isolators, which are strained in shear (continuously carrying the dead load). The absolute acceleration of the building can be much smaller than the PGA, with no amplification at higher floors. This is obtained at the price of large relative displacements between the building and the adjacent ground; this can be a problem for the design of the expansion joints and the connections with non isolated buildings of all the pipelines and service networks. The design of the isolation system, therefore, must reach a reasonable compromise between limitation of absolute accelerations and relative displacements. For the case of the IRIS NSSS, having a fixed-base first natural frequency of 5.91 Hz (on firm ground) and natural frequencies around 9 Hz for the vessel local motion, this led to a 0.7 Hz isolation frequency, i.e. to a value which can be seen as an upper limit for the parameter. If some equipment component (e.g., some wide span pipeline) has a lower natural frequency a local specific measure (stiffening or energy dissipation device) must be adopted.

The choice of 0.7 Hz as isolation frequency limits the relative displacement between the isolated building and the ground to 10 cm at the SSE level which is advantageous both for the performance of the isolators in beyond design conditions and for the design of steam lines connecting the NSSS building with the turbine units.

Dynamic modeling and fragility analysis criteria

In the following, to compute the fragility of the IRIS isolation system a simplified approach will be followed with reference to the following aspects.

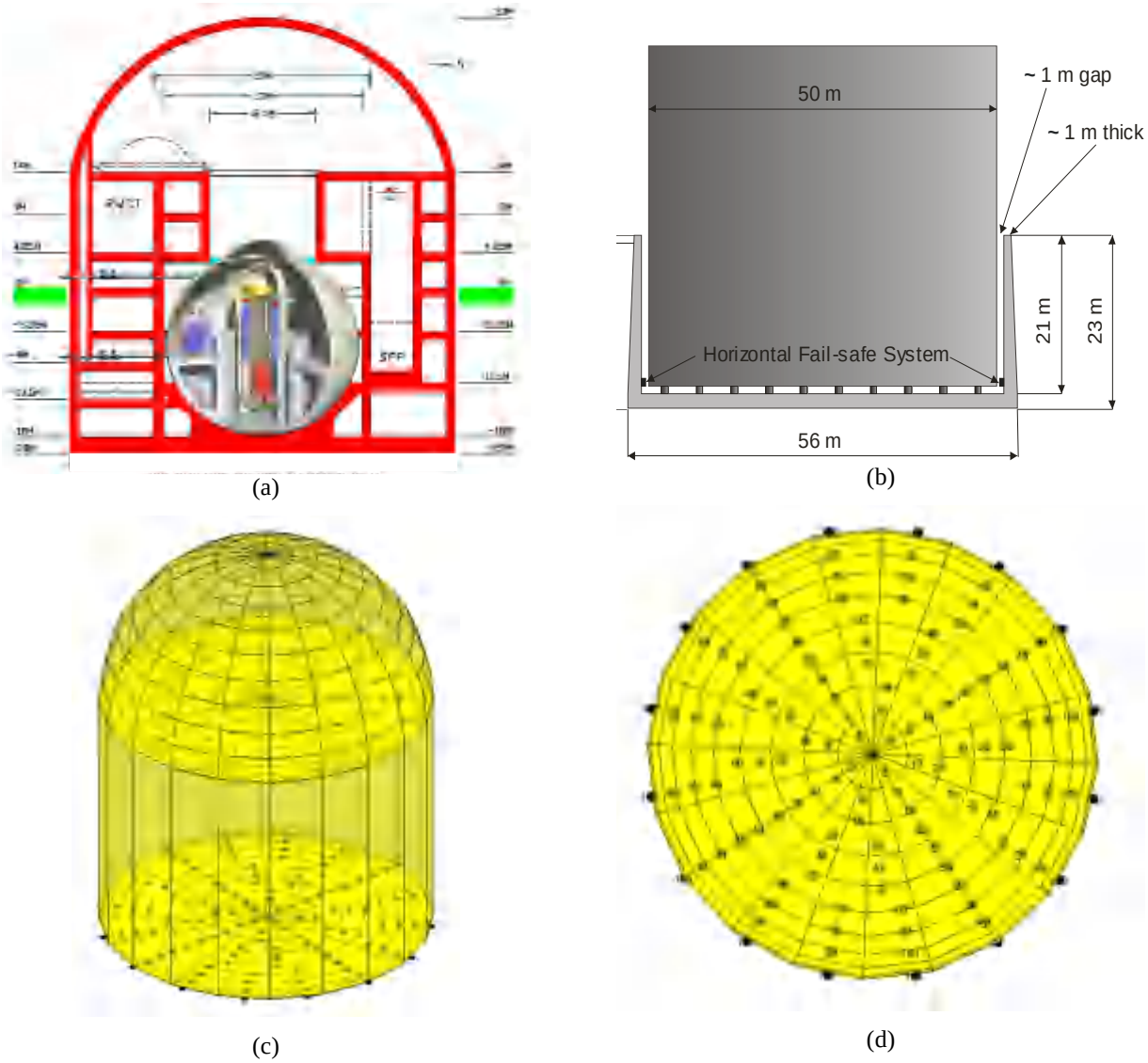

Fig. 2: IRIS NSSS building (a); isolation system (b); isolators layout (c-d)

- A 6-DOF plane model has been adopted for the reactor building, under the hypothesis that the isolated superstructure behaves like a rigid body; soil-structure interaction has been neglected.
- The behavior of isolators under horizontal and vertical loading has been regarded as independent; it is assumed that isolators behave as linear elastic under vertical loading, showing the same stiffness in tension and compression. Their non linear behavior under horizontal loading has been modeled according to the two-dimensional model described in [1].
- To define the limit state function (Fig. 1), it was assumed, as a tentative criterion, that under the static vertical load a 400% shear deformation leads to the attainment of an admissible peak tensile stress at the steel-

rubber interface. This rather drastic assumption allows for the definition of the limit domain in the σ-τ plane by the straightforward numerical methodology proposed in [5]. Subsequently, the domain is expressed in terms of the horizontal and vertical forces acting on the most severely strained isolator. In parallel research activity the refinement of the limit state function is pursued.

- The seismic input has been introduced by means of twenty artificial time histories, whose spectra individually match the response spectrum prescribed by Regulatory Guide 1.60.

Four independent random variables have been considered in the fragility analysis; two of them account for the uncertainty of the limit state function (Fig.1). A parabolic shape has been assumed, governed by two coefficients which have been taken as lognormal with mean value, equal to the one obtained via the procedure [5], and c.o.v. equal to 0.22.

The other two random variables account for the randomness of the dynamic properties of the isolator, represented via the model in [1]; according to this the restoring force is the sum of three contributions, i.e. an elastic-plastic model ($\boldsymbol{F_2}$ contribution) and two elastic non-linear springs, namely a non-linear elastic spring ($\boldsymbol{F_1}$) and an hardening spring ($\boldsymbol{F_3}$); the model allows to reproduce analytically some aspects of the experimental behavior of laminated rubber bearings. In light of these observations the resulting scheme for the Fujino model is represented in Fig. 3a [1].

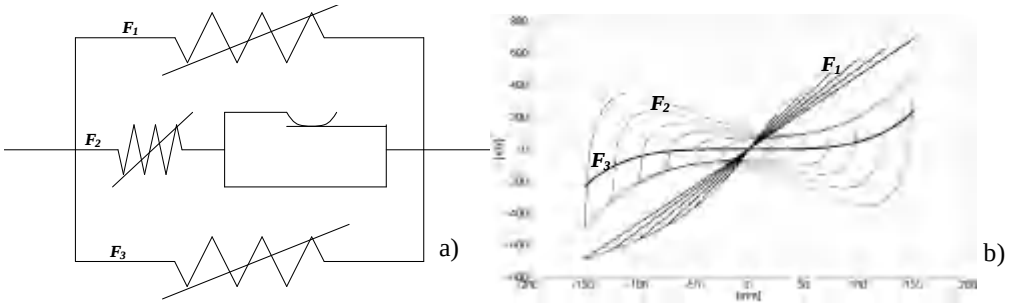

Fig. 3: Hysteretic model for the seismic isolators (a); $\boldsymbol{F_1}$,$\boldsymbol{F_2}$,$\boldsymbol{F_3}$ components of the total isolator reaction force $\boldsymbol{F}$ under cyclic loading (b)

From an analytical point of view the force-displacement relation for the first non-linear spring consists of

$$\boldsymbol{F}_1 = \boldsymbol{K}_1 \left[\beta + (1-\beta)\exp\left(-\frac{\boldsymbol{U}_{\max}}{\alpha}\right)\right] \boldsymbol{U} + \boldsymbol{a}\left[1-\exp(-\boldsymbol{b}|\boldsymbol{U}|)\right]\mathrm{sgn}(\boldsymbol{U}) \tag{9}$$

Where $\boldsymbol{U}$ is the relative displacement and $\boldsymbol{K_1}$, $\boldsymbol{a}$ e $\boldsymbol{b}$ parameters. In Equation (9), the first term reproduces the force linear evolution, while the second one the non-linear behavior. In Fig. 3b the $\boldsymbol{F_1}$ contribution is depicted for a cyclic experimental test as force-displacement diagram up to displacement values equal to 300% of the rubber height and the stiffness degradation during the variable cycle amplitude is highlighted.

The hysteretic contribution $\boldsymbol{F_2}$ is described by the differential equation

$$\dot{\boldsymbol{F}}_2 = \frac{\boldsymbol{Y_t}}{\boldsymbol{U_t}}\dot{\boldsymbol{U}} - |\dot{\boldsymbol{U}}|\left|\frac{\boldsymbol{F}_2}{\boldsymbol{Y_t}}\right|^{\boldsymbol{n}}\mathrm{sgn}\left(\frac{\boldsymbol{F}_2}{\boldsymbol{Y_t}}\right) \tag{10}$$

The values of $\boldsymbol{Y_t}$ and $\boldsymbol{U_t}$ are defined as

$$Y_t = Y_0(1+\left|\frac{U}{U_H}\right|^p) \quad ; \quad U_t = U_0(1+\frac{U_{\max}}{U_S}) \tag{11}$$

where Y_0 is the initial yielding force, U_0 the initial yielding displacement, U_H the displacement where hardening starts, U_S a parameter for controlling the degradation of the elastic stiffness of the elasto-plastic spring, U_{max} the maximum displacement experienced during the loading history, p a parameter governing the shape of the hardening branch. Fig. 3b depicts the hysteretic components F_2 when the displacement is imposed according to loading cycles of increasing amplitude.

Finally a new non-linear spring is introduced in parallel for capturing the increment of the tangential stiffness experienced by the devices at very high strain levels. This results in the F_3 contribution (see also Fig. 3b), defined mathematically as

$$F_3 = K_2\left|\frac{U}{U_H}\right|^r U \tag{12}$$

where r is the parameter to prescribe the shape of the hardening curve, K_2 the proportional constant to describe the contribution of the hardening spring to the other springs.

To account for the randomness of the dynamic properties of the isolator, represented via the model in [1], a first random variable has been introduced to control the stiffness of the elastic parts by modifying the K_1, a, K_2 and U_0 parameters. The second random variables affects the energy dissipated by the hysteretic portion by modifying the yielding force Y_0. The two r.v.'s are lognormal; for both the mean value is one, which means adopting the values obtained by fitting experimental results, and the c.o.v. is equal to 0.22.

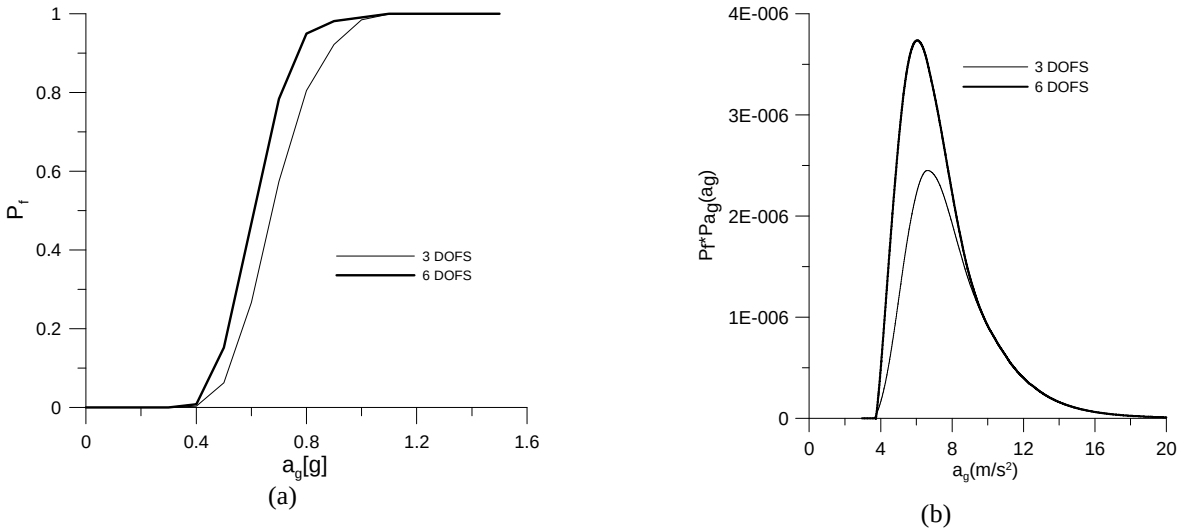

Fig. 4: (a) fragility function, (b) risk integrand function

In Fig. 4 the results of the analysis are presented; in 4a the fragility function relating the exceedance of the limit state function to the peak ground acceleration. In Fig. 4b the integrand function in the risk evaluation (eq. 2) is given; in the evaluation a prototype low-to-medium seismicity site has been considered, characterized by a return

period of about 10000 years for a 0.32 ***g*** PGA. The results here obtained are compared to those given in [13], where a 3-DOF plane model has been used in the dynamic analyses.

The curves given in Fig. 4b clearly point out the PGA range mostly contributing to the risk related to the isolators failure; this is the range in which both mechanical models and fragility analysis tools (e.g. the response surfaces) have to be refined and calibrated. Note that, even though the risk analysis has been here performed according to some crude assumptions, the capabilities of the proposed procedure are highlighted.

As a further development of the procedure, more consistent and refined criteria for defining the limit state function of the isolators are pursued; this activity, which is presently based on extensive finite element testing, will benefit, in the future, by the performance of an experimental campaign.

CONCLUSIONS

A procedure for estimating the fragility of seismic isolation systems in NPP buildings is under development and testing; in this paper a simple example has been shown illustrating the adopted criteria for evaluating the seismic performance of the isolation devices and the associated risk. The procedure delivers the risk associated to the isolators failure and the PGA range mostly contributing to the risk itself, this being a fundamental information for the calibration and refinement of mechanical models and fragility analysis tools.

ACKNOWLEDGMENTS

The financial support from CIRTEN (Consorzio Interuniversitario per la Ricerca Tecnologica Nucleare) is gratefully acknowledged. Marco Magli and Gianluca Barbaglia developed the isolated NPP model in partial fulfillment for the requirements of the Bachelor's Degree in Civil Engineering at Politecnico di Milano, under the guidance of the Authors. Their contribution is gratefully acknowledged.

REFERENCES

[1] Abe M., Yoshida J., Fujino Y., "Multiaxial Behaviors of Laminated Rubber Bearings and Their Modeling. II: Modeling", ***ASCE Journal of Structural Engineering***, Vol. 130, 2004, pp. 1133-1144.

[2] Bianchi G., Mantegazza D.C., Perotti F., "Dynamic modelling for the assessment of seismic fragility of NPP components", ***Proc. of SMiRT 19***, Toronto, Canada, August 2007.

[3] Carelli M.D. et al., "The Design and Safety Features of the IRIS Reactor", ***Nucl. Eng. Des.***, Vol. 230, 2004, pp. 151-167.

[4] CEN, 2005. Eurocode 8, Design of structures for earthquake resistance - Part 1. General rules, seismic actions and rules for buildings. EN 1998-1(2005).

[5] Corradi L., Domaneschi M. and Guiducci C., "Assessing the reliability of seismic base isolators for innovative power plant proposals", ***Proc. of SMiRT 20***, Helsinki, Finland, August 2009.

[6] De Grandis S., Domaneschi M. and Perotti F., "A numerical procedure for computing the fragility of NPP components under random seismic excitation", ***Nucl. Eng. Des.***, Vol. 239, 2009, pp. 2491-2499.

[7] Der Kiureghian A., "Non-ergodicity and PEER's framework formula", ***Earth. Eng. Struct. Dyn.***, Vol. 34, 2005, pp. 1643-1652.

[8] Faravelli L., "Response surface approach for reliability analysis", ***ASCE J. of Eng. Mech.***, Vol. 115, 1989, pp. 2763-2781.

[9] Forni M. et al., "Seismic Isolation of the IRIS Nuclear Plant", ***2009 ASME Pressure Vessels and Piping Conference (PVP)***, Prague, July 2009.

[10] Maioli A. et al., "Risk-Informed Design Process of the IRIS Reactor", Proc***. of ANS PSA'05 Conference***, San Francisco, September 2005, paper 138095.

[11] Perotti F. et al., "Seismic Isolation of the IRIS NSSS Building", ***Proc. of SMiRT 20***, Helsinki, Finland, August 2009.

[12] Towashiraporn P., "Building seismic fragilities using response surface metamodels". Thesis in partial fullfillment of PhD deg. in Civ. and Env. Eng., Georgia Institute of Technology, 2004.

[13] Bianchi G, Corradi Dell'Acqua L., Domaneschi M., Mantegazza D., Perotti F., "A procedure for the computation of seismic fragility of NPP buildings with base isolation", ***International Topical Meeting on Probabilistic Safety Assessment and Analysis – PSA2011***, Wilmington NC, USA, 2011. ISBN 978-0-89448-089-8.

RESPECTIVE ROLE OF THE VERTICAL AND HORIZONTAL COMPONENTS OF AN EARTHQUAKE EXCITATION FOR THE DETERMINATION OF FLOOR RESPONSE SPECTRA OF A BASE ISOLATED NUCLEAR STRUCTURE – APPLICATION TO GEN IV REACTORS

N.Moussallam[1], V.Vlaski[2]
[1]AREVA Engineering & Projects, Mechanical Engineering Lyon Department, Structural Analysis Section
[2]AREVA Engineering & Projects, Civil Structural Engineering Offenbach Department, Structural Dynamics Section
E-mail of corresponding author: nadim.moussallam@areva.com

ABSTRACT

Several nuclear energy systems, identified as GEN IV technologies, such as Liquid Metal Fast Breeder Reactor (LMFBR) must resist high temperature transients and do operate at relatively low internal pressure levels. Therefore, most of the components constituting these reactors are thin compared to their PWR counterparts. This induces a specific vulnerability to strong seismic loadings. For this reason, seismic base isolation is considered a very promising option. Its main goal, for this application, would be to decrease the loading on the components and systems by reducing the floor response spectra at their anchorage points. Despite some historical practices, the floor response spectra of a seismically isolated structure can not be properly determined using stick models or multi-degree of freedom spring mass models. Such models would actually lead to an over-estimation of the base isolation efficiency in the horizontal direction. Indeed, the vertical excitation component of the earthquake does excite some modes with significant local horizontal accelerations. As a result, the horizontal floor response spectra do exhibits significant peaks at frequencies higher than the isolation frequency. The representation of these local modes does generally require 3D modeling. The opposite phenomenon is also observed: the horizontal excitation does excite some modes with significant local vertical accelerations. Given that the horizontal excitation is filtered by the base isolation system, the vertical floor response spectra can be significantly reduced. By changing the vertical stiffness of the base isolation system or adding some damping in this direction useful design tools are available in order to influence both the horizontal and the vertical floor response spectra.

INTRODUCTION

In the recent decades, the seismic levels applied for the design of nuclear power plants have been constantly increased. Recent events in Japan, which have led to a halt in the functioning of the Kashiwazaki-Kariwa power plant in 2007 and the Fukushima accident in 2011 indicate that the design seismic levels may be subjected to further increase in a certain number of countries. As a result, it is becoming increasingly difficult to design a nuclear reactor in regions with high seismicity and the use of seismic base isolation system is expected to provide a much needed alternative to a constant strengthening of the structures, systems and components.

In the case of GEN IV reactors, and more specifically in the case of Liquid Metal Fast Breeder Reactors (LMFBR), several characteristics of their designs make the seismic problem even more stringent. Indeed, the primary and secondary circuits of these reactors are constituted of thin metallic vessels, shells and pipes, which are prone to buckling or plastic instability when submitted to dynamic loading. This is due for one part to the relatively low pressures inside these structures, when compared to the pressures encountered in usual light water reactors, and for the other part to the high thermal transients to which these structures may be submitted. Thin shells ensure a rapid conduction of the heat through the thickness, which keeps the peak thermal stresses in the allowable domain. A list of the design issues associated to the seismic loading for LMFBR is given in an AIEA report written by Gibert & Martelli [1].For LMFBR reactors of the 4th generation, whose safety level must be at least the same as the present safety level for GEN III reactors, it is foreseen that seismic base isolation systems will probably be required even for sites with moderate seismicity. The principal motivation in implementing these systems will be to lower the seismic loadings on the components and systems inside the buildings. In purely analytical terms, the isolation systems must be designed to produce as low as possible floor response spectra. This objective differs significantly from the one usually associated with seismic isolation systems in civil construction, which is to protect the buildings themselves. This may explain why the phenomena described in the present article seem to have been discovered only recently and are not addressed in the appropriate literature.

In the first part of this article, the expected "ideal" functioning of a seismic isolation system will be recalled, as well as some phenomena that are known to alter this "ideal" functioning. In the second part, it will be shown that the 3 dimensional nature of the seismic excitation might lead to spectra significantly different from the "ideal" ones for structures such as those encountered in the nuclear industry. The demonstration will be based on simple test cases. The third part illustrates the phenomena, as they are observed on a complete model of Gen IV nuclear island. A last part will concentrate on how the designer can improve the behavior of a seismically isolated structure.

"IDEAL" AND ACTUAL EFFECT OF A SEISMIC ISOLATION SYSTEM ON FLOOR RESPONSE SPECTRA FOR A PURELY HORIZONTAL EXCITATION

A seismic isolation system does basically act as a filter between the ground excitation and the isolated super-structure. An abundant literature exists on the subject, as for example the excellent book from Naeim and Kelly [2]. Many different systems are available, with low or high damping, pseudo-linear or completely non linear behavior. The principle is always to modify the dynamic behavior of a set of buildings denoted as the "super-structure" in order to increase the level of acceptable seismic loading. In the case of nuclear components design, the modification should uncouple the main buildings modes from the internal components modes, to avoid resonance phenomena. The range of components eigen frequencies being generally comprised between 3 and 20 Hz, the isolation system will classically be designed to shift the main horizontal building modes from a few Hz to below 1 Hz. This is achieved by introducing "soft" elements between the super-structure and the ground, the most classical of which are elastomeric rubber bearings. Isolation is usually not implemented in the vertical direction because the components sensitivity to vertical seismic loadings is lower.

The effect of the implementation of a horizontal isolation system below a super-structure is that the whole system "super-structure + isolation" have a behavior close to the one of a single degree of freedom oscillator. The super-structure being very stiff compared to the "soft" isolation system, it should almost not be excited by the filtered excitation signal. The floor response spectra in horizontal direction of such a structure are expected to:

- be constant along the height of the super-structure,
- exhibit a peak at the isolation frequency, which amplitude and width do only depend on the damping associated to the isolation system,
- exhibit a plateau after the peak, which value is equal to the value of the ground spectra for the isolation frequency.

An example of such expected "ideal" floor response spectra is given in Fig. 1, along with the ground response spectra corresponding to the time-history that have been used as an input. Such ideal floor response spectra can be obtained by simple spring-mass models.

Departing form this "ideal" behavior, it has been well established ([2], [3]) that even with a purely horizontal excitation, the floor response spectra of an isolated super-structure may exhibit some peaks at frequencies corresponding to the non isolated super-structure's modes, i.e. frequencies higher than the isolation frequency. The excitation of these higher frequency modes is due to the still existing (even if largely reduced) participation factors associated to these modes in the horizontal direction and to the damping effects. Indeed, for systems with high damping values, the damping forces between the ground and the isolated super-structure become significant and the frequency content of these forces is not filtered. For low values of damping, an illustration of a typical actual floor response spectrum obtained with a purely horizontal excitation in given in Fig. 2.

Moreover, recent studies [4] have underlined the fact that for seismically isolated structures, the rocking excitation, which effects are assumed to be negligible in most seismic analyses, may become significant. This is because the horizontal excitation's importance has been largely reduced by the isolation system. This aspect is difficult to treat since there is a lack of information and regulations concerning this type of excitation. No rocking excitation was considered in the analyses which results are presented here.

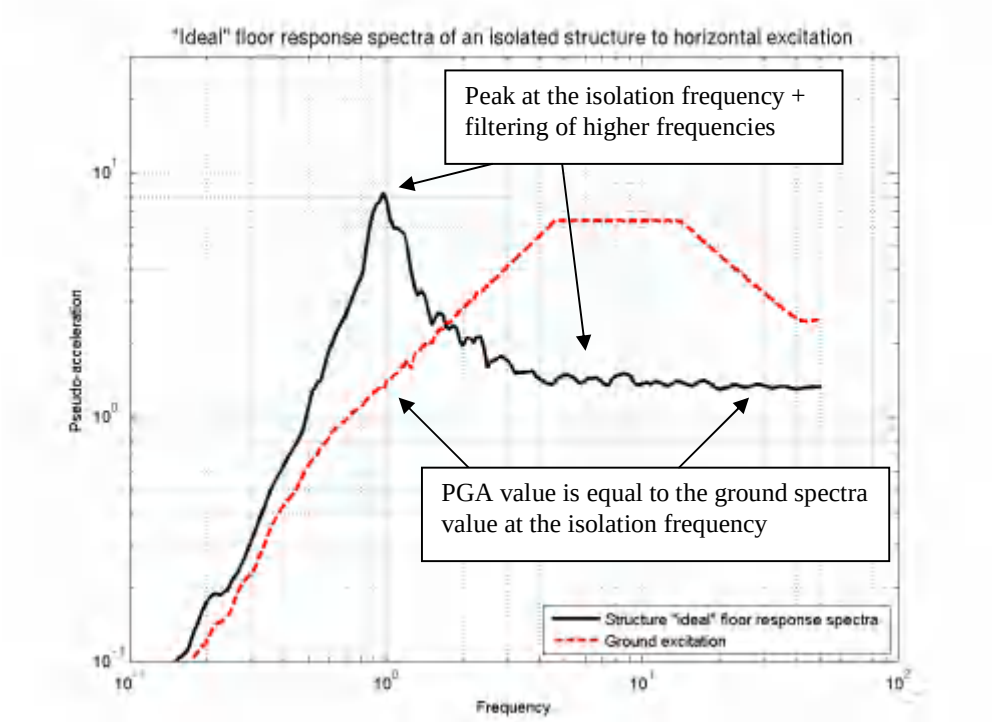

Fig.1: "Ideal" floor response spectra of an isolated structure to a purely horizontal excitation (time-history)

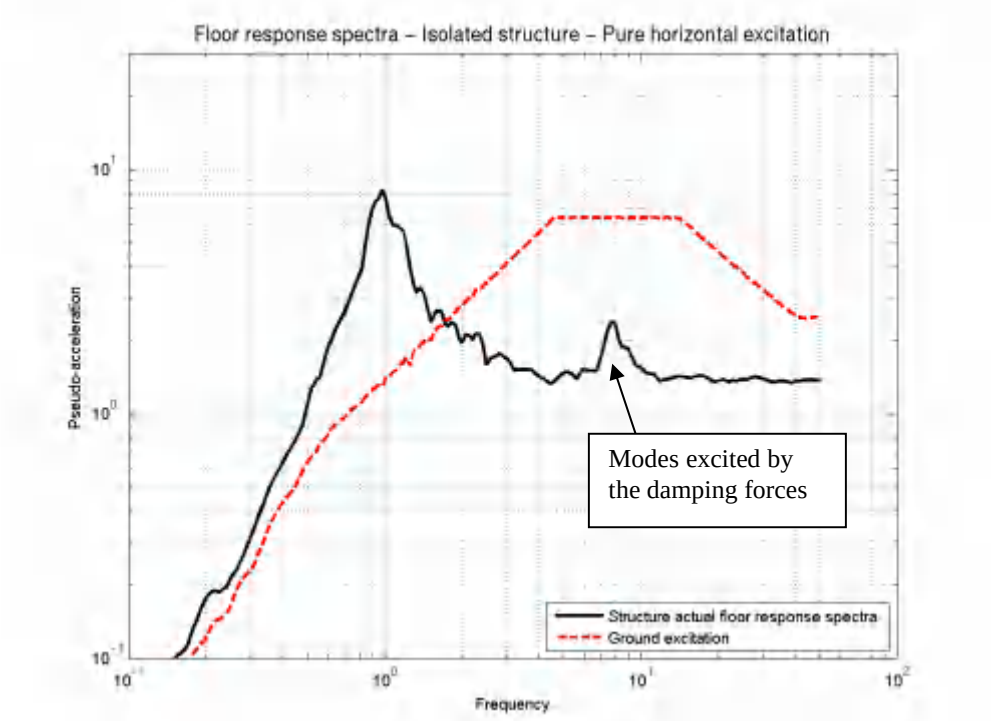

Fig.2: Actual floor response spectra of an isolated structure to a purely horizontal excitation (time-history)

INFLUENCE OF THE VERTICAL EXCITATION ON HORIZONTAL FLOOR RESPONSE SPECTRA - TEST CASES

If the whole system "super-structure + isolation" is assumed to be linear, the contribution of the vertical and horizontal seismic excitation can be computed separately and then linearly added to obtain the 3-dimensionnal response of the structure. This method is typically the one employed in many calculations of the behavior of a seismically isolated structure. The problem lies in the fact that it is very commonly assumed that floor response spectra in the horizontal direction are mainly due to the horizontal excitation and floor response spectra in the vertical direction are mainly due to the vertical excitation. Horizontal and vertical floor responses spectra are then computed with different simplified models, typically stick models, and it is assumed that the interaction is negligible. It will be demonstrated hereafter that this assumption is not valid for base isolated structures. Let us consider three very simple 2D structures:

- The first case is a perfectly symmetrical rectangular frame constituted of two lateral walls and two horizontal floors. It represents an autonomous well balanced building with a stiffness distribution exactly fitting its mass distribution and a regular stiffening of the walls by the floors. The structure is illustrated in Fig. 3a. The first vertical mode of this structure is illustrated in Fig 4a. A possible corresponding structure in a power plant is a containment building uncoupled from all other external buildings, as illustrated in Fig. 5a.
- The second case is similar to the first one, except for one lateral wall, which stiffness is twice lower than in the previous case. It represents the very common situation of a building linked to another structure on one side and self standing on the other side. It is also representative of any discrepancy between the stiffness distribution and the mass distribution within a building. Such discrepancy leads to modes which have significant participation factors in both the horizontal and the vertical directions. A purely vertical excitation of the structure will lead to significant horizontal displacement of certain points of this structure. The structure is illustrated in Fig. 3b. The first vertical mode of this structure is illustrated in Fig 4b. A possible corresponding structure in a power plant is a fuel building, rigidly linked to another stiffer building (containment or airplane crash shell) on one of its side, as illustrated in Fig 5b.
- The third case is similar to the first one, except for the upper floor that has been suppressed. It represents the case of large halls with wide lateral walls and a lack of floors linking these walls. It is also representative of any symmetrical structure for which a purely vertical mode with no participation in the horizontal direction can generate symmetrical horizontal displacement of several points of the structure. The structure is illustrated in Fig. 3c. The first vertical mode of this structure is illustrated in Fig 4c. Possible corresponding structures in a Gen IV power plant are the steam generator buildings, which are located outside the reactor building. The design of the steam generator might result in rather elongated buildings linked to the reactor building up to a certain altitude. A schematic of this configuration is given in Fig 5c.

For each of these three cases, the structure is supported on its two lower corners. The support for each corner is either fixed or mounted on a spring representing a horizontal isolation device. The isolation frequency is 1 Hz in the horizontal direction. All three structures have a main horizontal mode located at 1 Hz and representing more than 99 % of the participating mass in this direction. In the vertical direction, the isolation devices are 100 times stiffer than in the horizontal direction.

The three test cases were submitted simultaneously to synthetic acceleration time histories in the horizontal and vertical directions. The time histories correspond to the spectral curves of the European Utility Requirements [5] document for hard soil. The horizontal response spectra obtained on the upper part of the structure are given in Fig. 6a to Fig. 6c. On each part of the figure, the envelope response spectra of all points located on the upper part of the structure are given for one test case, with and without seismic isolation devices. Several observations can be derived from these figures:

- In all cases, except in the vicinity of the isolation frequency, the implementation of isolation devices in the model is resulting in significantly lower floor response spectra.
- Even though a modal analysis of these three isolated structures would define them as having a unique participating mode in the horizontal direction, it does not mean that the horizontal floor response spectra of these structures are identical. This is because, for an isolated structure, the vertical loading results in horizontal local displacements of the structure which are not negligible.
- The effect of the vertical acceleration on horizontal floor response spectra might significantly reduce the effectiveness of the seismic isolation system and become the leading constraint on the design of

components and systems. Therefore, the vertical and horizontal analysis shall be combined, if not carried at once, for determining the floor responses spectra of base isolated structures.

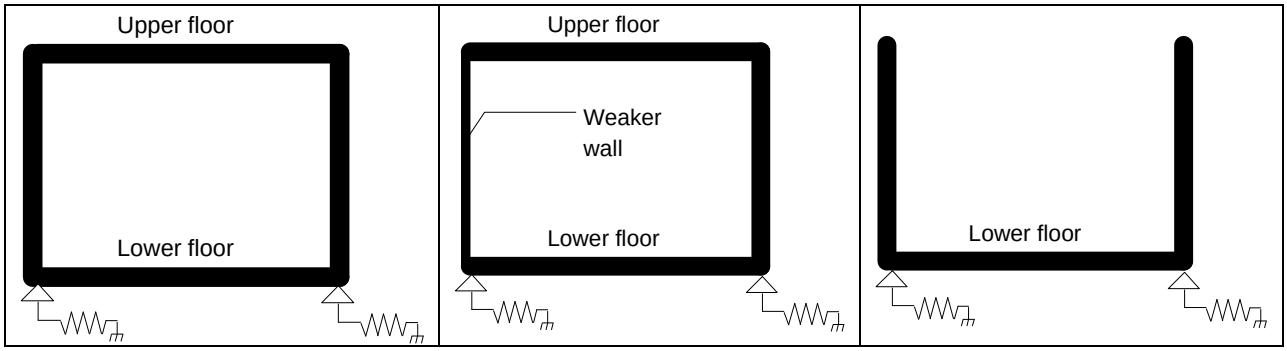

a) b) c)

Fig.3: Simple test case structures for the analysis – Horizontal support springs are either infinitely stiff (clamped structure) or tuned to produce a first translational mode at 1 Hz (isolated structure) - a) symmetrical closed frame b) unsymmetrical closed frame structure c) symmetrical open frame

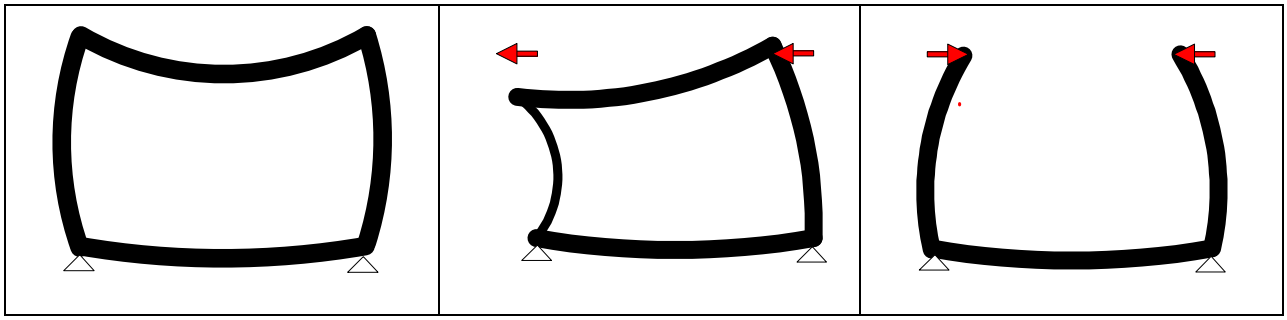

a) b) c)

Fig.4: Principal mode of the structure when excited in the vertical direction – Associated local horizontal displacement highlighted by the arrows - a) symmetrical closed frame b) unsymmetrical closed frame structure c) symmetrical open frame

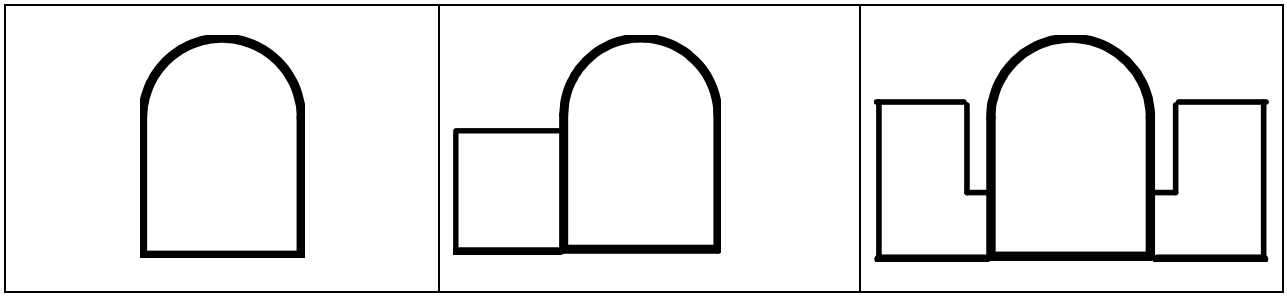

a) b) c)

Fig.5: Examples of possible arrangement of buildings for Gen IV reactors which have a behavior similar to the test cases - a) self standing containment building, assimilated with the symmetrical closed frame b) coupled fuel and containment building associated with the unsymmetrical closed frame structure c) Elongated steam generator buildings associated with the symmetrical open frame

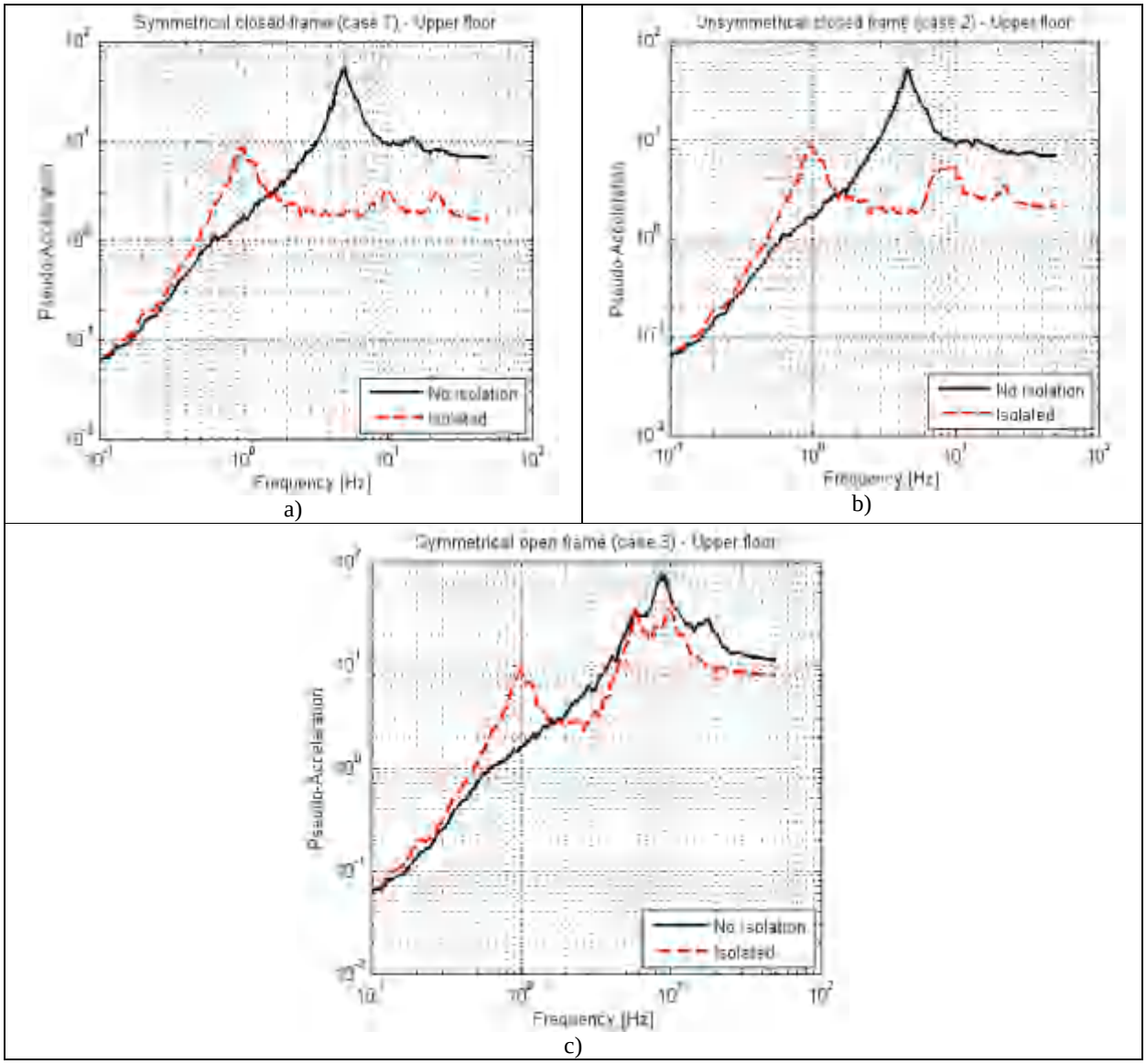

Fig.6: Horizontal response spectra on the upper part of the test case structures – a) symmetrical closed frame b) unsymmetrical closed frame structure c) symmetrical open frame

EXTENSION TO GEN IV BUILDINGS – RESPECTIVE INFLUENCE OF THE VERTICAL AND HORIZONTAL EXCITATIONS

LMFBR nuclear islands, such as planned today, may be prone to the kind of phenomena described in the previous paragraph. A dynamic analysis conducted on the preliminary design of a sodium fast reactor nuclear island developed by AREVA was conducted. Several time histories were given as input and the floor response spectra at different locations and altitudes inside the buildings were determined. The calculations were performed with and without the implementation of a seismic isolation system. The model was 3D and the seismic excitation was applied simultaneously in 3 orthogonal directions.

First of all, the efficiency of the seismic isolation system for reducing the horizontal floor response spectra in the frequency range of interest was confirmed. Fig. 7a illustrates the difference of horizontal floor response spectra at a given floor of the structure with and without isolation system. Reductions up to a factor 10 are achievable. Still, the potential for reduction is not as high as it would be expected because of the peaks due to the

vertical excitation. These peaks are altitude dependant, as illustrated in Fig. 7b. Fig. 7c shows the horizontal response spectra that would have been obtained with respectively purely horizontal and purely vertical excitations. The predominance of the vertical excitation on the higher frequency range is clear. Since the model is linear, the total response spectrum corresponds to an addition of the response spectra obtained with purely horizontal and purely vertical excitation.

Finally, if the vertical excitation has been demonstrated to have an influence on the horizontal response spectra, there is no reason for the horizontal excitation not to have the same kind of influence on the vertical response spectra. Indeed, some modes inducing significant local vertical accelerations are excited by the horizontal excitation. The implementation of a seismic isolation system does effectively filter the horizontal excitation, which means that these modes will be less excited. As a consequence, the vertical floor response spectra of the structure were found to be generally decreased by the implementation of the horizontal isolation system. This fact is illustrated in Fig. 7d. No mention of it was found in previous literature. Still, since the isolation system does also have a finite vertical stiffness, the change of vertical floor response spectra will also depend on this stiffness. The authors do not exclude that in some cases, because some vertical modes could be shifted toward lower frequency by the adjunction of this stiffness, the vertical floor response spectra might be actually augmented instead of decreased.

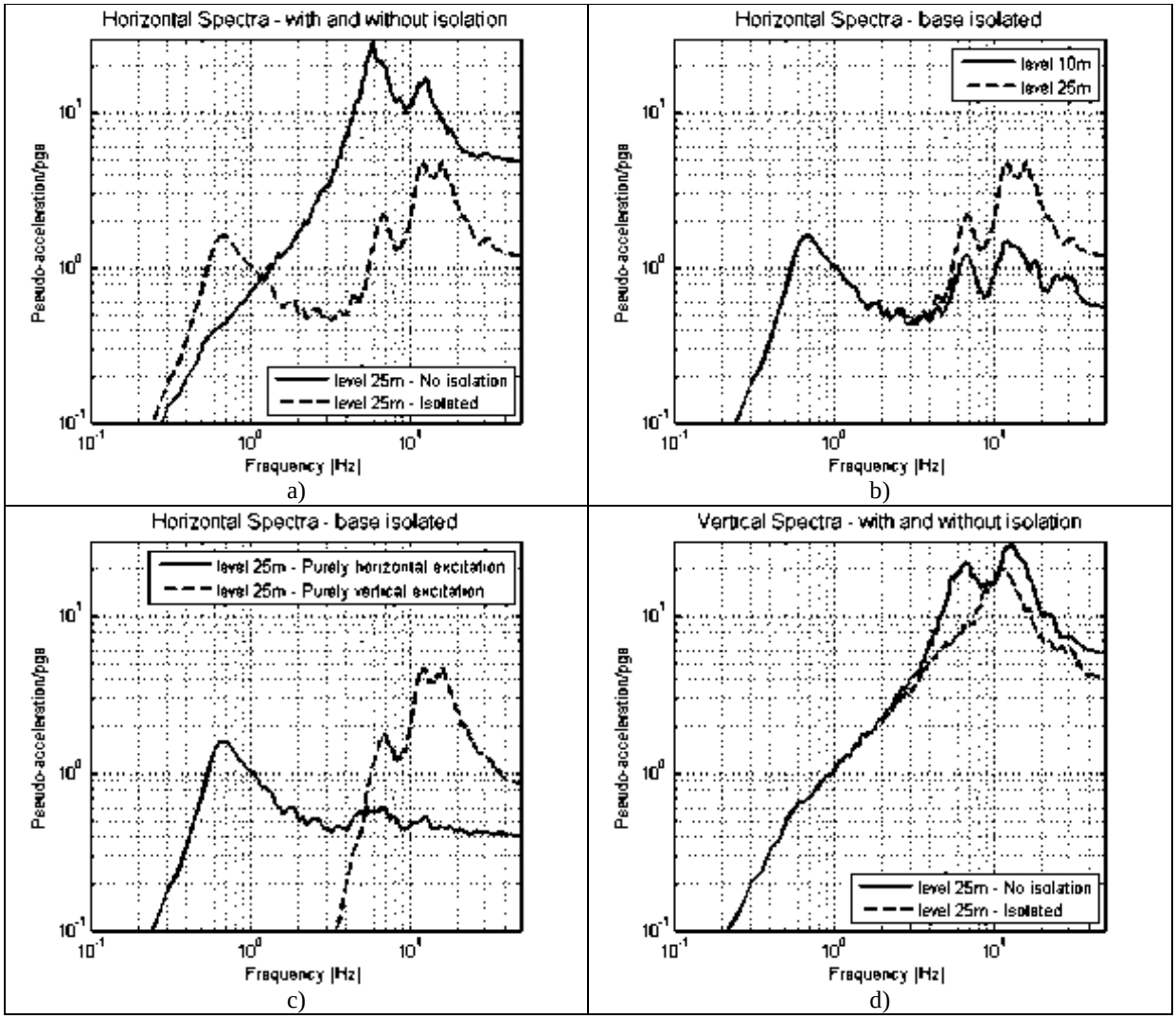

Fig.7: Calculated floor response spectra for a GEN IV structure – a) Horizontal floor response spectra with and without isolation. b) Horizontal spectra at two altitudes. c) Separation of the effects of the vertical and horizontal excitation on horizontal response spectra. d) Vertical floor response spectra with and without isolation.

DESIGN TOOLS TO ENHANCE THE BEHAVIOR OF A SEISMICALLY ISOLATED STRUCTURE

Based on the results presented in the previous paragraphs, it seems that some parameters are of unexpected importance for assessing, and possibly enhancing, the efficiency of a seismic isolation system. First of all, the soil-structure interaction in the vertical direction shall not be neglected. This interaction would affect the main vertical modes and therefore the positions of the peaks on the horizontal response spectra. The soil damping will directly affect the amplitude of these peaks. The vertical stiffness of the isolation system, generally considered of secondary importance, might prove a valuable tool to displace the peaks on the horizontal spectra as well as on the vertical spectra. Depending of the technology chosen for the isolation, it is more or less complicated to change the stiffness without moving the isolation frequency. The adjunction of damping devices, working in the vertical direction only and located in parallel with the isolation system allows a reduction of both the vertical and the horizontal response spectra. Finally, the building design can be modified to reduce the coupling between directions. Some changes of the sodium fast reactor design are typically envisaged for reducing the peaks on the horizontal response spectra.

CONCLUSION

Based on simple test cases and complete 3D calculation of a Gen IV reactor with base isolation system, the present paper demonstrates that the determination of the floor response spectra in an isolated structure requires a correct assessment of the influence of both the horizontal and vertical excitations. The vertical excitation results in some peaks at higher frequencies of the horizontal floor response spectra that would be missed by separated directional analyses traditionally performed with stick models.

The implementation of seismic isolation system in the horizontal direction has been found to also decrease the vertical response spectra of the structure. This is because some horizontal modes inducing vertical local acceleration are less excited.

Finally, the importance of the soil-structure interaction and of the stiffness of the isolation system in the vertical direction is underlined. Indeed, these parameters would significantly affect both the vertical and the horizontal floor response spectra. From a designer point of view, changing the vertical stiffness of the isolation system along with the possible adjunction of damping devices working in this direction might prove valuable tools to further decrease the floor response spectra.

REFERENCES

[1] Gibert, R.J., Martelli, A. “Seismic Analysis of liquid metal fast breeder reactors”, IAEA-TECDOC-514 ISSN 1011-4289, IAEA, Vienna, 1989.

[2] Naeim, F., Kelly, J.M. “Design of seismic isolated structures – From theory to practice”, John Wiley and Sons Inc, 1999

[3] Politopoulos, I., “A review of the adverse effects of damping in seismic isolation”, Earthquake Engineering & Structural Dynamics 2008, Vol 37, pp.447-465.

[4] Politopoulos, I., “Response of seismically isolated structures to rocking type excitations”, Earthquake Engineering & Structural Dynamics, 2010, Vol 39, pp.325-342.

[5] European Utility Requirements for LWR Nuclear Power Plants - Volume 2 Generic NI Requirements- Rev C, British Energy plc, Desarrollo Technologico S.L., Electricité de France, Fortum & Teollisuuden Volma Oy, NRG, SOGIN, Tractabel, UAK, Vattenfl/FKA, Verband der Elektrizitätswirtschaft, 2001

[6] Combescure D., “Structural Analysis and Optimization of the ITER-Tokamak Complex”, First Kashiwasaki International Symposium on Seismic Safety of Nuclear Installation, Workshop 2 - Seismic Isolation of Nuclear Facilities. 24-26 November 2010, Kashiwasaki, Japan.

[7] Germane L., “Seismic Isolation of the Jules Horowitz Reactor”, First Kashiwasaki International Symposium on Seismic Safety of Nuclear Installation, Workshop 2 - Seismic Isolation of Nuclear Facilities, 24-26 November 2010, Kashiwasaki, Japan.

[8] Moussallam N., “Seismic Isolation of GEN IV Reactors - Method for Determining the Floor Response Spectra in a Realistic Way”, First Kashiwasaki International Symposium on Seismic Safety of Nuclear Installation, Workshop 2 - Seismic Isolation of Nuclear Facilities. 24-26 November 2010, Kashiwasaki, Japan.

NAURAL SEISMIC BASE ISOLATION SYSTEM FOR RCC SRTCTURES

S.J.Patil[1], G.R.Reddy[2], Shivshankar[3], Ramesh babu[4], Jayalaxmi[3]
[1]. Heavy Water Board, Mumbai, India. [2.] BARC & HBNI, Mumbai, India. [3] NITK, Suratkal, India [4]. CPRI, Banglore,India.
e-mail of corresponding author : sjp_patil@yahoo.co.in

ABSTRACT

Generally seismic isolation is achieved by using laminated rubber bearings, lead bearings etc. as a supporting elements in structures. Very little work has been performed using soil as a base isolation media. Experiments and analytical work has been performed and found encouraging results. Details of this work are presented in this paper.

INTRODUCTION

Soil has very typical engineering properties. The soil in static condition and the same soil in dynamic condition exhibit entirely different engineering properties. Shear modulus of soil in static condition and that in dynamic condition varies largely. The soil properties can be altered by adding fibers or membranes. M.K. Yegian and U. Kadakal [1] have performed experimental work by using geo-synthetic material and shown that response of the structure can be altered. Fu Lin Zhou, et al., 2004 [2] have performed experiments on structures resting on sand layer. The properties also get affected by presence of water in the soil. Keeping the above facts in view, soil (river sand) was used as a base isolation material. Experiments were conducted on a RCC frame model placed on a layer of soil, a layer of soil mixed with water and a layer of soil provided with geo-membrane to evaluate the isolation effect under seismic conditions.

River sand having engineering properties shown in Table 1 was used in the experiments. Geo-membrane was used with a soil layer to know the effect of membrane on the performance of a soil layer.

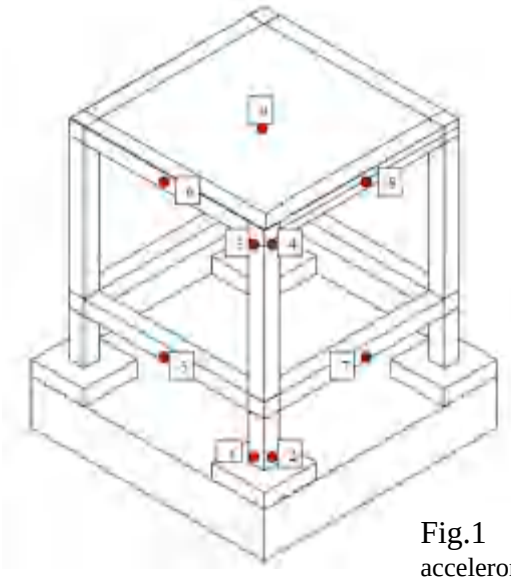

Fig.1 Location of accelerometers

Table 1: River sand properties

Property	Value	Property	Value
Gravel	5.6%	Cu	7.37
Coarse sand	19.4%	Cc	1.12
Medium Sand	53%	γdmax	1.71g/cc
Fine Sand	17.6%	γdmin	1.40g/cc
Silt + Clay	4.4%	Sp.gravity	2.66
D60	1.18mm	emax	0.77
D10	0.16mm	emin	0.48
D30	0.46mm		

ISOLATED FOOTING MODEL

RCC frame structure model of size 1.2 x 1.2 x 1.5 m height having column and beam c/s size of 0.1 x 0.1 m, roof slab thickness of 0.05 m and isolated footings of 0.3 x 0.3 x 0.1m was prepared as shown in Fig. 1 & 2(a). A metallic box of size 2.0 x 2.0 x 1.2 m height, filled with sand/ sand with geo-membrane layer with height of 300mm was used in the experiments. The model was kept on the soil layer. The test set up is shown in Fig 2(b).

Experiments were conducted [3] to see the effect of such layer on the structure. The model was tested on shake table and results were obtained.

Resonance search tests were conducted on the model with sinusoidal motion of 0.1g for fixed base (FXISO) model and 0.2g for other models with sweep rate of 1 octave/min in horizontal directions X, Y and vertical direction Z and natural frequencies of the model were established. Table 2 shows the frequencies of the model in different base conditions. It is seen that as compared to fixed base model frequencies, the frequencies of the model supported on dry soil, wet soil and soil with geo-membrane are reduced in all the three directions. The reductions in frequencies with dry sand are up to 16.16% and that with wet sand plus geo-membrane are up to 44.31%. The reduction in frequencies increases with geo-membrane.

(a)

(b)

Fig.2 a) Isolated footing model b) Shake table test set up

Table 2: Variation in natural frequency of isolated footing model from experimental results

Model condition	Frequency			Percentage variation		
	X	Y	Z	X	Y	Z
Fixed base (FXISO)	4.39	4.27	12.54			
Supported on a layer of dry sand (ISODRY)	3.90	3.58	11.60	-11.16	-16.16	-7.50
Supported on a layer of dry sand + geo-membrane (IDSGM)	2.82	2.58	10.69	-35.76	-39.58	-14.75
Supported on layer of saturated sand (ISOWET)	3.09	3.10	10.46	-29.61	-27.40	-16.59
Wet sand + Geo-membrane (ISOWETG)	2.51	2.38	10.12	-42.87	-44.31	-19.30

Table 3 shows the variation in damping ratios, which are estimated from the experimental results. The damping ratios are increased in horizontal directions (X and Y directions) as compared to FXISO case. For dry sand condition, increase in damping is 154.64% & 119.42% in X & Y directions respectively. Similar result is obtained for dry sand with geo-membrane condition except increase in damping in Y direction by 78.64%. The values of increase in damping for wet sand with geo-membrane condition are 97.62% and 80.58% for X and Y directions respectively.

Table 3: Variation in damping ratio of isolated footing model from experimental results

Sr. No.	Model condition	Damping ratio		Percentage variation	
		X	Y	X	Y
1	Fixed base (FXISO)	1.04	1.27		
2	Supported on a layer of dry sand(ISODRY)	2.64	2.79	154.64	119.42
3	Supported on a layer of dry sand + geo-membrane (IDSGM)	2.66	2.27	156.19	78.64
5	Wet sand + Geo-membrane (ISOWETG)	2.05	2.30	97.62	80.58

Table 4: ISOLATED FOOTING MODEL – Accelerations for IS code zone III time history

	Z3-FXISO	Z3-ISODRY		Z3-ISOWET		Z3-ISOWETG		Z3- IDSGM	
	MAX ACC	MAX ACC	%variation	MAX ACC	%variation	MAX ACC	%variation	MAX ACC	%variation
Roof level accelerometers									
A3 (Dir-X, location-beam-column junction at Roof level)	9.15	5.95	-34.97	6.10	-33.33	6.30	-31.15	5.50	-39.89
A6 (Dir-X, location-at mid span of roof beam)	7.41	5.45	-26.45	5.01	-32.39	5.63	-24.02	4.66	-37.11
A4 (Dir-Y, location-beam-column junction at Roof level)	11.60	5.29	-54.40	6.52	-43.79	5.93	-48.88	5.82	-49.83

Table 4 shows the variation in accelerations recorded by accelerometers located at different point on the model during shake table testing. The accelerations were recorded for model conditions FXISO, ISODRY, ISOWET, ISOWETG and IDSGM for IS code[4] zone III time history . Comparison has been done between the fixed base model and that the model with soil layers. In general there is a reduction in the accelerations recorded by all accelerometers. In case of dry sand layer below the footing, the accelerations are reduced by 26.45% to 54.4% for roof level accelerometers. For saturated sand layer, the decrease in accelerations is 32.39% to 43.79%. Similarly, the reductions in accelerations are recorded for wet sand layer with geo-membrane, which vary from 24.02% to 48.88% and that for dry sand layer with geo-membrane from 37.11% to 49.83%.

FREQUENCY RESPONSE SPECTRA: ZONE III TIME HISTORY

Fig.3 shows frequency response spectra of accelerations recorded by accelerometer A3 located at roof level of the model in X direction. The response acceleration is lower for all the models, as compared to FXISO model. The lower accelerations indicate increase in damping due to soil layer. Also there is a shift in the frequency on the lower side.

The frequency response spectrum of accelerations recorded by accelerometer A4 located at roof level in Y direction is shown in Fig. 4. The accelerations are lower for all the models i.e. ISODRY, IDSGM and ISOWET as compared to FXISO model. There is a reduction in peak response acceleration for ISODRY, IDSGM and ISOWET model as compared to FXISO model. Also there is a shift in the frequency on lower side.

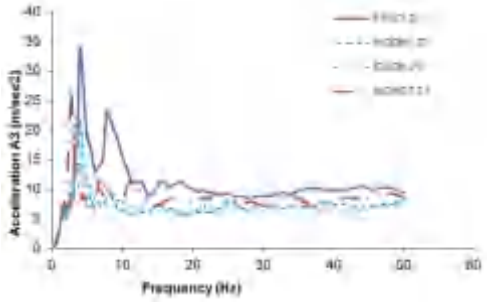

Fig. 3 – Spectra along X direction (A3)

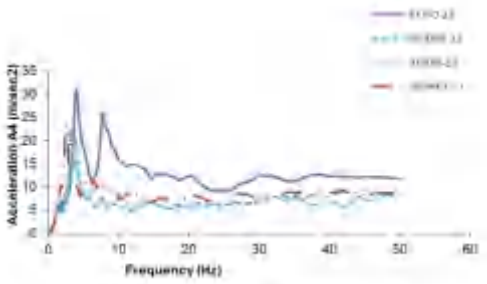

Fig. 4 – Spectra along Y direction(A3)

The response spectrum for acceleration recorded by accelerometer A6 located at roof level beam center to record the acceleration in the X direction is given in Fig. 5. The response accelerations for ISODRY, IDSGM and ISOWET are lower than the accelerations for FXISO case. There is a reduction in the peak response acceleration. There is a shift in the frequency on lower side as well.

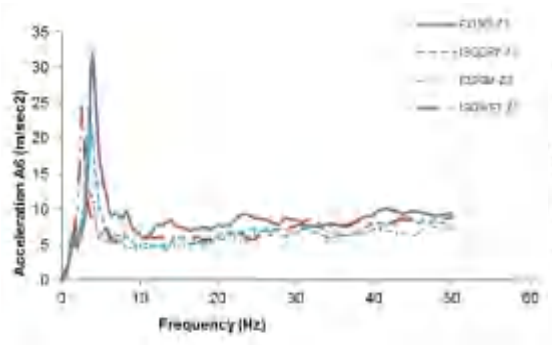

Fig. 5 Spectra along X direction(A6)

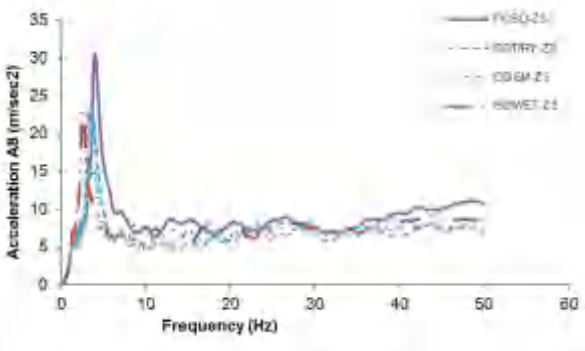

Fig. 6 Spectra along Y direction(A8)

The frequency v/s response acceleration spectrum for acceleration recorded by accelerometer A8 located at roof level beam to record acceleration in the Y direction are given in Fig. 6. The response accelerations are lower in case of models with soil layer as compared to the fixed base model. Also there is shift in the frequency on lower side as compared to fixed base frequency.

VARIATION IN TIME HISTORY

The graphs in Fig. 7 show the time histories of accelerometer A3 located at roof level, which has recorded the accelerations in X direction for FXISO model and other models with soil layer. It is seen from the above graphs

that the accelerations reaching to the structure are less if a sand layer is introduced between the foundations and base of a structure. The total energy reaching to the structure is also less as the area of the time history of models with soil layer is less than the FXISO model.

The Fourier transform amplitudes plotted for A3 signal in Fig. 8 confirms that i) there is a reduction in the frequency of models on the sand layer as compared to the frequency of fixed base model ii) Fourier amplitude is on lower side in all the models and lowest in case of ISODRY model as compared to the amplitude of FXISO model. This conclusion corroborates with above response spectrum analysis.

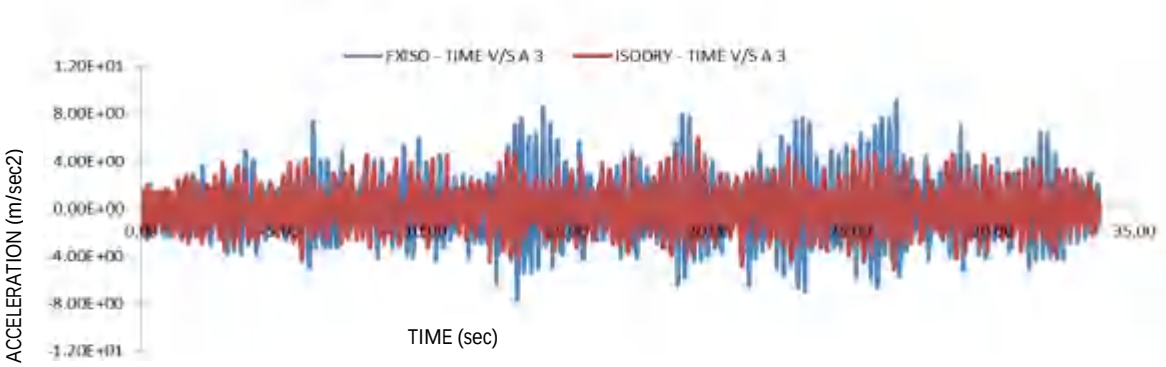

Fig.7(a) Time history along X direction (A3) for FXISO and ISODRY

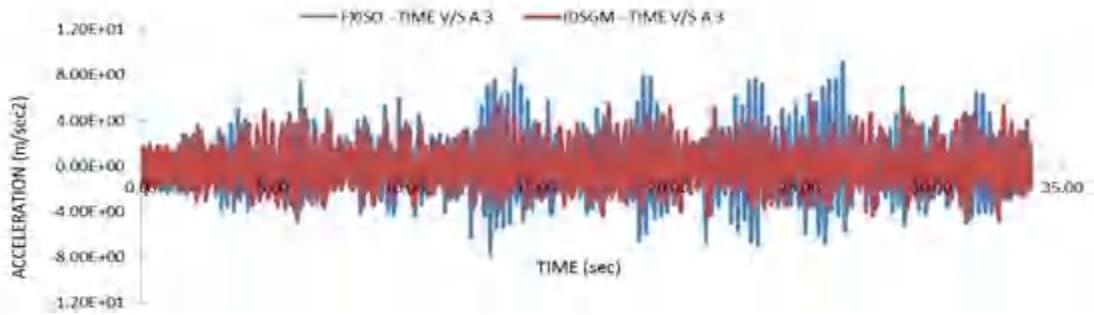

Fig.7(b) Time history along X direction (A3) for FXISO and IDSGM

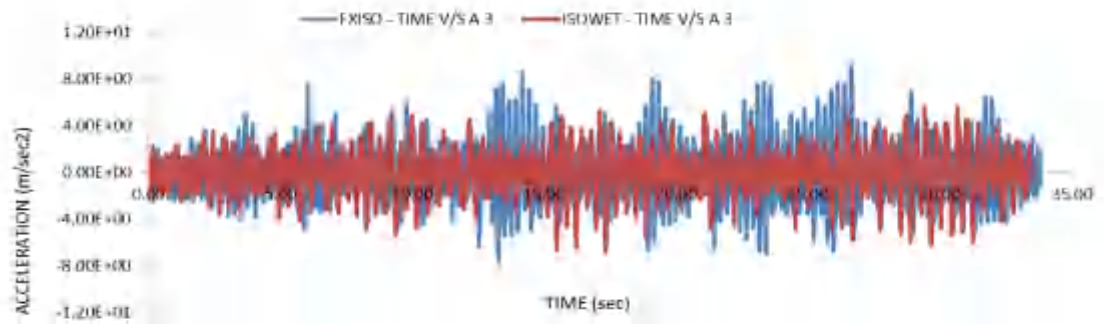

Fig.7(c) Time history along X direction (A3) for FXISO and ISOWET

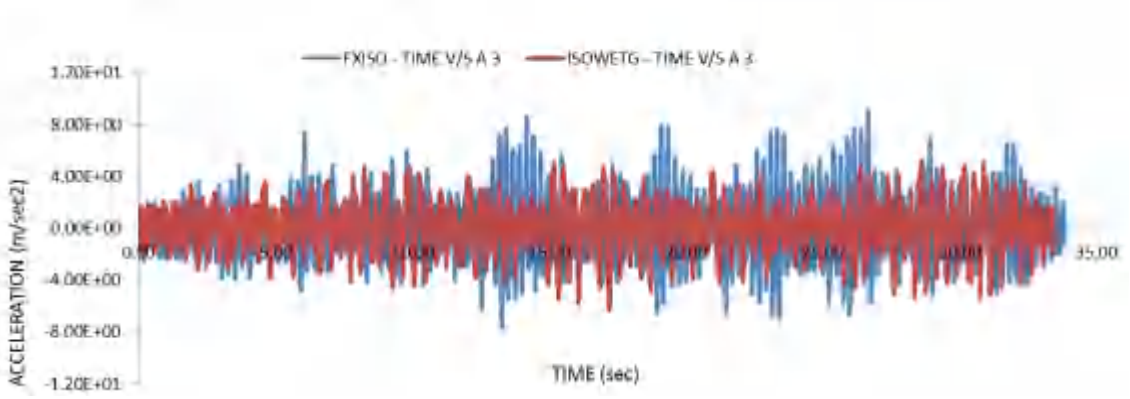

Fig.7(d) Time history along X direction (A3) for FXISO and ISOWETG

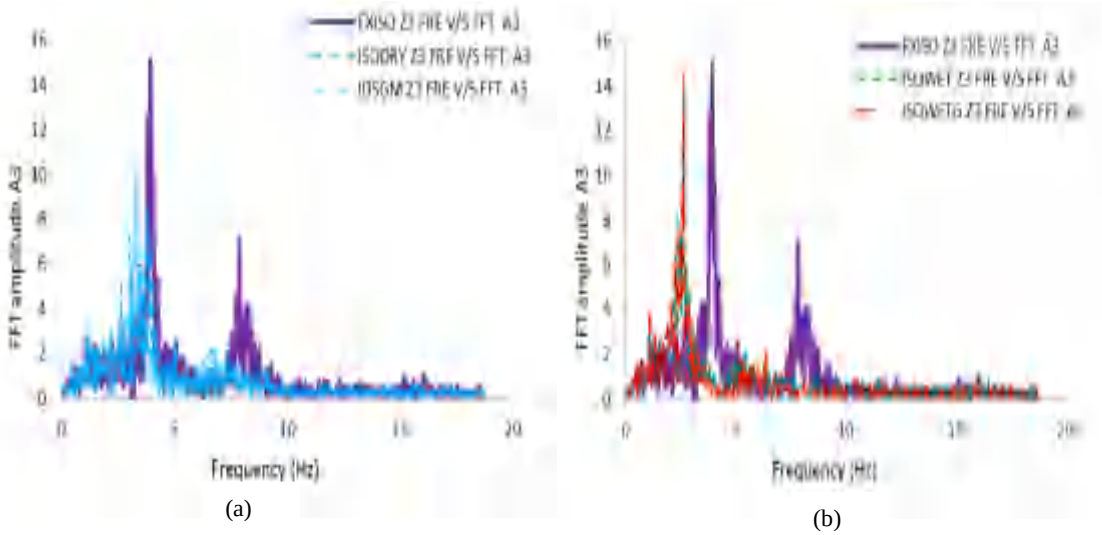

(a) (b)

Fig. 8 Fourier spectra along X direction

ANALYTICAL RESULTS

The frequencies, obtained from the above response spectrum analysis and Fourier analysis, are matching with the free vibration tests as shown in the Table 6. This infers that the strains built in the soil are similar both in free vibration and force vibration tests. Using the displacements measured at top of the footings (Fig 9) strains are calculated with soil thickness of 300 mm and corresponding strain based G values are obtained using Fig 10, which is generated using modulus reduction theory [5].

$$\frac{G}{G_{\max}} = K(\gamma, PI)\left(\sigma_m^{'}\right)^{m(\gamma,PI)-m_0}$$

$$K(\gamma, PI) = 0.5\left\{1+\tanh\left[\ln\left(\frac{0.000102+n(PI)}{\gamma}\right)^{0.492}\right]\right\}$$

$$m(\gamma, PI) - m_0 = 0.272\left\{1-\tanh\left[\ln\left(\frac{0.000556}{\gamma}\right)^{0.4}\right]\right\}\exp(-0.0145PI^{1.3})$$

$$n(PI) = 0.0 \text{ for PI} = 0$$

Where PI plasticity index for sand layer.

Using the strain based G values and equations for stiffness parameters based on the half space theory given in table 5, stiffness is calculated [6].

Table 5. Spring Constants Coefficients for Foundations on Homogeneous Half-Space

Direction of Motion	Equivalent Spring Constant for Rectangular Foundation
Horizontal	$K_H = 2(1+\nu)G\,\beta_X\sqrt{(BL)}$
Rocking	$K_R = (G/(1-\nu))\,\beta_\psi\,BL^2$
Vertical	$K_v=(G/(1-\nu))\beta_v\sqrt{(BL)}$

Where -

ρ = mass density of soil

V_s = Shear wave velocity of soil medium

$G = \rho V_s^2$

ν = Poisson's ratio of soil medium

R = equivalent radius for rectangular foundation ($R= \sqrt{BL/\pi}$ for translation and $R= \sqrt[4]{4BL^3} / 3\pi$ for rocking).

B = width of the foundation perpendicular to the direction of horizontal excitation

L = length of the foundation in the direction of horizontal excitation

β_x, β_ψ, and β_v are constants depending on ratio L/B

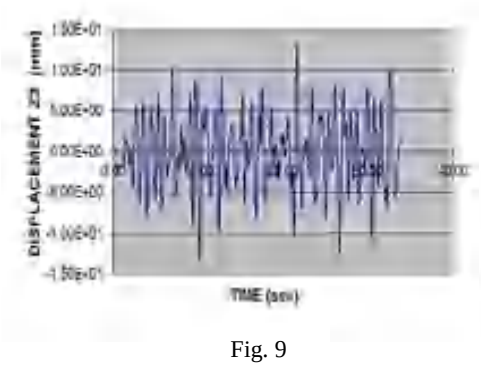

Fig. 9

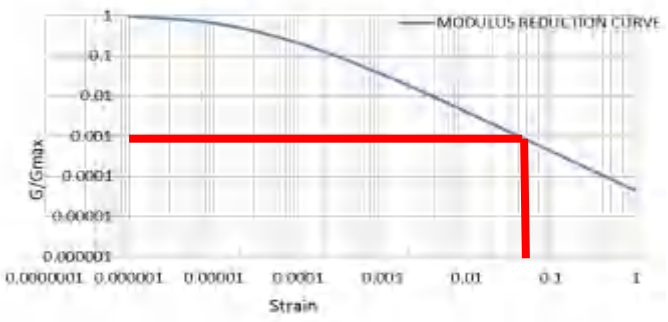

Fig. 10

FE model is generated by modeling beams and columns using beam elements and floor as shell elements. The footings are connected with soil springs evaluated above. The model was analyzed using SAP2000[7] software and the frequencies are tabulated in Table 6. Analytical frequencies for different models indicate that frequencies in all three directions for all the models on soil layer reduced as compared to fixed base model frequencies. This observation is similar to the one observed in experimental results.

Table - 6 Isolated footing model - Analytical & experimental frequencies

Model	Analytical		Experimental		Variation	
Type	X	Y	X	Y	X	Y
FXISO	4.27	4.27	4.39	4.27	-2.81	0.00
ISODRY	3.16	3.16	3.54	3.58	-12.03	-13.29
IDSGM	2.64	2.64	2.82	2.58	-6.82	2.27
ISOWET	2.97	2.97	3.09	3.10	-4.04	-4.38
ISOWETG	2.72	2.72	2.51	2.38	7.72	12.50

Comparison of analytical and experimental frequencies is shown in table 6. There is a good match between analytical and experimental frequencies the same are within 15% variation.

CONCLUSIONS

1. Introduction of soil layer between footing and hard foundation gives isolation effect to the structure. The degree of isolation will vary depending on the soil properties.
2. Maximum reduction in response acceleration is seen in case of ISODRY model followed by IDSGM, ISOWET and ISOWETG models.
3. Natural frequencies evaluated using stiffness based on the strain based G values. This approach can be used for evaluating natural frequencies of structure supported on soil layer used as a base isolation.

FUTURE STUDIES

The response has to be evaluated analytically and compared with the experimental results to complete the research work. An iterative procedure as explained in the text book [5] may be adopted and modifications may be suggested.

REFERENCES

1. Yegian M.K.& Kadakkal U.- Foundation isolation for seismic protection using a smooth synthetic liner. Journal Of Geotechnical And Geoenvironmental Engineering © ASCE / November 2004 / 1123.
2. Fu Lin Zhou, Zheng Yang, Wen Guang Liu And Ping Tan - New Seismic Isolation System For Irregular Structure With The Largest Isolation Building Area In The World (13 th World Conference on Earthquake Engineering Vancouver, B.C., Canada August 1-6, 2004 Paper No.2349).
3. Dynamic soil structure interaction effects in multistoried structures on homogeneous soil and geo-synthetic reinforced soil. A BRNS research report 2009. NITK Suratkal, India.
4. IS 1893, 2002 Criteria for earthquake resistant design of structures (part 1 general provisions and buildings)
5. Cramer Steven L., Geotechnical Earthquake Engineering, 2007.
6. IAEA TECDOC 1347 - Consideration of external events in the design of nuclear facilities other than nuclear power plants, with emphasis on earthquakes.
7. SAP2000® V10 Linear and Nonlinear Static and Dynamic Analysis and Design of Three Dimensional Structures.

ANALYSIS AND DESIGN OF SEISMIC ISOLATION SYSTEMS FOR NUCLEAR STRUCTURES

Y.-N.Huang[1], A.S.Whittaker[2], R.P.Kennedy[3], R.L.Mayes[4]
[1]Dept. of Civil Engineering, National Taiwan University, Taipei, 10617, TAIWAN
[2]The State University of New York at Buffalo, Buffalo, New York, NY 14260, UNITED STATES
[3]RPK Structural Mechanics Consulting, Escondido, California, CA92026, UNITED STATES
[4]Simpson Gumpertz & Heger, Inc., San Francisco, California, CA94105, UNITED STATES
E-mail of corresponding author: ynhuang@ntu.edu.tw

ABSTRACT

ASCE 43-05 presents two performance objectives for the design of nuclear structures: 1) 1% probability of unacceptable performance for 100% Design Basis Earthquake (DBE) shaking, and 2) 10% probability of unacceptable performance for 150% DBE shaking. To develop procedures for the analysis and design of base-isolated nuclear power plants (NPPs) to meet the intent of ASCE 43-05, we performed a series of nonlinear response-history analyses to study the impact of the variability in both earthquake ground motion and mechanical properties of isolation systems on the seismic responses of base-isolated NPPs. Computations were performed for three representative sites (rock and soil sites in the Central and Eastern United States and a rock site in the Western United States), three types of isolators (lead rubber, Friction Pendulum^{TM} and low-damping rubber bearings), and realistic mechanical properties for the isolators. Estimates were made of the ratio of the 99%-ile (90%-ile) response of isolation systems computed using a distribution of spectral demands and distributions of isolator mechanical properties to the median response of isolation systems computed using best-estimate properties and 100% (150%) spectrum-compatible DBE ground motions. Only the results for the soil site in the Central and Eastern United States and LR and FP bearings are presented.

INTRODUCTION

Base isolation has been used to protect buildings, bridges and mission-critical infrastructure from the damaging effect of earthquake shaking [1], [2]. It has been implemented in safety-related nuclear structures in France and South Africa [3]. In the United States, there are no applications of seismic isolation to nuclear structures at the time of this writing although some vendors of Nuclear Steam Supply Systems and power utilities are considering seismic isolation for new build plants.

Two ASCE standards are relevant to the analysis and design of nuclear power plants (NPPs): ASCE 4-98, *Seismic Analysis of Safety-related Nuclear Structures and Commentary* [4] and ASCE 43-05, *Seismic Design Criteria for Structures, Systems and Components in Nuclear Facilities* [5]. Section 1.3 of ASCE 43-05 presents dual performance objectives for nuclear structures: 1) 1% probability of unacceptable performance for 100% Design Basis Earthquake (DBE) shaking, and 2) 10% probability of unacceptable performance for 150% DBE shaking. ASCE Standard 4-98, which includes provisions for the analysis and design of seismic isolation systems, is being updated and the studies reported in Huang et al. [6], [7] provide related information regarding the analysis and design of seismic isolation systems for NPPs to aid in the update of ASCE Standard 4-98. This paper summarizes part of the studies and observations of Huang et al. [6], [7] with a focus on the soil sites in the Central and Eastern United States (CEUS). Information on the studies for rock sites in the CEUS and rock sites in the Western United States is presented in Huang et al. [6], [7].

The goals of the study were to 1) determine the ratio of the 99%-ile estimate of the displacement computed using a distribution of DBE spectral demands and distributions of isolator mechanical properties to the median isolator displacement computed using best-estimate properties and spectrum-compatible DBE shaking; and 2) determine the ratio of the 90%-ile estimate of the displacement computed using a distribution of 150% DBE spectral demands and distributions of isolator mechanical properties to the median isolator displacement computed using best-estimate properties and spectrum-compatible DBE shaking.

Computations were performed for representative rock and soil sites in the Central and Eastern United States (CEUS) and a rock site in the Western United States (WUS). Three types of isolators, namely, low-damping rubber, lead-rubber (LR) and Friction Pendulum (FP) bearings, and realistic mechanical properties for the isolators were used in the analysis. Only the results for the CEUS soil site and LR and FP bearings are presented in this paper. Those for the CEUS soil and WUS rock sites can be found in Huang et al. [6], [7].

The analyses presented in this paper do not consider torsional response of the isolated nuclear structure. If the increment in displacement response due to torsion is a significant percentage of the displacement at the center of mass of the isolated superstructure, the conclusions and recommendations presented below must be used with care. Further, the change in isolator mechanical properties over the course of earthquake shaking was not considered. The dual performance objectives of ASCE 43-05 were established to achieve a mean annual frequency of exceedance (MAFE) less than 10^{-5} for the first onset of significant inelastic deformation (FOSID) of safety-related structures, systems and components in conventional (non-isolated) nuclear facilities. However, the fragility curves for seismic isolation systems are much different from those for typical structural components in NPPs. A study is under way to judge the impact on the MAFE of the unacceptable performance of seismically isolated NPPs if the two performance objectives of ASCE 43-05 are used as the basis for design.

BASE ISOLATION SYSTEMS

Models of Isolation Systems

SAP2000 Nonlinear [8] was used to perform the response-history analysis of models of base-isolated NPPs. Each model was composed of a rigid mass supported by a link element representing the isolation system. Each model had three degrees of freedom: two horizontal and one vertical. The models for each type of the isolation systems used in the analysis are described below:

Lead-rubber (LR) isolation systems were modeled using the "Rubber Isolator" link element in SAP2000. This element has coupled plasticity properties for the two horizontal displacements and linear stiffness properties for the vertical displacement. The plasticity model is similar to that of Figure 1 but the transition between the elastic stiffness and the post-yield stiffness is continuous. To study a wide range of isolation-system properties, 9 best-estimate models were prepared with characteristic strength Q_d equal to 3%, 6% and 9% of the supported weight W, and T_d (the period related to the post-yield stiffness of the isolator K_d through W) equal to 2, 3 and 4 seconds. Parameter T_v (the period related to the vertical stiffness of the isolation system K_v through W) was set to 0.05 second. Only the results for T_d = 3 and 4 seconds and $Q_d = 3\%W$ and $6\%W$ are presented herein and the four models are termed LR_T3Q3, LR_T3Q6, LR_T4Q3 and LR_T4Q6.

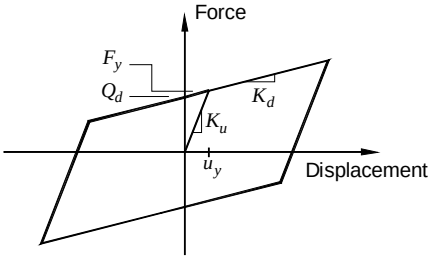

Figure 1: A force-displacement relationship similar to that used in the analysis for this study for LR bearings in the horizontal directions

Friction Pendulum™ (FP) isolators were modeled using the "Friction Isolator" link element that has coupled plasticity properties for the two horizontal directions and a gap element for vertical tensile forces. The coefficient of friction for FP bearings depends on the sliding velocity and is computed in SAP2000 using the following equation [9]:

$$\mu = \mu_{\max} - (\mu_{\max} - \mu_{\min}) \cdot e^{-aV} \tag{1}$$

where μ is the coefficient of sliding friction, varying between $\mu_{\max}$ and $\mu_{\min}$ (for high and very small velocities, respectively), a is a velocity-related parameter, and V is the sliding velocity. Nine best-estimate FP isolation-system models were analyzed in this study with $\mu_{\max}$ equal to 0.03, 0.06 and 0.09 and T_d equal to 2, 3 and 4 seconds but only the results for the three models with $\mu_{\max}$ equal to 0.03 and 0.06 and T_d equal to 3 and 4 seconds are presented. The four models are termed FP_T3Q3, FP_T3Q6, FP_T4Q3 and FP_T4Q6. The yield displacement was set at 1 mm for all FP models. (We note that the recently developed triple concave FP bearing can be configured to produce hysteresis loops similar to that of the LR bearing.)

Variations in properties of isolators

The mechanical properties of LR and FP seismic isolation bearings will tend to vary from the values assumed for design both a) at the time of fabrication due to variability in basic material properties, and b) over the lifespan of the nuclear structure due to aging, contamination, ambient temperature, etc. For LR bearings, the mechanical properties of the lead plug are a function of the confinement provided to the plug and the mechanical properties of the elastomer (rubber). For FP bearings, only the coefficient of sliding friction varies because the second-slope stiffness of the bearing is a function of the radius of the sliding surface, which is constructed to very tight tolerances. Importantly, the variability of the mechanical properties of an assembly of isolators (the isolation *system*) will be smaller than the variability of individual isolators.

To study the impact of the variations in mechanical properties of isolators on the response of base-isolated NPPs, 2 sets of 30 mathematical models were developed for each of the best-estimate models studied herein by modifying the values of key parameters of the best-estimate models. For LR models, Q_d, K_d and K_v were assumed to vary; and for FP models, only $\mu_{\max}$ was assumed to vary. One set of 30 models represents an isolation *system* with *excellent* control on the properties of individual isolators: the probability for the values of the key parameters of the isolation system described above to be within ±10% of the best-estimate values is 95% (Bin F1). The second set represents an isolation *system* with *good* control on the properties of individual isolators: the probability for the values of the key parameters of the isolation system to be within ±20% of the best-estimate values is 95% (Bin F2). We assume the distributions for the values of the key parameters to be normal. As an example, Figure 2 illustrates these distributions in parameters Q_d and K_d for LR isolation systems. Bins F1 and F2 likely address the permissible ranges of mechanical properties of an isolation system for NPP construction. Given that an isolation system consists of a large number of isolators, larger percentage variations in the mechanical properties of individual isolators might be acceptable.

To develop the 2 sets of 30 mathematical models, 2 bins of 30 scale factors were generated, where the factors for Bin F1 (F2) were obtained from a normal distribution with a mean of 1 and a standard deviation of 0.05 (0.1). Figure 3 presents the two normal distributions. For each of these curves in Figure 3, the area under the curve was divided into 30 equal segments; the *midpoint* value in each segment is used to form the factors for Bins F1 and F2.

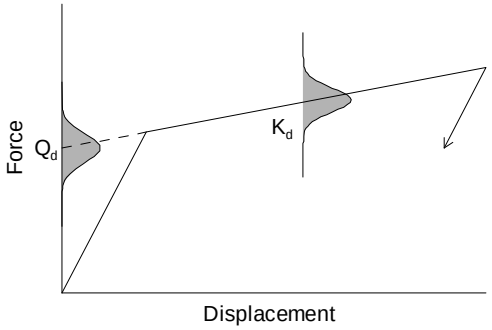

Figure 2: Variations in the mechanical properties of a LR isolation system

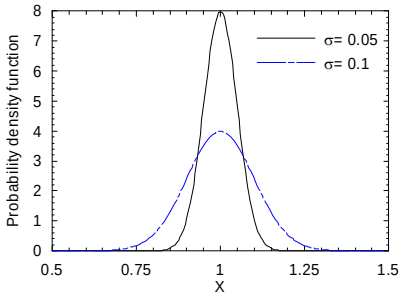

Figure 3: Normal distributions with a mean of 1 and standard deviations of 0.05 and 0.1

The generation of the 2 sets of 30 models for each LR isolation system is presented herein to demonstrate the process. For each best-estimate model of LR_T2Q3, LR_T3Q3 and LR_T4Q3, the values of Q_d, K_d and K_v were scaled by 2 sets of factors: [$F1_i^{Q_d}$, $F1_i^{K_d}$, $F1_i^{K_v}$] and [$F2_i^{Q_d}$, $F2_i^{K_d}$, $F2_i^{K_v}$], where $F1_i^{Q_d}$, $F1_i^{K_d}$ and $F1_i^{K_v}$ ($F2_i^{Q_d}$, $F2_i^{K_d}$ and $F2_i^{K_v}$) are the scale factors for Q_d, K_d and K_v, respectively, determined from the 30 scale factors in Bin F1 (F2) using the Latin Hypercube Sampling procedure [10] and i = 1 through 30. For each value of i, a new model was developed for each case of excellent and good control.

The procedures described above were repeated for the FP isolation system. The developed models were used in the response-history analysis to study the impact of variations in material properties of isolators on the response of base-isolated NPPs.

GROUND MOTIONS FOR A SOIL SITE IN CEUS

Design Basis Earthquake

The site of the Vogtle NPP in Waynesboro, Georgia is a representative soil site for NPPs in CEUS. The horizontal and vertical DBE spectra used in this study for the Vogtle site are presented in Figure 4. The horizontal spectrum of Figure 4 is a uniform-risk spectrum (URS) corresponding to a mean annual frequency of exceedance (MAFE) of 10^{-5} developed by the Southern Nuclear Operating Company for the Vogtle Early Site Permit (ESP) Application [11]. The horizontal DBE spectrum of Figure 4 was scaled by the V/H factors of 0.9 at periods smaller than 0.07 second (15 Hz) and 0.5 at periods greater than 1 second. Interpolation was used to determine the scale factors at periods between 0.07 and 1 second. The technical basis for the V/H scale factors for the spectra of Figure 4 is provided in [11].

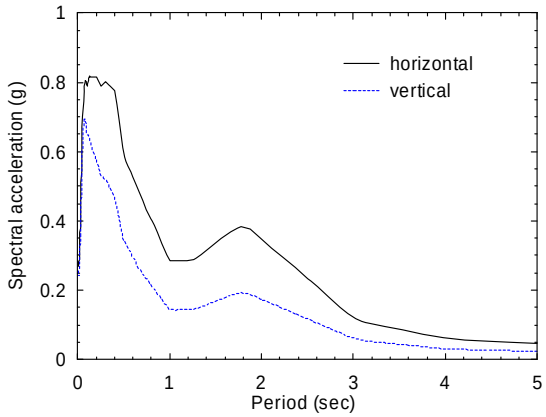

Figure 4: Horizontal and vertical 5% damped DBE spectra for the Votgle NPP site

DBE spectrum-compatible ground motions

Two bins of 30 sets of ground motions were developed for the response-history analysis to study the impact of the variability in earthquake ground motion on the response of base-isolated NPPs. In the first bin, termed DBE spectrum-compatible (DBE-SC) ground motions, both of the two horizontal components of each set of ground motions have 5% damped spectral accelerations similar to that of Figure 4. In the second bin, termed maximum-minimum spectrum-compatible (MM-SC) ground motions, the variability in spectral acceleration along three perpendicular directions is addressed in the scaling of ground motions. The development of these two bins of ground motions are summarized in this and the following subsections, respectively. More information can be found in [6].

Synthetic ground motions were developed in 2 steps. Step 1 involved the use of the deaggregtion data for the Vogtle site and the computer code "Strong Ground Motion Simulation" [12] to generate CEUS-type seed ground motions, which were then spectrally matched to the DBE spectra of Figure 4 in step 2 using the computer code RSPMATCH [13].

Thirty sets of DBE-SC ground motions were developed and each set of ground motions included 2 horizontal components and a vertical component. Panel a of Figure 5 presents a sample DBE-SC acceleration time series and panel b presents the target and achieved spectral accelerations for the time series of panel a. The spectral accelerations for the time series of panel a closely match the target. Panel a of Figure 6 presents the spectral accelerations for horizontal component 1 of all 30 sets of DBE-SC ground motions. Each spectrum of Figure 6a closely matches the target.

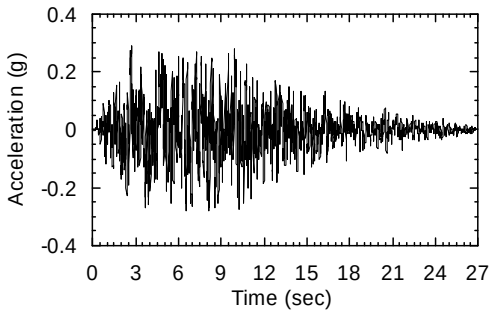

a. time series (horizontal component 1)

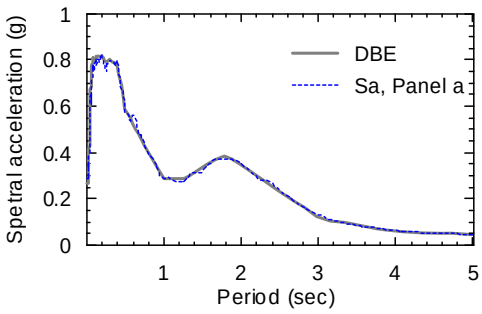

b. spectral acceleration (horizontal component 1)

Figure 5: Sample DBE-SC acceleration time series and the corresponding 5% damped response spectra

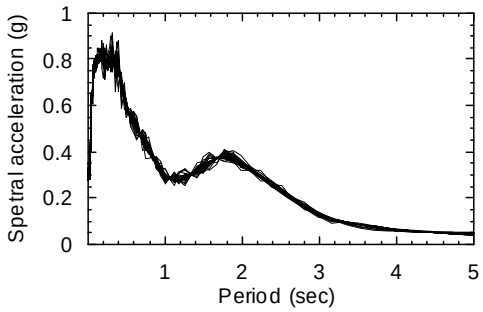

a. spectral acceleration (DBE-SC, horizontal component 1)

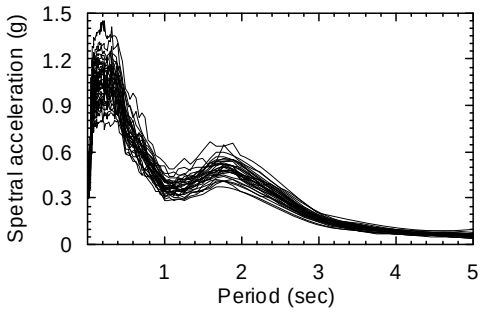

b. spectral acceleration (MM-SC, maximum component)

Figure 6: Five-percent damped response spectra for the DBE-SC and MM-SC ground-motion bins

Maximum-minimum spectra compatible Ground motions

A second set of 30 pairs ground motions, MM-SSC ground motions, were developed by amplitude scaling the 30 sets of DBE-SC ground motions to represent the maximum spectral demand and the demand at the orientation perpendicular to the maximum direction, termed the *minimum* demand. The maximum spectral demand at a given period was defined as the maximum of the spectral accelerations at orientations between 0° to 180° for a pair (the two orthogonal horizontal components) of ground motions [14].

For each set of DBE-SC motions, the 2 horizontal components were amplitude scaled by F_{H_i} and $1/F_{H_i}$, respectively, and the vertical component was amplitude scaled by F_{V_i}. Note that the geometric-mean spectrum for the two scaled horizontal components of a set of ground motions remains the same as the horizontal DBE spectrum of Figure 4. The factors F_{H_i} (F_{V_i}) with $i = 1,30$ were determined using a lognormal distribution with the median of 1.3 (1.0) and logarithmic standard deviation of 0.13 (0.18) using the Latin Hypercube Sampling procedure. Panel b of Figure 6 presents the spectral accelerations for the horizontal component 1 (i.e., the maximum component) of all 30 sets of MM-SC ground motions.

The distribution of F_{H_i} was based on the study of Huang et al. [14], where the median ratio of maximum to geometric-mean (hereafter termed geomean[1]) spectral demands was shown to vary between 1.2 and 1.4 and the logarithmic standard deviation of the ratio varied between 0.11 and 0.13 at periods greater than 2 seconds.

ANALYSIS SETS

Response-history analysis was performed for two intensities of shaking: 1) 100% DBE shaking, using the 60 sets of DBE-SC and MM-SC ground motions, and b) 150% DBE shaking, using the DBE-SC and MM-SC ground motions but with the amplitude of the acceleration time series multiplied by 1.5.

[1] The geomean demand at a given period is computed as the square root of the product of the spectral demands for two orthogonal horizontal ground-motion components.

At each intensity level, 4 sets of analyses were performed for each of the best-estimate models for this study and the corresponding property-varied models. Table 1 summarizes the 4 analysis sets used in this study, denoted G0, M0, M1 and M2.

Set G0 involves response-history analysis of a best-estimate model subjected to 100% and 150% of the 30 sets of DBE-SC ground motions and produces 30 realizations for each of peak bearing displacement and shearing force in the horizontal plane. Here the letter G stands for geomean since the target horizontal DBE spectrum of Figure 4 is a geomean of two horizontal components and the number 0 is used to denote analysis performed using best-estimate models. The data developed from analysis of Set G0 is used to benchmark all other results.

Set M0 is similar to Set G0 but uses 100% and 150% of the 30 sets of MM-SC ground motions. For Set M1 (M2), each of the 30 models associated with a given best-estimate model and mechanical-property scale factors of Bin F1 (F2) is analyzed using the 100% and 150% of 30 sets of MM-SC ground motions. At a given intensity, Sets M1 and M2 each produce 900 realizations (30 sets of ground motions × 30 models) for peak horizontal bearing displacement and transmitted shearing force. Only the results for bearing displacement are presented herein. The results for transmitted shearing force can be found in Huang et al. [6], [7].

Table 1: Analysis sets for this study

Set	Ground motions		Number of models	Quality control	Number of realizations
	Intensity	Bin			
G0	100%,150%	DBE-SC	1	N/A	30
M0	100%,150%	MM-SC	1	N/A	30
M1	100%,150%	MM-SC	30	excellent	900
M2	100%,150%	MM-SC	30	good	900

ANALYSIS RESULTS FOR SOIL SITES IN CEUS

Peak displacement

All realizations in an analysis set are assumed to distribute lognormally with median (θ) and logarithmic standard deviation (β). Table 2 presents θ and β of peak displacement for each case, model and shaking intensity analyzed in this study. The key observations are presented below.

1) For a given model and shaking intensity, the values of θ for M0, M1 and M2 are identical or nearly identical. The median response for analyses accounting for variability in the mechanical properties of the isolation system (i.e., M1 and M2) can be estimated without bias using analysis of a best-estimate model (i.e. M0).
2) The ratio of θ for M0 to G0 ranges between 1.2 and 1.35. If analysis is performed using DBE-SC ground motions (i.e., Set G0), the median displacement should be increased by 20% to 35% to address variability in spectral demands for soil sites in CEUS.
3) The values of β for peak displacement range between 0.1 and 0.3.

Table 2: Medians (θ) and dispersions (β) of peak displacement

Model	100% DBE								150% DBE							
	θ (mm)				β				θ (mm)				β			
	G0	M0	M1	M2	G0	M0	M1	M2	G0	M0	M1	M2	G0	M0	M1	M2
LR_T3Q3	289	349	348	347	0.13	0.18	0.18	0.19	467	558	557	555	0.12	0.15	0.15	0.16
LR_T3Q6	204	264	263	263	0.16	0.24	0.23	0.24	368	456	455	454	0.15	0.21	0.21	0.22
LR_T4Q3	227	274	274	274	0.13	0.20	0.20	0.20	352	425	426	427	0.11	0.18	0.18	0.18
LR_T4Q6	195	238	238	238	0.15	0.23	0.23	0.23	309	373	374	374	0.16	0.23	0.23	0.23
FP_T3Q3	246	303	303	303	0.14	0.20	0.19	0.20	433	523	523	523	0.12	0.15	0.15	0.15
FP_T3Q6	140	190	190	189	0.21	0.30	0.30	0.31	308	391	391	391	0.18	0.25	0.24	0.25
FP_T4Q3	193	240	240	240	0.15	0.22	0.22	0.22	325	403	403	403	0.12	0.19	0.19	0.19
FP_T4Q6	128	168	168	168	0.20	0.29	0.28	0.29	255	319	319	319	0.18	0.26	0.25	0.26

Response scale factors for design

As noted previously, ASCE 43 writes that nuclear structures should achieve two performance goals: 1) less than 1% probability of unacceptable performance for DBE shaking, and 2) less than 10% probability of unacceptable performance for shaking equal to 150% of the DBE ground motion. Factors are presented in Table 3 to scale the median peak displacements for Sets G0 and M0 and 100% DBE shaking to the responses corresponding to 1) 1% probability of exceedance (PE) for Sets M1 and M2 for 100% DBE shaking, and 2) 10% PE for Sets M1 and M2 for 150% DBE shaking.

If response-history analysis is performed using only the DBE-SC ground motions, the factors in the 2nd through 5th columns of Table 3can be used to address the influence of both maximum-demand orientation and the variation in the material properties of isolation systems on responses. The factor corresponding to 1% (10%) PE at 100% (150%) DBE shaking ranges between 1.8 (2.3) and 2.8 (3.9) in Table 3. If response-history analysis is performed using the MM-SC ground motions, the factors in the 6th through 9th columns of Table 3 can be used to address the impact of variation in isolator material properties on response. The factor corresponding to 1% (10%) PE at 100% (150%) DBE shaking ranges between 1.3 (1.2) and 1.8 (1.4) in Table 3.

Table 3: Ratios of displacement for 1% (10%) exceedance probability at 100% (150%) DBE to $\theta_{G0,DBE}$ and $\theta_{M0,DBE}$

Model	$\frac{D_{M1,DBE,99th}}{\theta_{G0,DBE}}$	$\frac{D_{M1,150\%DBE,90th}}{\theta_{G0,DBE}}$	$\frac{D_{M2,DBE,99th}}{\theta_{G0,DBE}}$	$\frac{D_{M2,150\%DBE,90th}}{\theta_{G0,DBE}}$	$\frac{D_{M1,DBE,99th}}{\theta_{M0,DBE}}$	$\frac{D_{M1,150\%DBE,90th}}{\theta_{M0,DBE}}$	$\frac{D_{M2,DBE,99th}}{\theta_{M0,DBE}}$	$\frac{D_{M2,150\%DBE,90th}}{\theta_{M0,DBE}}$
LR_T3Q3	1.83	2.34	1.85	2.37	1.51	1.94	1.53	1.96
LR_T3Q6	2.22	2.91	2.24	2.93	1.72	2.26	1.73	2.27
LR_T4Q3	1.92	2.36	1.93	2.37	1.60	1.96	1.60	1.96
LR_T4Q6	2.06	2.58	2.07	2.58	1.69	2.11	1.69	2.11
FP_T3Q3	1.93	2.57	1.95	2.58	1.57	2.09	1.58	2.09
FP_T3Q6	2.72	3.83	2.80	3.85	2.00	2.82	2.06	2.83
FP_T4Q3	2.09	2.65	2.10	2.66	1.68	2.13	1.68	2.13
FP_T4Q6	2.52	3.44	2.56	3.45	1.93	2.63	1.96	2.64

CLOSING REMARKS

Nonlinear response-history analyses have been performed to study the impact of the variability in both earthquake ground motion and mechanical properties of isolation systems on the seismic responses of base-isolated NPPs. Three types of isolation systems were studied, including LR and single concave FP isolation systems. The analyses were performed for representative rock and soil sites in CEUS and a rock site in WUS but only the results for LR and FP bearings and the selected soil site in the CEUS have been presented here. Key conclusions for the CEUS soil site are summarized below:

1) For a given model, the ratio of median displacement for Set M0 to Set G0 generally ranges between 1.2 and 1.35. The median responses for analyses using DBE-SC ground motions in both horizontal directions should be amplified to address the known variability in spectral demands.
2) The ratios of median responses for Set M1 to Set M0 and those for Set M2 to Set M1 are either equal to or very close to 1 for all cases considered. The median response for analyses accounting for the variability in isolator material properties (i.e., M1 and M2) can be estimated without bias using analysis of a best-estimate model (i.e. M0).
3) The factors to scale the median displacements for Sets G0 and M0 and 100% DBE shaking to the displacements corresponding to 1) 1% PE for Sets M1 and M2 for 100% DBE shaking and 2) 10% PE for Sets M1 and M2 for 150% DBE shaking were studied. The factor for 10% PE and 150% DBE shaking is greater than that for 1% PE and 100% DBE shaking. Analysis of isolator capacity and clearance to surrounding structure can be based on 10% PE for 150% DBE shaking. For Set G0, 10% PE and 150% DBE shaking, the upper bound of the scale factor for LR and FP isolation systems are 2.9 and 3.9, respectively at the representative soil site in CEUS.
4) The difference in the factors to scale the results of analysis of best-estimate models and 100% DBE shaking to 10% PE and 150% DBE shaking for Sets M1 and M2 is negligible.

REFERENCES

[1] Mayes, R. L., Button, M. R. and Jones, D. M. (1998) "Design issues for base isolated bridges: 1997 revised AASHTO code requirements." *Proceedings*, Structural Engineering World Congress, San Francisco, CA.
[2] Naeim, F., and Kelly, J. M. (1999). *Design of seismic isolated structures: from theory to practice*, John Wiley, NY.
[3] Eidinger, J. M., and Kelly, J. M. (1985). "Seismic isolation for nuclear power plants: technical and non-technical aspects in decision making." *Nuclear Engineering and Design*, 84(3), 383-409.
[4] American Society of Civil Engineers (ASCE). (2000). "Seismic analysis of safety-related nuclear structures and commentary." *ASCE 4-98*, ASCE, Reston, VA.
[5] American Society of Civil Engineers (ASCE). (2005). "Seismic design criteria for structures, systems, and components in nuclear facilities." *ASCE/SEI 43-05*, ASCE, Reston, VA.
[6] Huang, Y.-N., Whittaker, A. S., Kennedy, R. P., and Mayes, R. L. (2009). "Assessment of base-isolated nuclear structures for design and beyond-design basis earthquake shaking." *MCEER-09-0008*, Multidisciplinary Center for Earthquake Engineering Research, State University of New York, Buffalo, NY.
[7] Huang, Y.-N., Whittaker, A. S., Kennedy, R. P., and Mayes, R. L. "Beyond-design basis nuclear structures of base isolated nuclear structures." Paper in preparation, *Earthquake Engineering and Structural Dynamics*.
[8] Computers and Structures, Inc. (CSI). (2007). *SAP2000 user's manual – version 11.0*. Berkeley, CA.
[9] Constantinou, M. C., Tsopelas, P., Kasalanati, A., and Wolff, E. D. (1999). "Property modification factors for seismic isolation bearings." *MCEER-99-0012*, Multidisciplinary Center for Earthquake Engineering Research, State University of New York, Buffalo, NY.
[10] Nowak, A. S., and Collins, K. R. (2000). *Reliability of structures*, McGraw-Hill, Boston.
[11] Southern Nuclear Operating Company (SNOC). (2008). *Vogtle Early Site Permit Application*, SNOC. < http://adamswebsearch2.nrc.gov/idmws/ViewDocByAccession.asp?AccessionNumber=ML081020073 >
[12] Halldorsson, B. (2004). <civil.eng.buffalo.edu/engseislab/ products.htm> Engineering Seismology Laboratory, State University of New York, Buffalo, NY.
[13] Abrahamson, N.A. (1998). "Non-stationary spectral matching program RSPMATCH." PG&E, Internal Report.
[14] Huang, Y.-N., Whittaker, A. S., and Luco, N. (2008). "Maximum spectral demands in the near-fault region." *Earthquake Spectra*, 24(1), 319-341.

REDUCTION OF SEISMIC RESPONSE OF BUILDING USING BASE ISOLATION

P. N. Dubey[1], G. R. Reddy[1], K K Vaze[1], H S Kushwaha[2] and S K Deb[3]
[1]Reactor Safety Division, Bhabha Atomic Research Centre, Mumbai, INDIA-400085
[2]Raja Ramanna fellow, Bhabha Atomic Research Centre, Mumbai, INDIA-400085
[3]Department of Civil Engineering, IIT, Guwahati, INDIA-781 039
E-mail of corresponding author: pndubey@barc.gov.in

ABSTRACT

The base isolation is aimed to attenuate the horizontal accelerations transmitted to the superstructure. The isolators attempt to decouple the superstructure from the strong components of horizontal ground motion. Isolators have low horizontal stiffness and they are placed between the structure and foundation. This makes the natural frequency of the structure of the order of 0.5 Hz of less, which enables the structure to experience low accelerations. Thus the structure along with the isolators acts like filter and will not respond to higher frequencies (> 0.5Hz). To study the behaviour of base isolated buildings under actual earthquakes, two numbers of three-storied RCC framed buildings have been constructed at IIT, Guwahati campus, one of the highest seismic zones (Zone-V) of India. Between two experimental buildings, one is on base isolator and other with conventional rigid foundation. Initially isolated building was constructed on Lead Plug Bearing (LPBs) and later LPBs were replaced by Laminated Rubber Bearing (LRBs) by lifting the building. Accelerometers are installed at first and third floors of both the buildings in order to record and compare the seismic responses of base isolated and conventional foundation buildings. The experimental buildings experienced actual earthquakes for both types of base isolators. A study has been made on the data recorded on both the buildings for both the cases of base isolation and the difference between recorded responses of isolated building using two different types of isolators have also been highlighted. Improvements required in the conventional analysis procedures are clearly brought out in this paper.

INTRODUCTION

The isolators attempt to decouple the building or structure from the horizontal components of the ground motion. Isolators have low horizontal stiffness and they are placed between the superstructure and foundation. This makes the natural frequency of the whole system including the structure to the order of 0.5 Hz of less, which eventually makes the structure to experience low accelerations as shown in Fig.1. Thus the structure along with the isolators acts like filter and will not respond to higher frequencies (> 0.5Hz).

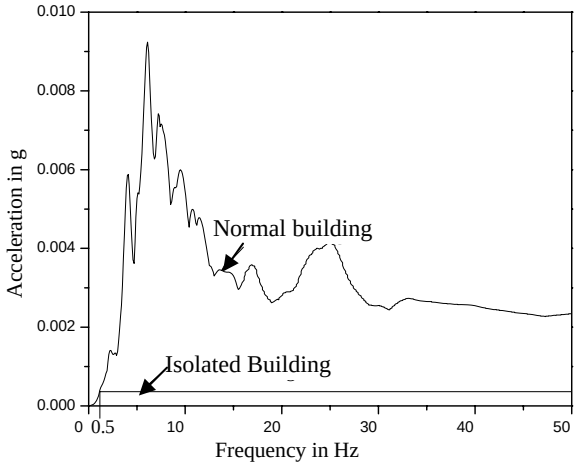

Fig. 1: Typical design response spectrum for normal and base isolated buildings

Recently Kelly compiled the literature in design, analysis, experiments and application of base isolators to structures and published a book [1]. From this book it is observed that there is no literature on behavior of base isolated structure subjected to real earthquake. In present work response of normal and isolated buildings have been

recorded under real earthquakes, which would help to build more confidence in utilities and promote indigenous design, manufacturing and use of base isolation technique in India. To study the behavior of isolated building under actual earthquake scenario, two numbers of three-storeyed framed RCC buildings with similar construction, one building with conventional foundation (here onwards called as normal building) and other with base isolation as shown in Fig. 2(a), were-built at IIT, Guwahati campus. Guwahati is situated in the most severe seismic zone (Zone-V) of Northeast India. Northeast India is lying at the juncture of Himalayan arc to the north and Burmese arc to the east, and is one of the most seismically active regions of the world. Eighteen large earthquakes (M ≥7.0) including two great earthquakes (M ≥ 8.0) occurred in this region during the last 100 years [2]. The experimental building is 4.5mx3.3m area and the orientation of X and Z-axes of the buildings are shown in Fig. 2(c). The Y-axis is aligned with the height of the building. Initially for the base isolation, four numbers of Lead Plug Bearings (LPB) as shown in Fig. 2(b), with 50T vertical load capacity have been used under each column of the building and latter on these isolators were replaced by Laminated Rubber Bearings (LRBs) by lifting the building on hydraulic jacks and actual earthquake data were recorded on both the buildings. A twelve channel dynamic structural recording system has been employed for recording the seismic ground motion and structural response of normal and isolated buildings [3]. One tri-axial force balance accelerometer has been installed on the ground to capture earthquake induced ground motion and four numbers of accelerometers have been installed at 1st floor and 3rd floor of the buildings to record the bi-directional accelerations. Five numbers of actual earthquake data were recorded on experimental buildings with LPB isolation and further after replacement of LPBs by LRBs, seven numbers of real earthquake data have been recorded. The real earthquake data recorded with LPB isolation on November 06, 2006 and earthquake data with similar origin, depth and magnitude has been recorded on September, 03, 2009 with LRB isolation. A comparative study between recorded data has been made to investigate the effectiveness of two types of base isolation used separately. The magnitude of earthquake on November 06, 2006 was 5.2 on Richter scale with focal depth of 122.6 km (24.736^{o} N, 95.223^{o} E) and epicenter is in the Southeast to the site of the buildings, whereas the magnitude of earthquake on September, 03, 2009 was 5.9 on Richter scale with focal depth of 100 km (24.3^{0} N, 94.6^{0} E) and epicenter is in the Southeast of the site of buildings at Myanmar-India border. From the analysis and actual seismic records on experimental buildings, improvements required in the conventional analysis procedures are clearly brought out in this paper to obtain realistic structural seismic response.

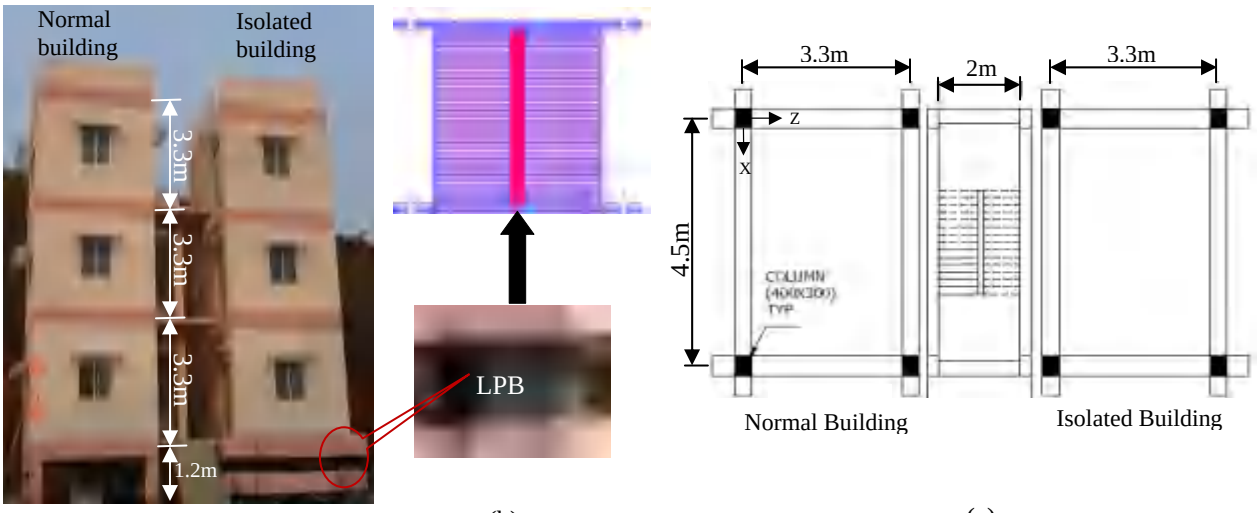

Fig. 2: (a) Experimental buildings at IIT, Guwahati; (b) Lead plug bearing (c) Plan view of the buildings

SEISMIC BASE ISOLATORS

Base isolation is a technique to reduce the acceleration transferred to structure from the ground and hence prevent the damage to buildings during an earthquake. Use of base isolation technique is very common in New Zealand, Japan, Italy and USA, however use of same is very limited in India. Commonly two types of base isolators are used viz. laminated rubber bearing and lead plug bearing. The lead plug bearing consists of alternate layers of metal and rubber with central lead plug as shown in Fig. 3(a), to control the lateral displacement by hysteretic deformation of lead. The re-crystallization temperature of lead is 25^{0}F, therefore lead can plastically deform under

earthquake forces and regain its original shape when forces are removed and also it can take large numbers of load reversal cycles of plastic deformation without losing strength [4]. The laminated rubber bearing is similar as lead plug bearing without central lead plug as shown in Fig. 3(b). The central lead plug in LPB absorbs the seismic energy by hysteretic deformation of lead hence lesser seismic response however in case of LRBs more lateral displacements can be expected. Both the base isolators used for base isolation of experimental building are consisting of 28 numbers of 4mm thick steel shims and 29 numbers of 7 mm thick rubber layers with 460 mm diameter and 355 mm height. The diameter of central lead plug in LPB is 40mm.

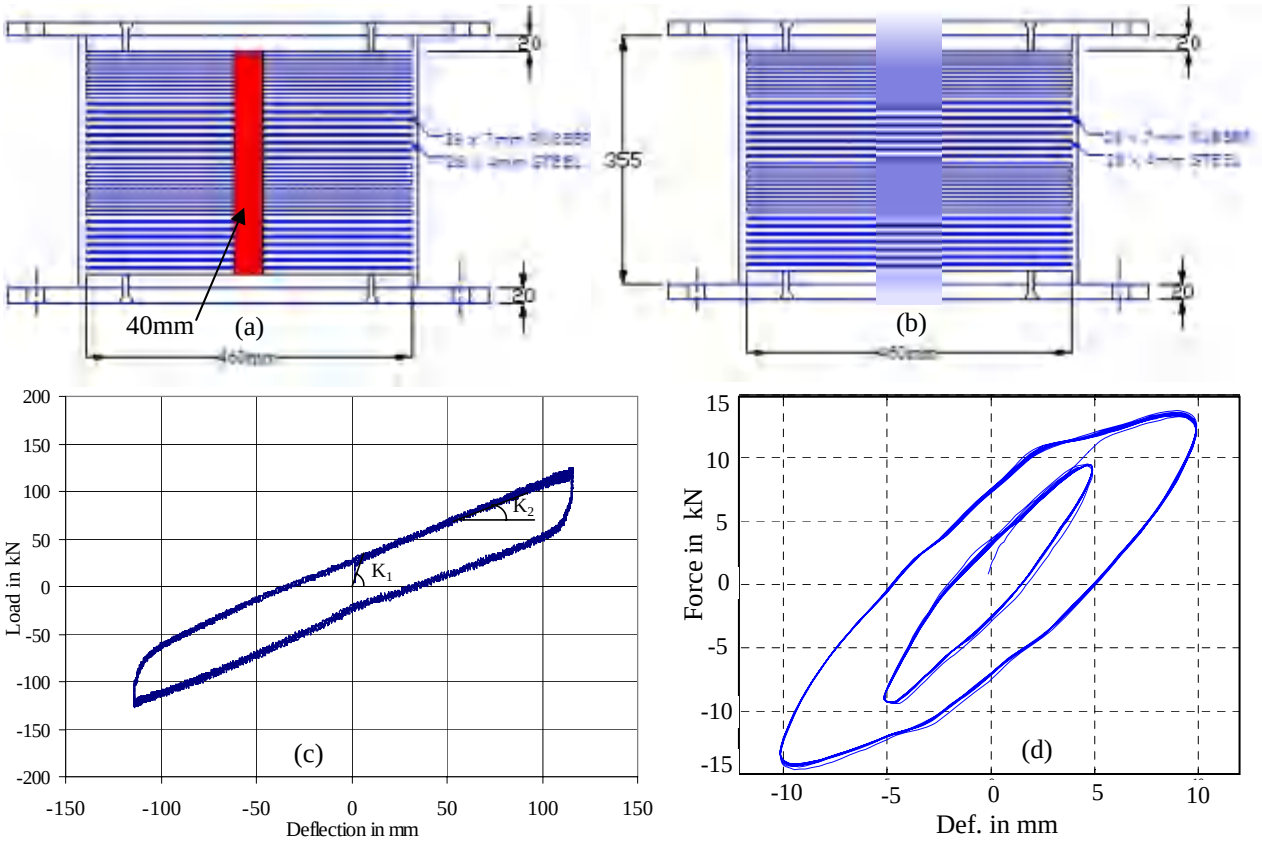

Fig. 3: (a) Dimensions of LPB; (b) Dimensions of LRB; (c) Cyclic load-deflection curve for LPB; (d) Cyclic load-deflection curve for LRB

The vertical stiffness of single LPB is 806.64 kN/mm and horizontal stiffness of isolator considering the first slope (K_1) is 17.18 kN/mm and 0.7968kN/mm for second slope (K_2) as shown in Fig. 2(c). The vertical stiffness of other type of isolator used i.e. LRB is 753kN/mm and experimentally derived horizontal stiffness from cyclic force-displacement curve as shown in Fig. 3(d), is 2.0kN/mm.

RECORDED RESPONSE OF THE BUILDINGS UNDER ACTUAL EARTHQUAKE

Among twelve recorded actual earthquakes, the earthquake data on November 06, 2006 with LPB isolation and September, 03, 2009 with LRB isolation on experimental buildings along with ground motion records have been discussed under following headings.

Recorded Response with LPB Isolator

The recorded response on 1st and 3rd floors in Z-direction of normal and base isolated buildings with LPBs have been plotted in Figs. 4 & 5 and corresponding ground motion record has also been plotted in Fig. 6. It can be observed from Figs. 4(a) & (b), that there is 4.8 times reduction in seismic response at 3rd floor of base isolated building as compared to normal building. Similarly 2.6 times reduction can also be observed from Figs. 5(a) & (b), at 1st floor of the isolated building as compared to normal building. The recorded response of isolated building is

lesser than the response of normal building and ground motion records, which depicts the effectiveness of base isolation. There is amplification of response from ground to 3rd floor of the normal building, whereas almost same response can be observed at 1st and 3rd floor of isolated building, which is a desired characteristic of base isolated system.

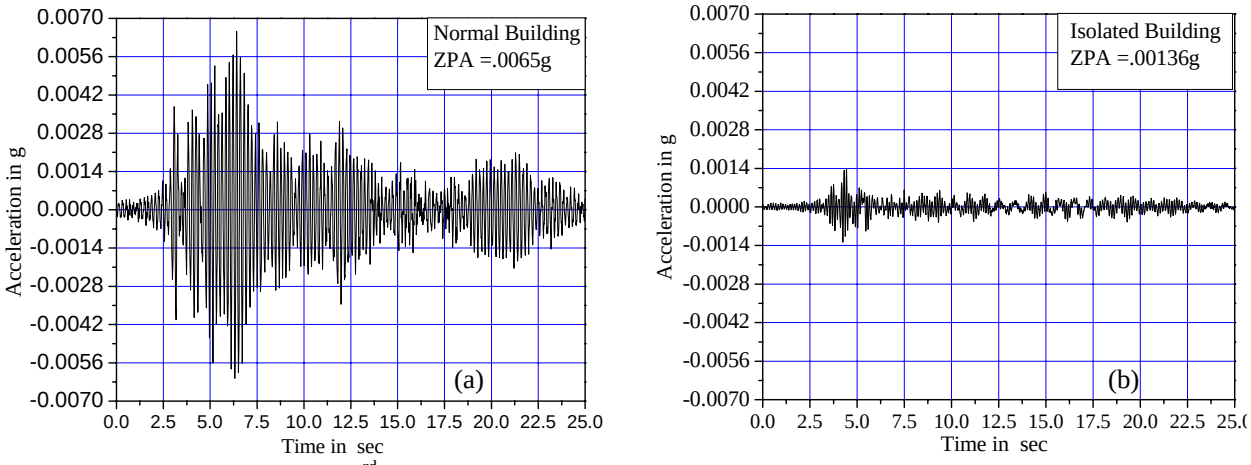

Fig. 4: Recorded response at 3rd floor in Z-direction, (a) Normal building; (b) Isolated building with LPB

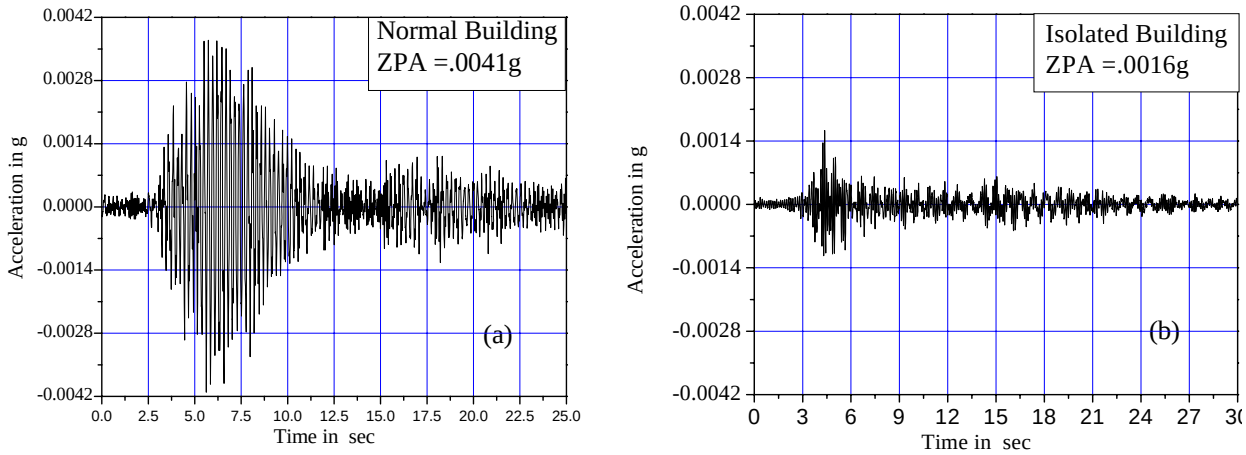

Fig. 5: Recorded response at 1st floor in Z-direction, (a) Normal building; (b) Isolated building with LPB

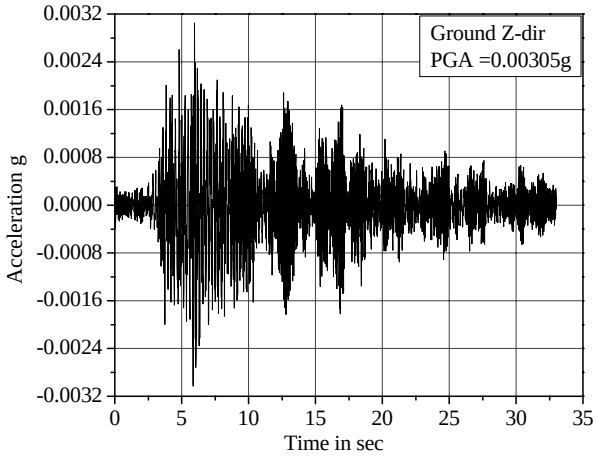

Fig. 6: Recorded ground motion acceleration in Z-direction on Nov 06, 2006

Recorded Response with LRB Isolator

The recorded response on 1st and 3rd floors in Z-direction of normal and base isolated buildings with LRBs have been plotted in Figs. 7 & 8 and corresponding ground motion record has also been plotted in Fig. 9. It can be observed from Figs. 7(a) & (b), that there is 2.3 times reduction in seismic response at 3rd floor of base isolated building as compared to normal building. Similarly 1.8 times reduction as shown in Figs. 8 (a) & (b) can also be observed at 1st floor of the isolated building as compared to normal building. The recorded response of isolated building is lesser than normal building similar to previous case, which depicts the effectiveness of base isolation using LRBs. The response of isolated building is more uniform from 1st floor to 3rd floor as compared to previous case. The earthquake occurred on September 03, 2009 was of higher magnitude even then the percentage reduction in seismic response is more in case of LPB isolators.

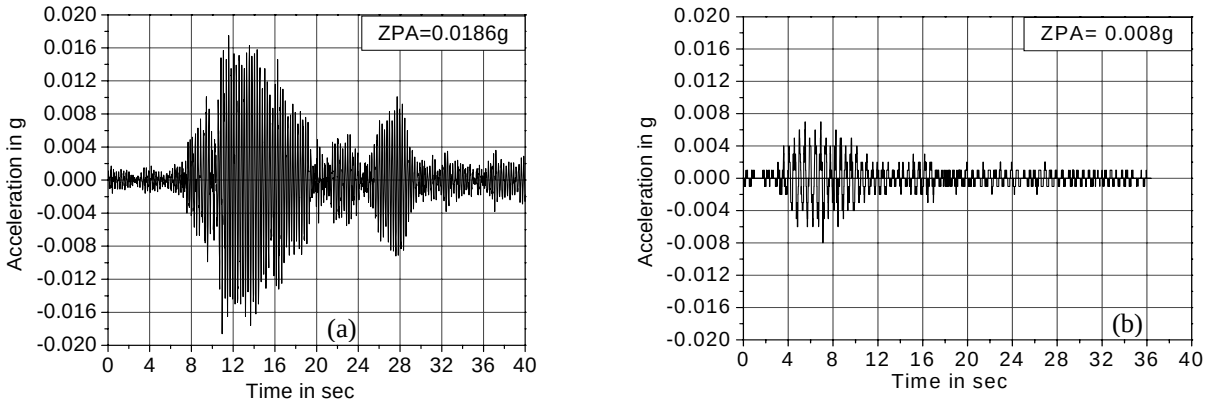

Fig. 7: Recorded response at 1st floor in Z-direction, (a) Normal building; (b) Isolated building with LRB

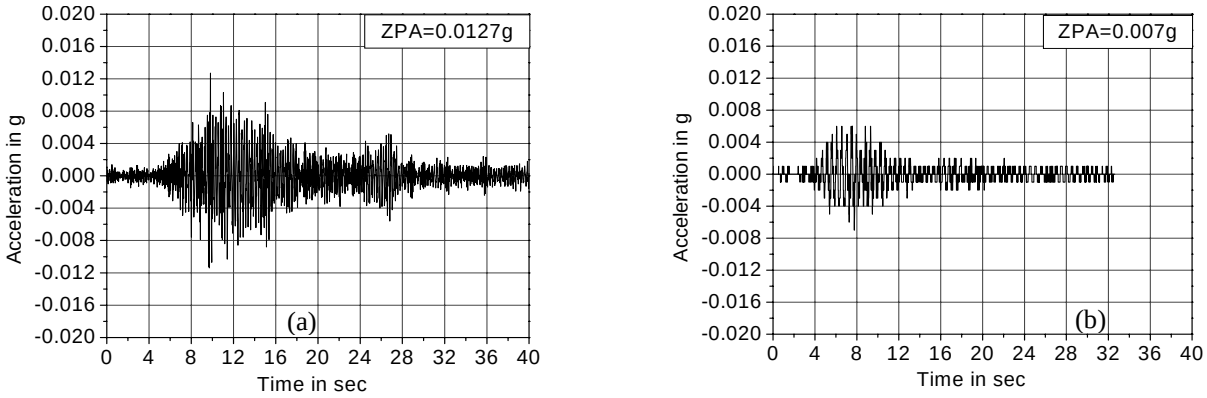

Fig. 8: Recorded response at 1st floor in Z-direction, (a) Normal building; (b) Isolated building with LRB

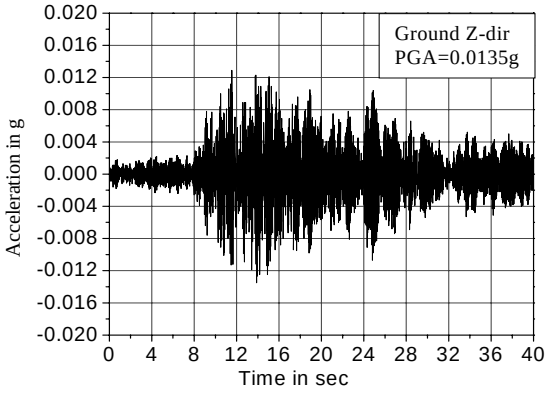

Fig. 9: Recorded ground motion acceleration in Z-direction on Sept 03, 2009

FREE VIBRATION ANALYSIS OF EXPERIMENTAL BUILDINGS

Analysis of Normal Building

Using conventional design approach, analysis of normal building has been performed by ignoring the stiffness of the in-fills walls and only considering the masses of the in-fill walls. The masses of infill walls have been lumped at the nodes of respective floor beams as shown in Fig. 10 (a). The first mode frequencies obtained in Z and X-directions are 1.25Hz and 1.54Hz respectively with 76% mass participation. Free vibration analysis is also performed considering frequency independent soil springs, whose properties are obtained using the formulae given in ASCE 4-98 [5] and from the analysis it is found the effect of soil springs are insignificant and frequencies and participation factors were unaltered.

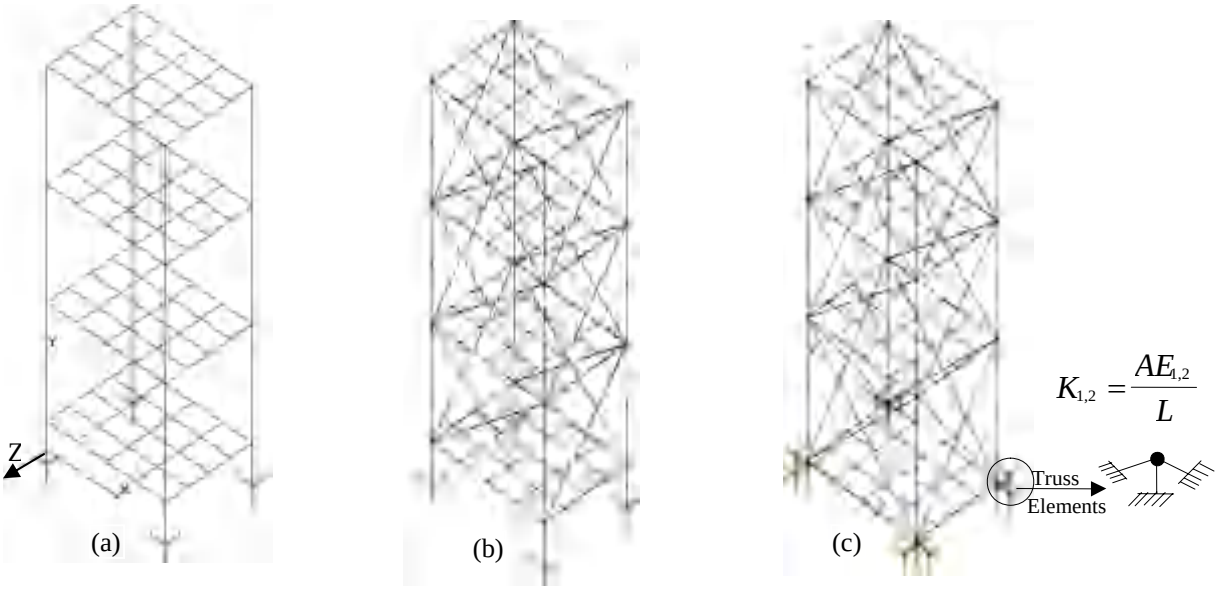

Fig. 10: (a) FE model of normal building without infill wall; (b) FE model of normal building with in-fill wall as equivalent strut; (c) FE model of isolated building

Later to investigate the effect of infill walls on natural free vibration characteristics of normal building, stiffness of infill walls have been modelled as equivalent diagonal struts [6] as shown in Fig.10 (b), and equivalent struts geometric parameters have been calculated from the geometry of the brick wall using the procedures explained in reference [7]. The first fundamental frequencies in Z and X-directions are 4.42Hz and 5.65 Hz with 81% and 82% mass participations respectively. It is clearly understood from this analysis that there is significant contribution of infill walls in increasing the fundamental frequency of normal building.

Analysis of Isolated Building

Isolated building has been FE modelled same as normal building and initially LPB isolators were modelled with second slope stiffness (K_2), where yielding of lead was assumed, however later it was realised that the seismic excitation is very low to cause any yielding in central lead plug. Hence the modal frequencies thus obtained were very low as compared to modal peaks in the recorded data. Later the isolators have been modelled as nonlinear truss elements as shown in Fig. 10 (c). The first lateral stiffness (K_1) of LPB isolator corresponding to un-yielded lead and the 2nd lateral stiffness (K_2) of LPB corresponding to nonlinearly deforming lead plug as shown in Fig. 3(c), have been modelled using Eq. (1).

$$K_{1,2} = (AE_{1,2})/L \quad (1)$$

Where E_1 and E_2 are the elastic modulus corresponding to first and second stiffness as discussed above.
A, L= area and length of truss element respectively.

It can be observed from the analysis results listed in Table-1, that there is significant mass participation in 2nd modes in horizontal direction considering the duel slope model of isolators, whereas total mass was participated in 1st mode when second slope was only considered for modelling the isolators. Non-yielding of lead plug due to low earthquake excitation imparts higher stiffness to isolators and hence frequency of isolated building is higher in this situation.

Table 1: Modal frequencies and mass participation of isolated building

Dual Slope					2nd Slope				
Mode No	Freq (Hz)	Mass Participation in kg			Mode	Freq (Hz)	Mass Participation in kg		
		M_x	M_y	M_z			M_x	M_y	M_z
1 (Z-dir)	2.07	0	0	98718	1 (X-dir)	0.796	0	0	116000
2 (X-dir)	2.53	104000	0	0	2 (Z-dir)	0.812	116000	0	0
4 (Z-dir)	7.58	0	0	17367	6 (Y-dir)	10.10	0	112000	0
5 (X-dir)	8.42	12211	0	0					

Time history analysis has also been performed for above two cases using recorded ground time history on November 06, 2006 as base excitation to isolated building and the corresponding response spectrum have been plotted in Figs. 11(a) & (b). It can be observed that in case of dual stiffness modelling of isolator the analytical spectral peaks are more close to recorded spectral peaks as compared to single stiffness i.e. in 2nd slope case. This analysis also depicts that for small input excitations the deflection of the isolator is small to cause yielding in lead plug and hence natural vibration characteristic is governed by the elastic slope (K_1) and higher.

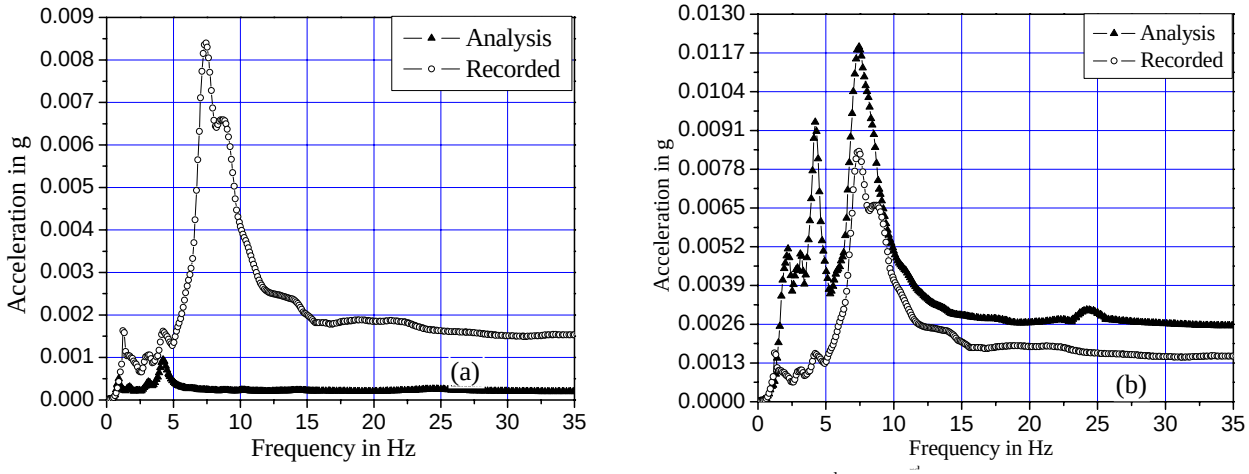

Fig. 11: (a) Recorded and analysis response spectrum corresponding to 2nd slope of isolator; (b) Recorded and analysis response spectrum corresponding to dual slope of isolator.

CONCLUSION

From the FE analysis of normal building it is observed that there is significant contribution of in-fill walls in the dynamic characteristic of the normal building, whereas effect of same is insignificant in case of isolated building because of rigid body motion of the structure above the isolator. The recorded response of isolated building using two types of base isolators is much lesser than the response of normal building, which depicts the effectiveness of base isolation. The percentage reduction in seismic response is higher in case of base isolation using lead plug bearing. The input seismic excitation is very low to cause yielding of lead plug and therefore frequency of isolated building is higher in this situation. The initial stiffness (un-yielded lead plug) of LPB is higher that can provide rigidity under lateral service loads such as wind loads. The spectral peaks are more close to recorded response when LPB isolators are modelled as dual slope nonlinear truss element as compared to single slope model.

Since there is significant contribution of infill walls on dynamic characteristics of normal building, the structural members should be designed for two levels of earthquakes, one low level earthquake at which infill walls are intact and other high level (design) earthquake at which infill walls are failed, because the acceleration

corresponding to increased frequency due to infill walls may be higher than acceleration at lower frequency in design spectrum. Similarly in case of isolated building, modal frequencies are higher in case of un-yielded lead plug condition at low level of earthquakes, which may correspond to higher acceleration than design spectrum. Therefore structural members of isolated building needs to be checked for a limiting earthquake level at which lead core is un-yielded otherwise isolated building may attract higher acceleration corresponding to un-yielded lead plug frequency, which is higher than the design frequency. The deformations may exceed the design value at an earthquake which is lower than the design earthquake.

REFERENCES

[1] J. M. Kelly and Farzad Naeim, "Design of Seismic Isolated Structures, From Theory to Practice".
[2] J.R. Kayal "Seismicity of northeast India and surroundings- Development over the past 100 years" Journal of Geographics, Jan 1998, vol. XIX No.1 pp 9 to 34.
[3] S.K. Deb, A. Dutta, "Verification test of a prototype two storeyed RCC framed building subjected to actual earthquakes" Project report for 8th technical programme discussion meeting.
[4] "Introduction to physical metallurgy" by Sidney H Avner, second editionTata McGraw-Hill Education.
[5] Seismic analysis of safety-related nuclear structures and commentary, ASCE 4-98
[6] Hemant B. Kaushik, Durgesh C. Rai, and Sudhir K. Jain, "Code approaches to seismic design of masonry-in-filled reinforced concrete frames: A state-of-the-art review" Earthquake Spectra, Volume 22, No. 4, pages 961–983, November 2006; © 2006, Earthquake Engineering Research Institute.
[7] Federal emergency management agency (FEMA)-306, "Evaluation of earthquake damaged concrete and masonry walls buildings" 1998.

SHAKE TABLE TESTS TO INVESTIGATE THE ISOLATION EFFECT OF GEOMEMBRANE IN SOIL

B.R.Jayalekshmi[1], R.Shivashankar[1], Katta Venkataramana[1], R.Ramesh Babu[2], G. R.Reddy[3]
[1] National Institute of Technology Karnataka, Surathkal, India - 575025
[2] CPRI , Bangalore, India
[3] BARC, Mumbai, India
E-mail of corresponding author: br.jaya@gmail.com

ABSTRACT

Base isolation and other structural control systems are being developed to minimize the earthquake damage by reducing seismic structural response. Over the years, several types of base isolators have emerged and been installed worldwide in structures to dissipate the seismic energy transmitted to the structure. Generally a base isolator shifts the natural period of the building away from that of the predominant period of the most probable earthquakes and provides additional damping to absorb the energy. The present study focuses on the efficacy of soil and a layer of smooth geosynthetic membrane placed in soil in reducing the seismic response of a structure. Shake table tests are carried out in a 3mx3m tri-axial shaker system with six degrees of freedom. A steel tank fixed to the shake table is used as a container for soil and soil reinforced with smooth geosynthetic membrane. 1/3rd scaled model of a single storey, single bay reinforced concrete space frame with isolated footing has been cast. This model is placed over sand and sand with geomembrane in the steel tank. Sand in dry and saturated conditions are used. Response of the structure is recorded with accelerometers placed at the roof level.

Sine sweep tests are carried out on the structure with fixed base and the structure resting on different soil conditions to assess the effect of soil and soil isolation on the dynamic characteristics of the structure. For this, sinusoidal motion in the range of frequency of 1 to 50 Hz is applied in all three directions with a sweep rate of 1 octave per minute. The structure with different base conditions is subjected to motion corresponding to the response spectrum of Zone III as per the recommendations of Indian standard IS 1893(Part1):2002 to identify the effect of soil isolation on the seismic response. Analysis of results shows considerable reduction in the natural frequency and a reduction in maximum acceleration at the roof level by 40% due to soil isolation with geomembrane. It is concluded that smooth geomembrane and sand acts together as an isolator system in reducing the seismic response of the structure. A concept of using a smooth geosynthetic liner underneath building foundations to dissipate earthquake energy through sliding along the geosynthetic interface can be adopted as an alternative low cost seismic base isolation technique.

INTRODUCTION

Base isolation provides a very effective means of mitigating seismic and vibrational responses in the equipment and systems in nuclear power plants. The reduction in the natural frequency of structures may cause the structural period to be shifted to the right of the falling curve of response spectra given in IS 1893:2000, resulting in a reduced seismic structural response compared to a fixed base structure.

A smooth synthetic liner placed within a soil deposit can dissipate earthquake energy through deformations along the liner interface, thus reducing the intensity of the propagating shear waves. Such a system is referred to as soil isolation because the soil layer above the liner is isolated from the underlying soil deposit that is experiencing the seismic shaking. Soil isolation can be potentially beneficial if applied in the construction of new buildings, slopes, embankments, and reclaimed land using hydraulic fill [1] that is known to liquefy during seismic shaking [2], [3],[4]. For soil isolation to function properly, an allowance has to be made for the deformations to occur along the liner. In addition, the permanent deformations associated with the movement along the isolation liner need to be within acceptable limits if soil isolation is used to protect an overlying building or other structures[5]. The concept of foundation isolation is similar to base isolation except that, in this case, the entire building is isolated from the ground through the use of a geosynthetic liner. Under strong ground shaking the smooth geosynthetic liner underneath the building foundation dissipates earthquake energy thus transmitting reduced accelerations to the overlying structure [6].

The objective of the present research is to evaluate the efficiency of homogeneous soil and soil reinforced with geomembrane in reducing the seismic wave transmission to the building. It is aimed to estimate the response behaviour of reinforced concrete structures with isolated foundation, resting on a shallow soil stratum of

homogeneous or reinforced soil and to study the efficiency of the slip deformations along the geosynthetic interface in reducing the transmission of the base motion to the superstructure.

EXPERIMENTAL SET UP

A 1/3rd scaled model of a single storey, single bay RC space frame with isolated footing was cast. Sufficient mass was added to the structure to maintain the fundamental frequency in the range of 3 Hz to 10 Hz, which corresponds to structures with maximum spectral acceleration according to the response spectra for rock and soil site for 5% damping as given in IS 1893(Part I): 2002[7].

Structure

The size of model is 1.2m X 1.2m c/c between columns.The height of the model up to the top of slab from the top of footing is 1.5m. The slab thickness is 50 mm with reinforcement of 6 MS @ 100 mm c/c both ways at both top and bottom. Plinth beams and columns are 100mm X 100mm with 4-8Tor and stirrups of 3 MS @ 75mm c/c. Roof Beams are 100mm X 100mm with 4-8Tor, stirrups of 3 MS @ 75mm c/c. The isolated footing is 350mm X 350mm X 100mm with 6 MS @ 100mm c/c both ways at both top and bottom. Concrete of Grade M25 was used. A schematic model of the structure is shown in Fig.1.

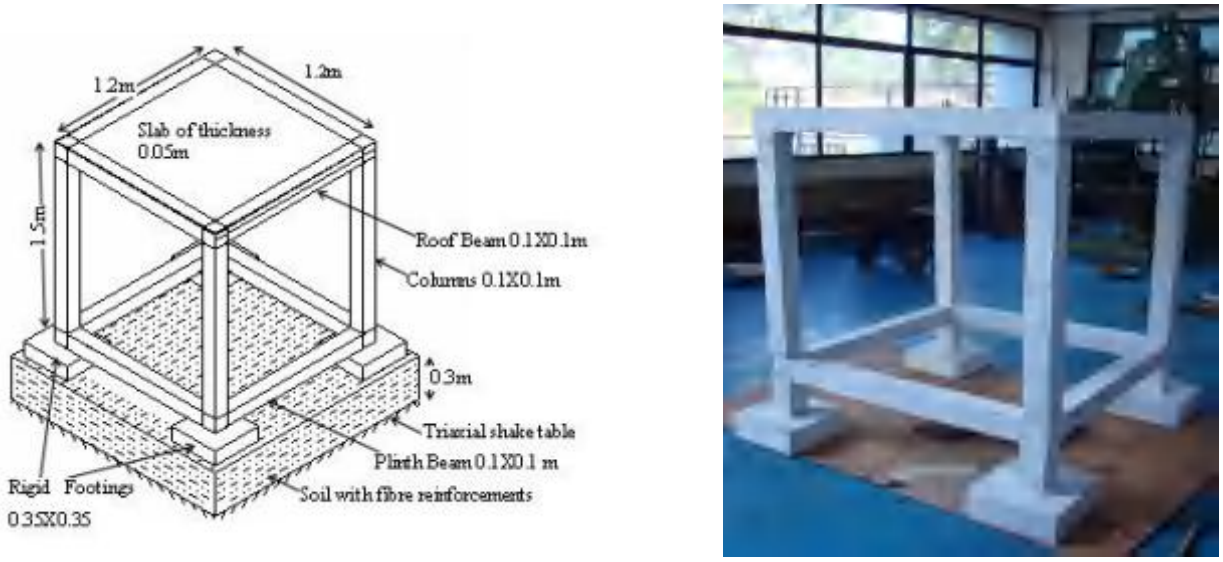

(a) (b)

Fig.1: (a) Geometric details of the model (b) Model of the structure

Base isolation

The supporting soil or reinforced soil was filled to a depth of 300mm in a rigid steel tank of size 2mx2m. The supporting soil used for base isolation was well graded dry and saturated dense sand. Polyethlene geomembrane with very low friction coefficient was used. Dense sand was reinforced with this geomembrane which is embedded horizontally in the soil at one third height from the top of soil layer.

EXPERIMENTAL PROCEDURE

The tri-axial shaker system of Earthquake Engineering and Vibration Research Centre (EVRC) at Central Power Research Institute (CPRI), Bangalore, India, was used to carry out the tests on the models. The Tri-axial shaker system consists of 4 vertical and 4 horizontal linear servo hydraulic actuators to provide the motion inputs to the shake table. The t able dimension is 3 m × 3 m with six degrees of freedom, 3 translational and 3 rotational, and a maximum payload of 100 kN. Experimental setup on the triaxial shaker system is shown in figure 2.

Fig.2 : Experimental setup on the triaxial shaker system

A three dimensional single storey building model with isolated footing was placed on the shaking table and its response to harmonic and simulated earthquake motion was measured. Sine sweep test were carried out to find the natural frequency of the fixed structure as well as the structure resting on different soils. Seismic excitations corresponding to seismic zone-III as given in IS: 1893(Part I): 2002 was given to structural model with various base conditions and the response was measured. Comparative studies were carried out by testing the building model placed on different types of soil bed and with fixed base.

To study the response of the fixed base structure, the isolated footings of the model were anchored to the shake table. Accelerometers were placed at the roof level to get the response to the excitations. They were placed at the beam column junction and at the mid span of the roof beam in X and Y directions. Locations of accelerometers are listed in Table 1.

Table 1: Location details of accelerometers

Location of Accelerometers	Direction	Accelerometer Nos.	Location Details
Roof Level	X	A1	At the mid span of roof beam
		A2	At the beam column junction
	Y	A3	At the mid span of roof beam
		A4	At the beam column junction

The structural response to harmonic and earthquake motions was measured. To study the effect of soil, the rigid steel tank was fixed to tri-axial shaker system and a layer of soil or reinforced soil of 300mm thickness was filled inside the tank. Subsequently the building model was placed over the soil bed and the response to shaking was recorded. To study the isolation effect of geomembrane, polyethlene geomembrane with very low friction coefficient was embedded horizontally in the soil at 200mm from the bottom of soil layer and the structural response was measured.

INPUT MOTION

Sine Sweep Test

In this test, a sinusoidal input with continuously varying frequency was applied to the structure for determining the natural frequency of the models. A sinusoidal motion with amplitude of 0.lg was applied in all three directions i.e. X, Y, Z for the structure with fixed base without causing any damage to the rigid structural model.

The response of the structure supported on soil was very less for this amplitude sinusoidal motion. Since the amplitude of motion does not alter the natural frequency of a system, a higher amplitude of 0.2g, which gives a recordable response in the structure was applied to the structure resting on soil. The range of frequency was 1 to 50 Hz. The sweep rate applied was 1 octave per minute. The fundamental natural frequency of the fixed base and compliant base structures was obtained from the frequency response function of the structural response.

Design Response Spectrum for Zone III

Design response spectrum refers to an average smoothened plot of maximum acceleration as a function of frequency or time period of vibration for a specified damping ratio for earthquake excitations at the base of a single degree of freedom system. The design response spectra corresponding to seismic zone-III as given in IS: 1893(Part I): 2002 are shown in Figure 3. In this figure, X and Y denote the two horizontal directions (N-S and E-W) and Z denotes the vertical direction. These spectra were used for the testing of models as explained.

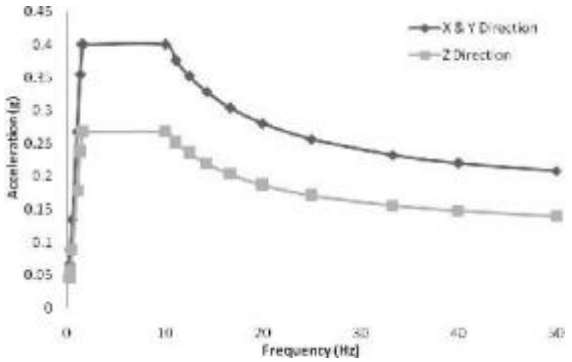

Fig.3: Design response spectra for seismic zone III

RESULTS AND DISCUSSIONS

A study of single bay single storey structural model with isolated footing, resting on various soil conditions, dry sand, dry sand reinforced with geomembrane, saturated sand and saturated sand reinforced with geomembrane is considered. The variation in natural frequencies from experimental results is presented. The variation of maximum acceleration at the roof level is studied for all accelerometer locations for various base conditions. Response spectrum analysis and time history analysis are carried out using spectrum compatible time history for zone III.

Variation in natural frequency

The variation in natural frequency has been studied on structure with the different cases mentioned above. The variation in the natural frequency of the structure from experimental results is tabulated in the Table 2. It is observed that the natural frequency decreases with the increase in flexibility of supporting soil.

Table 2: Variation in fundamental frequency of structural model

Base conditions	Natural frequency(Hz)		
	X	Y	Z
Fixed Base	4.218	4.125	23.25
Dry Sand	3.75	3.5	16
Dry Sand + Geomembrane	3	3	13
Wet Sand	2.5	2.5	12.5
Wet Sand + Geomembrane	2	2	12

Analysis of Table 2 shows that the natural frequency of the fixed base structure is reduced by incorporating a finite mass of soil or reinforced soil below the structure. The effect is more prominent for sand reinforced with the geomembrane layer. The reduction in natural frequency is 28.9 % due to the base with geomembrane reinforced dry sand and 52.6% due to the base with geomembrane reinforced saturated sand. It is also observed that the effect of wet sand itself is nearly 40% and this may be due to the fact that the pore pressure in sand increases due to the excitation and results in a more flexible base. The presence of geomembrane in sand increases the flexibility of the structure thus reducing the natural frequency.

Variation in structural response for Zone III design spectrum

Representative time history of responses at the mid span of the roof beam in X direction for supports with dry sand and dry sand reinforced with geomembranes are shown in figures 4 to 5. The accelerometer recordings represent the responses at the beam column junction and at the mid span of the roof beam in X and Y directions. Table 3 represents the variation in maximum acceleration for excitation corresponding to Zone III. Frequency response spectrum curves for the responses recorded in the accelerometers at the roof level for the structural model subjected to the time history of acceleration corresponding to Zone III are shown in figures 7 to 12. Comparison of structural responses for different base conditions of the structure with dry and wet sand with reinforcement is presented.

Comparison of time history responses at the mid span of the roof beam in X direction presented in figures 4 to 5 and Table 3 shows a reduction in the maximum acceleration values from 7.41 m/sec^2 for a fixed base to 5.45 m/sec^2 for base with dry sand, 4.66 m/sec^2 for base with dry sand & geomembrane. The maximum acceleration at the roof level is reduced by 46% due to the supporting base reinforced with geomembrane. Table 3 shows similar reduction in the structural response recorded by other accelerometers.

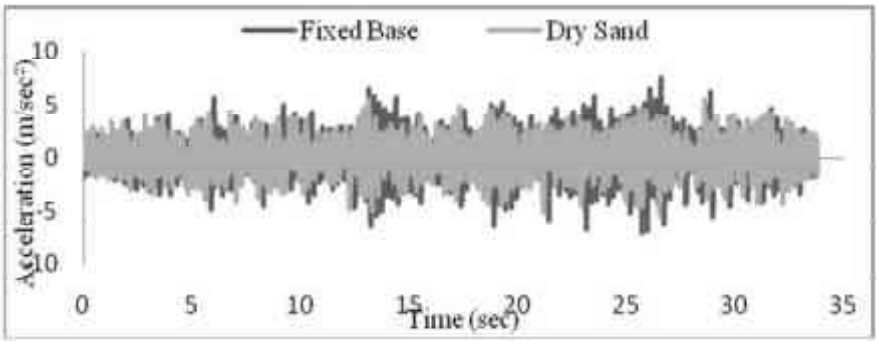

Fig.4 : Time history of response at the mid span of roof beam in X direction for base with dry sand

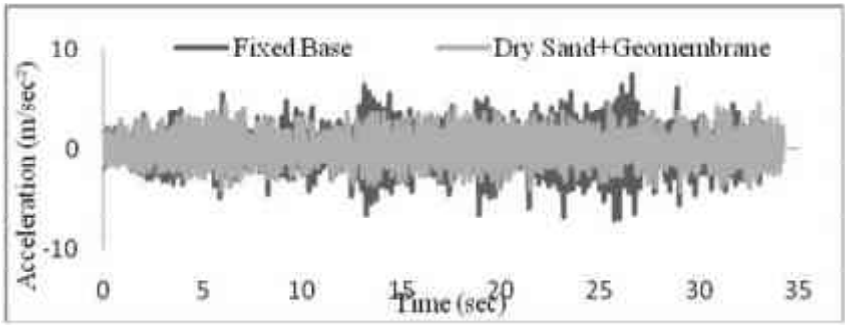

Fig.5 : Time history of response at the mid span of roof beam in X direction for base with dry sand & geomembrane

Table 3 : Variation in maximum acceleration for Zone III

Base Condition	Maximum Acceleration in Accelerometers (m/sec$^{2)}$			
	A2 (X-dir)	A1 (X-dir)	A4 (Y-dir)	A3 (Y-dir)
Fixed Base	9.14	7.41	11.75	7.29
Dry Sand	5.95	5.45	5.28	5.04
Dry Sand +Geomembrane	5.5	4.66	5.82	5.71
Wet Sand	5.33	6	5	5.67
Wet Sand + Geomembrane	5.17	6	5.17	5.83

Frequency response spectrum curves in Figures 6 to 11 show that there is a lateral shift in the fundamental natural frequency of the structure by incorporating the flexibility in the base. It is also seen clearly that the amplitude is considerably reduced for all frequencies upto 50Hz representing an isolation effect. The reduction is maximum for the base reinforced with geomembrane.

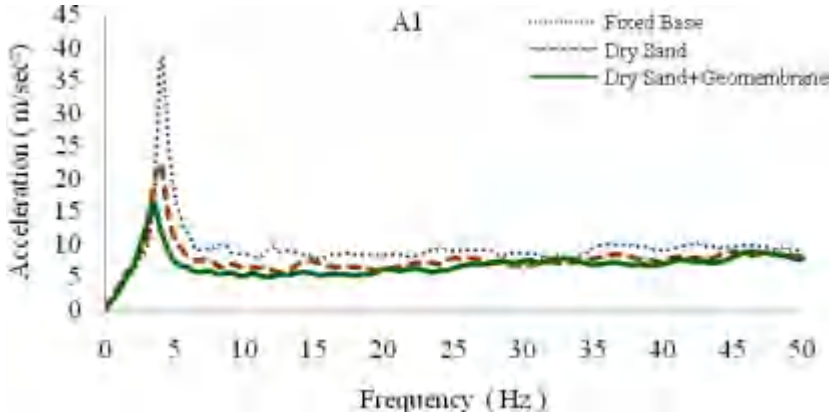

Fig.6 : Frequency response spectrum of response at the mid span of roof beam in X direction for base with dry sand

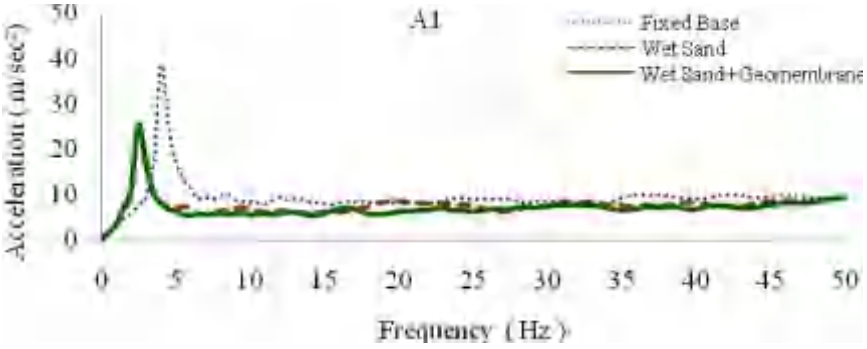

Fig.7 : Frequency Response Spectrum of response at the mid span of roof beam in X direction for base with wet sand

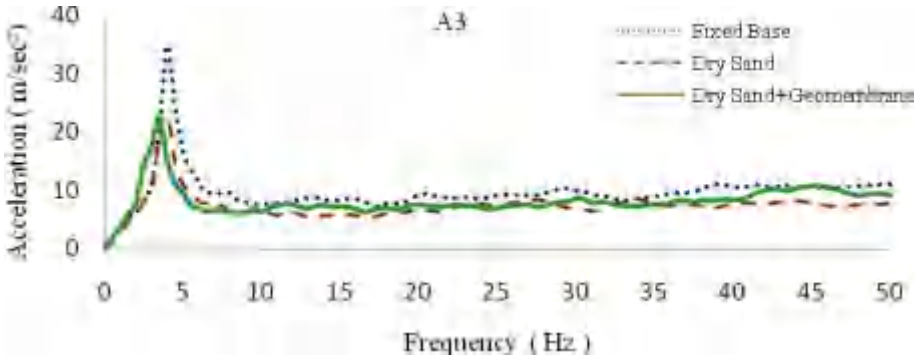

Fig.8 : Frequency Response Spectrum of response at the mid span of roof beam in Y direction for base with dry sand

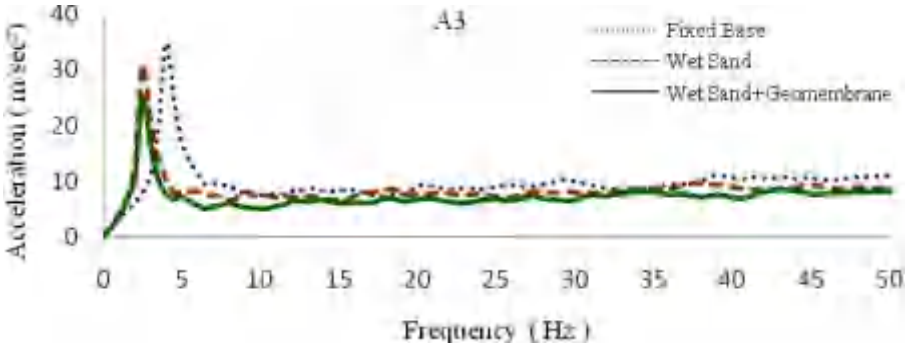

Fig.9 : Frequency Response Spectrum of response at the mid span of roof beam in Y direction for base with wet sand

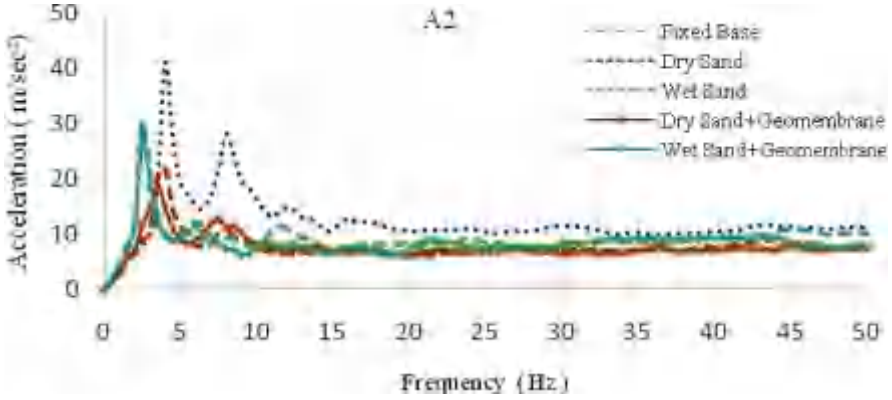

Fig.10 : Frequency response spectrum of response at the beam column junction in X direction for different base conditions

In general it is seen that the base with dry or wet sand reinforced with geomembrane reduces the natural frequency of the structure and the response in the structure to the maximum. This may be due to the slip deformations generated along the geosynthetic interface which reduces the transmission of the base motion to the superstructure.

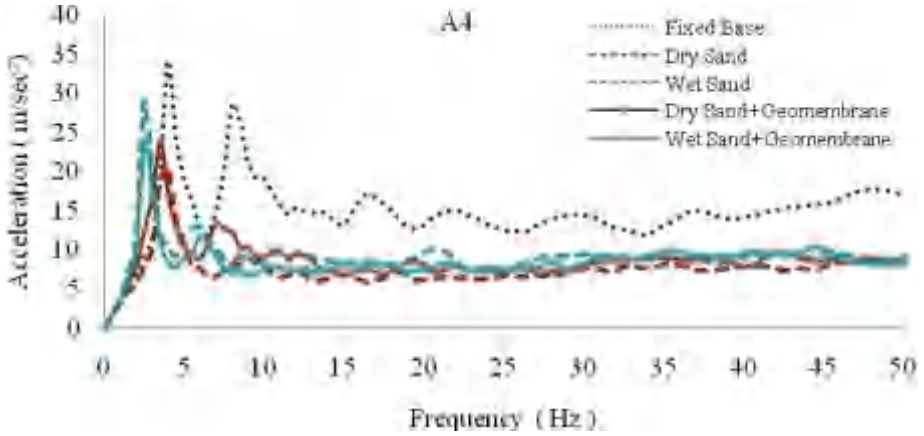

Fig.11 : Frequency response spectrum of response at the beam column junction in Y direction for different base conditions

CONCLUSION

The following conclusions are drawn from the study,

1. The natural frequency of a structure is reduced considerably by the addition of a finite mass of soil to the fixed base. The response in the structure is also reduced due to the addition of soil at the base for an input base motion corresponding to design spectrum for Zone III.

2. Sand in saturated condition acts as a very good base isolator.

3. Geomembrane reinforced wet sand as a base isolation medium causes maximum reduction in the response of the structure.

4. The concept of base isolation with soil or reinforced soil for reducing the natural frequency of the structure and reducing the transmitted base motion intensity can be an economical alternative for conventional methods.

REFERENCES

[1] Yegian, M.K. and Harb, J. (1995) "Slip Displacements of Geosynthetic Systems Under Dynamic Excitations," Earthquake Design and Performance of Solid Waste Landfills, *ASCE Geotechnical Special Publication No. 54*.
[2] Yegian, M.K. and Kadakal, U. (1998a). "Dynamic Response Analysis Procedure for Landfills with Geosynthetic Liners" *ASCE Journal of Geotechnical and Geoenvironmental Engineering*,
[3] Yegian, M.K. and Kadakal, U. (1998b). "Geosynthetic Interface Behavior Under Dynamic Loads" *The Geosynthetic International Journal,* Volume 5.
[4] Yegian, M.K., Yee, Z.Y., and Harb J.N. (1995). "Response of Geosynthetics Under Earthquake Excitations," *Geosynthetics '95 Conference*, Nashville, TN.
[5] Yegian, M. K., and Catan, M. (2004). "Soil isolation for seismic protection using a smooth synthetic liner," *Journal of Geotechnical and Geoenvironmental Engineering*, 1131–1139.
[6] Yegian, M.K., Kadakal, U. and Catan, M. (1999). "Geosynthetic for Earthquake Hazard Mitigation". *Geosynthetics '99 Boston*.
[7] IS 1893 (Part I): 2002, "Criteria for Earthquake Resistant Design of Structures - General provisions and Buildings", Bureau of Indian Standards, New Delhi.

LIMIT STATE DOMAIN OF HIGH DAMPING RUBBER BEARINGS IN SEISMIC ISOLATED NUCLEAR POWER PLANTS

G. Bianchi[1], L. Corradi[2], M. Domaneschi[3], D. C. Mantegazza[1], F. Perotti[4], A. Ravez[5]
[1]MSc, Consultant at Politecnico di Milano, Principal of Bianchi Mantegazza Studio, ITALY
[2]Professor of Structural Mechanics, Energy Dept., Politecnico di Milano, ITALY
[3]PhD, Dept. of Structural Engineering, Politecnico di Milano, ITALY
[4]Professor of Structural Dynamics, Dept. of Structural Engineering, Politecnico di Milano, ITALY
[5]MSc, Dept. Of Structural Engineering, Politecnico di Milano, ITALY
e-mail of corresponding author: perotti@stru.polimi.it

ABSTRACT

The paper describes the work performed at Politecnico di Milano in the field of seismic isolation of nuclear power plants buildings. Within this activity, the development of reliable and efficient FE models in ANSYS® has been pursued along with the definition of a limit state domain for first damage in High Damping Rubber Bearing (HDRB) devices. The paper is settled into a wider procedure aiming at providing a reliable, effective and robust method to evaluate the seismic fragility of base isolated nuclear power plants.

INTRODUCTION AND SCOPE

This work is framed into the research activity performed at Politecnico di Milano within the field of seismic isolation of NPP (Nuclear Power Plant) buildings, with specific attention to the IRIS™ project (International Reactor Innovative and Secure™), a medium size pressurized water reactor under development by an international consortium [1]. The work presented here is part of a procedure described by F. Perotti et al. [2], proposing an innovative approach for the evaluation of seismic fragility for isolated buildings, based on the following steps:

- step 1: performance of laboratory tests on high damping rubber and HDRB isolating devices;
- step 2: development of a reliable and efficient isolator FE model, taking into account all significant sources of mechanical and geometrical nonlinearities; the model, after having been validated against experimental data, will be used to simulate additional and more complex numerical tests;
- step 3: FE model calibration based on laboratory tests;
- step 4: statement of the limit state condition for the isolator, expressing the interaction between horizontal and vertical load at first damage and failure;
- step 5: performance of the fragility analysis for the isolation system.

A first set of laboratory tests on 1:2 scale HDRB devices designed for IRIS™ NPP was performed by ENEA and CIRTEN at CESI-ISMES [3] (Bergamo, Italy) and FIP Industriale S.p.A [4] (Padova, Italy) laboratories, in June 2010. The test results, integrated, where necessary, with experimental data from the literature, were analyzed in order to define the future experimental test campaign required to accomplish step 1, and to tune the analytical and numerical models of HDRB devices.

In a previous work by this research group [5], a robust procedure for developing a FE model of a HDRB device, properly tuned on experimental data, was addressed. The most suitable element type, mesh refinement and analysis control parameters were identified and verified by comparing numerical results to laboratory tests.

In the present paper, the development of a new FE model of a HDRB device has been pursued in ANSYS®, mainly aimed at the definition of a reliable limit state domain under seismic excitation, which represents step 4 in seismic fragility evaluation procedure. A comprehensive study of the global and local behaviour of numerical and analytical models is first presented, under the hypothesis of fully incompressible rubber material. Delamination damage condition is then accounted by Yen-Caiazzo limit state domain [12][13], tuned to rubber tensile strength provided by the manufacturer and maximum tangential stress taken from experimental tests under vertical load [4]. First damage domain is finally addressed, in terms of HDRB global actions, by means of combined FE modelling and analytical treatment.

HDRB DEVICE PROPERTIES AND LABORATORY TESTS

Geometrical data for the IRIS™ designed HRDB device were taken from [4] and are listed in Tab. 1. Mechanical properties were retrieved from experimental tests performed by ENEA on 1:2 scale devices [4] and from

the analysis of a set of literature experimental tests on rubber specimens [6][7][8][9]. Mechanical parameters are then used to calibrate the rubber constitutive law by means of a fitting procedure, performed in ANSYS® environment [10].

	full scale	1:2 scale	
Isolator external diameter	1000	500	[mm]
Design vertical load	8000	2000	[kN]
Steel reinforcing plate diameter	980	480	[mm]
Thickness of the internal steel plates	4	2	[mm]
Number of elastomeric layers	10	10	[ ]
Thickness of one elastomeric layer	10	5	[mm]
Total rubber thickness	100	50	[mm]
First shape factor	24	24	[ ]
Second shape factor	9.6	9.6	[ ]
Dynamic shear modulus (at 100% def.)	1.4	1.4	[MPa]

Tab. 1: Full scale and 1:2 scale HDRB parameters

Six 1:2 scale isolators were tested in two sessions. The first [3] comprised vertical loading tests, quasi-static horizontal loading tests and dynamic horizontal loading tests. The second [4], also aimed at investigating isolator failure, comprised a vertical loading failure test and a horizontal quasi-static loading failure test.

Tests showed a vertical failure mode consisting in a radial expulsion of internal steel plates and rubber (Fig. 1b). Horizontal failure occurred during the second cycle at 350% deformation, when the external rubber cover suddenly broken, revealing the failure due to the partial detachment of an internal plate (Fig. 1a).

(a)  (b) 

Fig. 1: Horizontal (a) and vertical (b) loading HDRB failure tests

Since no experiments had been already performed to determine actual rubber properties, an analysis of three standard experimental test curves (Uniaxial Tension: UT, Biaxial Tension: BT, Pure Shear: PS) was performed on literature data [6][7][8][9], for different G* shear moduli. The analysis identified similar experimental curves by scaling each case by corresponding G* ratio. Thus G* = 1.4 MPa rubber tests were generated by scaling literature rubber tests. The Simple Shear (SS) test has been obtained from horizontal loading test on 1:2 scale isolators.

HDRB STRESS ANALYSIS

Constitutive law and hyperelastic parameters assessment

In a previous study performed by this research group [5], Ogden, Mooney-Rivlin and Polynomial hyperelastic constitutive laws for elastomeric materials were analysed by an analytical and numerical HDRB model, in order to identify the most promising law in reproducing experimental behaviours. Benchmarks identified the Polynomial 2-Parameters (POLY-2P) constitutive law as the most suitable model for the scope. The present study confirmed previous results, for a different HDRB geometry, in terms of quality of simulation of the HDRB experimental behaviour. Elastic potential function for POLY-2P is reported eq. 1:

$$W = \sum_{i+j=1}^{2} c_{ij} (\bar{I}_1 - 3)^i (\bar{I}_2 - 3)^j + \sum_{k=1}^{2} \frac{1}{d_k} (J-1)^{2k} \quad (1)$$

c_{10}, c_{01}, c_{02}, c_{20} and c_{11} parameters depend on the actual material, while the volumetric part (d_1 and d_2) is ignored in fulfilment to the hypothesis of fully incompressible rubber. Parameters have been evaluated by fitting

laboratory rubber specimen curves quoted in the previous paragraph. Four fitting combinations (Tab. 2) have been defined by including different experimental tests in the fitting procedure, in order to evaluate the stability and convergence sensitivity of the constitutive law. Convergence and accuracy tests were performed by comparing numerical and analytical solutions with the experimental curves, in terms of global reactions. Fitting combination 301 has been identified as the most suitable and will be assumed in all subsequent analyses.

FITTING	**TESTS**				**POLY-2P PARAMETERS [MPa]**						
	UT	BT	PS	SS	c_{10}	c_{01}	c_{20}	c_{11}	c_{02}	d_1	d_2
301	**x**	**x**	**x**	**x**	**7.97E-01**	**-5.91E-02**	**1.61E-02**	**-5.29E-03**	**1.10E-03**	-	-
302	x	-	x	x	-8.99E-01	1.72E+00	-1.46E-01	8.85E-01	-7.30E-01	-	-
303	x	x	-	x	6.84E-01	8.82E-02	3.80E-02	-6.90E-02	1.42E-02	-	-
304	-	x	x	x	1.40E+00	-4.10E-01	-7.22E-02	8.38E-02	-1.10E-02	-	-

Tab. 2. Fitting combinations for Polynomial 2P hyperelastic constitutive law

Numerical model

A parametric FE model of the full scale HDRB was assembled according to geometrical properties listed in Tab. 1 and to the following criteria (Fig. 2):

- *Finite elements*. SOLID185 element for bricks (linear 3D 8-nodes element with 3 DOF at each node, with hyperelasticity, large deflection and large strain capabilities; allowing a mixed formulation for simulating deformations of fully incompressible hyperelastic materials). The integration method is the Uniform Reduced Integration with hourglass control. SHELL281 for steel shell elements (4+4 nodes element with 3+3 DOF at each node, allowing for finite membrane strains); overall number of DOF is about 220'000;
- *Constraints.* At top and bottom face a 20 mm steel plate has been modelled as a node with a rigid link to the corresponding rubber disc; at each steel-rubber interface, the connection between the upper and lower nodes and rubber surfaces is provided by means of node-to-node rigid links;
- *Material*. POLY-2P hyperelastic constitutive law has been adopted (Tab. 2, fitting combination 301);
- *Boundary conditions and loads*. Boundary conditions and loads act at top and bottom nodes. The horizontal action is applied as an imposed horizontal displacement in *x* direction. Bottom node is always fixed, while upper node constraint prevents displacement along *y* and all rotations.

The global response of the model was investigated by comparing the numerical solution with experimental results, for the following cases:

- vertical load up to 80'000 kN (Fig. 3b): the agreement is poor since compressibility was not included;
- horizontal displacement up to 350% of the rubber thickness (0 kN and 80'000 kN vertical load, Fig. 3a): there is a good agreement between the experimental and the numerical solution which confirm POLY-2P constitutive model ability to reproduce the HDRB global behaviour, when properly tuned; moreover, vertical load does not affect the horizontal stiffness, mainly due to the HDRB high second shape factor.

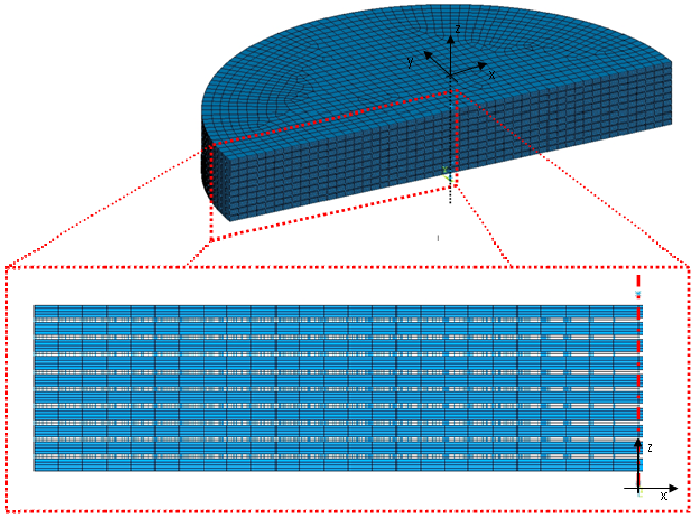

Fig. 2. HDRB FE model. Approximate number of DOFs: 220'000

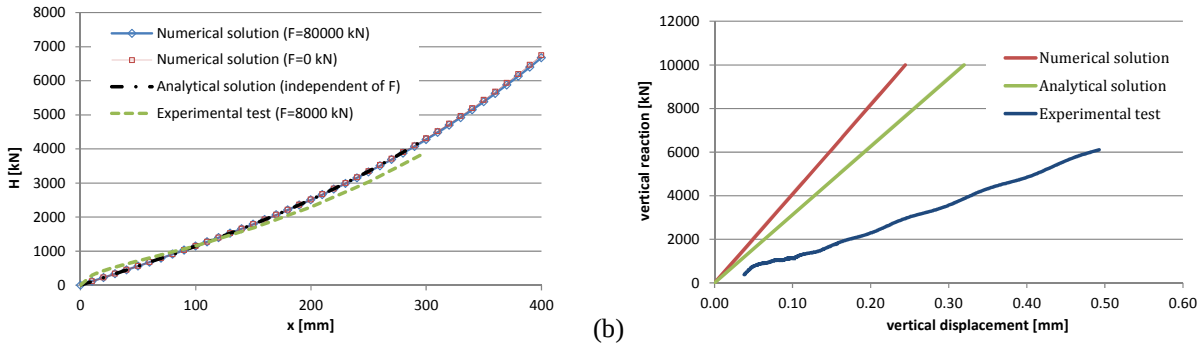

(a) (b)

Fig. 3: Numerical, analytical and experimental HDRB horizontal (a) and vertical (b) stiffness

Analytical model

Corradi et al. [11] proposed two approximate analytical solutions for a single rubber layer subjected to vertical load (linear elastic incompressible material, small displacements), and to horizontal displacement (hyperelastic incompressible material, large displacement), as shown in Fig. 4. The two solutions, applied also in [5], are here further developed in order to reproduce the stress distribution evaluated by numerical FE analyses. The main purpose is to obtain a reliable analytical solution to assess an analytical limit state domain.

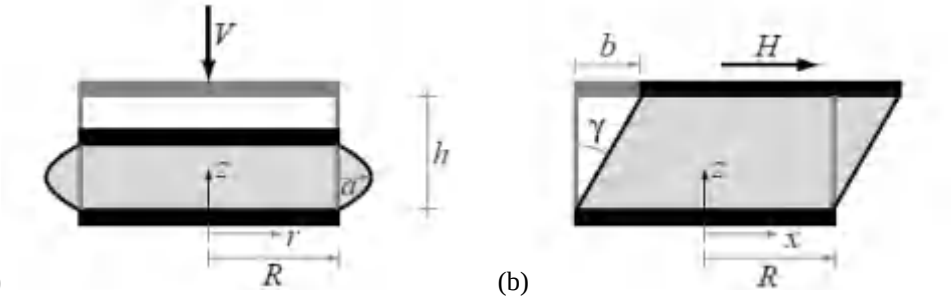

(a) (b)

Fig. 4: Single rubber layer analytical solutions scheme. (a): vertical load; (b): horizontal displacement

In terms of stresses induced by vertical load, the Corradi model shows a good agreement with the numerical solution (Fig. 5a, Fig. 6a). In terms of stresses induced by horizontal displacements, on the other hand, the Corradi model introduces an artificial constraint on displacement along the *z*-axis, thus the vertical resultant is not necessarily zero. Comparing the behaviour of the numerical FE solution for HDRB device and the analytical solution for single rubber layer it can be noted that:

- the shear stress (Fig. 6a and b) does not depend on the interaction among layers: all layers of the isolator can be modelled as individual single rubber layers. Corradi analytical model is thus in good agreement with numerical results;
- the Corradi analytical solution (not shown) is different from the numerical complete HDRB behaviour in terms of vertical stress σ_z, due to horizontal displacement. In this respect, the influence of multilayered geometry cannot be neglected, leading to global compression and tension areas (Fig. 8) which are not described by the analytical model.

The Corradi solution has been here extended by introducing a new hypothesis on the shape of the σ_z stresses under horizontal loading. A shape function has been defined on the basis of the general stress behaviour observed on the numerical results, and, in particular, within the area subjected to positive (tension) σ_z stresses. The normal tension stress due to horizontal load has been stated as a function of the value of the parameter *k* (ratio of horizontal displacement to total rubber height), of the height *z* of the layer and on the abscissa *x* (Fig. 4b). The function has a sinusoidal variation in terms of *x*, with a phase depending on *z* and *k* (eq. 2, Fig. 5b):

$$\sigma_z = 1 \cdot k \cdot \sin\left(\frac{\pi x}{R} + \frac{k\pi}{3R}\left(z - \frac{H}{2}\right)\right) \qquad (2)$$

The resultant force calculated on the symmetry vertical plane is always zero under horizontal loading, as the wave length of function in eq. 2 is equal to R.

In terms of global reactions, Fig. 3a shows a good matching between the analytical and numerical solutions, only for horizontal displacement. Concerning local stresses, σ_z due to vertical load (Fig. 5a) and τ_{xz} due to vertical load (Fig. 6a) and horizontal displacement (Fig. 6b) are in good agreement, when numerical FE solution for complete isolator is compared with analytical solution for a single rubber layer. σ_z stresses due to horizontal displacement (Fig. 5b), approximated by shape function in eq. 2, are in good agreement with numerical solution, in particular in traction zones (Fig. 8) for k>200%.

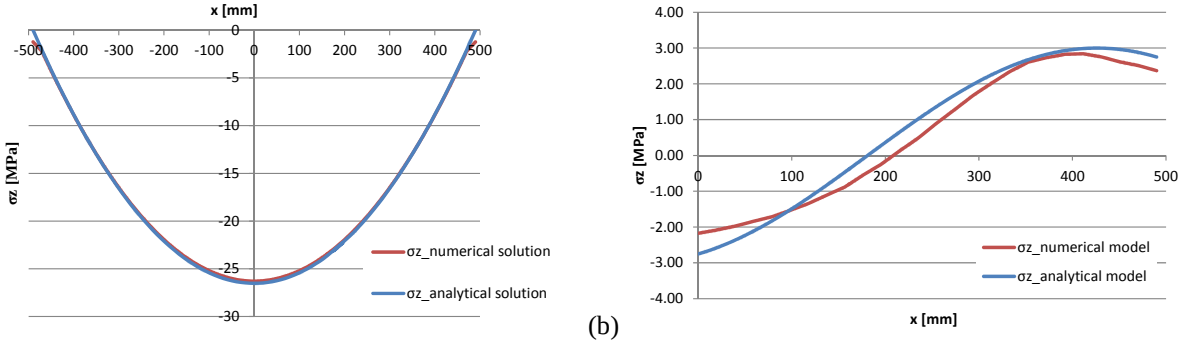

(a) (b)

Fig. 5: analytical and numerical σ_z stresses in HDRB: vert. load 10'000 kN (a), k=300% horizontal displ. (b)

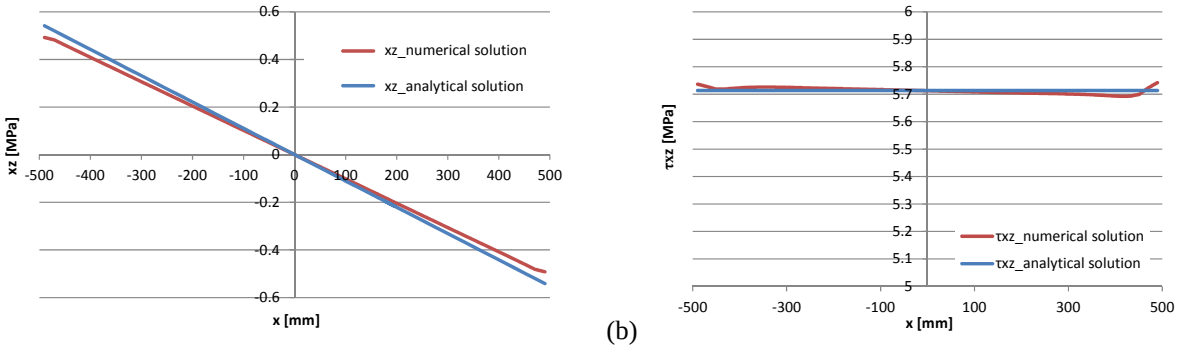

(a) (b)

Fig. 6: analytical and numerical τ_{xz} stresses in HDRB: vert. load 10'000 kN (a), k=300% horizontal displ. (b)

HDRB LIMIT STATE DOMAIN

Rubber compounds may suffer damage and failure for delamination (detachment of rubber layers from steel plates), tensile rupture (rubber ultimate strength under tension), tearing (indefinite propagation of a crack), fatigue (indefinite propagation of a crack, induced by a large number of stress cycles) and cavitation (large or indefinite expansion of small holes due to hydrostatic tension). Delamination damage condition is accounted in present study.

Yen-Caiazzo limit state domain

Failure tests on HDRB showed that delamination initiates on isolator sides (Fig. 1a). Coherently, the numerical and analytical stress fields exhibit the highest values in the same regions on sides (maximum shear and tension stress). The σ/τ limit domain in [12] [13] was adopted for first damage (eq. 3a)

$$\left(\frac{\sigma_{3T}}{S_{3T}}\right)^2+\left(\frac{\tau_{13}}{S_{130}}\right)^2=1 \tag{3a}$$

$$S_{130}=\frac{2Fh}{\pi R^3}=\frac{2*20000*5}{\pi 245^3}=4.33MPa \tag{3b}$$

$$S_{3T}=17.5MPa \tag{3c}$$

where σ_{3T} is the tensile stress orthogonal to rubber plane, S_{3T} is the tensile strength, τ_{13} is the shear stress and S_{130} is the reference shear strength. Strength parameters were determined from data provided by the manufacturer [4]: tensile strength is 17.5 MPa while shear strength was calculated from the vertical load (20'000 kN, 1:2 scale isolator) that caused the first change in vertical stiffness. The analytical solution [11] for vertical load

provides corresponding shear stress, at isolator sides (eq. 3b). First damage is assumed to occur when a single point of the isolator reaches the limit state condition. Regions with high compression stresses (Fig. 8) are not considered in this study, since there was no experimental evidence of damages in these regions for actual geometry and loading.

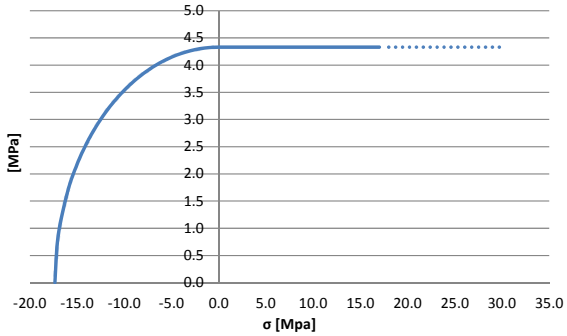

Fig. 7: Yen–Caiazzo first damage domain, for S_{130}=4.33 MPa and S_{3T}=-17.5 MPa (σ>0 compression, in figure)

Numerical and analytical limit state domains

Regions where first damage due to delamination is expected to occur are those where normal stresses are tractions and shear stresses due to vertical load sum to shear stresses due to horizontal displacement, with same sign. Fig. 8 shows locations of these critical points in a HDBR, where Yen-Caiazzo limit state [12][13] is firstly reached.

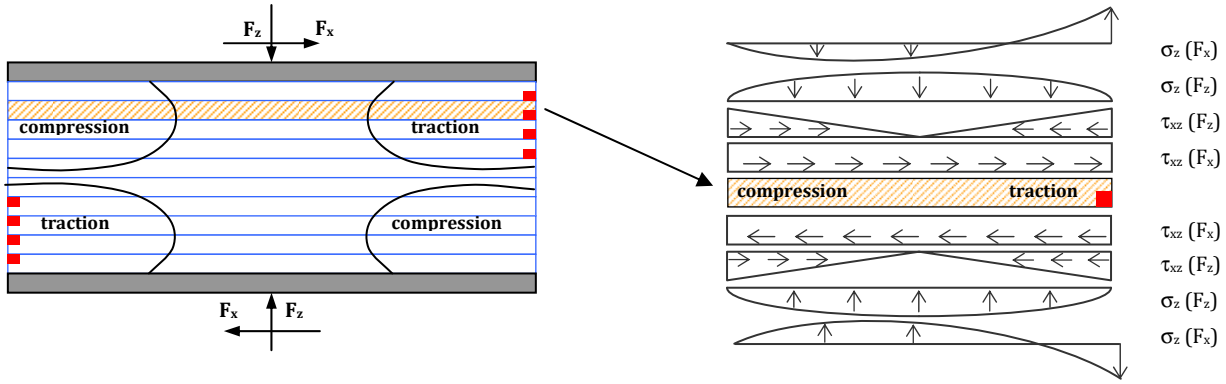

Fig. 8: Critical points in a HDRB and qualitative stress state in a rubber layer located in the isolator top half

The numerical H-V domain (Fig. 10a) was computed imposing a vertical load and determining the corresponding horizontal displacement *k* (Fig. 10b) that causes a single point to reach the first damage condition.

For the analytical domain statement (Fig. 10a), shear and normal stresses due to vertical load and shear stress due to horizontal displacement are retrieved from Corradi analytical solution [11] for a single rubber layer, while for the normal stress due to horizontal displacement $\sigma_{3T} = 1 \cdot k$ is assumed (eq. 2, calculated at HDRB middle height *z*=H/2, at side *x*=R). The procedure in Fig. 9 is applied to calculate the analytical domain in terms of global forces, for a given *k*:

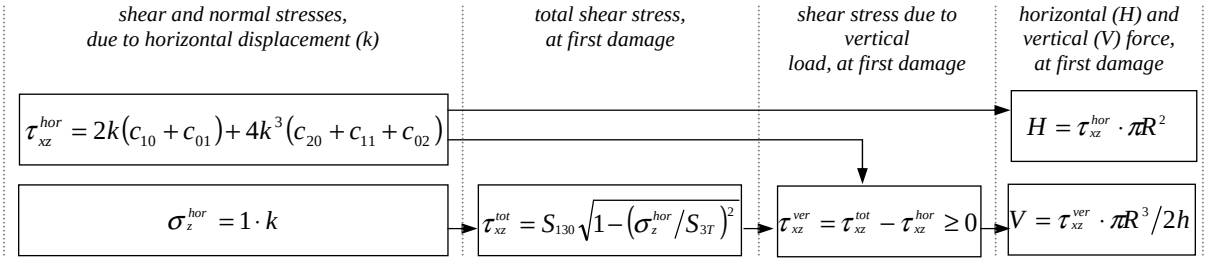

Fig. 9: Procedure for analytical domain calculation, in terms of global forces, for a given *k* horizontal displacement

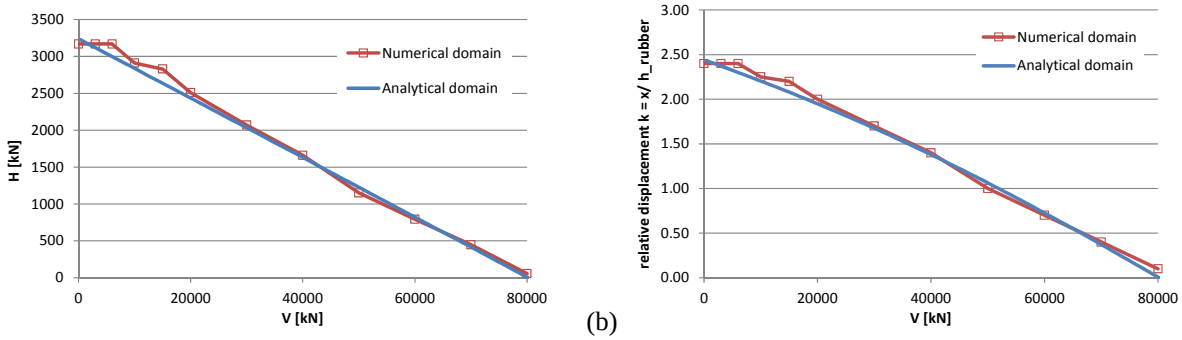

(a) (b)

Fig. 10: Analytical and numerical first damage domains (full scale) in terms of vertical and horizontal forces (a), and relative horizontal displacement *k* at which first damage condition is reached for a given vertical load (b)

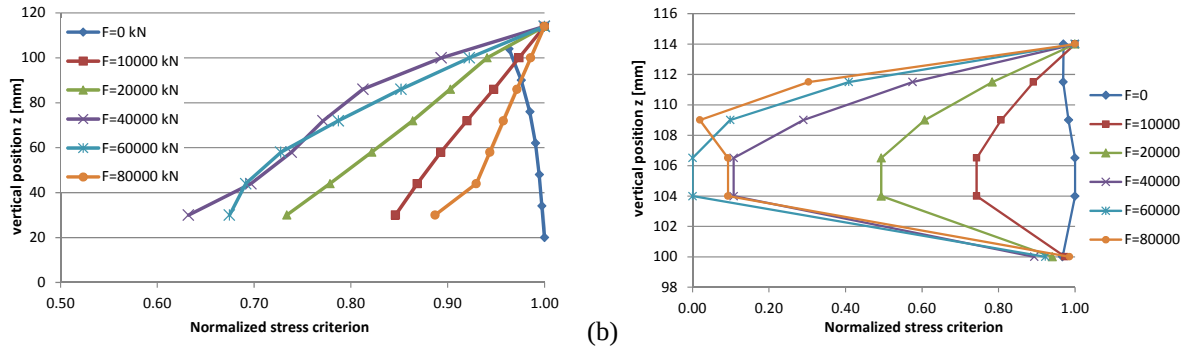

(a) (b)

Fig. 11: Normalized stress criterion, (a) at different location in the isolator (maximum value at each layer), (b) at different location in a single rubber layer, extracted form the isolator

CONCLUSIONS AND FUTURE DEVELOPMENTS

The first part of the work addressed the stress state in the HDRB device. A refined FE model of a single rubber layer was set to perform preliminary evaluation on mesh sensitivity and potential sources of numerical instabilities (see also [5]). It has been shown how the number of FEs adopted in thickness plays a crucial role in tangential stresses due to vertical load, whose magnitude affects the limit state domain significantly. Furthermore, global behaviour of the FE model was compared to experimental results performed at FIP laboratories on 1:2 scale isolator [4]. The comparison showed optimum agreement in terms of horizontal stiffness, while vertical stiffness is highly affected by the exact estimation of rubber compressibility.

Corradi et al. [11] proposed an analytical formulation for stresses in a single rubber layer, subjected to vertical and horizontal loading separately, based on approximate solution in large displacement, for different hyperelastic constitutive laws. The Corradi solution was found to be accurate in predicting all but one stress state also in the HDRB complete device, since rubber layers behave almost as a single individual rubber layers acting in series. The present work extended and applied this solution to the complete isolator, allowing predicting also vertical normal stresses in the isolator, which is significantly different than the Corradi solution for a single rubber layer. The proposed Modified Corradi analytical formulation was compared to numerical solutions and was considered to be accurate in predicting the stress field in the HDRB, subjected to vertical load and horizontal displacement, at least in regions where first damage is more likely to occur.

Extensive numerical tests were performed to verify the possibility to decouple horizontal and vertical actions (see also [5]) . The error due to superimposing the effects of each load condition was found small enough to confirm the validity of the analytical solution for first damage domain assessment.

Rubber compounds may suffer damage and fail for delamination, tensile rupture, tearing, fatigue and cavitation. Delamination damage condition is accounted in present study by a Yen-Caiazzo limit state domain [12][13], tuned against mechanical properties provided by the manufacturer, in terms of rubber tensile strength and maximum tangential stress due to maximum vertical load [3][4]. In the second part of the work, the HDRB first damage domain was addressed by means of both the FE model and analytical solution. The two approaches led to

very close bi-dimensional first damage domains, expressed in terms of maximum horizontal load for a given vertical load. The domain represents the combination of forces that generates the very first damage at a single location inside the HDRB, whose bearing capacity and stiffness properties are still unchanged.

The study has been developed for fully incompressible rubber, although significant results were obtained in case of nearly incompressible rubber, which will become a future development for the current research.

The results obtained from the first application of step 1 to 4 of the seismic fragility evaluation procedure presented in Perotti et al. [2], also allows defining which mechanical parameters are necessary to be required from the manufacturer.

REFERENCES

[1] Forni M., Poggianti A., Bianchi F., Forasassi G., Lo Frano R., Pugliese G., Perotti F., Corradi dell'Acqua L., Domaneschi M., D. Carelli M., Ahmed A.M., Maioli A., "Seismic Isolation of the IRIS Nuclear Plant", *ASME pressure Vessel and Piping Conference (PVP 2009)*, Prague, Czech Republic, July 26-30, 2009.

[2] De Grandis S., Domaneschi M., Perotti F., "A numerical procedure for computing the fragility of NPP components under random seismic excitation", *Nuclear Engineering and Design*, 239, p. 2491-2499, 2009.

[3] CESI S.p.A., ENEA Centro Ricerche Bologna, "Rapporto di prova CESI B0020266", 2010

[4] FIP Industriale S.p.A., ENEA Centro Ricerche Bologna, "Rapporto di prova FIP Industriale VP 59/10", 2010

[5] G. Bianchi, L. Corradi dell'Acqua, M. Domaneschi, D. C. Mantegazza, F. Perotti, "High Damping Rubber Bearing (HDRB) isolating devices for nuclear power plants: FE modelling and damage characterization", *SEWC 2011 - Structural Engineering World Congress*, Como, April 2011

[6] S.B. Bhoje, P. Chellapandi, S. Chetal, R. Muralikrishna, T. Salvaraj, "Comparison of computer simulated and observed force deformation characteristics of anti-seismic devices and isolated structures", *Final report of a research project 1996-1999*, International Atomic Energy Agency, Vienna (Austria), IAEA-TECDOC-1288, pp:105-130

[7] IAEA-TECDOC-1288, "Verification of analysis methods for predicting the behaviour of seismically isolated nuclear structures". *Final report of a research project 1996–1999*

[8] IAEA-RC-624.3 IWGFR/96, "Intercomparison of analysis methods for seismically isolated nuclear structures", *Papers and working materials presented at the 3rd research coordination meeting*, Hertford, UK, 25-29 May 1998

[9] Forni M., Martelli A., Dusi A., Castellano G., "Hyperelastic Models of Steel – Laminated Rubber Bearings for Seismic Isolation of Civil Buildings and Industrial Plants", *International ABAQUS User's Conference*, Paris, France, p. 273-287, May 31- June 2 1995.

[10] ANSYS Release 12, Theoretical manual.

[11] Corradi dell'Acqua L., Domaneschi M., Guiducci C., "Assessing the reliability of seismic base isolators for innovative power plant proposals", *20th International Conference on Structural Mechanics in Reactor Technology (SMiRT20)*, Espoo Finland, August 9-14, 2009.

[12] Xiao J.R., Gillespie, JR, "A Phenomenological Mohr–Coulomb Failure Criterion for Composite Laminates under Interlaminar Shear and Compression", *Journal of Composite Materials*, 41: 1295, 2007.

[13] Yen C.F., Caiazzo A. "Innovative processing of multifunctional composite armor for ground vehicles", US Army Research Laboratory, ARL-CR-484, Aberdeen Proving Ground, MD.

[14] UNI EN 15129:2009 – Anti-seismic devices.

COMPARISON OF RECORDED RESPONSE OF CONVENTIONAL AND BASE ISOLATED BUILDINGS WITH ANALYSIS

V.K.Mahadik[a], D.K.Paul[b], G.R.Reddy[a], P.N.Dubey[a], S.K.Deb[c]
[a] Reactor Safety Division, Bhabha Atomic Research Centre, Mumbai, India
[b] Department of Earthquake Engineering, IIT-Roorkee, Uttarakhand, India.
[c] Department of Earthquake Engineering, IIT-Guwahati, Assam, India.

ABSTRACT

Base Isolation is regarded as a promising solution for earthquake resistant design which result in significantly low floor accelerations, and inter storey drifts. This ensures the safety of structural as well as non-structural elements, thereby keeping the building operational even after a severe earthquake. Seismic base isolation technique is very useful for cost effective seismic design of nuclear structures. The effectiveness of a base isolation system is governed by bilinear characteristics offered by the isolators. The present work attempts to study the effectiveness of base isolation over conventional seismic construction, using a case study of identical conventional and isolated building constructed for experimental purposes in Guwahati, a seismically active region in India. The comparisons of analytical results with the records for two low intensity earthquakes indicate the effectiveness of base isolation in the initial stiffness range of the isolation system when none of the isolators yield.

KEY WORDS: Base Isolation, Lead Rubber Bearings, Low intensity earthquakes.

INTRODUCTION

There are several options for seismic design of a building with a given configuration. Linear elastic seismic design for a severe earthquake will result in an uneconomical and impractical building. In conventional seismic design, plastic deformations in beams and columns help in absorbing the damaging effects of earthquakes. This is the most widely used design concept across the world. However, the displacements generated may be large enough to cause the collapse of non-structural elements, thereby preventing the structure from being operational after the earthquake. Base isolation offers a solution for buildings which are required to remain operational after a severe earthquake. For a study of characteristics of base isolated structures, two buildings (Fig-1) with identical configuration have been constructed in IIT-Guwahati [1], located in one of the highly active seismic zone in India. One of the buildings has been constructed using conventional earthquake resistant design procedure, and the other uses seismic base isolation (lead laminated rubber bearings) for mitigating earthquake effects. The buildings are instrumented to record floor accelerations at the first floor and the roof level for real earthquakes. A comparison of the conventional and base isolated buildings subjected to two low intensity earthquakes, with their respective recorded and analytical response is presented.

BILINEAR CHARACTERISTICS

The reduction of storey shears, storey drifts and floor spectral accelerations is realised in base isolation design by two modifications in the dynamic characteristics of the structure - a time period shift by introduction of flexible mounts and additional damping offered by the isolators by hysteretic energy dissipation [2], [3], [4], [5]. When a base isolated building is subjected to a low intensity earthquake, the isolators are subjected to very low horizontal forces, preventing them from yielding. Thus for low intensity earthquakes, the isolators remain in the initial stiffness region. There is, however; a slight time period shift due to the lesser initial stiffness of the isolators compared to the stiffness of the ground storey columns. There is no role of hysteretic damping since yielding of isolators does not take place. Thus whatever reductions occur in shears and spectral accelerations at low intensity earthquake are attributed to the slight shift in the time period [4]. Only for moderate or high intensity earthquakes, both time period shift and additional hysteretic damping contribute in the significant reduction of shears and spectral acceleration.

Fig-1: Conventional Building (Left) & Isolated Building (Right)

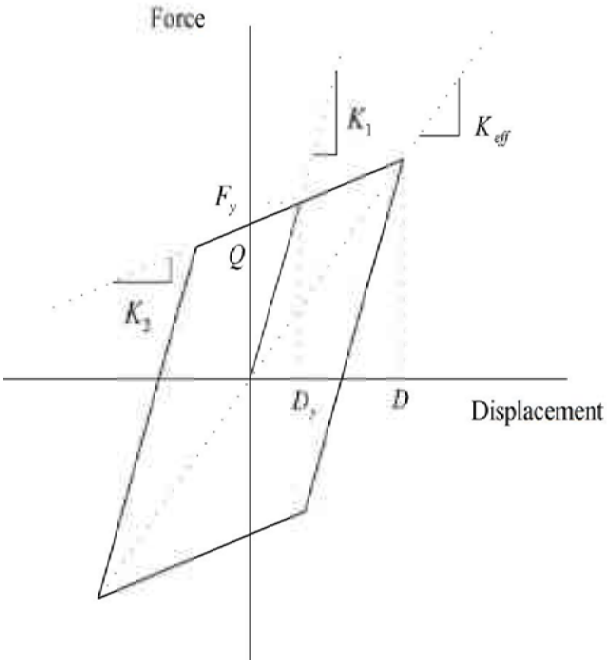

Fig-2: Bilinear Force Deformation Curve

The behavior of almost all of the isolator devices is represented mathematically by a bilinear force-deformation curve as depicted in Fig-2 [4], [6], [7]. The characteristic strength Q, initial stiffness K_1, post yield stiffness K_2 are sufficient to define the bilinear behavior of any type of isolator, and are referred to as bilinear characteristics. The bilinear characteristics Fig-2 have been related to the material properties of the isolator and its geometry [3], [4], [7]. For analysis of a base isolated building, an experimental cyclic shear test of the prototype isolator device is mandatory [8], [9], and the resulting force-deformation curve is used to define the required bilinear characteristics. In this paper, the study of base isolated buildings is limited to the use of lead laminated rubber bearings (LLRB) for seismic isolation. The experimental force deformation curve obtained for the lead laminated rubber bearing used in the isolated building is shown in Fig-3 [1]. The bilinear characteristics obtained from a cyclic shear test of the isolator used for the experimental building are presented in Table-1. In base isolated buildings, the superstructure behaves in a linear elastic manner as the inter storey drifts in the building are considerably low even in a severe earthquake. The hysteretic energy dissipation due to large plastic deformations is localized and limited to the isolators. Isolators are designed to maintain their vertical load carrying capacity under large shear deformation.

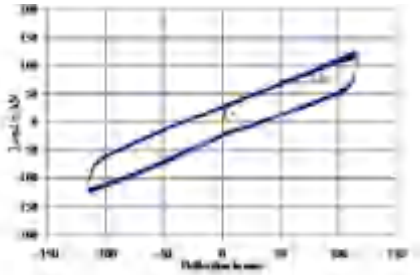

Fig-3: Experimental Force-Deformation Curve

Table-1: Experimental Bilinear Characteristics

Quantity	Value
Characteristic strength (kN), Q	25.7
Initial stiffness (kN/m), K_1	13525
Post-yield stiffness (kN/m), K_2	838
Yield force (kN), F_y	27.4
Yield Displacement (mm), D_y	2.03

ANALYSIS FOR RECORDED LOW INTENSITY EARTHQUAKES

An analytical 3-D model of the building is generated in SAP-2000 [10], accounting for the effects of infill and soil structure interaction [11]. The impedances for equivalent soil springs [12], [13], used to model the effects of

soil stiffness are evaluated and soil springs are modeled using link element [11]. The building is analyzed for two low intensity earthquakes that have actually occurred (designated as EQ-1 (Fig-4) occurred on 6-November, 2006 and EQ-2 (Fig-5) occurred on 10-November, 2006).

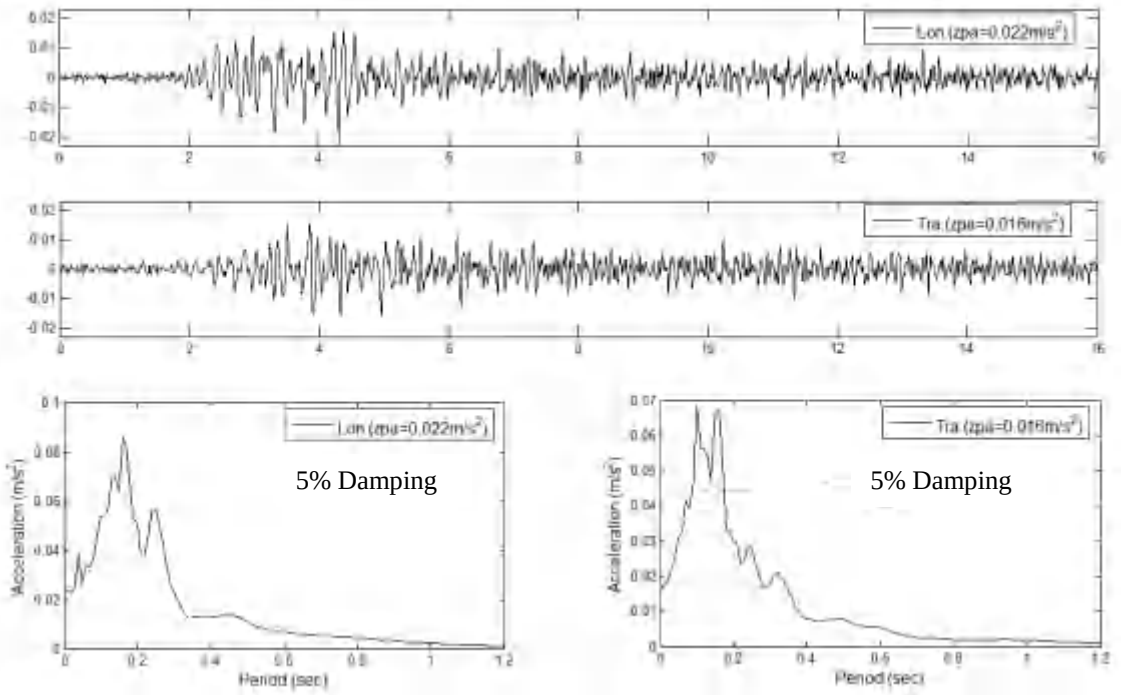

Fig-4: EQ1—Longitudinal and Transverse motions and their Acceleration Spectra

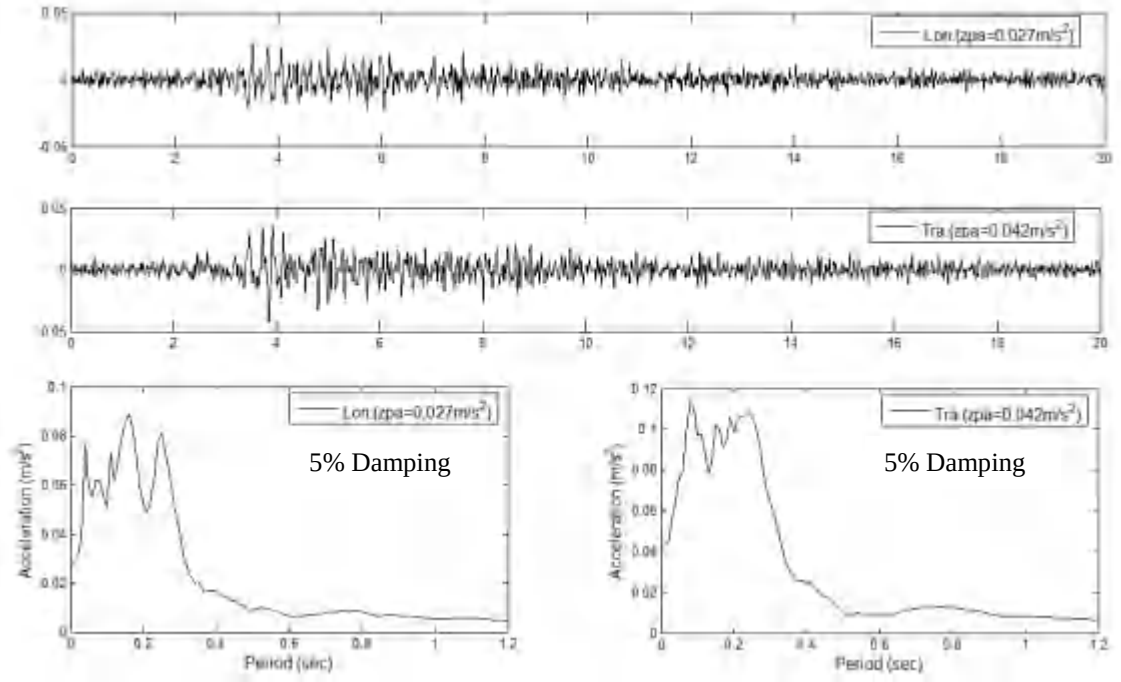

Fig-5: EQ2—Longitudinal and Transverse motions and their Acceleration Spectra

The isolators are modeled in SAP by using the link element [11]. The initial stiffness, yield force and the post yield stiffness ratio are specified as obtained (Table-1) from the experimental force deformation curve.

Modeling of the superstructure and soil is similar to that done in case of the conventional building. The isolated building is analyzed for the two recorded earthquakes- EQ-1 (Fig-4) and EQ-2 (Fig-5).

Recorded motion of the buildings for EQ-1 and EQ2, in form of roof acceleration time history for longitudinal as well as transverse directions is available for both the buildings. In addition longitudinal and transverse acceleration time history records at the ground floor just above the isolation plane are available. Acceleration time history for transverse direction on the ground floor of the conventional building is also available. From analysis, the corresponding acceleration response time histories are obtained. A comparison of 5% damped acceleration spectra of these analytical and recorded time histories are presented in Figs.6-11. For a relative comparison of response of conventional and isolated building, their spectra are plotted to the same scale.

EFFECTIVENESS OF SEISMIC ISOLATION

The recorded earthquakes EQ-1 and EQ-2 are of low intensities with the maximum peak ground acceleration of 0.022m/s^2 and 0.047m/s^2 respectively. A higher time period of the isolated building as compared to the conventional building is responsible for the reduction of its acceleration response as seen in Figs.6-11. Further it is seen that the reduction in peak spectral acceleration of the records is more significant as compared to the peak spectral values obtained from the analysis. This implies that the time period shift which is responsible for the reduction in response has been under estimated in the analysis, which leads to a conclusion that the actual initial stiffness of the isolators is much less than the initial stiffness used in the analysis (determined from experimental cyclic shear test).

The difference in the peak values of recorded floor acceleration in comparison with analysis are tabulated in Table-2. The values indicate that difference in analysis and records of base isolated building is more significant as compared to conventional building. Moreover, while the analytical peak floor accelerations in conventional building are an under estimate of the peak accelerations obtained from instrumental records, analysis of base isolated building gives much higher peak floor accelerations than the instrument records. Here it is expected that a modified analysis of conventional building should yield higher floor acceleration as compared to the present analysis and a modified analysis of the isolated building should yield lower floor accelerations as compared to the present analysis.

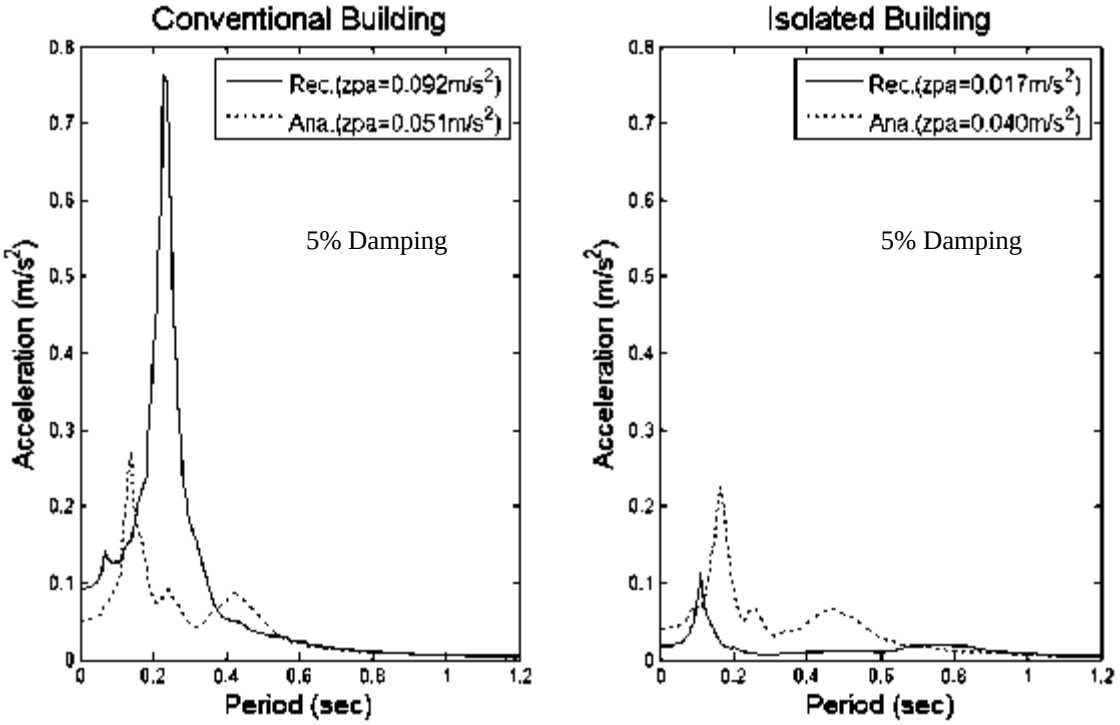

Fig-6: Comparison of Roof Acceleration Spectra for EQ-1—Longitudinal Direction

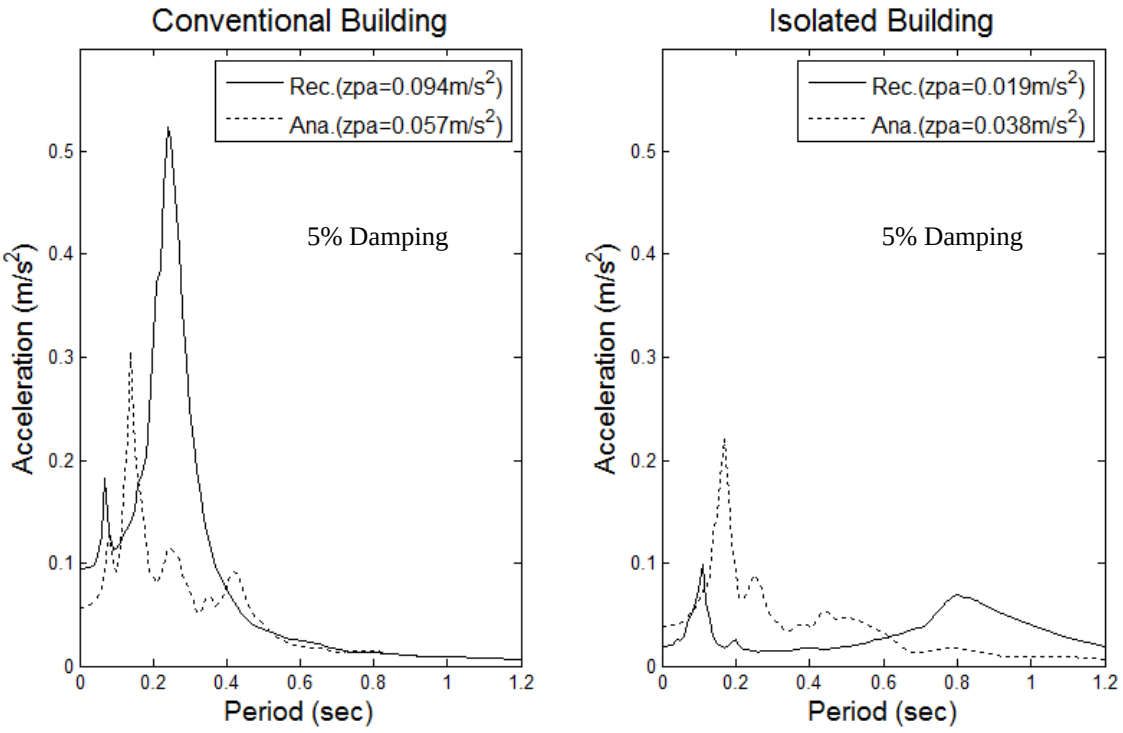

Fig-7: Comparison of Roof Acceleration Spectra for EQ-2—Longitudinal Direction

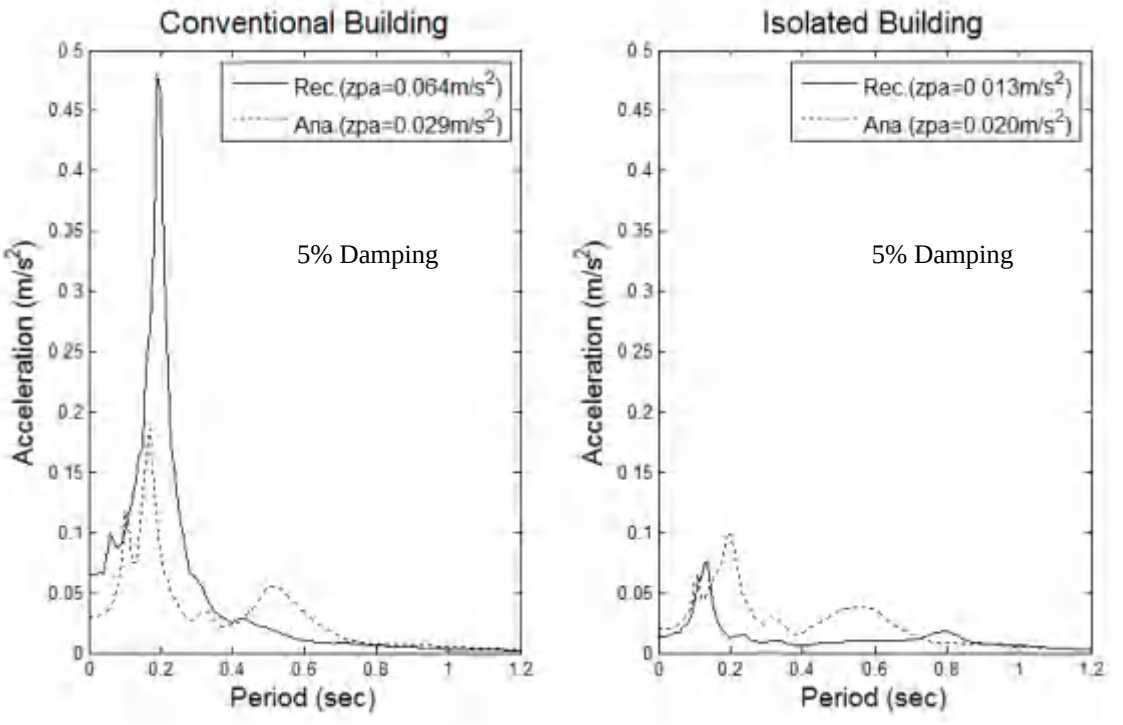

Fig-8: Comparison of Roof Acceleration Spectra for EQ-1—Transverse Direction

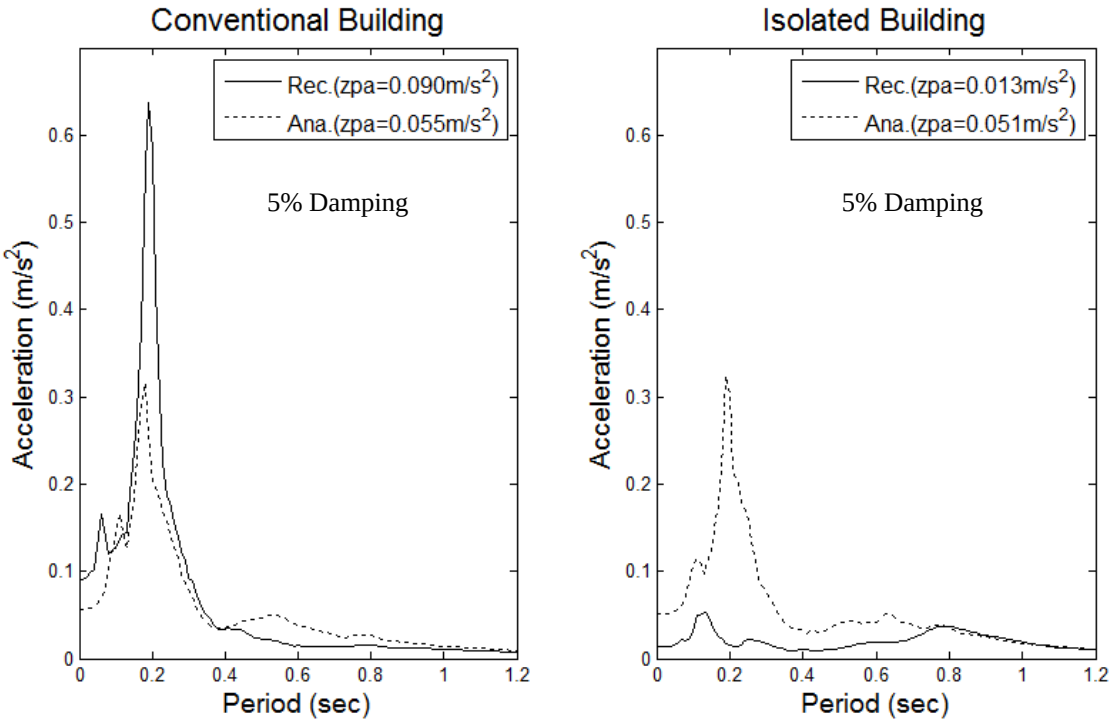

Fig-9: Comparison of Roof Acceleration Spectra for EQ-2—Transverse Direction

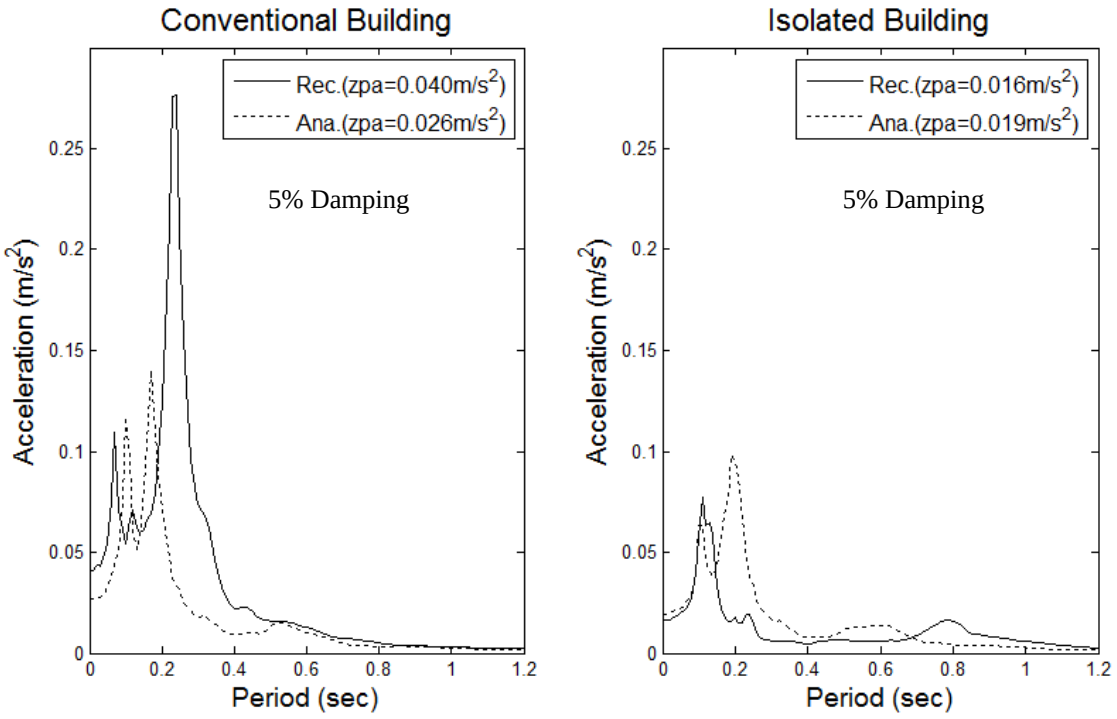

Fig-10: Comparison of Ground floor Acceleration Spectra for EQ-1—Transverse Direction

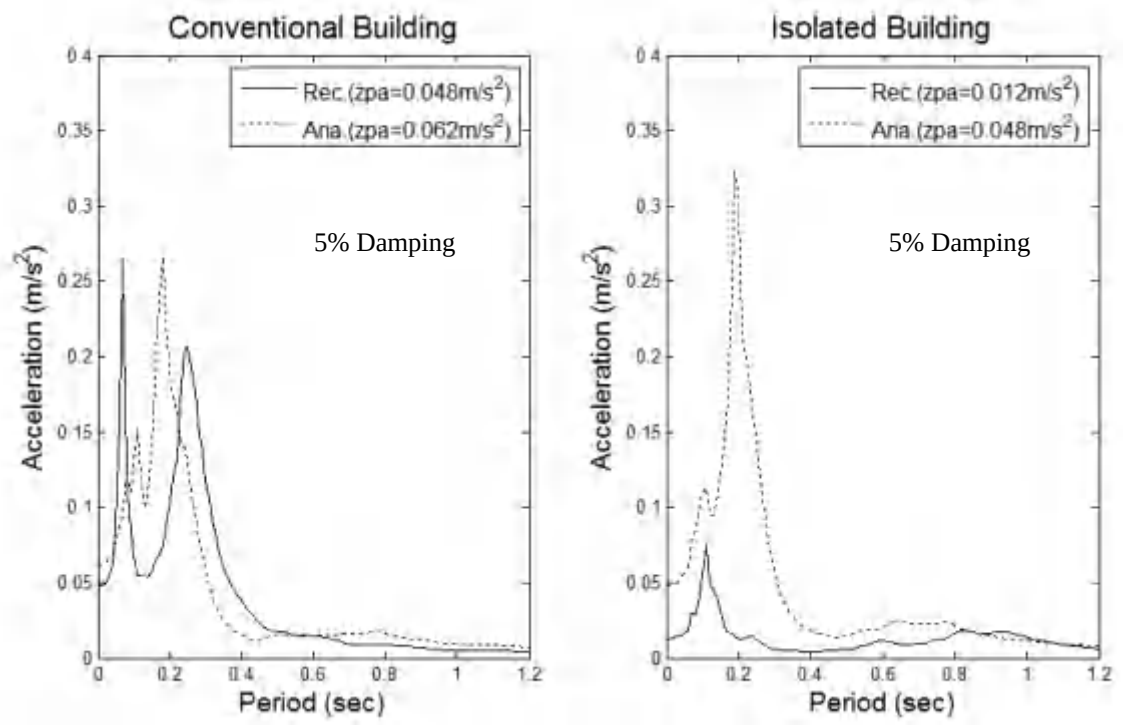

Fig-11: Comparison of Ground floor Acceleration Spectra for EQ-2—Transverse Direction

Table-2: Percentage Difference between Recorded and Analytical Peak Acceleration Response

		Longitudinal		Transverse	
		Conventional	Isolated	Conventional	Isolated
EQ-1	Roof	44.6	135.3	54.6	53.8
	Ground	-	-	35.0	18.8
EQ-2	Roof	39.4	100.0	38.8	292.3
	Ground	-	-	29.2	300.0

-Instrumental records not available for ground floor in longitudinal direction

The difference between the results of analysis and the values obtained using instrumental records for the conventional building can be explained as followed:

- Infills are modelled as a diagonal strut. The earthquake is of a considerably small intensity. There is a possibility of the entire infill acting as a shear panel (for the low intensity earthquakes considered). This would significantly increase the stiffness of the conventional building.
- In modelling the frame, gross cross sectional area for the columns and beams have been taken. A free vibration testing of the frame structure would have given a better estimation of stiffness at low level excitations
- At low intensity earthquake, a conventional structure is expected to exhibit low damping. The present analysis assumed 5% damping in all modes. An assumption of reduced damping values is required for an accurate estimation of the spectral acceleration.

The difference in analysis and observations of the base isolated building can be explained as followed

- The large differences in the analysis and records of base isolated building indicate that the actual value of initial stiffness at a low level intensity is much smaller than the value evident from the experimental cyclic shear test. A free vibration testing of the base isolated structure would have given a better estimation of the initial stiffness of isolators at low level excitations.
- The rubber compound used in the LLRB may have a considerable amount of damping. Considering this damping in the analysis would reduce the spectral acceleration. Therefore damping of the isolator need to be evaluated accurately.
- The infill modelling as explained for conventional building would significantly alter the stiffness of the base isolated building.

CONCLUSIONS

In this paper, a comparative study of conventional and base isolated buildings at actual low level excitation is carried out. A complete 3D model of the buildings considering the effects of infill and soil stiffness is used for the analysis. The comparison observed in the analysis and the instrumental records for both conventional and base isolated buildings indicate a similar trend in the spectral accelerations. However, some differences are evident. These discrepancies indicate a modelling deficiency with respect to stiffness and damping of the structural elements, infill and the isolators. In the analysis, gross cross sections of the beams and columns have been considered. There may be some effective reduction in the gross stiffness at low level excitations, which has not been considered. The earthquakes considered in the present study are of a very low intensity. At such low intensity excitations, the conventional building is expected to exhibit low value of damping in contrast to 5% damping which is assumed in the present analysis. It is also possible that the infill wall acts as a shear panel for such low intensity excitations, whereas the present analysis considers the infill acting as equivalent diagonal strut. The stiffness and damping characteristics of the isolators that have been used are derived from an experimental cyclic shear test, where the isolator was subjected to significantly large deformations. The applicability of these values of stiffness and damping at low level excitations is questionable. The comparison of analysis of the base isolated building with the instrumental records indicate that the initial stiffness of the isolator for low level excitation should be much less than its value for an excitation resulting in significant shear deformation of the isolators. A free vibration test of the two structures would have given a better estimation of the stiffness and damping characteristics of the test structures at low intensity excitations.

REFERENCES

[1] P.N. Dubey, G.R. Reddy, K. K. Vaze, A.K. Ghosh, H.S. Kushwaha, S.K. Deb, Performance of Base Isolated RCC Framed Building under Actual Earthquake, Journal of Structural Engineering, 35 (3) (2008), pp 147-153
[2] J.M. Kelly, Earthquake-Resistant Design with Rubber, Springer, London, 1997.
[3] F. Naeim, J.M. Kelly, Design of seismic isolated structures from theory to practice, Wiley, New York, 1999.
[4] P. Komodromos, Seismic Isolation for Earthquake-Resistant Structures, WIT Press, Southampton, Boston, 2000.
[5] R.I. Skinner, W.H. Robinson, G.H. McVerry, An Introduction to Seismic Isolation, John Wiley & Sons, England, 1993.
[6] T.V. Pradeep Kumar, D.K. Paul, Force-Deformation Behaviour of Isolation Bearings, Journal of Bridge Engineering, ASCE, 12 (4) (2007), pp.527-529.
[7] H. Masahiko, O. Shin, Response Control and Seismic Isolation of Buildings, Taylor & Francis, New York, 2006.
[8] FEMA-356 , Prestandard and Commentary for the Seismic Rehabilitation of Buildings, Federal Emergency Management Agency, Washington, D.C.. , 2000.
[9] UBC-1997, Uniform Building Code, Volume-2, pp- 9-38 & 405-416.
[10] CSI (Computers amd Structures Inc.), SAP2000 v14, Static and Dynamic Finite Element Analysis of Structures, CSI, Berkeley, 2009.
[11] CSI (Computers amd Structures Inc.), SAP2000 v14 Analysis Reference Manual, CSI, Berkeley, 2009.
[12] George Gazetas, Formulas and Charts for Impedances of Surface and Embedded foundations, Journal of Geotechnical Engineering, ASCE, 117 (9) (1991), pp.1363-1381.
[13] J.E. Bowles, Foundation Analysis and Design, McGraw-Hill Book Co., Singapore, 1997.

DEVELOPMENT OF LEVEL-1 PSA METHOD APPLICABLE TO JAPAN SODIUM-COOLED FAST REACTOR: (2) SEISMIC RESPONSE ANALYSIS CONSIDERING CHARACTERISTICS OF THE ADVANCED SEISMIC ISOLATION SYSTEM

K. Minagawa[1], S. Fujita[1], A. Yamaguchi[2], T. Takata[2], K. Kurisaka[3]
[1]Department of Mechanical Engineering, School of Engineering, Tokyo Denki University, Tokyo, Japan
[2]Department of Energy and Environment Engineering, Osaka University, Osaka, Japan
[3]Advanced Nuclear System R&D Directorate, Japan Atomic Energy Agency, Ibaraki, Japan
E-mail of corresponding author: minagawa@cck.dendai.ac.jp

ABSTRACT

This paper deals with seismic response analysis and sensitivity analysis of a seismic isolation system. Rubber bearings have a hardening property in horizontal direction and a softening property in vertical direction in case of large deformation. Therefore the analyses considered nonlinearity of rubber bearings. Both horizontal and vertical nonlinear characteristics of rubber bearings were explained by multi-linear model. Mass point analytical models were applied. At first, seismic response analysis was executed in order to investigate influence of nonlinearity of rubber bearing upon response of the building. Then sensitivity analysis was executed. Parameters of rubber bearings, oil dampers and the building were fluctuated, and influence of dispersion of these parameters upon response of building was investigated. As a result, it was confirmed that nonlinear properties of rubber bearings have influence on response of the building and inner equipment.

INTRODUCTION

Japan Atomic Energy Agency (JAEA) has been developing Japan Sodium-cooled Fast Reactor (JSFR) in the fast reactor cycle technology development project. The JSFR employs passive safety architectures and an advanced seismic isolation system as innovative technologies. Since no one has established the level-1 PSA method that can provide the evaluation of these innovative technologies, JAEA, Tokyo Denki University and Osaka University have started a joint study to develop the level-1 PSA method that is applicable to JSFR since August 2010. This study includes the level-1 PSA related to internal events and a seismic event as a representative external event in Japan.

The advanced seismic isolation system that is applied to the JSFR consists of rubber bearings and oil dampers. Generally, rubber bearings deform linearly and have linear stiffness against seismic load in both horizontal and vertical direction. However, hardening in horizontal direction and softening in vertical direction occur in case of large input. In seismic PSA, it is important to consider these nonlinear characteristics.

This paper describes results of seismic response analysis and sensitivity analysis of the advanced seismic isolation system. The seismic response analysis considered nonlinearity of laminated rubber bearings. In the sensitivity analysis, parameters of the rubber bearings, the oil dampers and the building were fluctuated, and influence of dispersion of these parameters upon response of building was investigated.

ANALYTICAL CONDITION

In this chapter, analytical models and input waves for the seismic response analysis and the sensitivity analysis are described. a reactor building is modeled to simple mass point model, and rubber bearings are modeled in consideration of nonlinear stiffness. Seismic wave for design is applied for the analysis.

Modeling of Reactor Building

A reactor building was modeled to a three mass points model, that is to say isolation layer, lower layer of structure and upper layer of structure [1]. Deformation of isolation device is predominant compared with it of the upper structure in isolated building, so the modeling to mass points is permissible for this fundamental investigation. Figure 1 shows analytical model for horizontal direction and Fig. 2 shows it for vertical direction. The mass m_{s1} corresponds to floor where a reactor and important equipment are installed. Analytical model for vertical direction includes the ground layer. On the other hand, horizontal model does not include ground layer. This is because

horizontal stiffness of rubber bearings is so small compared with ground that dynamic behavior of ground can be ignored. Tables 1 and 2 indicate parameters of the analytical model. These parameters are based on an actual design of a nuclear power plant.

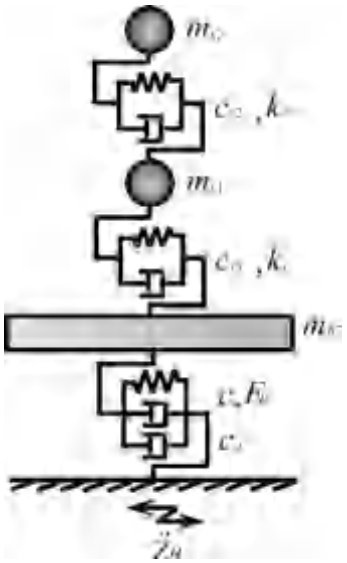

Fig. 1: Analytical model (Horizontal)

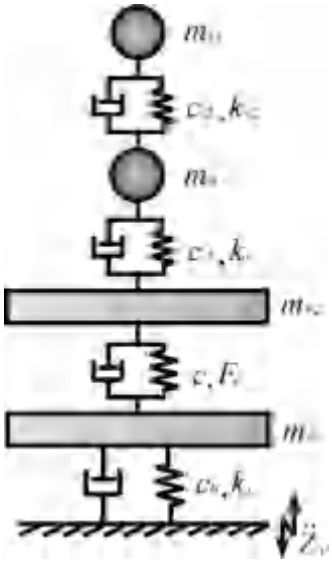

Fig. 2: Analytical model (Vertical)

Table 1: Analytical parameter of building (Horizontal)

	Caption	Median	Variation coefficient	Log. standard variation
m_{b2}	Mass of isolation layer	46.0x10^6[kg]	0.10	0.10
m_{s1}	Mass of 1st layer of building	111x10^6[kg]	0.10	0.10
m_{s2}	Mass of 2nd layer of building	13.2x10^6[kg]	0.10	0.10
F_R	Restoring force of rubber bearings			
k_{s1}	Stiffness of 1st layer of building	99.4x10^9[N/m]	0.13	0.13
k_{s2}	Stiffness of 2nd layer of building	11.7x10^9[N/m]	0.13	0.13
c	Damping coefficient of rubber bearings	12.6x10^6[Ns/m] (2[%])	0.10	0.10
c_d	Damping coefficient of oil dampers	270x10^6[Ns/m] (43[%])	0.10	0.10
c_{s1}	Damping coefficient of 1st layer of building	332x10^6[Ns/m] (5[%])	0.25	0.25
c_{s2}	Damping coefficient of 2nd layer of building	39.3x10^6[Ns/m] (5[%])	0.25	0.25

Table 2: Analytical parameter of building (Vertical)

	Caption	Median	Variation coefficient	Log. standard variation
m_{b1}	Mass of ground layer	22.9x10^6[kg]	0.10	0.10
m_{b2}	Mass of isolation layer	46.0x10^6[kg]	0.10	0.10
m_{s1}	Mass of 1st layer of building	111x10^6[kg]	0.10	0.10
m_{s2}	Mass of 2nd layer of building	13.2x10^6[kg]	0.10	0.10
k_{b1}	Stiffness of ground layer	1.18x10^{12}[N/m]	0.20	0.20
F_r	Restoring force of rubber bearings			
k_{s1}	Stiffness of 1st layer of building	1.15x10^{12}[N/m]	0.13	0.13
k_{s2}	Stiffness of 2nd layer of building	184x10^9[N/m]	0.13	0.13
c_{b1}	Damping coefficient of 1st layer of building	22.7x10^9[Ns/m]	0.20	0.20
c_{b2}	Damping coefficient of rubber bearings	341x10^6[Ns/m] (2[%])	0.10	0.10
c_{s1}	Damping coefficient of 1st layer of building	1.13x10^9[Ns/m] (5[%])	0.25	0.25
c_{s2}	Damping coefficient of 2nd layer of building	151x10^6[Ns/m] (5[%])	0.25	0.25

Modeling of Rubber Bearing

Rubber bearings have linear stiffness in the normal deformation range. However rubber bearings have nonlinear stiffness in case of large deformation. Figure 3 shows the horizontal restoring property of rubber bearings, and Fig. 4 shows the vertical restoring property of rubber bearings. Tables 3 and 4 indicate parameters of the rubber bearing models.

As shown in Fig. 3, rubber bearings have hardening property in horizontal direction, which is caused by strain hardening of rubber material [2]. In addition, once the hardening occurs, the hardening displacement shifts in accordance with the following equation.

$$\delta_1' = \delta_1 + \alpha\left(\delta_{\max} - \delta_1\right), \qquad \delta_2' = \delta_2 + \alpha\left(\delta_{\max} - \delta_1\right) \tag{1}$$

Where δ_1' δ_2' are the new hardening displacement, $\delta_{\max}$ is the maximum displacement which rubber bearing experienced.

As shown in Fig. 4, vertical stiffness of rubber bearings is linear for compressive load, but has a softening property for tensile load. This softening property is caused by static deformation of rubber bearings by gravity. Therefore the 1st softening load P_1 is the load that makes rubber bearings natural length, and that is equivalent to weight of the upper structure. The Accumulative strength P_2 - P_1 is equivalent to allowable tensile load.

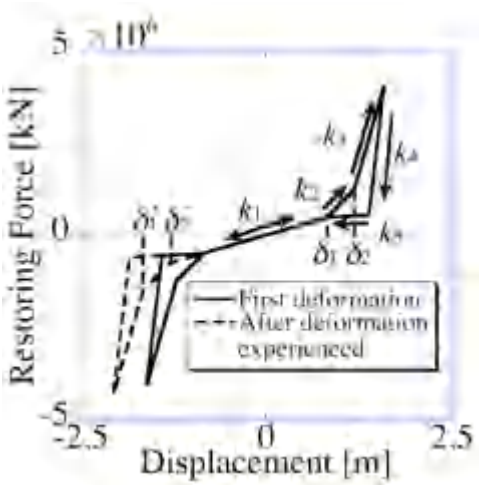

Fig. 3: Restoring model of rubber bearing (Horizontal)

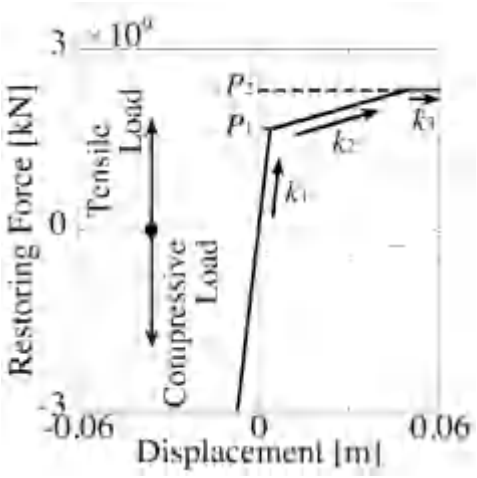

Fig. 4: Restoring model of rubber bearing (Vertical)

Table 3: Analytical parameter of rubber bearings (Horizontal)

	Caption	Median	Variation coefficient	Log. standard variation
k_1	1st stiffness	$580\text{x}10^6$[N/m]	0.10	0.10
k_2	2nd stiffness	$2.03\text{x}10^9$[N/m] ($3.5k_1$)	0.10	0.10
k_3	3rd stiffness	$6.96\text{x}10^9$[N/m] ($12k_1$)	0.10	0.10
k_4	4th stiffness	$17.1\text{x}10^9$[N/m] ($29.5k_1$)	0.10	0.10
k_5	5th stiffness	$116\text{x}10^6$[N/m] ($0.2k_1$)	0.10	0.10
δ_1	1st hardening displacement	0.826[m]	0.10	0.10
δ_2	2nd hardening displacement	1.19[m]	0.10	0.10
F_1	1st hardening load	$479\text{x}10^6$[N]	linked with k_1 and δ_1	
F_2	2nd hardening load	$1.22\text{x}10^9$[N]	linked with k_1 and δ_1	
α	Repetition factor	0.45	0.10	0.10

Table 4: Analytical parameter of rubber bearings (Vertical)

	Caption	Median	Variation coefficient	Log. standard variation
k_1	1st stiffness	428 x10^9 [N/m]	0.10	0.10
k_2	2nd stiffness	14.3x10^9[N/m] (k_1/30)	0.10	0.10
k_3	3rd stiffness	0 [N/m]	0	0
P_1	1st softening load	479x10^6[N]	0.10	0.10
$P_2 - P_1$	Accumulative strength	1.22x10^9[N]	0.10	0.10

Input Wave

A wave shown in Fig. 5 was used as an input wave for horizontal direction. This wave is suitable for seismic design of a nuclear power plant. A wave of which amplitude is 2/3 of the wave for horizontal direction is used as an input wave for vertical direction. These waves are called Ss wave in this paper. Amplitude of the Ss wave is varied in analyses in order to investigate relationships between response and earthquake level.

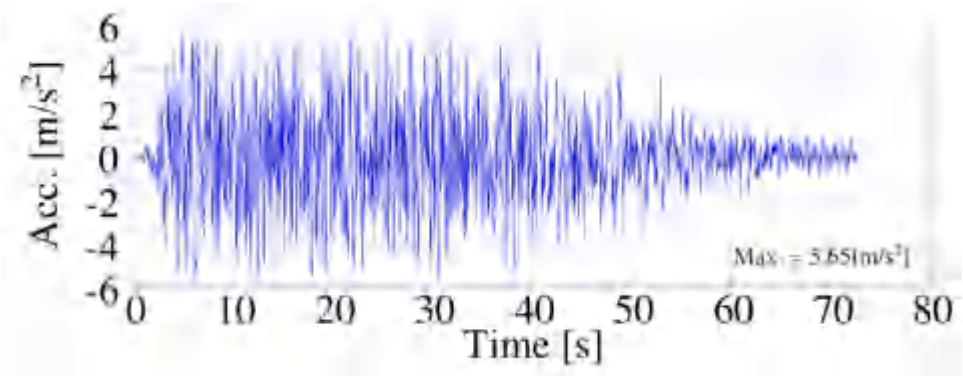

Fig. 5: Input wave

SEISMIC RESPONSE ANALYSIS

In order to investigate influence of nonlinearity of rubber bearings on response of the building, seismic response analysis was executed. The median parameters of the building and rubber bearings were used for the analysis. The amplitudes of input wave were varied in order to investigate relationships between the input earthquake level and the response.

Horizontal Direction

Figure 6 shows relationships between input earthquake level and the maximum response. In Fig. 6, response acceleration is it of the mass m_{s1} where a reactor and important equipment are installed, and response displacement indicates deformation of rubber bearings. It is confirmed from Fig. 6 that the maximum response displacement exceeds the 1st hardening displacement when the input earthquake level is 2.4, and it exceeds the 2nd hardening displacement when the input earthquake level is approximately 4. The response acceleration increases nonlinearly according to the hardening of the rubber bearings. On the other hand, the response displacement increases linearly. The reason is that the hardening displacement increases according to Eq. (1), and the maximum response displacement occurred after the hardening displacement increased.

Figure 7 shows response acceleration spectra of input earthquake level of 3.0 and 5.0. These spectra were computed from response of the mass m_{s1}, so response of a reactor and equipment installed in mass m_{s1} can be evaluated. These spectra contain results of rubber bearings having linear property in order to investigate influence of nonlinearity. The 1st hardening occurred in the case of input earthquake level of 3.0, and the 2nd hardening occurred in the case of 5.0. When input earthquake level is 3.0, the spectrum of nonlinear simulation is almost same as linear. On the other hand, when input earthquake level is 5.0, the spectrum of nonlinear simulation is large compared with linear. Therefore hardening of the rubber bearings affects response of a reactor and important equipment that were installed in the building.

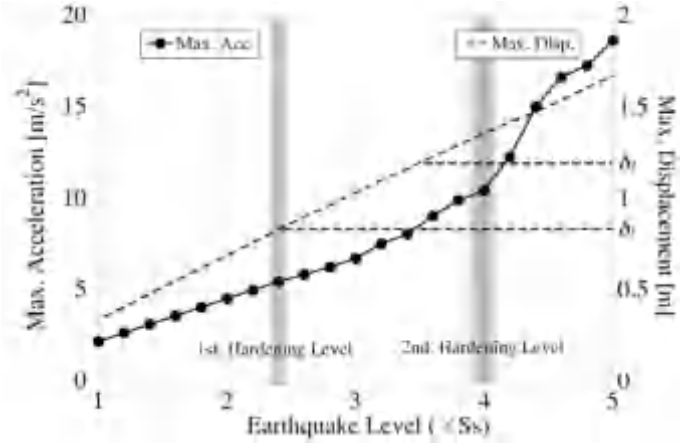

Fig. 6: Relationship between input earthquake level and Max. response (Horizontal)

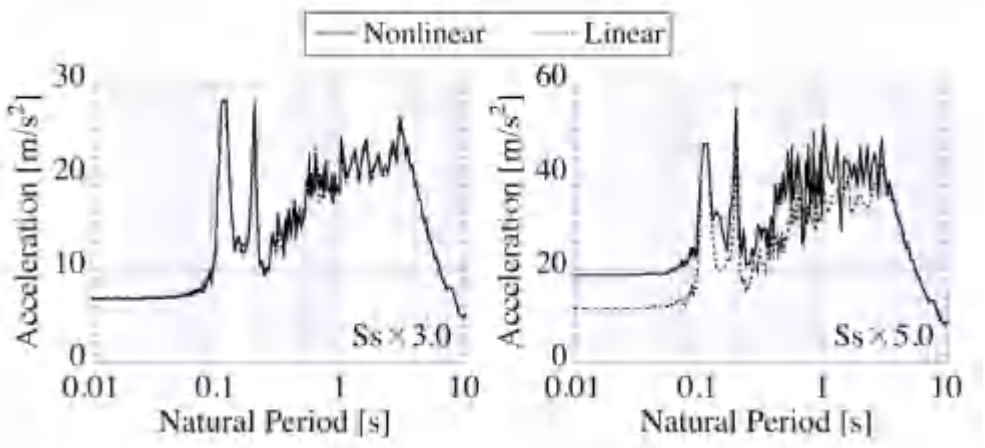

Fig. 7: Floor response spectra (Horizontal)

Vertical Direction

Figure 8 shows relationships between input earthquake level and the maximum response. In Fig. 8, response acceleration is it of the mass m_{s1}, and response displacement is deformation of rubber bearing. The 1st softening occurred when the input earthquake level is more than 1.2, and the 2nd softening occurred when the input earthquake level is more than 3.2. The increment of response displacement increases with an increase of input earthquake level, because of the softening of rubber bearings. The increment of response acceleration increases as well, because compressive load increases by softening.

Figure 9 shows response acceleration spectra of input earthquake level of 3.0 and 5.0. These spectra were computed from response of the mass m_{s1} as well as Fig. 7. The 1st softening occurred in the case of input earthquake level of 3.0, and the 2nd softening occurred in the case of 5.0. As shown in Fig. 9, predominant frequencies of spectra considering nonlinear properties are broader than results of the linear system. The reason is that various modes were excited by the impact load when stiffness of the rubber bearings shifts from k_2 to k_1. Therefore the softening of rubber bearings affects response of a reactor and important equipment that were installed in the building.

SENSITIVITY ANALYSIS

In order to investigate influence of parameter of the building and rubber bearings, sensitivity analysis was executed. In this analysis, a parameter whose sensitivity is investigated was fluctuated in consideration of fabrication accuracies, and other parameters retained median value. The dispersion was given by logarithmic normal distribution [3]. The upper and lower limit values of fluctuated parameters were yielded from Eq. (2).

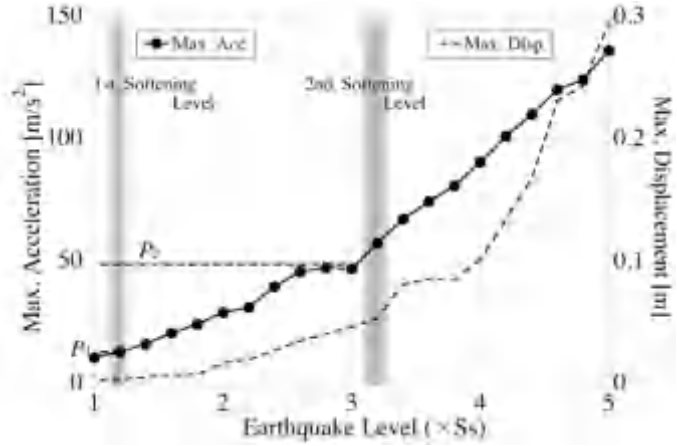

Fig. 8: Relationship between input earthquake level and Max. response (Vertical)

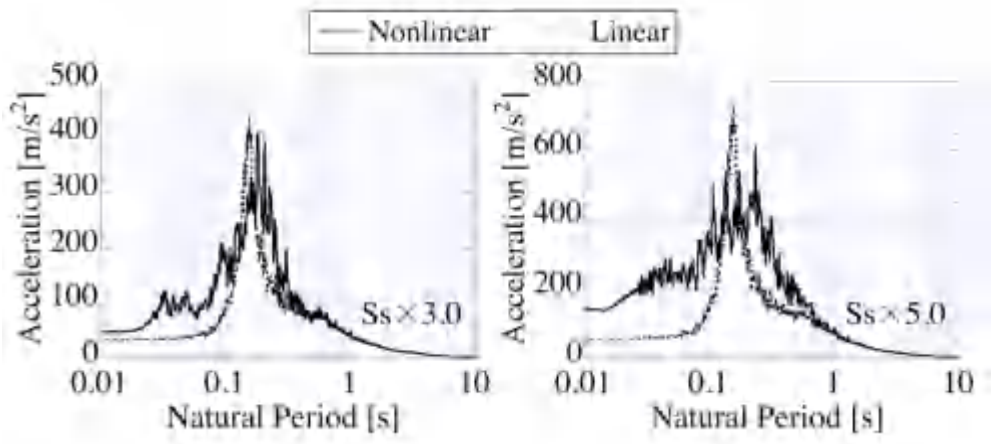

Fig. 9: Floor response spectra (Vertical)

$$X_{Upper} = \exp\left(\log X + \xi\right), \qquad X_{Lower} = \exp\left(\log X - \xi\right) \tag{2}$$

Where X_{Upper} is an upper limit value of a parameter, X_{Lower} is a lower limit value, X is a median value and ξ is a logarithmic standard variation shown in tables 1 to 4. Sensitivities were calculated from the maximum response acceleration of the mass m_{s1} where a reactor and important equipment are installed, and the sensitivities were error ratio to analysis result without any variations.

Horizontal Direction

Figure 10 shows analytical results for horizontal direction. It is confirmed that sensitivities of parameters of the building are dominant in the case of normal input earthquake level (Ss x 1). On the other hand, sensitivities of parameters of the rubber bearings, especially the 2nd hardening displacement δ_2, are dominant in the case of large input earthquake level (Ss x 5). This is because the isolation period became low in consequence of 2nd hardening, and it came close to the natural period of superstructure.

Vertical Direction

Figure 11 shows analytical results for vertical direction. It is confirmed that sensitivities of parameters of the rubber bearings are dominant. In addition, masses of the building m_{b2}, m_{s1}, m_{s2} have high sensitivity because they influence on the isolation period. The stiffness and the damping coefficient of ground k_{b1}, c_{b1} have high sensitivity as well because their logarithm standard variations were high compared with the other.

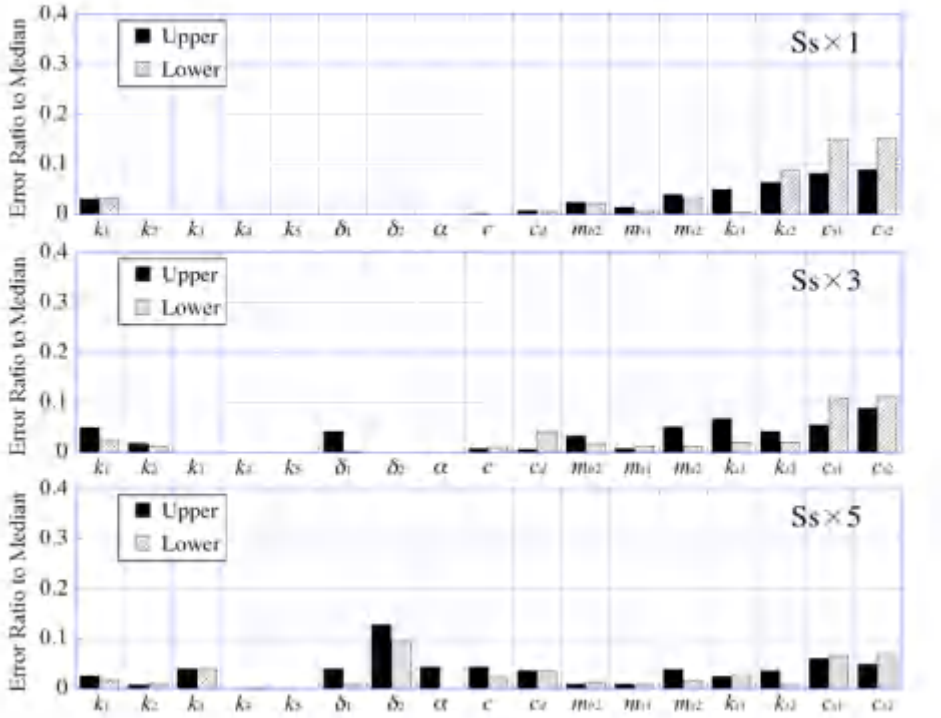

Fig. 10: Results of sensitivity analysis (Horizontal)

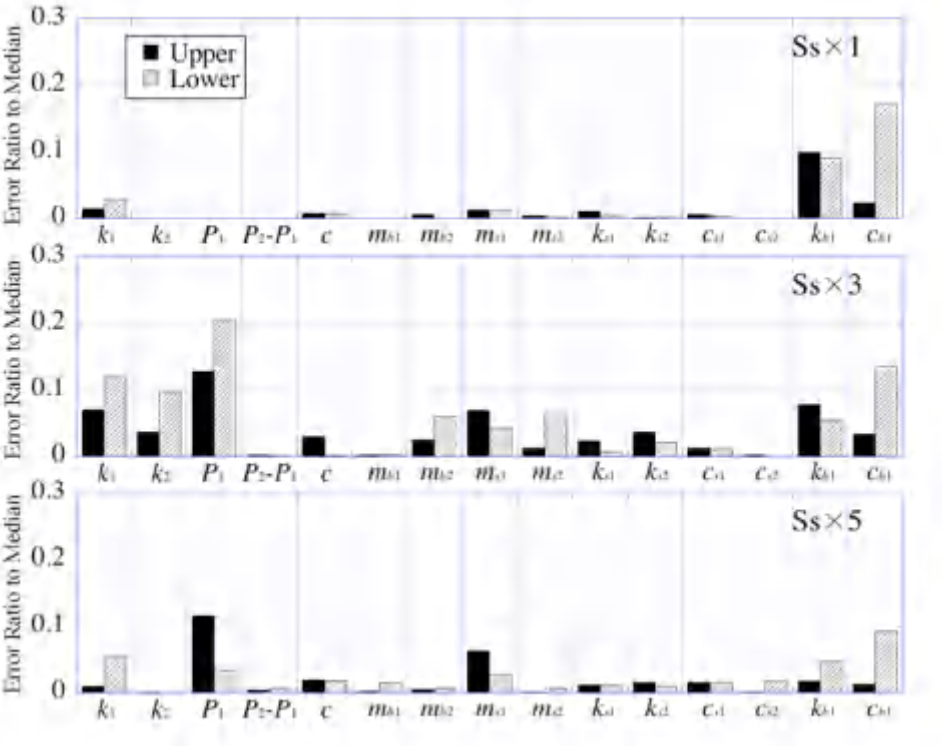

Fig. 11: Results of sensitivity analysis (Vertical)

CONCLUSION

This paper dealt with the seismic response analysis and sensitivity analysis of the seismic isolation system, and the analyses considered nonlinearity of rubber bearings. The results of this paper are summarized as follows.

Nonlinear properties of rubber bearings appeared when input earthquake level is 2.4 times of the design wave in horizontal direction, and 1.2 times in vertical direction. Therefore the consideration of the nonlinear properties is needed in probabilistic approaches of seismic isolation system.

The horizontal isolation period came close to the natural period of superstructure by hardening of rubber bearings. As a result, horizontal response of the building increased.

The softening of rubber bearings in vertical direction caused impact load in compressive direction.

Nonlinear properties of rubber bearings have influence on the floor response spectra. Therefore the properties affect equipment installed in the building.

Parameters of rubber bearings have high sensitivity.

ACKNOWLEDGEMENT

The present study incorporates the results from "Development of level-1 PSA method for Japan sodium-cooled fast reactor" entrusted to Japan Atomic Energy Agency by the Ministry of Education, Sports, Science and Technology (MEXT). The authors would like to express their appreciations to Mr. T. Kodaira and Mr. M. Oguro of graduate school of Tokyo Denki University for their devoted assistance.

REFERENCES

[1] Japan Electric Association, "Japan Electric Association Guide 4614-2000", Japan Electric Association, 2000, pp. 5-18, [in Japanese].

[2] Katoh, A., Nagura, S., Nojima, O., Yoneda, G.,, "Study on concept of seismic isolation type plant for FBR: Part 28 Ultimate Behavior of Base-Isolated Reactor Building (Sensitivity Analysis on Hysteresis Curve Modeling Method)", *Proceedings of Architectural Institute of Japan*, 1993, pp. 1595-1596, [in Japanese].

[3] Endo, M., Uryu, M., Imazuka, Y., Yamazaki, T., Yoshida, S., Nakanishi, R., "Fragility evaluation of base-isolated building: Part2: Evaluation of fragility curve considering bumping against retaining wall", *Proceedings of Architectural Institute of Japan*, 2007, pp. 943-944, [in Japanese].